



**HAL**  
open science

# Multisensory (visuo-proprioceptive) integration and sensory transformations for upper-limb control in humans : towards an improved sensory clinical assessment for stroke patients

Jules Bernard-Espina

► **To cite this version:**

Jules Bernard-Espina. Multisensory (visuo-proprioceptive) integration and sensory transformations for upper-limb control in humans : towards an improved sensory clinical assessment for stroke patients. *Neurons and Cognition [q-bio.NC]*. Sorbonne Université, 2023. English. NNT : 2023SORUS008 . tel-04051192

**HAL Id: tel-04051192**

**<https://theses.hal.science/tel-04051192>**

Submitted on 29 Mar 2023

**HAL** is a multi-disciplinary open access archive for the deposit and dissemination of scientific research documents, whether they are published or not. The documents may come from teaching and research institutions in France or abroad, or from public or private research centers.

L'archive ouverte pluridisciplinaire **HAL**, est destinée au dépôt et à la diffusion de documents scientifiques de niveau recherche, publiés ou non, émanant des établissements d'enseignement et de recherche français ou étrangers, des laboratoires publics ou privés.

# Sorbonne Université

Ecole Doctorale Cerveau Comportement Cognition (ED3C)

*Integrative Neuroscience and Cognition Center, Université Paris Cité, CNRS UMR 8002*

**Multisensory (visuo-proprioceptive) integration  
and sensory transformations for upper-limb control in humans:  
*towards an improved sensory clinical assessment for stroke patients.***

Par Jules Bernard-Espina

Thèse de doctorat de Neurosciences

Dirigée par Marc Maier

Co-encadrée par Michele Tagliabue

Présentée et soutenue publiquement le 19/01/2023

Devant un jury composé de :

Assaiante Christine, Directrice de Recherche, CNRS

Rapporteure

Crèvecoeur Frédéric, Professeur, Université catholique de Louvain

Rapporteur

Roby-Brami Agnès, Directrice de Recherche Emérite, INSERM

Examinatrice

Berret Bastien, Professeur, Université Paris Saclay

Président du jury, Examinateur

Maier Marc, Professeur Emérite, Université Paris Cité

Directeur de thèse

Tagliabue Michele, Ingénieur de Recherche, Université Paris Cité

Co-encadrant



*« Personne, il est vrai, n'a jusqu'à présent déterminé ce que peut le corps [...] Le corps, par les seules lois de sa nature, peut beaucoup de choses dont son esprit reste étonné. »*

*Spinoza, L'Ethique (1677)*

# Résumé

Pour contrôler nos mouvements avec précision, le cerveau combine de multiples sources d'information sensorielle, telles que la proprioception et la vision. Les déficits proprioceptifs, fréquemment observés chez les patients victimes d'accident vasculaire cérébral (AVC), ont ainsi un impact majeur sur le contrôle et la récupération de la motricité volontaire. Une bonne compréhension des déficits proprioceptifs est donc essentielle à la rééducation post-AVC. Cependant, à ce jour, aucun consensus ne s'est dégagé sur l'évaluation des déficits proprioceptifs. Une réinterprétation de la littérature, à travers le prisme des récentes théories sur l'intégration sensorielle, suggère que ce qui est communément nommé « déficit proprioceptif » dans le domaine clinique pourrait confondre d'autres fonctions cognitives, telles que la capacité à réencoder les informations proprioceptives dans un autre espace sensoriel (nommée transformation sensorielle). Le premier objectif de cette thèse est de réconcilier les résultats, en apparence contradictoires, d'un grand nombre d'études cliniques à l'aide d'une approche théorique nous permettant de proposer une nouvelle stratification des patients victimes d'AVC. Celle-ci apparaît cohérente avec la localisation des lésions cérébrales rapportée dans les études citées : les patients présentant des lésions dans le cortex pariétal postérieur, impliqué dans la capacité à lier les informations proprioceptives et visuelles, ont tendance à présenter un déficit fonctionnel du membre supérieur mis en évidence spécifiquement par les tests cliniques impliquant des transformations sensorielles. Le deuxième objectif de cette thèse est d'étudier comment les transformations sensorielles influencent l'intégration visuo-proprioceptive. En utilisant la réalité virtuelle, nous avons réalisé une série d'expériences comportementales, avec des sujets sains, afin de tester expérimentalement les prédictions de notre modèle théorique dans le but de développer de nouvelles techniques d'évaluation sensorielle. Nous observons que les transformations sensorielles influencent l'intégration visuo-proprioceptive en modulant la dépendance visuelle ou proprioceptive des sujets en fonction du contexte de la tâche expérimentale. Enfin, le troisième objectif de cette thèse est d'étudier les facteurs qui peuvent altérer les transformations sensorielles. Nous apportons de nouveaux arguments soutenant le rôle central de la gravité dans la perception spatiale. Dans leur ensemble, ces résultats établissent un nouveau cadre conceptuel, permettant de mieux comprendre les déficits sensoriels, et ouvrent la voie à l'émergence d'approches innovantes pour l'évaluation et la rééducation post-AVC.

**Mots-clés** : coordination œil-main ; principe de vraisemblance maximum ; intégration multi-sensorielle ; transformation sensorielle ; AVC ; proprioception ; compensation visuelle.

# Abstract

The control of hand movements arises from the integration of multiple sources (modalities) of sensory information, such as proprioception and vision. For this reason, proprioceptive deficits often observed in stroke patients have a significant impact on the integrity and recovery of motor functions. A better understanding of proprioceptive deficits is therefore critical for the rehabilitation of stroke patients. Despite its importance, to date, no consensus has emerged on the assessment of proprioceptive deficits. A reinterpretation of the literature on stroke proprioceptive deficits through the prism of recent sensory integration theories suggests that what is termed “proprioceptive deficits” in the clinical field would encompass other cognitive functions, such as the ability to re-encode proprioceptive (spatial) information in higher-order sensory spaces (referred to as sensory transformations). The first goal of this thesis is to reconcile the apparently contradictory results of a large number of clinical studies by use of optimal sensory integration modelling. This theoretical approach provides a novel rationale for an improved stratification of stroke patients according to their sensory deficits. This new stratification was found to be consistent with the location of brain lesions reported in stroke studies: patients with lesions in the posterior parietal cortex, which is known to be involved in linking proprioceptive and visual information, tend to show a functional upper limb deficit specifically in the proprioceptive assessment tasks requiring sensory transformations. The second goal of this thesis is to study how sensory transformations affect optimal visuo-proprioceptive integration. For this purpose, we used virtual reality behavioural experiments, with healthy participants, to experimentally test the predictions of our newly developed model, and prepare the ground for new sensory assessment techniques in upper limb rehabilitation after stroke. We found that sensory transformations affect visuo-proprioceptive integration by modulating the subjects’ reliance on visual or proprioceptive cues depending on the task context. Finally, the third goal of this thesis is to study the factors which can influence sensory transformations negatively. We show that head-gravity misalignment interferes with sensory transformations, supporting the theorized central role of gravity in spatial perception. Altogether, these results provide a novel framework to better understand sensory deficits and may lead to innovative approaches to stroke assessment and rehabilitation.

**Keywords:** eye-hand coordination; maximum likelihood principle; multisensory integration; cross-modal sensory transformation; stroke; proprioception assessment; visual compensation.

# Contents

|  |             |
|--|-------------|
| <b>Résumé</b>  | <b>i</b>    |
| <b>Abstract</b>  | <b>ii</b>   |
| <b>Contents</b>  | <b>iii</b>  |
| <b>Remerciements</b>   | <b>iv</b>   |
| <b>Curriculum</b>  | <b>vii</b>  |
| <b>List of figures</b>   | <b>viii</b> |
| <b>List of tables</b>  | <b>x</b>    |
| <b>List of abbreviations</b>   | <b>xi</b>   |
| <br>   |             |
| <b>1 Introduction</b>  | <b>1</b>    |
| 1.1 Proprioceptive, visual and vestibular systems                                  | 3           |
| 1.2 Reference frames for sensory encoding  | 8           |
| 1.3 Multisensory integration   | 14          |
| 1.4 Proprioceptive deficits and visual compensation in stroke                      | 22          |
| 1.5 Goals and research questions   | 33          |
| <b>2 Methods</b>   | <b>37</b>   |
| 2.1 Study 1 – Reinterpretation of the stroke literature on proprioceptive deficits | 37          |
| 2.2 Study 2 – Sensory transformations affecting visuo-proprioceptive integration   | 41          |
| 2.3 Study 3 – Gravitational influence on sensory transformations                   | 52          |
| <b>3 Common theoretical approach</b>   | <b>58</b>   |
| 3.1 Extended Concurrent Model  | 58          |
| 3.2 Application of the model for proprioceptive tasks                              | 60          |
| 3.3 Application of the model for visual tasks                                      | 63          |
| 3.4 Application of the model for visuo-proprioceptive tasks                        | 65          |
| 3.5 Application of the model for cross-modal tasks                                 | 67          |
| 3.6 Description of the model fitting procedures                                    | 69          |
| <b>4 Results</b>   | <b>75</b>   |
| 4.1 Study 1 – Reinterpretation of the stroke literature on proprioceptive deficits | 75          |
| 4.2 Study 2 – Sensory transformations affecting visuo-proprioceptive integration   | 83          |
| 4.3 Study 3 – Gravitational influence on sensory transformations                   | 96          |
| <b>5 Discussion</b>  | <b>107</b>  |
| 5.1 Study 1 – Reinterpretation of the stroke literature on proprioceptive deficits | 107         |
| 5.2 Study 2 – Sensory transformations affecting visuo-proprioceptive integration   | 111         |
| 5.3 Study 3 – Gravitational influence on sensory transformations                   | 116         |
| 5.4 Common theoretical approach  | 120         |
| 5.5 From assessment to rehabilitation  | 122         |
| <b>6 Perspectives</b>  | <b>126</b>  |
| 6.1 A new paradigm for the assessment of proprioception                            | 126         |
| 6.2 Possible applications for the assessment of other neurological deficits        | 129         |
| <b>7 Conclusion</b>  | <b>132</b>  |
| <br>   |             |
| <b>References</b>  | <b>133</b>  |
| <br>   |             |
| <b>Appendix</b>  | <b>147</b>  |
| A. Software development for our study on multisensory integration                  | 147         |
| B. Previous models of optimal multisensory integration                             | 149         |
| C. Scientific contribution   | 151         |
| D. Articles published in the context of the thesis                                 | 153         |

# Remerciements

Il m'est bien étrange de signer ce manuscrit avec mon seul nom, tant il est collectif. Il n'aurait jamais vu le jour sans un improbable concours de circonstances qui m'a mené à des rencontres déterminantes.

Tout d'abord, Agnès et Bastien, merci pour votre implication depuis le début, du comité de suivi de thèse jusqu'au jury. Merci Christine et Frédéric pour votre engagement en tant que rapporteurs. Merci à vous quatre du temps que vous avez consacré à lire et évaluer mon travail.

Michele, Marc, je ne vous remercierai jamais assez de m'avoir accueilli dans votre équipe, et de m'avoir fait confiance pour développer ensemble ce projet de recherche. Vous avez toujours été disponible l'un comme l'autre, à mon écoute et en soutien. Pendant ces trois années, j'ai eu la chance d'apprendre à vos côtés, particulièrement avec toi Michele. Et j'ai tant appris ! Vous m'avez transmis votre sens pédagogique et votre rigueur, que je continuerai à aiguiser. Vous êtes un modèle pour le scientifique que j'aspire à être. Je tiens également à remercier l'École Doctorale Cerveau-Cognition-Comportement (ED3C) qui m'a fait confiance en m'accordant une bourse de doctorat pour ces trois années, ainsi que le Centre National d'Études Spatiales (CNES), le CNRS, et l'Université Paris Cité. Sans leur soutien financier, cette thèse n'aurait pu exister.

Merci à toute mon équipe de recherche, vous avez tous et toutes été d'un soutien si précieux. La thèse est une épreuve qu'il me semble impossible de traverser seul. Mathieu, Desdemona, David, merci pour votre bienveillance et disponibilité, François, merci pour tes cours qui m'ont permis (enfin !) de comprendre le système vestibulaire. Et tous mes co-thésards, merci à vous, nous nous sommes serré les coudes dans les moments les plus difficiles, en partageant nos galères de C++, en s'offrant bubble tea, maté, kimchi, kouign-amann et gâteaux basques : Corentin, Dongkyun, Esteban, Flavia, Louis, Louise, Marin, Mérie, merci ! Merci également à Joe. Bien que vous fassiez partie de notre équipe je ne vous ai jamais rencontré, pourtant mon travail découle directement du vôtre, aussi bien sur les aspects théoriques que pratiques. Et bien sûr, merci Carole pour ton aide, nous ne pourrions pas faire grand-chose sans toi !

Si je suis arrivé jusqu'ici aujourd'hui, c'est aussi en grande partie grâce à l'Institut de Formation en Masso-Kinésithérapie (IFMK) Saint-Michel. J'ai eu la chance lors de mes études de kinésithérapie de pouvoir participer à mon premier projet de recherche, et c'est ce qui m'a amené sur ce chemin passionnant qu'est la thèse. Merci Fabien pour la confiance que tu m'as accordé, de l'IFMK jusqu'au World Congress of Physiotherapy. Merci Lucas et Hermann d'avoir partagé avec moi ces premiers pas dans la recherche. Merci Thomas, Helena et Caroline du soutien que vous m'avez apporté. Merci Stéphane, Julien et Jean, vous avez été mon premier jury d'experts. C'est en partie grâce à vous tous que j'ai acquis la confiance nécessaire pour poursuivre dans cette voie.

Merci à toute l'équipe de rééducation de Garches qui a animé en moi la passion pour les neurosciences. Merci Élisabeth de m'avoir accueilli dans ton service. Merci Alex, Erika et Magalie, vous avez été mes guides pendant ces deux années passées avec vous, et vous restez à mes yeux un modèle pour la rééducation neurologique. Merci Céline, Djamel et Samuel, de m'avoir fait découvrir la recherche clinique à l'hôpital, c'est un véritable espoir pour la suite, d'allier science et clinique. Merci à toi Julie, il est rare et précieux d'entretenir une telle relation de confiance entre kinésithérapeute et médecin. J'ai énormément appris à tes côtés. Merci pour ton implication au début de ma thèse. Notre projet de recherche ensemble n'a malheureusement pas pu voir le jour, mais je suis convaincu que ce n'est que partie remise.

Merci Sophie, de m'avoir accueilli dans ton master et de me faire confiance aujourd'hui encore. Le master BME a été un tremplin, tant pour la formation qu'il offre que pour les rencontres qu'il a provoquées. Je suis honoré d'y participer aujourd'hui, comme alumni et comme enseignant grâce à Michele.

A toute cette grande famille, merci de m'avoir accueilli à la croisée des mondes de la recherche et de la rééducation. J'espère faire encore un long chemin avec vous tous.

Au-delà du monde clinique et académique, j'ai eu la chance d'être entouré par tant de personnes qui m'ont offert soutien, courage et inspiration. C'est aussi grâce à vous tous que j'ai pu mener ce travail à son terme. Merci Martino et Guillaume pour votre aide mathématique. J'ai hâte de collaborer avec vous sur vos projets d'apnée et triathlon ! Merci Claire et Çağlar pour les nombreuses discussions scientifiques et philosophiques. Vous êtes une source d'inspiration pour

moi. Merci Élise et Léa, mes kinés préférées, toujours au rendez-vous. Wilfried, Sophie, vous avez aussi été présents lorsque j'en ai eu le plus besoin, merci. Merci à ma famille d'apnéistes, les Adriens, le Benoit (l'unique), Dom (le super coach), vous m'avez donné force, courage et persévérance. Lukas, Chau, Theo, Maëlig, Yvan, mes amis depuis le master, nous avons partagé ensemble ce parcours du combattant, merci. Victoria, merci d'avoir partagé les derniers instants de cette thèse. Merci Hélène, même si nous sommes loin aujourd'hui, tu fais incontestablement partie des personnes qui m'ont permis de me construire, et m'ont soutenu dans les différentes étapes qui m'ont menées jusqu'ici.

Et mes deux familles. Merci à ma famille d'adoption, Alain, Michèle, Thalia, Benjamin et mes nouveaux partenaires de Lego Yliann et Louna. Merci pour tout le ~~hum~~ soutien que vous m'apportez. Grâce à vous, j'ai gravi plusieurs cols, au sens figuré comme au sens propre. Merci Papa, merci Mamita, vous m'avez toujours soutenu dans mes choix, quels qu'ils soient : de la physique à la kinésithérapie, en passant par la danse contemporaine, pour enfin arriver aux neurosciences. Sans bien savoir où j'allais à priori, chaque petite brique de liberté que vous m'avez offerte m'a permis de me structurer et d'évoluer vers celui que je suis aujourd'hui. Et ce n'est que le début. Merci Nenette, ma grande petite sœur. Nous sommes loin géographiquement, mais proches dans l'adversité.

Enfin, Lloydie, tu mérites une place à part dans ces remerciements. Je te dois tant ! Ton soutien sans faille pendant ces trois années m'a permis de tenir. Je ne peux pas imaginer être arrivé jusqu'au bout sans toi. Au bout de la thèse, mais aussi des autres épreuves qui se sont présentées. Même dans les traversées les plus difficiles, la vie est douce à tes côtés. Merci du fond du cœur.

À vous qui vous apprêtez à lire cet ouvrage, merci et bonne lecture.

# Curriculum

## Professional

---

- 2019-2022: PhD candidate at INCC (Université Paris Cité, CNRS, UMR 8002).  
Spatial Orientation team (Dir. Mathieu Beraneck and Desdemona Fricker).
- 2015-2017: Physiotherapist at Raymond Poincaré Hospital, Garches.  
Neurological Rehabilitation and post-intensive care Unit.

## Teaching and Tutoring

---

- 2015-2022: At the Institut de Formation en Masso-Kinésithérapie (IFMK) Saint-Michel, Paris:  
- Teaching electromyography, respiratory and neurological rehabilitation;  
- Tutoring end-study dissertations.
- 2019-2022: At the Université Paris Cité:  
- Teaching “Introduction to Virtual and Augmented Reality”:  
virtual reality for neurorehabilitation (Master 2, BME Paris);  
- Tutoring one physiotherapy student for a research project on sensory  
assessment (one month internship);  
- Tutoring three Master students (BME Paris, two months FABlab project) on  
the development of a new sensory assessment method;  
- Tutoring one Master student (BME Paris, two months internship) working on  
the testing phase of a new sensory assessment method.

## Scientific/Clinical Education

---

- 2022-2023: Diplôme Inter-Universitaire (DIU) of Vestibular Rehabilitation.  
Sorbonne Université, Paris.
- 2019: Master in Biomedical Engineering (BME Paris). Neurosciences, with honors.  
Arts et Métiers ParisTech & Université Paris Descartes, Paris.
- 2015 : State-registered diploma of Physiotherapy.  
IFMK Saint-Michel, Paris.
- 2012 : Bachelor (3rd year) in Scientific communication and mediation, with honors.  
Université Paris Diderot, Paris.
- 2011 : Bachelor (2nd year) in Physics (DEUG), with honors.  
Université Paris Diderot, Paris.

# List of figures

## **Introduction**

|  |    |
|--|----|
| Figure 1-1   Proprioceptive, visual and vestibular pathways.....   | 3  |
| Figure 1-2   Proprioceptors.....   | 5  |
| Figure 1-3   The eye.....  | 6  |
| Figure 1-4   The inner ear and the vestibular system .....   | 7  |
| Figure 1-5   Topographic maps for proprioceptive and visual sensory information .....                          | 9  |
| Figure 1-6   Sensory encoding in “extra” sensory spaces .....  | 11 |
| Figure 1-7   Gravity links the reference frames used for perception and action .....                           | 13 |
| Figure 1-8   Sensus Communis.....  | 14 |
| Figure 1-9   Statistical optimality in multisensory integration.....   | 15 |
| Figure 1-10   Application of the Concurrent Model for a multisensory (visuo-proprioceptive) reaching task..... | 18 |
| Figure 1-11   Cross-modal visuo-proprioceptive task with sensory transformations.....                          | 19 |
| Figure 1-12   Potential sensory transformation in uni-modal proprioceptive tasks .....                         | 21 |
| Figure 1-13   Global incidence of stroke .....   | 23 |
| Figure 1-14   Spot a stroke, use the BE-FAST acronym.....  | 23 |

## **Methods (Study 1)**

|   |    |
|---|----|
| Figure 2-1   Four categories of proprioceptive assessments..... | 39 |
|---|----|

## **Methods (Study 2)**

|  |    |
|--|----|
| Figure 2-2   Experimental set-up.....                                  | 42 |
| Figure 2-3   Representation of the experimental paradigm .....         | 43 |
| Figure 2-4   Virtual reality experimental tasks .....                  | 45 |
| Figure 2-5   Illustration of the visuo-haptic sensory conflict .....   | 47 |
| Figure 2-6   Example of subject responses and associated analysis..... | 49 |

## **Methods (Study 3)**

|                                       |    |
|---------------------------------------|----|
| Figure 2-7   Experimental setup ..... | 53 |
|---------------------------------------|----|

## **Common theoretical approach**

|  |    |
|--|----|
| Figure 3-1   Extended Concurrent Model.....  | 59 |
| Figure 3-2   Unimodal proprioceptive tasks without necessity of sensory transformations .....                      | 61 |
| Figure 3-3   Unimodal proprioceptive tasks with the necessity of sensory transformations.....                      | 62 |
| Figure 3-4   Unimodal proprioceptive tasks with potential sensory transformations.....                             | 63 |
| Figure 3-5   Unimodal visual tasks without the necessity of sensory transformations. ....                          | 63 |
| Figure 3-6   Unimodal visual tasks with the necessity of sensory transformations .....                             | 64 |
| Figure 3-7   Visuo-proprioceptive tasks without the necessity of sensory transformations.....                      | 65 |
| Figure 3-8   Visuo-proprioceptive tasks with the necessity of sensory transformations for the retinal signals..... | 66 |
| Figure 3-9   Visuo-proprioceptive tasks with the necessity of sensory transformations for the joints signals.....  | 67 |
| Figure 3-10   Cross-modal visuo-proprioceptive tasks.....  | 68 |

|   |    |
|---|----|
| Figure 3-11   Visuo-proprioceptive reaching of a visual target.....   | 69 |
| Figure 3-12   Model parameters for fitting stroke literature data (Study 1) .....   | 70 |
| Figure 3-13   Model parameters for fitting experimental data of the study on the effect of sensory transformations on visuo-proprioceptive processing (Study 2) ..... | 72 |
| Figure 3-14   Model parameters for fitting experimental data of the study on the gravitational effect on sensory transformations (Study 3).....                       | 74 |

**Results (Study 1)**

|   |    |
|---|----|
| Figure 4-1   Data and predictions of performance variability in different sensory assessments.... | 78 |
| Figure 4-2   Cortical areas potentially involved in proprioceptive and sensory transformations... | 82 |

**Results (Study 2)**

|   |    |
|---|----|
| Figure 4-3   Average subject responses .....  | 84 |
| Figure 4-4   Response patterns for unimodal haptic and visual tasks .....   | 85 |
| Figure 4-5   Differential effects of spatial mirror transformations on response variability in haptic and visual unimodal tasks ..... | 87 |
| Figure 4-6   Response patterns for multimodal visuo-haptic tasks .....  | 89 |
| Figure 4-7   Comparison between multimodal and unimodal tasks .....   | 90 |
| Figure 4-8   Visual weight of each multisensory visuo-haptic task, working plane orientation and visual noise level .....             | 92 |
| Figure 4-9   Comparisons between model predictions and experimental data.....   | 95 |

**Results (Study 3)**

|  |     |
|--|-----|
| Figure 4-10   Effect of posture (seated vs. supine) on performance.....              | 97  |
| Figure 4-11   Response variability and visual weights as a function of posture ..... | 99  |
| Figure 4-12   Inter-individual analyses.....   | 101 |
| Figure 4-13   Model predictions as a function of seated vs. supine posture.....      | 105 |
| Figure 4-14   Response errors in the Straight Neck Experiment.....                   | 106 |

**Discussion**

|   |     |
|---|-----|
| Figure 5-1   Correspondence between clinical assessment tasks and experimental (haptic and visuo-haptic) tasks..... | 113 |
|---|-----|

**Perspectives**

|   |     |
|---|-----|
| Figure 6-1   Proprioceptive assessment tasks using a forced choice paradigm.....                | 127 |
| Figure 6-2   Preliminary results of 12 healthy subjects in the sensory assessment protocol..... | 128 |
| Figure 6-3   Clinical expression of apraxia .....   | 129 |
| Figure 6-4   Patient with pusher syndrome.....  | 130 |

**Appendix A**

|  |     |
|--|-----|
| Figure A-1   Communication between the haptic device and the virtual reality system..... | 147 |
|--|-----|

# List of tables

## **Introduction**

|  |    |
|--|----|
| Table 1-1   Description of the most commonly used methods for the assessment of proprioceptive function post-stroke..... | 25 |
|--|----|

## **Common theoretical approach**

|  |    |
|--|----|
| Table 3-1   Representation of the two alternative Concurrent Models..... | 73 |
|--|----|

## **Results (Study 1)**

|  |    |
|--|----|
| Table 4-1   Performance variability reported in studies involving healthy subjects ..... | 76 |
| Table 4-2   Performance variability reported in studies involving stroke patients.....   | 77 |

## **Results (Study 2)**

|  |    |
|--|----|
| Table 4-3   ANOVA main and interaction effects for the unimodal tasks .....  | 86 |
| Table 4-4   ANOVA main and interaction effects for the multisensory tasks .....  | 88 |
| Table 4-5   Difference between H, V and VH response variability .....  | 91 |
| Table 4-6   ANOVA main and interaction effects for the visual weight.....  | 92 |
| Table 4-7   Hotelling T-Squared value (and associated p-value) between the model predictions and experimental data ..... | 94 |
| Table 4-8   Model parameter values for the Extended Concurrent Model .....   | 96 |

## **Results (Study 3)**

|  |     |
|--|-----|
| Table 4-9   ANOVA main and interaction effects.....  | 98  |
| Table 4-10   Coefficient of correlation R (and associated p-value) between variability and visual dependency ..... | 100 |

## **Discussion**

|   |     |
|---|-----|
| Table 5-1   Predicted impairment in the different sensory assessments based on the sensory deficit type ..... | 110 |
|---|-----|

# List of abbreviations

**aB-AP:** Asymmetric Between-Arms Proprioceptive tasks

**aB-A<sub>VP</sub>:** Asymmetric Between-Arms Visuo-Proprioceptive tasks (Visual compensation)

**BSMT:** Bimanual Sagittal Matching Test

**CNS:** Central Nervous System

**ECM:** Extended Concurrent Model

**ExJ:** Extra-Joint

**ExR:** Extra-Retinal

**fMRI:** Functional Magnetic Resonance Imaging

**FPT:** Finger Proprioception Test

**H:** Haptic tasks

**H<sub>//</sub>:** Haptic Parallel task

**H<sub>Λ</sub>:** Haptic Mirror task

**IPD:** Interpupillary Distance

**IPS:** Intra-Parietal Sulcus

**J:** Joint

**LOC:** Lateral Occipital Cortex

**M1:** Primary Motor Cortex

**MLP:** Maximum Likelihood Principle

**MPT:** Mirror Position Test

**MRI:** Magnetic Resonance Imaging

**MS:** Motor Sequences Test

**MV:** Matching to a Visual Image

**OFA:** Occipital Face Area

**PET:** Positron Emission Tomography

**P:** Proprioceptive deficit

**P-P:** Unimodal Proprioceptive Task (Proprioceptive target – Proprioceptive response)

**PPC:** Posterior Parietal Cortex

**P+T:** Proprioceptive and Sensory Transformations deficit

**RT:** Reaching Test

**S1:** Primary Somatosensory Cortex

**S2:** Secondary Somatosensory Cortex

**sB-AP:** Symmetric Between-Arms Proprioceptive tasks

**sB-A<sub>VP</sub>:** Symmetric Between-Arms Visuo-Proprioceptive tasks (Visual compensation)

**SLD:** Shape or Length Discrimination

**SMG:** Supramarginal Gyrus

**SPL:** Superior Parietal Lobule

**STG:** Superior Temporal Gyrus

**T:** Sensory Transformation deficit

**TDT:** Threshold Detection Test

**TLT:** Thumb Localization Test

**TMS:** Transcranial Magnetic Stimulation

**UDT:** Up or Down Test

**V:** Visual tasks

**V<sub>//</sub>:** Visual Parallel task

**V<sub>∧</sub>:** Visual Mirror task

**V1:** Primary Visual Cortex

**VIP:** Ventral IntraParietal area

**VH:** Visuo-Haptic tasks

**V//H//**: Visuo-Haptic Parallel task

**V $\wedge$ H//**: Visual Mirror - Haptic Parallel task

**V//H $\wedge$** : Visual Parallel - Haptic Mirror task

**Vn**: Visual tasks, with visual noise

**Vn//**: Visual Parallel task, with visual noise

**Vn $\wedge$** : Visual Mirror task, with visual noise

**VnH**: Visuo-Haptic tasks, with visual noise

**Vn//H//**: Visuo-Haptic Parallel task, with visual noise

**Vn $\wedge$ H//**: Visual Mirror - Haptic Parallel task, with visual noise

**Vn//H $\wedge$** : Visual Parallel - Haptic Mirror task, with visual noise

**V-P**: Cross-modal Visuo-Proprioceptive task (Visual target – Proprioceptive response)

**VR**: Virtual Reality

**V-V**: Unimodal Visual Task (Visual target – Visual response)

**V-VP**: Visuo-proprioceptive reaching (Visual target – Visuo-Proprioceptive response)

**W-AP**: Within-Arm Proprioceptive tasks

**W-AVP**: Within-Arm Visuo-Proprioceptive tasks (Visual compensation)

**WPT**: Within-arm Position Test

# 1 Introduction

When performing goal-oriented hand movements, such as reaching and grasping an object, the central nervous system (CNS) uses multiple sensory signals. In particular, vision and proprioception allow for comparison of the hand position and configuration with the location/orientation of the object to be grasped (the target). Sensory information about hand and target position are key to movement planning and execution. In the context of brain lesions, such as in stroke, proprioceptive deficits are extremely common (Connell et al., 2008; Kessner et al., 2016) and contribute significantly to the patient's motor and functional disability (Turville et al., 2017; Zandvliet et al., 2020). Despite the clinical relevance, both assessment and rehabilitation of proprioceptive function of the upper limb lack consensus and provide contrasting results (Findlater and Dukelow, 2017). Furthermore, it remains unclear to which extent stroke patients with proprioceptive impairments are able to compensate for their deficits with visual feedback to guide hand movements (Darling et al., 2008a; Herter et al., 2019; Scalha et al., 2011; Semrau et al., 2018). It is therefore critical to understand how proprioception is processed in the CNS, how it interacts with visual processing, and how it leads to motor action.

Recent findings suggest that, when reaching or grasping an object, visual and/or proprioceptive sensory signals can be encoded in multiple concurrent reference frames (McGuire and Sabes, 2009; Tagliabue and McIntyre, 2014, 2011, 2008). These reference frames can either directly reflect the nature of the sensory system from which the information originates (e.g. the retinal reference for vision, and the joint reference for proprioception) or they can reflect a more complex combination of sensory signals (i.e. body-centered encoding of the hand position requiring the processing of inverse kinematics of joint signals, or external encoding with respect to a gravitational reference requiring the integration of graviceptor signals, or with respect to external visual landmarks that are integrated into an allocentric representation of the movement). This process of encoding information in a reference frame different from the receptor that originally encoded it, will in the following be referred to as *sensory transformation*.

A particular case of sensory transformation can be observed when, even in the absence of visual feedback of the hand, the CNS encodes the proprioceptive signals from the arm in a visual

## **Introduction: Proprioceptive, visual and vestibular systems**

reference (Arnoux et al., 2017; Jones and Henriques, 2010; McGuire and Sabes, 2009; Pouget et al., 2002; Sarlegna and Sainburg, 2007; Tagliabue and McIntyre, 2013). These experimental results with healthy subjects suggest that in purely proprioceptive tasks (when only proprioceptive feedback of the hand is available, but not visual), the sensory processing of joint signals involves sensory transformations. This is likely also the case in some proprioceptive assessment methods used to evaluate proprioceptive deficits post-stroke.

The first goal of this thesis is to reinterpret and reconcile the apparently contradictory results of a large number of clinical studies on stroke proprioceptive deficits, and provide a novel rationale for an improved stratification of stroke patients according to their sensory deficits, by distinguishing purely proprioceptive deficits from deficits of sensory transformations. In continuity with the first goal, the second aim of this thesis is to study the role of sensory transformations in uni- and multi-sensory processing. This would provide additional evidence for distinguishing, and not confounding, proprioceptive processing from processing of sensory transformations. This would further clarify the potential role of sensory transformations in the ability to use vision to compensate for a proprioceptive deficit. Finally, the third goal of this thesis is to study the factors which can influence sensory transformations. In order to apprehend these three different aspects, we used an interdisciplinary approach, combining behavioral experiments and mathematical modeling.

In this first chapter, I will present the general framework of this thesis, from the sensory systems involved in reaching and grasping, to the multisensory integration, and finally I will describe the standard clinical methods for the assessment of proprioceptive deficits and visual compensation mechanisms post-stroke. In the second chapter, I will detail our methodological approach, which is built on three complementary and interconnected blocks: targeted literature review, behavioral experiments, and mathematical modeling. The third chapter will present the results obtained and/or published in the course of this thesis, describing visual and proprioceptive processing in different contexts. The fourth chapter will constitute a general discussion of the results, which provide altogether a novel framework to better understand sensory upper limb deficits. Finally, in the fifth chapter, I will provide some perspectives on potential clinical applications of our results, and present a new experimental paradigm aiming to improve screening and quantification of sensory deficits in stroke patients.

### 1.1 Proprioceptive, visual and vestibular systems

Sensorimotor control relies on the CNS ability to integrate concomitant sensory information arising from the external environment and from the body itself. Since Aristotle, and his description of sensation in *De Anima* (350 BC), it is commonly accepted that humans possess five different senses which are: sight, hearing, taste, smell, and touch. Modern neurosciences, however, count more senses. They are, perhaps, subtler senses which may be less obvious to conscious perception, but which are equally essential to interact with our environment. Among them are proprioception and the vestibular sense, which are often referred to as the sixth and seventh senses (not always with the same priority ranking). These two sensory systems, together with vision, contribute to spatial orientation, balance, and sensorimotor coordination.

Proprioception, vision, and the vestibular sense (as well as the other senses) are characterized by a group of sensory cells (receptors) that transduce specific stimuli (light, mechanical pressure, stretching...) and transmit the resulting neural signal to multiple regions of the brain where it is processed and interpreted (see Figure 1-1). In the following introductory sections, I will describe briefly the physiology and anatomy of these three sensory systems.

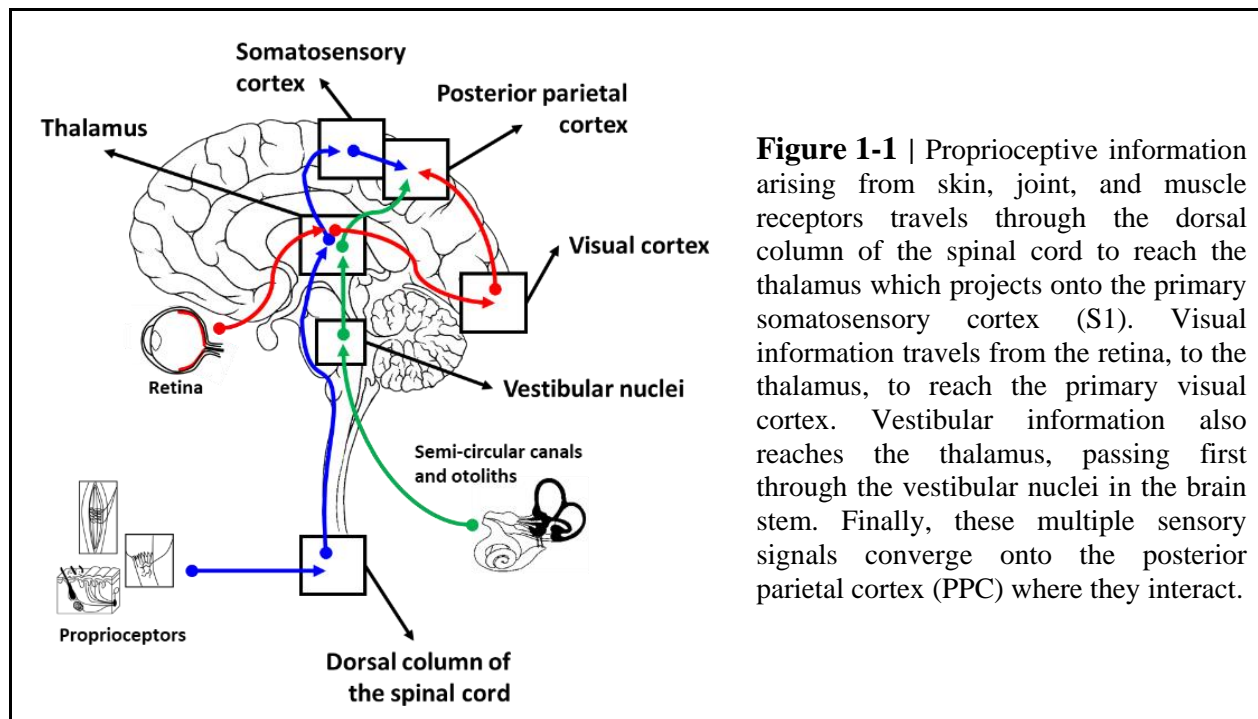


**Figure 1-1** | Proprioceptive information arising from skin, joint, and muscle receptors travels through the dorsal column of the spinal cord to reach the thalamus which projects onto the primary somatosensory cortex (S1). Visual information travels from the retina, to the thalamus, to reach the primary visual cortex. Vestibular information also reaches the thalamus, passing first through the vestibular nuclei in the brain stem. Finally, these multiple sensory signals converge onto the posterior parietal cortex (PPC) where they interact.

### **1.1.1 Proprioceptive system**

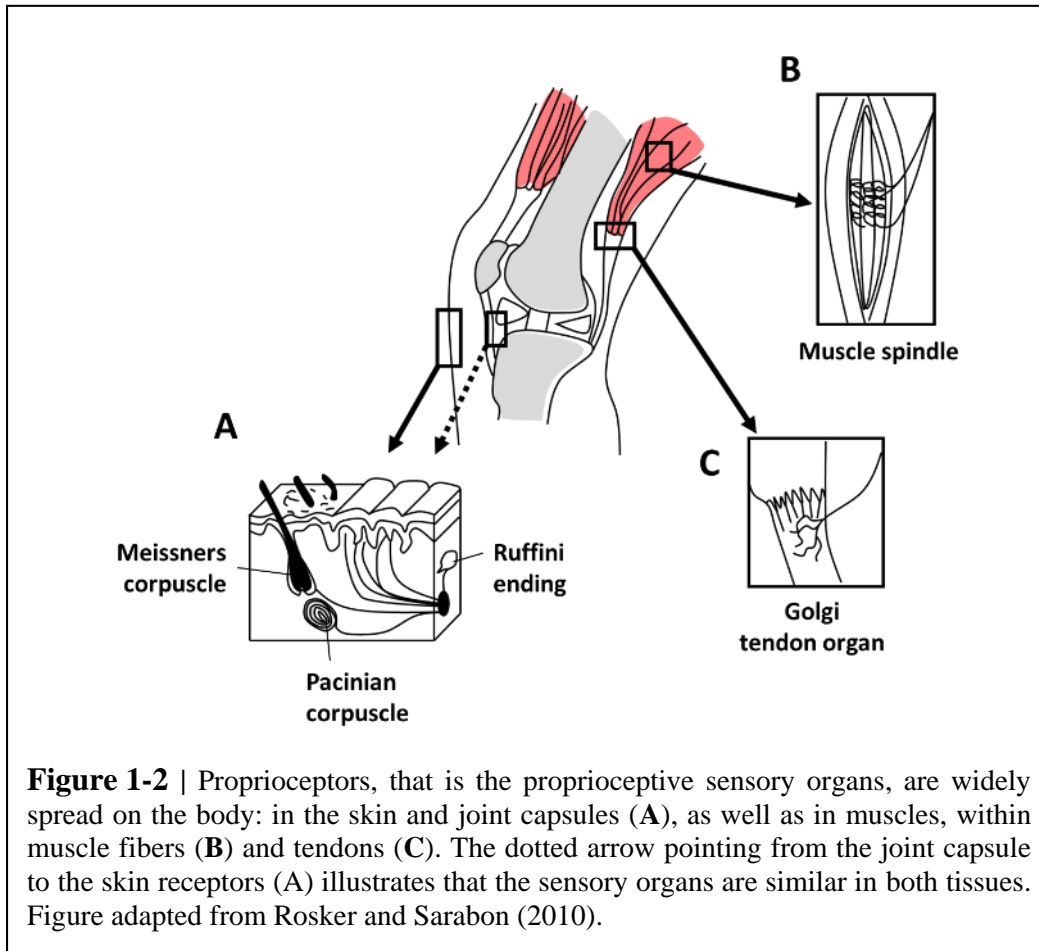
The term “proprioception” has received different definitions and conceptualizations, and thus can be confusing. Sherrington (1907) coined proprioception from Latin *prōprius* (“one’s own”) and *perception*. He stated, “In muscular receptivity we see the body itself acting as a stimulus to its own receptors—the proprioceptors.” Traditionally, proprioception refers to conscious sensations of limb position and movement (Proske and Gandevia, 2012). Also referred to as “kinesthesia” (from Ancient Greek *kinéō*, “to move” and *aísthēsis*, “sensation”), a term which has been introduced by Bastian (1887), specialists in the medical field sometimes distinct proprioception and kinesthesia, as the joint position sense only (posture) and the sense of joint motion respectively (Han et al., 2016). However, joint position and movement senses are inherent to one another. As a consequence, “proprioception” and “kinesthesia” are often used as synonymous (Han et al., 2016; Stillman, 2002).

In this thesis, I will use the term proprioception in the largest sense: including both conscious joint position and movement senses. As well, in the most literal interpretation of Sherrington (1907), I will refer to proprioceptors, not just as the receptors concerned with muscular sensitivity, but as all receptors providing the sense of joint position and movement: receptors located in muscles, in joint capsules, and in the skin (tactile receptors) (Collins, 2009; Proske and Gandevia, 2012). Therefore, the proprioceptive sense, as it is described here, may be interpreted as being similar to the haptic sense, which corresponds to the active exploration of object shape/orientation/direction that stimulates directly the proprioceptors.

#### ***The variety of proprioceptors***

Skin receptors (Meissner corpuscles, Pacinian corpuscles, Ruffini endings) provide information about skin stretch and pressure, similarly to joint capsule receptors with Ruffini-like endings, comparable to the cutaneous Ruffini endings, and Paciniform corpuscles which respond to stretching and local compression respectively (Figure 1-2A). In the muscles, muscle spindles (Figure 1-2B) and Golgi tendon organs (Figure 1-2C) provide information about muscle stretch and exerted force, respectively (Proske and Gandevia, 2012; Rosker and Sarabon, 2010). Mechanoreceptors in joint capsules and skin are most numerous in the human hand, with over

17,000 units, whereas muscle spindles and Golgi tendon organs are less represented, with about 4,000 and 2,500 units respectively for the whole arm (Johansson and Vallbo, 1979; Rosker and Sarabon, 2010).

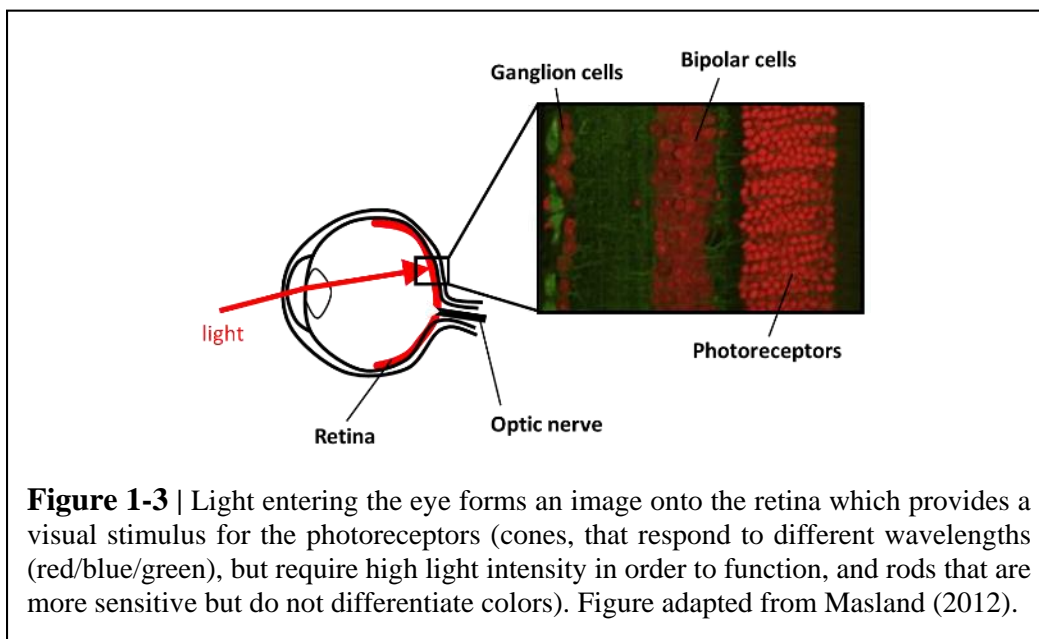


### *From the periphery to the cortex*

Somatosensory information from the skin, muscles and joint capsules is conveyed to the CNS by dorsal root ganglion neurons innervating the limbs. Through the dorsal column of the spinal cord to ventral posterior lateral and medial nuclei of the thalamus, it reaches the primary somatosensory cortex (S1) and is finally distributed within the posterior parietal cortex (PCC) where information from other sensory systems also converges (Delhaye et al., 2018) (see Figure 1-1).

### 1.1.2 Visual system

Visual perception originates in the retina, which contains light sensitive receptors: the photoreceptors (Figure 1-3). The visual information is conveyed to the occipital cortex through the optic tract, and the lateral geniculate nucleus of the thalamus (Usrey and Alitto, 2015). From the visual cortices, it is then passed to other cortical areas, among which the PPC, where convergence with proprioceptive information occurs (Huang and Sereno, 2018; Sereno and Huang, 2014) (see Figure 1-1).

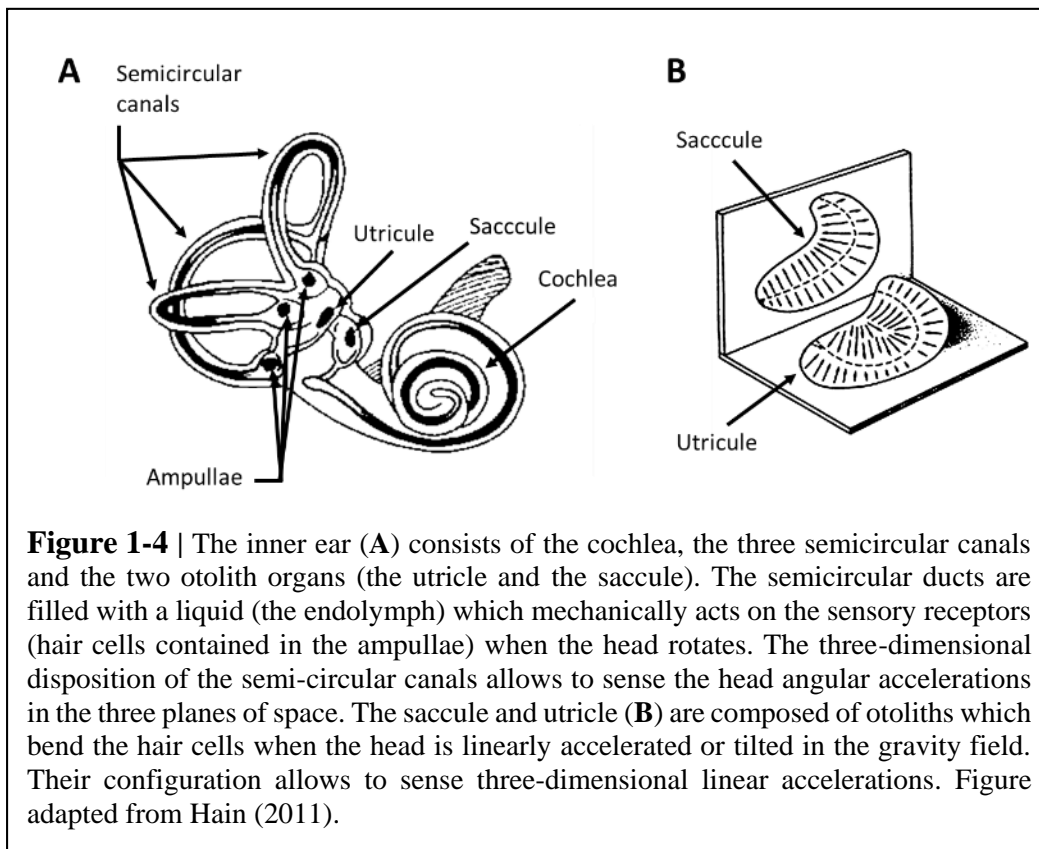


Visual information from each eye provides a two dimensional image in the primary visual cortex, and from the two (slightly different) two-dimensional images, in later visual areas, the CNS is able to create a three-dimensional representation of the environment, as well as of the body parts that are in the visual field (Finlayson et al., 2017).

### 1.1.3 Vestibular system

The vestibular system, located in the inner ear, is composed of five sensory receptors: three semi-circular canals and two otolith organs (Figure 1-4). The three semi-circular canals are

sensitive to head rotations (three-dimensional angular accelerations) in three planes, one horizontal and two vertical, which are roughly perpendicular to one another. The two otolith organs, the utricle in the horizontal plane and saccule perpendicular to the horizontal plane, detect linear accelerations in the three-dimensional directions of space, as well as the head orientation with respect to gravity (Khan and Chang, 2013). Indeed, the equivalence principle, introduced by Einstein (1907), states a “complete physical equivalence of a gravitational field and a corresponding acceleration of the reference system.” Therefore, both linear accelerations of the head and static orientations of the head relative to the gravitational field result in the same sensory signals in the otoliths.



Vestibular information is conveyed to the CNS through the vestibular nuclei, through the ventral posterior nucleus of the thalamus and finally reaches the PPC where it may be compared to proprioceptive and visual information (Khan and Chang, 2013) (Figure 1-1).

## **Introduction: Reference frames for sensory encoding**

The vestibular pathway (as well as the proprioceptive and visual pathways) described here and in Figure 1-1 is intentionally simplified (the complete networks are highly distributed in the brain, see for review: Büttner-Ennever, 1999; Cullen, 2019; Hitier et al., 2014). I chose to focus on the PPC, since it is known to be involved in reaching due to convergence of vestibular, proprioceptive and visual information.

### **1.2 Reference frames for sensory encoding**

Sensory information arises in parallel from these different sensory receptors, which encode the intensity and duration of the sensory stimuli, as well as their location and physical properties (stretch, compression, colors, ...) depending on the receptor specificities. Receptor activation is the initial step in sensory processing. Stimuli location is decrypted through the receptive fields of sensory neurons: each sensory neuron conveys information coming from a specific location (e.g. a specific area of the skin for a Meissner corpuscule, or of the visual field for a photoreceptor of the retina) which will be represented in topographic maps onto the cortex (i.e. somatotopy in the somatosensory cortex and retinotopy in the occipital cortex).

#### **1.2.1 Retinotopic and somatotopic reference frames: early stage of sensory encoding**

For vision and proprioception, the cortical areas involved in the early stages of sensory processing are unimodal: concerned only with a single modality.

Proprioceptive information is initially represented in a somatotopically organized reference frame in which sensory stimuli are referred to distinct locations on the skin, joints or muscles (McGuire and Sabes, 2009; Tamè et al., 2017, 2014). The somatotopic organization in the primary somatosensory cortex (S1) in humans has been determined with cortical electrical stimulation of patients undergoing neurosurgery: the stimulation of specific areas of S1 elicited sensation of touch or movement of specific body parts (Penfield and Boldrey, 1937). Today, cortical electrical stimulation of S1 is actively studied, both in non-human primates and humans, as a means to restore proprioceptive feedback for patients who suffer from a complete loss of somatosensation such as in spinal cord injury (Armenta Salas et al., 2018; London et al., 2008). This “native”, somatotopic,

reference frame for proprioception (in the largest sense, including tactile sensation) represents the first step of cortical encoding for the proprioceptive signals. In this thesis, I will refer to this native reference frame as “joint space” or “joint reference frame” where the sensory stimuli are expressed in joint coordinates (Figure 1-5A).

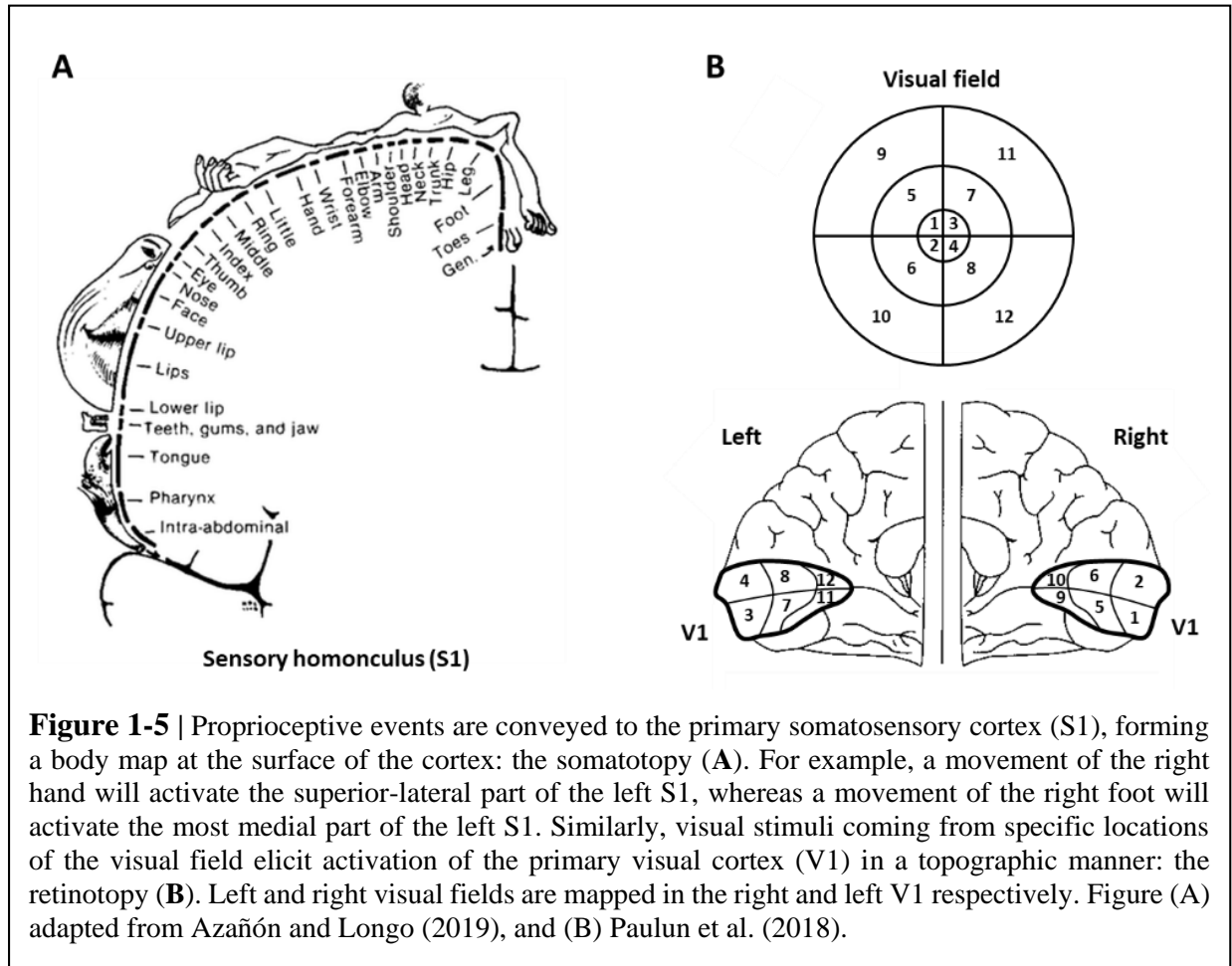


**Figure 1-5** | Proprioceptive events are conveyed to the primary somatosensory cortex (S1), forming a body map at the surface of the cortex: the somatotopy (A). For example, a movement of the right hand will activate the superior-lateral part of the left S1, whereas a movement of the right foot will activate the most medial part of the left S1. Similarly, visual stimuli coming from specific locations of the visual field elicit activation of the primary visual cortex (V1) in a topographic manner: the retinotopy (B). Left and right visual fields are mapped in the right and left V1 respectively. Figure (A) adapted from Azañón and Longo (2019), and (B) Paulun et al. (2018).

Similarly, early visual processing represents stimuli in a retinotopic organization (McGuire and Sabes, 2009): topographic maps of the visual field were drawn from the study of war wounds during World War I, which in some cases affected specifically focal regions of the occipital cortex. These studies provided the foundation of modern knowledge of visual fields (Fishman, 1997). The link between the visual fields and the topographic organization of the occipital cortex was further studied with both electrical stimulations of the occipital cortex, which was found to elicit visual perceptions at specific locations of the visual field (Brindley and Lewin, 1968), and Magnetic

Resonance Imaging (MRI) which allowed the precise identification of the retinal projection onto the cerebral cortex (Fishman, 1997). This “native”, retinotopic, reference frame for visual information will be referred to as “retinal space” or “retinal reference frame” in the following, where the visual stimuli are expressed in retinal coordinates (Figure 1-5B).

Even though these two native reference frames, “joint” and “retinal”, seem to be sufficient to perform some specific tasks (Arnoux et al., 2017; Azañón et al., 2010; Tagliabue and McIntyre, 2013), for most actions, evidence suggests that several reference frames are used in parallel in which the sensory information is encoded in other coordinates than simply “joint” or “retinal” (Arnoux et al., 2017; Azañón et al., 2010; McGuire and Sabes, 2009; Pouget et al., 2002; Tagliabue and McIntyre, 2013; Tamè et al., 2017).

### **1.2.2 Higher level sensory representations: “extra” reference frames in the posterior parietal cortex**

In further stages of sensory processing, the unimodal sensory information from proprioceptive, visual and vestibular systems converges on multimodal association areas of the cortex such as the posterior parietal cortex (PPC). From the retinal space and the joint space, sensory signals can be re-encoded in more complex and integrated reference frames which correspond to a combination of the original sensory signals with additional sensory information. Several reference frames, that can be used to represent visual and/or proprioceptive signals, have been described in the literature. Depending on the task to be performed, the sensory information can be encoded in hand-, body-, head-, eye-, world- or gravity-centered coordinates (Duhamel et al., 1997). In this thesis I will use the generic terms “extra-joint” and “extra-retinal” space to refer to the non-native reference frames for the encoding of proprioceptive and visual signals, respectively. Therefore, “extra-joint” encoding of the hand position could be: body-, head- or eye-centered, or even allocentric (world- or gravity-centered). The “extra-retinal” encoding of an object to be grasped (its position and orientation) could be: body-, head- or hand-centered, and also world- or gravity-centered.

Re-encoding sensory information from the native reference frame to “extra” reference frames is termed *sensory transformation*. This process is necessary to perform numerous tasks. For

instance, to plan the movement trajectory to reach a visual target, sensory transformations are necessary to account for eye, head and body movements that may occur between target acquisition and reaching movement and thus provide a stable representation of hand and the target position (Duhamel et al., 1997; Pouget et al., 2002; Tagliabue and McIntyre, 2011). For example, to represent a visual object with respect to the hand, the visual signals on the retina would have to follow a sequence of sensory transformations: from eye- to head centered coordinates taking into account the eye position, from head- to body-centered coordinates integrating head position signals, and finally from body- to hand-centered coordinates using hand position signals (Pouget et al., 2002) (see Figure 1-6).

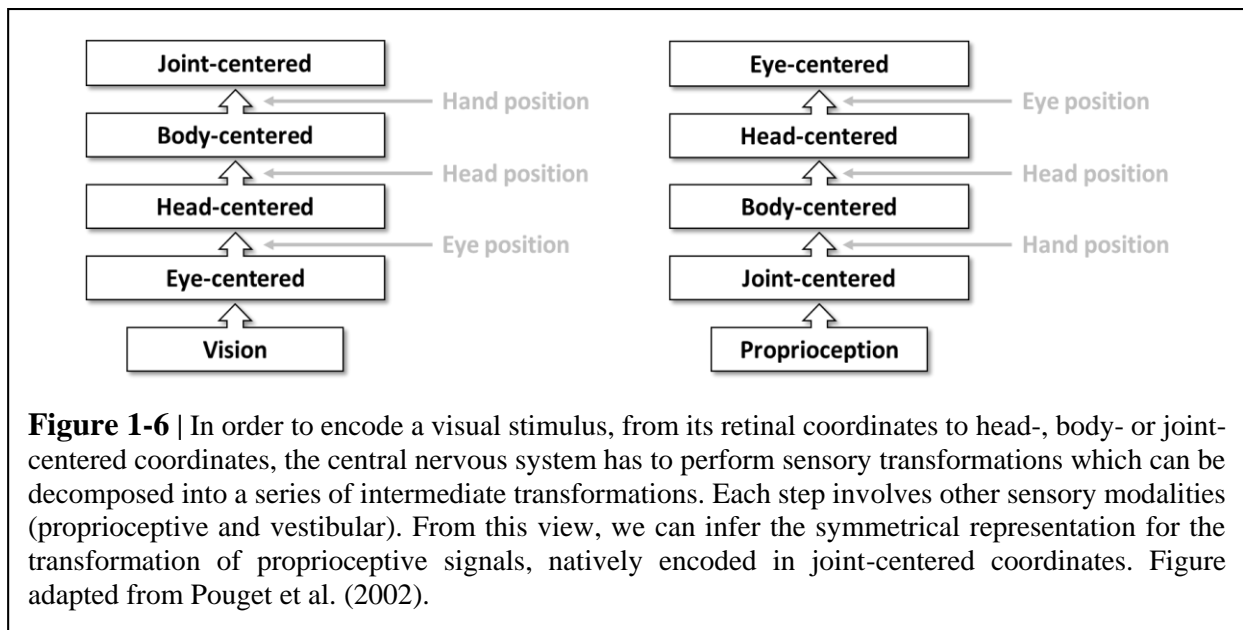


**Figure 1-6** | In order to encode a visual stimulus, from its retinal coordinates to head-, body- or joint-centered coordinates, the central nervous system has to perform sensory transformations which can be decomposed into a series of intermediate transformations. Each step involves other sensory modalities (proprioceptive and vestibular). From this view, we can infer the symmetrical representation for the transformation of proprioceptive signals, natively encoded in joint-centered coordinates. Figure adapted from Pouget et al. (2002).

It has been shown that, when reaching to a memorized visual target with the unseen hand, proprioceptive information about the hand can be encoded in retinal (eye-centered) space. Experiments (Engel et al., 2002; Jones and Henriques, 2010), involving a gaze shift after the visually memorized target had disappeared from sight, showed that the pointing errors were affected by the gaze deviation. Moreover, Jones and Henriques (2010) have shown that, even in the case of a proprioceptive target (e.g. the tip of the left thumb), in the complete absence of vision of the target (as of the reaching hand), reaching to the memorized proprioceptive target was also

affected by the gaze deviation. Their results suggest that the position of the hand can be partially encoded in retinal space, and are consistent with the overlapping neuronal receptive field for the proprioceptive and visual signals in the PPC (Huang and Sereno, 2018; Sereno and Huang, 2014).

Similarly, visual information can be encoded not only in retinal space, but also in non-retinotopic reference frames (i.e., “extra-retinal” space), such as in body-, head-, or world-centered coordinates (Chafee et al., 2007; Duhamel et al., 1997, 1992; Olson, 2003; Snyder et al., 1998; Tagliabue and McIntyre, 2011). Electrophysiological studies with neural population recordings show that different areas of the PPC encode visual stimuli in a body-, head-, or world-centered reference frame depending on whether the visual stimulus is close to some parts of the body (body-centered) or in a fixed spatial location while the eyes move (head-centered) or the head moves (world-centered) (Bottini and Doeller, 2020; Buneo and Andersen, 2012; Chen et al., 2018; Duhamel et al., 1997; Snyder et al., 1998).

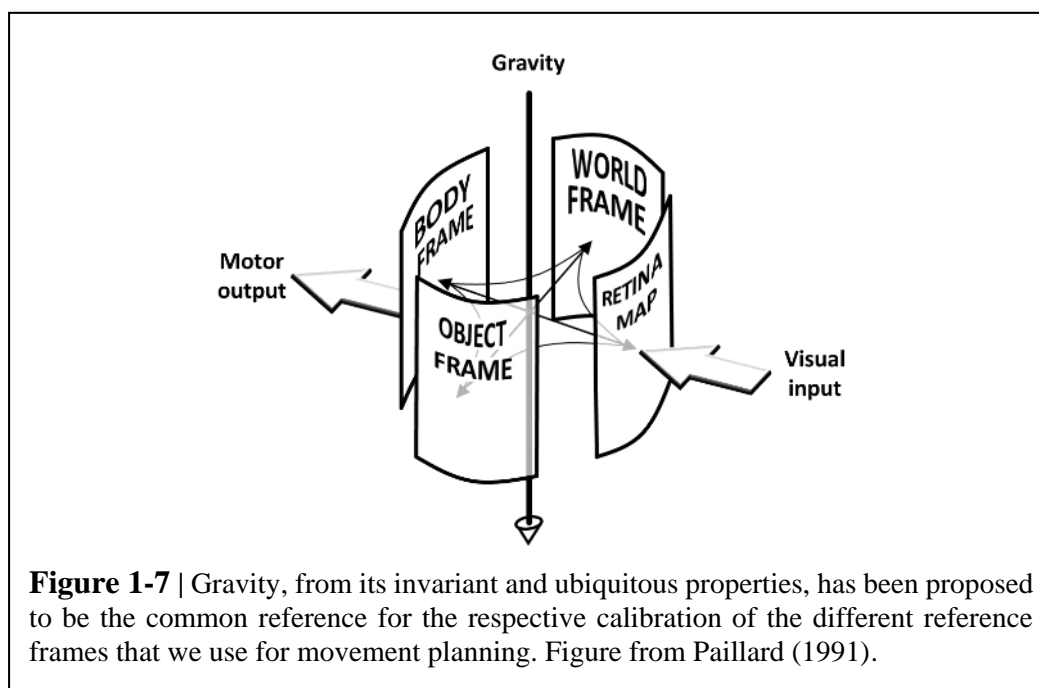
Regardless of the sensory cues available (vision and/or proprioception), the PPC seems to have multiple, concurrent, representations of the movement to perform, expressed in different coordinate systems (Buneo and Andersen, 2012). These concurrent encodings seem to exist in parallel, and can be used and combined in a flexible manner depending on the task context (Burgess, 2008; Chen et al., 2018; Tamè et al., 2017).

### **1.2.3 The contribution of gravity for sensory encoding**

Another solution to encode sensory signals in a stable representation regardless of head/body movements is to use a gravito-centered reference frame. In different regions of the PPC, Rosenberg and Angelaki (2014) showed that some neurons encode the orientation of an object (visually perceived) to be reached in gravito-centered coordinates. Psychophysics experiments seem to support this result. In their study, Niehof et al. (2017) asked subjects to memorize visual line orientation during head movements (lateral tilts with respect to the vertical) in the absence of external visual landmarks. They showed that the brain relies primarily on a gravito-centered reference for the memorized visual orientation in the frontal plane. In other studies, when subjects performed arm movements either following visual line orientations or pointing to visual targets,

movement pattern errors suggest gravity can be used as a reference for the combination of visual and proprioceptive information (Darling et al., 2008b; Scotto Di Cesare et al., 2014).

It has been hypothesized that gravity might play a fundamental role in the reciprocal calibration between visual and proprioceptive senses, since it can be both seen (the pull of gravity on surrounding objects, together with the horizontal plane, defines a three-dimensional Cartesian frame for visual images) and felt (mechano-receptors detect gravity action on our body, and the otolith organs provide complementary information) (Lacquaniti et al., 2015). Paillard (1991) first mentioned the role of gravity for sensorimotor control. He proposed that the ubiquitous and invariant vertical orientation of gravity is a crucial factor for linking together the different reference frames that are needed for perception and action (see Figure 1-7).



Recent studies support Paillard's intuition (Bernard-Espina et al., 2022; Darling et al., 2008b; Niehof et al., 2017; Scotto Di Cesare et al., 2014; Tagliabue et al., 2013; Tarnutzer et al., 2012, 2010): when the head or body is not aligned with the gravitational vertical, errors of reaching movements increase, which reflects the increased difficulty to perform the necessary sensory transformations.

### 1.3 Multisensory integration

The concept of multisensory integration was proposed by Aristotle to explain how the different senses provide together a unified perception of our environment. The *sensus communis*, the combination of all senses, was understood to be seated in the heart. It is in the 17<sup>th</sup> century, by the time of Descartes, that this faculty was thought to be located in the brain (Figure 1-8).

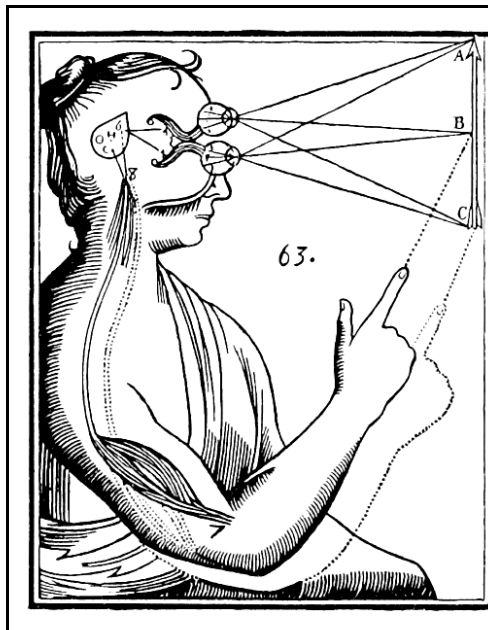


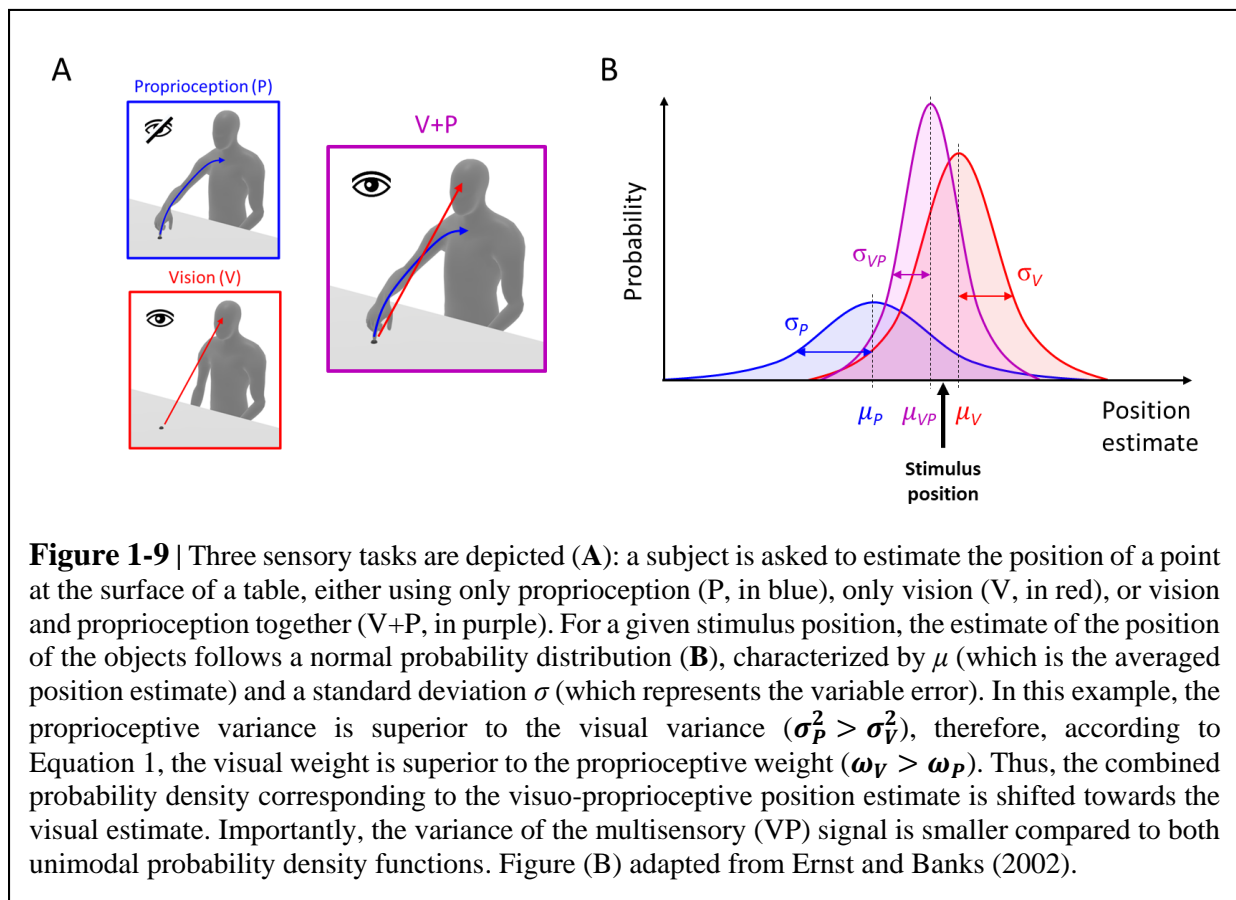
**Figure 1-8** | Illustration of multisensory perception by René Descartes in *Treatise on Man* (French: *L'Homme*, published 1664, posthumously). Sensory, i.e. visual and proprioceptive, signals travel via their respective nerves to the *Sensus Communis*, located in the pineal gland and considered the center of multisensory integration (as well as of cognition). Note: the subject looks at the object 'A-C' and simultaneously points with the arm at its center 'B' so that visual and proprioceptive spatial information coincide.

In modern neuroscience, multisensory integration refers to the combination of two, or more, sensory modalities. It can be understood as a way to reduce perceptual bias and errors by multiplying the amount of sensory information available to the CNS. The resulting multimodal and unified perception is more precise and accurate compared to each one of the unimodal perceptions taken individually (Ernst and Banks, 2002; Ghahramani et al., 1997; O'Reilly et al., 2012; Tagliabue and McIntyre, 2014).

#### 1.3.1 Statistical optimality in multisensory integration

When trying to estimate the position of an object in space, perceived with a single sensory modality (e.g. visual or proprioceptive) (see Figure 1-9A), our estimates are characterized by a

statistical distribution with a mean position estimate  $\mu$  (which is the most likely estimate of the object position based on the unimodal sensory perception) and a variance  $\sigma^2$  representing the sensory system variability due to various sources of noise in the nervous system (Faisal et al., 2008) (Figure 1-9B). Several studies have shown that when combining both visual ( $E_V$ ) and proprioceptive ( $E_P$ ) estimates, the redundant visual and proprioceptive sensory information are optimally combined and weighted according to the Maximum Likelihood Principle (MLP) in order to statistically minimize the variability of the visuo-proprioceptive estimate  $E_{VP}$  (van Beers et al., 1996; Ernst and Banks, 2002):  $E_{VP} = \omega_V \times E_V + \omega_P \times E_P$ , where  $\omega_V$  and  $\omega_P$  are the optimal sensory weights corresponding to the minimal variance of  $E_{VP}$  ( $\sigma_{VP}^2$ ).



The optimal values of the sensory weights are reported in Equation 1 and depend on the relative variance of the visual and proprioceptive sensory signals. The more variable is

## **Introduction: Multisensory integration**

proprioception compared to vision, the more sensory weight will be given to vision (and less to proprioception), and vice versa:

$$\begin{aligned}\omega_V &= \frac{\sigma_P^2}{\sigma_P^2 + \sigma_V^2} \\ \omega_P &= \frac{\sigma_V^2}{\sigma_P^2 + \sigma_V^2}\end{aligned}\tag{Equation 1}$$

with:  $\omega_V + \omega_P = 1$

As a consequence of sensory weighting the visuo-proprioceptive position estimate  $E_{VP}$ , and hence its mean  $\mu_{VP}$  will be biased toward one of the unimodal position estimates (visual,  $E_V$ , or proprioceptive alone,  $E_P$ ) (see Figure 1-9B).

The MLP also predicts that the variance of  $E_{VP}$  ( $\sigma_{VP}^2$ ) is lower than both of  $E_V$  and  $E_P$  variances ( $\sigma_V^2$  and  $\sigma_P^2$  respectively) (Equation 2).

$$\sigma_{VP}^2 = \frac{\sigma_V^2 \sigma_P^2}{\sigma_P^2 + \sigma_V^2}\tag{Equation 2}$$

This is reflected in Figure 1-9 by the probability distribution of  $E_{VP}$  which is “thinner” compared to  $E_V$  and  $E_P$  ( $\sigma_{VP}^2 < \sigma_V^2$  and  $\sigma_{VP}^2 < \sigma_P^2$ ).

### **1.3.2 Optimal multi-sensory integration for hand control**

Applying this concept to arm (reaching) movements adds additional complexity to the sensory processing as compared to simple perceptual tasks: when reaching an object, to match the position and orientation of the object with that of the hand, the latter must be displaced from its initial position by a distance and in a direction that are represented by the movement vector  $\Delta$ . The movement vector  $\Delta$  can be computed by subtracting the estimated position of the hand from the estimated target position. A direct interpretation of the above mentioned literature on position estimation would suggest that the CNS constructs two representations: a single representation of the target, and another of the hand, using all sensory modalities available (van Beers et al., 1996; Ernst and Banks, 2002). The optimal target and hand estimates (according to the MLP) would then be subtracted to compute the optimal movement vector  $\Delta$ . However, it was shown that this

approach fails to describe some experimental observations (McGuire and Sabes, 2011, 2009; Tagliabue et al., 2013; Tagliabue and McIntyre, 2013, 2012, 2011, 2008).

An alternative approach, called “Concurrent Model” (Tagliabue and McIntyre, 2014), postulates that visual and proprioceptive sensory information about the target and the hand (response) are first encoded and compared in the reference frame of the respective receptors: retinal and joint reference for vision and proprioception, respectively. From the unimodal hand-response estimates, it is then possible to compute intermediate movement vectors in each reference frame ( $\Delta V$  and  $\Delta P$  for the visual and proprioceptive space respectively, shown in Equation 3):

$$\begin{aligned}\Delta V &= E_{T,V} - E_{R,V} \\ \Delta P &= E_{T,P} - E_{R,P}\end{aligned}\tag{Equation 3}$$

where T and R subscripts indicate an information about the target and the response respectively, so  $E_{T,V}$  and  $E_{R,V}$  are the visual estimates, and  $E_{T,P}$  and  $E_{R,P}$  the proprioceptive estimates for the target and response positions. For each sensory modality, the comparison ( $\Delta V$  and  $\Delta P$ ) is characterized by a variance corresponding to the sum of the variances of the target and response estimations (Equation 4):

$$\begin{aligned}\sigma_{\Delta V}^2 &= \sigma_{T,V}^2 + \sigma_{R,V}^2 \\ \sigma_{\Delta P}^2 &= \sigma_{T,P}^2 + \sigma_{R,P}^2\end{aligned}\tag{Equation 4}$$

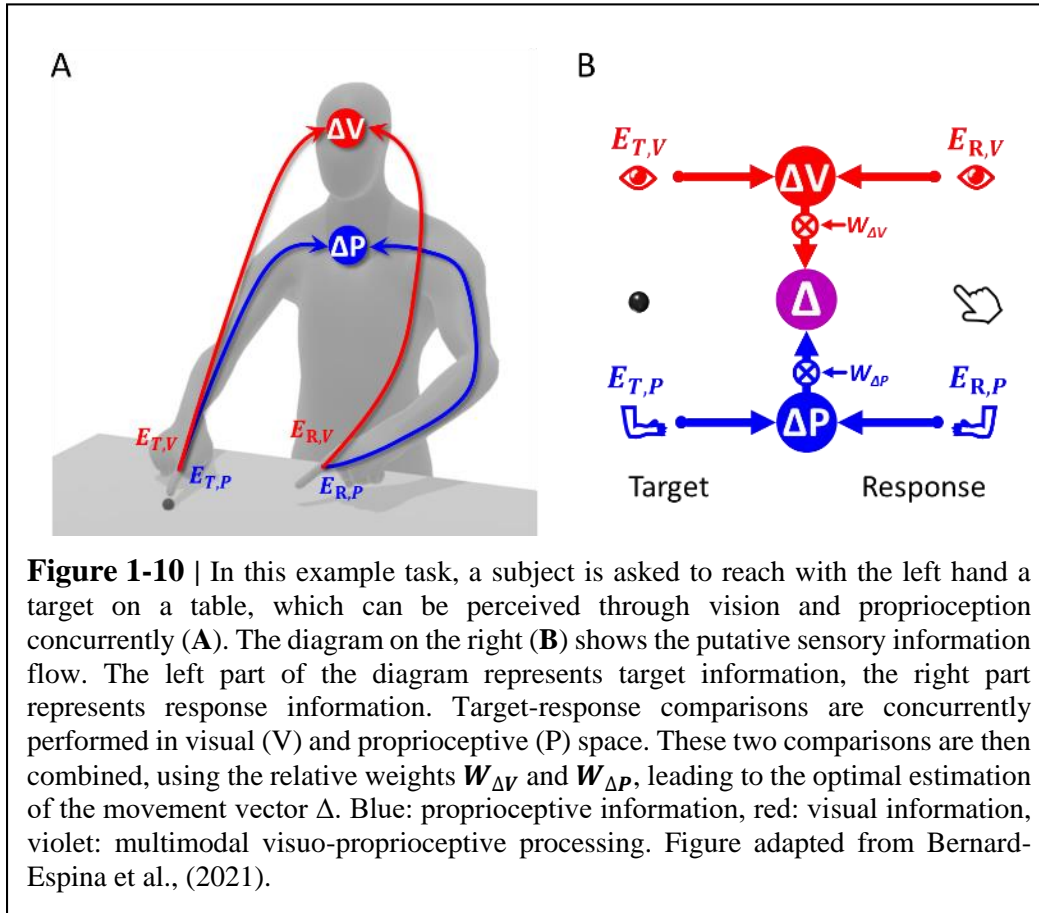
Figure 1-10 shows how sensory signals are conceptually processed in a visuo-proprioceptive reaching task according to the Concurrent Model.

The MLP predicts that in order to maximize the precision of the estimated movement vector  $\Delta$ , the concurrent visual and proprioceptive comparisons must be combined, as in Equation 5.

$$\begin{aligned}\Delta &= \omega_{\Delta V} \cdot \Delta V + \omega_{\Delta P} \cdot \Delta P \\ \omega_{\Delta V} &= \frac{\sigma_{\Delta P}^2}{\sigma_{\Delta V}^2 + \sigma_{\Delta P}^2} \\ \omega_{\Delta P} &= \frac{\sigma_{\Delta V}^2}{\sigma_{\Delta V}^2 + \sigma_{\Delta P}^2}\end{aligned}\tag{Equation 5}$$

## Introduction: Multisensory integration

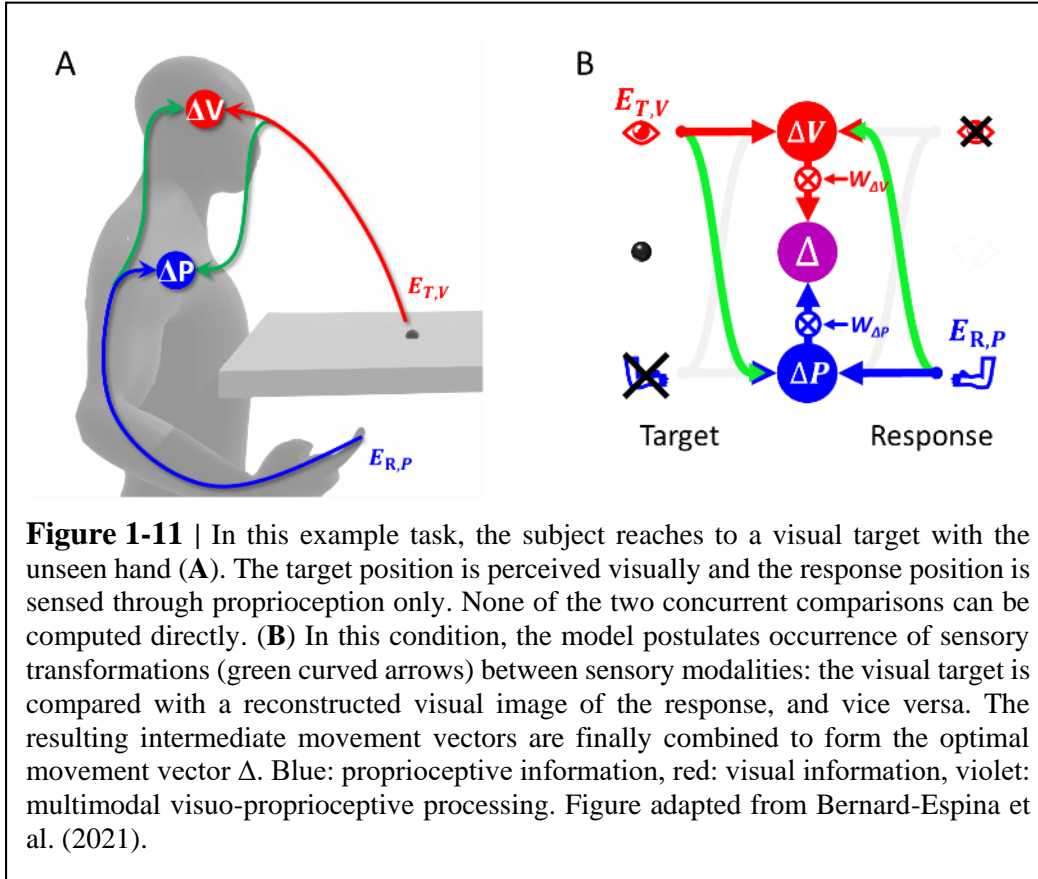
Thus, the movement vector is the weighted sum of the concurrent target-response comparisons, and each comparison is associated to a weight,  $\omega_{\Delta V}$  and  $\omega_{\Delta P}$ , whose value depends on the relative variance of the two comparisons.



### 1.3.3 Accounting for sensory transformations

A fundamental characteristic of the Concurrent Model is to explicitly account for the ability to perform sensory transformations. In the case where some sensory information is not available, e.g. when the target position can be perceived only visually while the response position only through proprioception (Figure 1-11), none of the two concurrent comparisons can be computed directly because the target and the response position are acquired through different sensory systems and hence they are not encoded in the same reference frame. However, these comparisons can be performed through two mutually nonexclusive possibilities: first, the visually perceived position

of the target may be encoded in a proprioceptive space; second, the response position, provided through proprioception, may be encoded in visual space.



It has been experimentally shown that sensory transformations intrinsically add noise to the sensory processing (Burns and Blohm, 2010; Tagliabue et al., 2013). To represent this phenomenon, the sensory transformations from proprioception to vision, and from vision to proprioception are characterized by a specific variance,  $\sigma_{P \rightarrow V}^2$  and  $\sigma_{V \rightarrow P}^2$ . The variability associated with the two concurrent visuo-proprioceptive comparisons is given in Equation 6. The indentation is used to facilitate the distinction between the variance associated with the target and response encoding (the same type of indentation will be used throughout the manuscript).

|                         | Target  | Response  |            |
|-------------------------|---|---|------------|
| $\sigma_{\Delta V}^2 =$ | $\sigma_{T,P}^2$                              | $+ \sigma_{R,P}^2 + \sigma_{P \rightarrow V}^2$ | Equation 6 |
| $\sigma_{\Delta P}^2 =$ | $\sigma_{T,V}^2 + \sigma_{V \rightarrow P}^2$ | $+ \sigma_{R,P}^2$                              |            |

## Introduction: Multisensory integration

In contrast to the task represented in Figure 1-10 and Equation 5, in this condition the two concurrent comparisons are not fully independent, because they are partially computed from the same information  $E_{T,V}$  and  $E_{R,P}$  (Figure 1-11B). In this case, Equation 5 must be modified to take into account the covariance between proprioceptive and visual target-response comparisons,  $cov(\Delta P, \Delta V)$ :

$$\begin{aligned} w_{\Delta V} &= \frac{\sigma_{\Delta P}^2 - cov(\Delta P, \Delta V)}{\sigma_{\Delta V}^2 + \sigma_{\Delta P}^2 - 2 \cdot cov(\Delta P, \Delta V)} \\ w_{\Delta P} &= \frac{\sigma_{\Delta V}^2 - cov(\Delta P, \Delta V)}{\sigma_{\Delta V}^2 + \sigma_{\Delta P}^2 - 2 \cdot cov(\Delta P, \Delta V)} \end{aligned} \quad \text{Equation 7}$$

For the example of Figure 1-11,  $cov(\Delta P, \Delta V) = \sigma_{T,V}^2 + \sigma_{R,P}^2$ , that is the common variance component between  $\sigma_{\Delta P}^2$  and  $\sigma_{\Delta V}^2$ . Therefore, Equation 7 becomes:

$$\begin{aligned} w_{\Delta V} &= \frac{\sigma_{V \rightarrow P}^2}{\sigma_{V \rightarrow P}^2 + \sigma_{P \rightarrow V}^2} \\ w_{\Delta P} &= \frac{\sigma_{P \rightarrow V}^2}{\sigma_{V \rightarrow P}^2 + \sigma_{P \rightarrow V}^2} \end{aligned} \quad \text{Equation 8}$$

It follows that the relative weights between the two concurrent target-response comparisons depend on the noisiness of the two sensory transformations, which is consistent with experimental observations (Burns and Blohm, 2010; Tagliabue et al., 2013).

If it is straightforward that sensory transformations must be used when a direct target-response comparison is not possible (example task of Figure 1-11A). In purely proprioceptive tasks, however, where both target and response are sensed through proprioception (see Figure 1-12A for an example), the assumption is that target-response comparison would take place in the joint space (Figure 1-12A).

In this condition the variability associated with the two concurrent comparisons is given in Equation 9:

$$\begin{aligned} \sigma_{\Delta V}^2 &= \sigma_{T,P}^2 + \sigma_{P \rightarrow V}^2 + \sigma_{R,P}^2 + \sigma_{P \rightarrow V}^2 \\ \sigma_{\Delta P}^2 &= \sigma_{T,P}^2 + \sigma_{R,P}^2 \end{aligned} \quad \text{Equation 9}$$

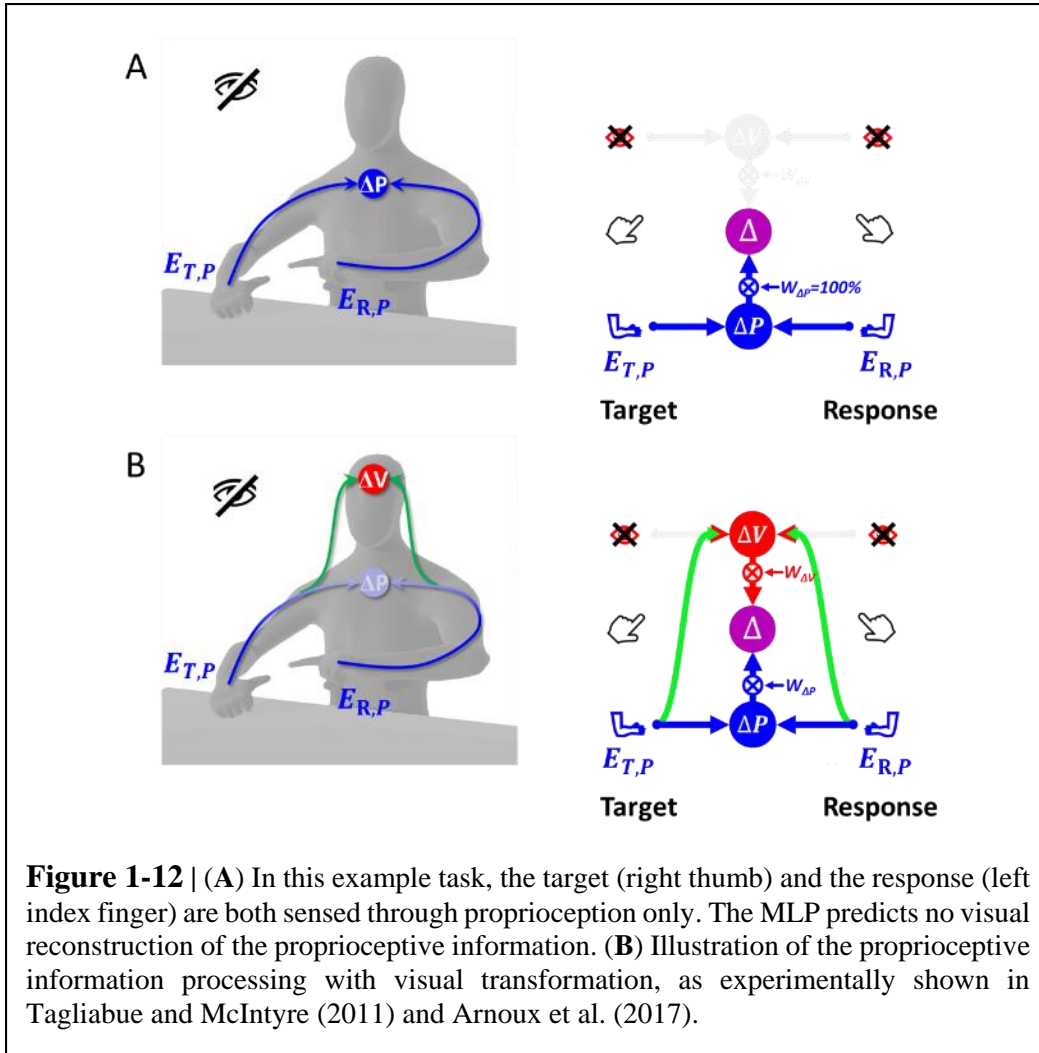


**Figure 1-12** | (A) In this example task, the target (right thumb) and the response (left index finger) are both sensed through proprioception only. The MLP predicts no visual reconstruction of the proprioceptive information. (B) Illustration of the proprioceptive information processing with visual transformation, as experimentally shown in Tagliabue and McIntyre (2011) and Arnoux et al. (2017).

In this condition, the target-response comparison in the visual space ( $\sigma_{\Delta V}^2$ ) fully covaries with the target-response comparison in the proprioceptive space ( $\sigma_{\Delta P}^2$ ). When replacing the terms of Equation 9 in Equation 7, we obtain the optimal weight of Equation 10, meaning that, as represented in Figure 1-12A, the MLP predicts no advantage of using the reconstructed visual representations of the task, because it does not add any information.

$$\begin{aligned} w_{\Delta V} &= 0 \\ w_{\Delta P} &= 1 \end{aligned} \quad \text{Equation 10}$$

There is evidence, however, that sensory transformations are performed even when it does not appear strictly necessary: that is even when the object and the hand can be both seen, or both

sensed through proprioception, before movement onset (Sarlegna et al., 2009; Sarlegna and Sainburg, 2009, 2007; Sober and Sabes, 2005) and during movement execution (Arnoux et al., 2017; Cluff et al., 2015; Crevecoeur et al., 2016; Tagliabue and McIntyre, 2014, 2013, 2011). In particular, in a similar task as the one presented in Figure 1-12A, Arnoux et al. (2017) and Tagliabue and McIntyre (2013) provided evidence that the proprioceptive signals are partially encoded in the visual space (Figure 1-12B). Therefore, the variance of the movement vector  $\Delta$  becomes a function of the variance of both proprioceptive signals  $\sigma_p^2$  and sensory transformations  $\sigma_{p \rightarrow v}^2$ .

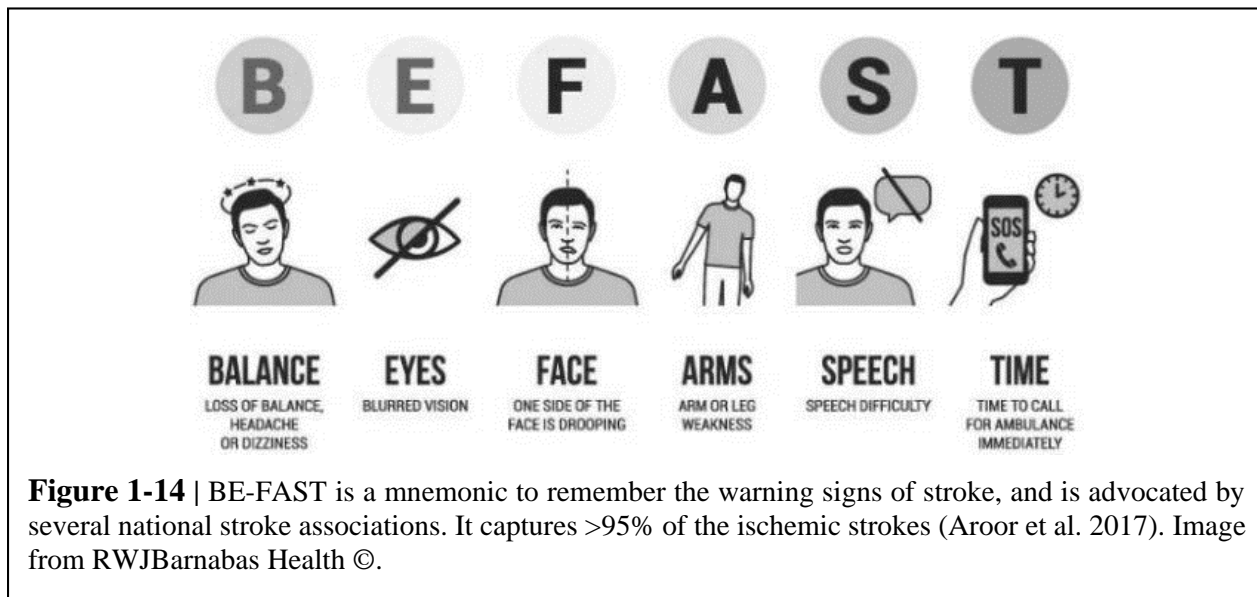
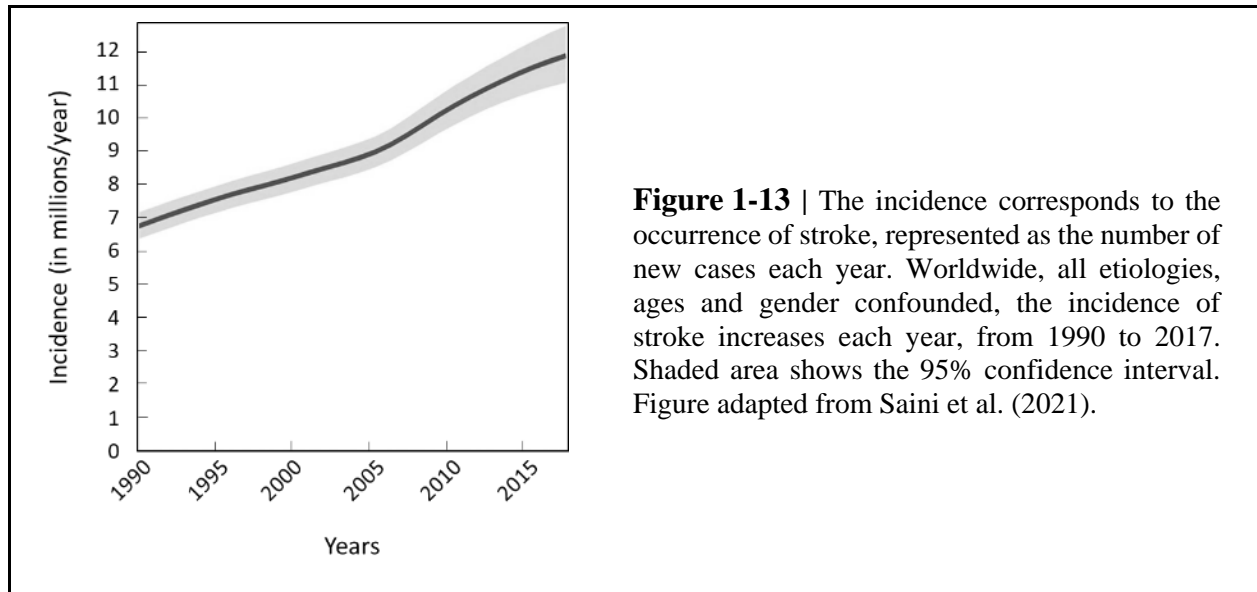
Interestingly, among the variety of proprioceptive assessment tasks that are used in post-stroke rehabilitation, some are similar to the tasks presented in Figure 1-11 and Figure 1-12. This suggests that the clinical assessment of proprioceptive function post-stroke, as it is practiced today, may confound proprioception and sensory transformations.

## **1.4 Proprioceptive deficits and visual compensation in stroke**

### **1.4.1 Definition and epidemiology of stroke**

The World Health Organization defined stroke as “rapidly developed clinical signs of focal (or global) disturbance of cerebral function, lasting more than 24 hours or leading to death, with no apparent cause other than of vascular origin” (Donkor, 2018). It was first described by Hippocrates (500 BC), and named after the ancient Greek word *apoplexia* which literally means “struck down”. Nowadays, although the term apoplexia has been replaced by stroke, the sudden onset of symptoms, often fatal, reminds us of the primary definition. As a matter of fact, stroke is the second leading cause of both disability and death worldwide (Saini et al., 2021), and its incidence continues to grow (Figure 1-13).

The most common clinical signs are balance disorders, weakness in the arm, leg or one side of the face, trouble speaking and trouble seeing (Figure 1-14). These first symptoms generally appear a few seconds or minutes after stroke onset, and are the cerebral signs of a vascular dysfunction: the interruption of blood flow (or insufficient blood flow) in the brain, resulting in oxygen and glucose deprivation, rapidly causes cellular death which is irreversible.



Brain ischemia is responsible for 87% of strokes, and is caused by the presence of a thrombus (blood clot) or embolus blocking an artery or a blood vessel irrigating the brain. Intracranial hemorrhage, which is bleeding within the brain, is the second cause of strokes (13%). It can occur after the rupture of an artery or a blood vessel, most frequently caused by trauma, hypertension, and cerebral aneurism (localized weakening and dilation of a blood vessel) (Go et al., 2014).

Even though rapid medical care efficiently reduces the long term functional deficits, stroke remains a serious condition from which patients rarely fully recover: among patients who received thrombolysis (which consists in injecting medication to provoke the lysis of the blood clot after an ischemic stroke), more than 35% of patients still present functional deficits which negatively impact activities of daily living (ADL) one year after (Alawieh et al., 2018). Motor weakness (hemiparesis), asymmetrical muscular tone (spasticity), sensory loss (hemiparesthesia), as well as deficits of executive function, affecting working memory, spatial attention and action planning, play an important role in the functional performance and autonomy in ADL (Tasseel-Ponche et al., 2015; Vallar, 1997).

Rehabilitation, as well as functional compensatory strategies, are the main approaches for improving post-stroke function. But evidence based practice, especially for somatosensory deficits, is weak and it remains a major challenge (Stinear et al., 2020). In the following, I will focus on proprioceptive deficits, and visual compensation mechanisms.

### **1.4.2 Upper limb proprioceptive deficits post-stroke**

Proprioceptive deficits can be observed in a large percentage, up to 60%, of individuals following stroke (Connell et al., 2008; Kessner et al., 2016). These impairments are clearly correlated with functional deficits (Meyer et al., 2016, 2014; Rand, 2018; Scalha et al., 2011). In particular, reaching (Zackowski, 2004), manual dexterity (Carlsson et al., 2019) and inter-limb coordination (Torre et al., 2013) appear to be negatively affected by proprioceptive deficits. Moreover, sensory recovery is a predictive factor for functional recovery (Turville et al., 2017; Zandvliet et al., 2020).

Yet, the assessment of proprioceptive function is often overlooked, and no consensus seems to have emerged regarding proprioceptive assessment methods (Pumpa et al., 2015; Saeys et al., 2012; Santisteban et al., 2016; Simo et al., 2014). For the assessment of upper-limb function, no less than 48 different clinically validated (standardized) measures are used in clinical practice and research (Santisteban et al., 2016). A high discrepancy between studies was found, as only 15 of the 48 outcome measures are used in more than 5% of the studies. In particular, only few studies specifically assess proprioceptive function: The Nottingham Sensory Assessment, one of the most

commonly used standardized scales, and gold standard for proprioceptive function, was applied in only 0.6% of studies reviewed by Santisteban et al. (2016). Moreover, current clinical practice does not systematically use standardized scales (Matsuda et al., 2019; Pumpa et al., 2015; Saeys et al., 2012; Santisteban et al., 2016; Simo et al., 2014). This lack of consensus is a major shortcoming for meta-analysis of recovery of upper limb function after stroke (Findlater and Dukelow, 2017).

### **1.4.3 Proprioceptive tests in the clinical practice**

All existing proprioceptive assessment methods are relevant from a functional point of view, but their differences pose a challenge for their comparability. The commonly used tests, both in clinical practice (Pumpa et al., 2015) and in clinical research are described in Table 1-1.

**Table 1-1** | Description of the most commonly used methods for the assessment of proprioceptive function post-stroke.

---

#### **Thumb Localization Test (TLT)**



Assesses the ability of a subject to localize a body part (thumb). The physiotherapist positions the affected arm of the patient who then has to point, without vision, to the affected thumb with the other, less-affected hand (*Dukelow et al., 2012; Meyer et al., 2016; Otaka et al., 2020; Rand, 2018*).

*Image from Otaka et al. (2020).*

#### **Up or Down Test (UDT)**



Assesses the ability of a subject to detect the direction of joint rotation. The physiotherapist moves a single joint of the patient whose vision is occluded (interphalangeal joint for example). The subject is then asked to report the up or down movement direction. This test is part of the Fugl-Meyer Assessment for the Upper Extremity and the Rivermead Assessment of Somatosensory Performance (*Birchenall et al., 2019; Carlsson et al., 2019; Frenkel-Toledo et al., 2019; Kessner et al., 2019; Pennati et al., 2020; Rand, 2018; Saeys et al., 2012; Scalha et al., 2011; Simo et al., 2014; Zandvliet et al., 2020*).

*Image from Medistudents ©.*

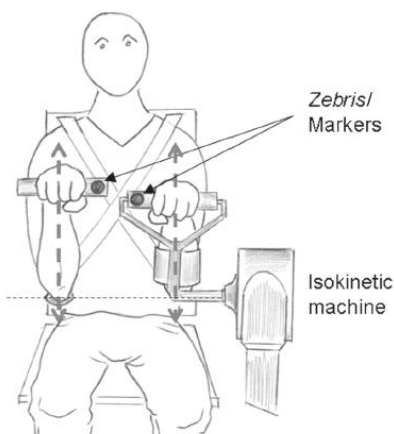
**Table 1-1 (continued)**

**Mirror Position Test (MPT)**



Assesses the ability of a subject to perceive the angular configuration of a particular joint (abduction of the shoulder for example). The physiotherapist positions a joint of the patient's affected arm in the absence of vision. The patient is then asked to mirror the position with the other, less-affected arm. This task can also be performed using a robotic device. This test is part of the Nottingham Sensory Assessment (*Ben-Shabat et al., 2015; Connell et al., 2008; Dukelow et al., 2010; Findlater et al., 2018; Gurari et al., 2017; Herter et al., 2019; Iandolo et al., 2014; Meyer et al., 2016; Rinderknecht et al., 2018; Sallés et al., 2017; Scalha et al., 2011; Semrau et al., 2018; Zandvliet et al., 2020*). *Image from Gurari et al. (2017).*

**Bimanual Sagittal Matching Test (BSMT)**



Assesses the ability of the patients to reproduce with their unaffected hand the trajectory/position of the affected hand which is passively driven by a robotic device along the sagittal plane (*Torre et al., 2013*).

*Image from Torre et al. (2013).*

**Within-arm Position Test (WPT)**

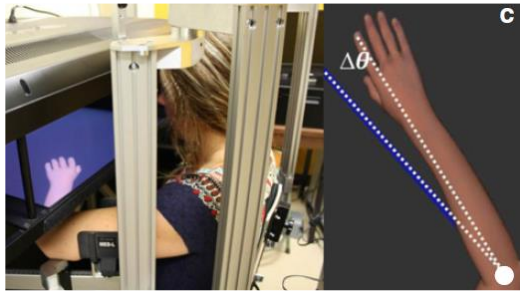


Assesses the ability of a subject to perceive and reproduce without vision the angular configuration of one joint (flexion of the elbow for example). A robot passively moves the arm of the patient to a position to be memorized and then back to the initial configuration. Subsequently, the subject is asked to move the arm actively to the remembered position, or the arm is passively moved and the subject is asked to indicate when the memorized position has been reached (*Contu et al., 2017; Gurari et al., 2017; dos Santos et al., 2015*).

*Image from Gurari et al. (2017).*

Table 1-1 (continued)

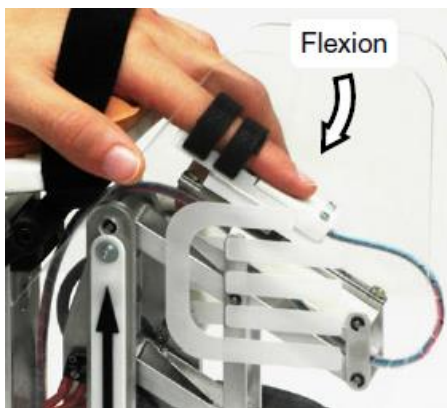
### Matching to a Visual Image (MV)



Assesses the ability of a subject to localize in space his/her unseen arm or hand relative to a visual reference. A visual image, that could be a lever or a virtual hand with a given orientation, is shown to the subject. The subject is then asked, without visual feedback, to reproduce the same orientation with his/her hand. The vision of the hand can be occluded by a box covering the hand, or by wearing a virtual reality headset that does not render the subject's hand (*Deblock-Bellamy et al., 2018; Turville et al., 2017*).

*Image from Turville et al. (2017).*

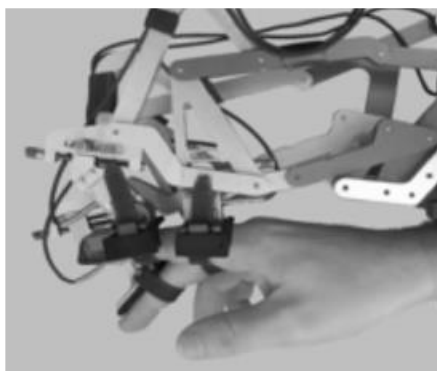
### Threshold Detection Test (TDT)



Assesses the patient's ability to detect hand displacements of various magnitudes. Using a robotic device, a joint (elbow, wrist, metacarpophalangeal) is first moved from a starting to a reference position. Then, a second movement from the starting position in the same direction, but not with the same amplitude, is operated by the robot. The subject is asked to assess whether the second movement was larger or smaller than first one. The threshold detection value is measured (*De Santis et al., 2015; Ingemanson et al., 2019; Rinderknecht et al., 2018; Simo et al., 2014*).

*Image from Rinderknecht et al. (2018).*

### Finger Proprioception Test (FPT)



Assesses the patient's ability to detect whether the index finger is aligned (in flexion/extension) with the middle finger. The two fingers are passively moved by a robotic device in a crossing flexion/extension movement. For each finger-crossing movement, the patient is asked to report when the two fingers are directly aligned relative to each other (*Ingemanson et al., 2019*).

*Image from Ingemanson et al. (2019).*

**Table 1-1 (continued)**

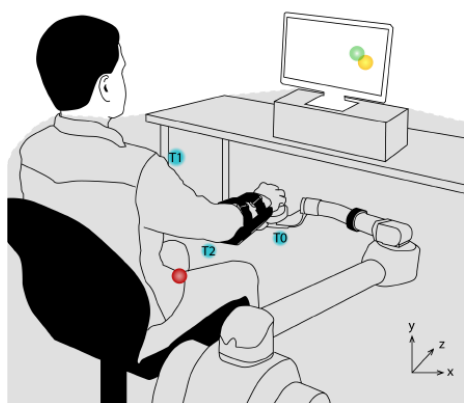
**Motor Sequences Test (MS)**



Assesses the patient’s ability to localize a body part (fingers). The subject is asked to touch with the thumb pad (I) the other finger pads (II, III, IV, V) with eyes closed. Motor sequences with alternating movements between the thumb and the other fingers are used: for example, touching with I the other fingers in the following order: II, III, IV, V and then V, IV, III, II (Scalha et al., 2011).

*Image from Scalha et al. (2011).*

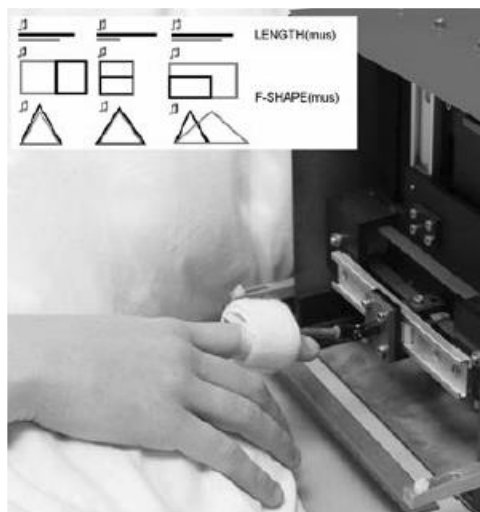
**Reaching Test (RT)**



Assesses the patient’s ability to localize in space his/her unseen arm relative to a visual reference. A visual target (real or on a screen) is shown and the subject asked to reach to the memorized target, without visual feedback of the reaching hand (Elangovan et al., 2019; Scalha et al., 2011; Valdes et al., 2019).

*Image from Valdes et al. (2019).*

**Shape or Length Discrimination (SLD)**



Assesses the patient’s ability to discriminate object shapes and dimensions without vision. Different objects of familiar geometric shapes, everyday objects or segments of different lengths are presented to the patient whose vision is occluded. Either with passive movements (operated by a robotic device or a physiotherapist) or active movements, the patient interacts with the different objects. The subject is asked to report the perceived shape, object or length (Carlsson et al., 2019; de Diego et al., 2013; Matsuda et al., 2019; Metzger et al., 2014; Sallés et al., 2017; Turville et al., 2017; Van de Winckel et al., 2012).

*Image from Van de Winckel et al. (2012).*

### **1.4.4 Different proprioceptive assessments, different outcomes**

Although each one of the tests described in Table 1-1 involves proprioception, they are clearly different. For instance, some tests involve one articular chain only (Up or Down Test, Threshold Detection Test, Within-arm Position Test), whereas others involve two distinct articular chains (two arms for Mirror Position Test and Thumb Localization Test, or two fingers for Finger Proprioception Test and Motor Sequences Test). When two articular chains are involved, the patient is either asked to mirror the joint configuration (Mirror Position Test, Finger Proprioception Test), or to point to a body part (e.g. thumb of the affected arm: Thumb Localization Test and Motor Sequences Test). It is noteworthy that some other tests do not rely on proprioceptive inputs only, but use visually remembered references (Matching to a Visual Image, Reaching Test, Shape or Length Discrimination).

Experimental observations suggest that these methodological differences can lead to different diagnostics (Dukelow et al., 2012; Gurari et al., 2017; Hirayama et al., 1999; Ingemanson et al., 2019): one and the same patient can perform differently depending on specific proprioceptive assessments, leading to strongly assessment-dependent diagnostics. In the following paragraphs, I highlight some of the similarities and differences between these proprioceptive assessment tasks, with a comparative approach from experiments with healthy subjects.

#### ***Within-arm Position Test (WPT) vs. Mirror Position Test (MPT)***

Gurari et al. (2017) characterized the ability of chronic stroke patients and healthy controls to match elbow flexion/extension positions using two approaches: the MPT performed with a physiotherapist versus the WPT under robotic control. The large majority of stroke patients showed impairments in the mirror task (MPT), but no difference with the control group in the within-arm task (WPT). These different outcomes could be due to lateralized sensory deficits observed after stroke (Connell et al., 2008; Kessner et al., 2016) resulting in asymmetries that may affect the between-arms comparison in the mirror task, but not the unilateral within-arm task. A non-exclusive alternative explanation for the difference in performances (and hence diagnostics) may reside in stroke lesions that could have damaged brain networks specifically involved in the mirror but not in the within-arm task (Iandolo et al., 2018). This second hypothesis was supported by the

## **Introduction: Proprioceptive deficits and visual compensation in stroke**

results of Torre et al. (2013), where stroke patients performed the bimanual sagittal matching tests (BSMT). The achievement of BSMT does not require mirroring of the hand position with respect to the body midline, because both hands move along the sagittal plane, close to each other. The performance (precision) of the patients in this study is similar to that observed in within-arm tasks (Contu et al., 2017; Rinderknecht et al., 2018; dos Santos et al., 2015) and appears better than for the MPT (Herter et al., 2019; Ingemanson et al., 2019), suggesting that stroke lesions can affect the sensory processing necessary to mirror the hand position with respect to the body midline without affecting the between-arms communication per se.

### ***Mirror Position Test (MPT) vs. Thumb Localization Test (TLT)***

Outcomes of MPT and TLT assessment tasks are poorly correlated (Kenzie et al., 2017) and do not reliably identify a proprioceptive deficit within the same patients (Dukelow et al., 2012). Estimated prevalence of proprioceptive deficits using these two tests varied by a factor of two (Meyer et al., 2016). A clear difference between the two tasks, which might explain the different outcomes, is the use of a left/right symmetric (MPT) vs. an asymmetric joint configuration in the TLT. Studies on healthy subjects comparing analogous symmetric and asymmetric inter-manual proprioceptive tasks suggest that these tests differ by the way the joint information from the two arms is processed (Arnoux et al., 2017). More precisely, it was proposed that symmetric and asymmetric inter-manual proprioceptive tasks differ by the encoding of the proprioceptive signals. In symmetric tasks, the proprioceptive signals can be encoded in the reference frame of origin (joint space), whereas in asymmetric tasks, sensory transformations are performed to re-encode the proprioceptive signals in extra-joint spaces, such as a visual reference. Stroke lesions may differentially damage brain areas involved in the specific sensory processing characterizing symmetric and asymmetric tasks.

### ***Thumb Localization Test (TLT) and Finger Proprioception Test (FPT) vs. Up or Down Test (UDT)***

TLT and FPT showed poor correlations with the UDT (Ingemanson et al., 2019; Lanska and Kryscio, 2000), and prevalence of proprioceptive deficits assessed with TLT increased by a

factor of three compared to the UDT (Hirayama et al., 1999). The difference between the unimanual UDT and both the inter-manual TLT and FPT, which uses two fingers of the affected hand, suggests that the different outcomes do not originate from involving only the affected limb. A key difference between these tasks resides in using a single (UDT) vs. two articular chains (TLT and FPT). Research on healthy subjects, comparing analogous proprioceptive tasks, supports differential proprioceptive processing in these two situations (Tagliabue and McIntyre, 2013): sensory transformations are involved in the latter.

### ***Within-arm Position Test (WPT) vs. Reaching Test (RT)***

Performance errors in the WPT are only poorly correlated with errors in the RT (Darling et al., 2008a). This result is most likely due to the obvious difference between the sensory information available in these two tasks: the target position is either memorized through proprioception (WPT) or through vision (RT). These tasks have been compared in healthy subjects and have been shown to require different sensory processing, namely sensory transformation between visual and proprioceptive spaces (Tagliabue et al., 2013; Tagliabue and McIntyre, 2011).

### ***Summary for the proprioceptive assessments***

To summarize this section, overall, we found that the comparison of different studies on proprioceptive assessments reveal high discrepancies, that can lead to different diagnostics. In particular, the proprioceptive assessment tasks that involve two articular chains differ from the tasks that are unimanual and involve a single joint. Furthermore, the outcome of asymmetric assessment tasks (when the two arms are not in the same configuration with respect to the body midline) differ from that of symmetric tasks. Finally, tasks that involve a visual target also differ in terms of sensory processing of the proprioceptive information compared to unimanual proprioceptive assessment tasks. Therefore, the assessment tasks that are currently used in the clinic and in the clinical research appear inherently different: some might assess other sensory functions (sensory transformations) and not the integrity of proprioception per se.

If it appears that the sensory processing of proprioceptive information is different across the various proprioceptive assessment tasks, the comparative analysis of some studies also suggests

that the ability of patients to compensate the proprioceptive deficit with vision depends on the task under consideration (Darling et al., 2008a; Herter et al., 2019; Scalha et al., 2011; Semrau et al., 2018; Torre et al., 2013).

### **1.4.5 Different visual compensation assessments, different outcomes**

Although empirical evidence suggests that vision is helpful to compensate a proprioceptive deficit (Pumpa et al., 2015), the methodologies of studies addressing this question are hardly comparable (Darling et al., 2008a; Herter et al., 2019; Scalha et al., 2011; Semrau et al., 2018; Torre et al., 2013).

Visual feedback of the hand appears to improve the patient's performance in some tasks, such as the Motor Sequences Test (Scalha et al. 2011) and the Reaching Test (Darling et al. 2008a; Scalha et al. 2011). On the other hand, in a large-scale study where patients were assessed using a Mirror Position Test, up to 80% of patients with proprioceptive deficits were not able to improve their performance when visual feedback of both arms was available (Semrau et al. 2018; Herter et al. 2019). The important difference between Mirror Position Test (MPT) and both Motor Sequences Test (MS) and Reaching Test (RT), is the different way visual information can be used. In both tasks where vision significantly improves performance in patients (i.e. MS and RT), the hand (or finger) reaches the same spatial position of the target: the tasks can hence be accomplished by simply matching the visually acquired target position and the visual feedback of the hand (or finger). In the MPT in contrast, the patient does not have to reach the spatial location of the target, but its mirror position: the patient must thus “flip”, relative to the body midline, the image of the arms to achieve the task. This suggests that the ability to use visual information to compensate for proprioceptive deficits in reaching (MS and RT), but not in mirror tasks (MPT), could be due to specific difficulties in performing “mirroring” of visual information, involving the necessity of sensory transformations to re-encode retinal signals in another reference frame to accomplish the task. Consistent with this interpretation, patients were shown to be able to significantly improve their performance with vision in the Bimanual Sagittal Matching Test which does not require “mirroring” of visual information, because their hands moved parallel to the sagittal plane and close to each other (Torre et al. 2013).

## **1.5 Goals and research questions**

The main goal of this thesis is to provide a novel conceptual framework to better understand the nature of proprioceptive deficits post-stroke, and to which extent these deficits can be compensated with vision. To this end, three studies were undertaken focused on the central processing of proprioceptive and visual information when using the upper limb. In these three projects the experimental results are interpreted through the prism of a common theoretical approach based on statistical optimality (see the theoretical framework presented in section 1.3).

### **1.5.1 Study 1 – Reinterpretation of the stroke literature on proprioceptive deficits**

In the first study, we propose a new analysis and re-classification of the assessment techniques commonly used in clinical practice and stroke research, based on the hypothesis that altered sensory transformation processing forms an essential part of what has (perhaps misleadingly) been termed proprioceptive post-stroke deficits. Indeed, I will show that these clinical assessments are very similar to some experimental tasks performed with healthy subjects, for which proprioceptive signals can be encoded in the reference frame of origin (joint space), or in higher-order (“extra”) sensory spaces, depending on the task context. It is therefore critical to distinguish between the modality of the sensory inputs provided by a particular assessment of sensory deficits post-stroke, proprioception, and the potential sensory transformations that ensue during achievement of the assessment task.

Based on a non-systematic review of the literature, we compare our theoretical predictions to empirical data and propose a new stratification for stroke patients based on the nature of their sensory deficits. Finally, we review lesion-behavior and brain imaging studies after stroke in the framework of this novel classification and attempt to relate brain structures to either purely proprioceptive deficits or deficits in sensory processing.

This leads to the following key question:

**Q1. How does sensory transformation processing interact with proprioceptive deficits post-stroke, and how does it affect the patients’ ability to visually compensate for these deficits?**

### **1.5.2 Study 2 – Sensory transformations affecting visuo-proprioceptive integration**

Through the prism of the reinterpretation of the proprioceptive deficits and their compensation using vision in the first study, we explore experimentally the link between sensory transformations and sensory processing in tasks replicating the characteristics of the different clinical assessments (proprioceptive, and visual-compensation tasks). Using a virtual reality set-up combined with a motorized haptic feedback system, we asked healthy subjects to reproduce the same orientation (parallel task), or the mirror orientation (mirror task) of an object relative to the sagittal plane. We used a haptic feedback system to mimic proprioceptive tasks, based on the assumption that the haptic sense relies mainly on proprioceptive perception (see section 1.1.1). Different sensory conditions were tested:

- haptic tasks, where the object could only be perceived haptically,
- visual tasks, where the object could only be perceived visually,
- and visuo-haptic tasks, where the object could be perceived both visually and haptically.

In opposition to the parallel tasks, for the mirror tasks, the mirror spatial transformation necessitates sensory transformations of the available visual and/or haptic information, from the native to “extra-” reference frames. The visuo-haptic tests consist of different combinations of mirror/parallel visual and haptic tasks in order to study how sensory transformation of one sensory modality affects multi-sensory integration. Different levels of noise were used in order to decrease the precision of the visual estimate of object orientation, and to study the effect of a sensory perturbation on our multisensory integration tests. Preliminary (unpublished) results obtained with former versions of this experimental protocol showed that the spatial mirror transformation did not equally affect task precision depending on the working plane orientation, especially for the visual mirror task. This is in accordance with studies on visual symmetries and mental rotations which suggest that visual vertical symmetries (symmetries with respect to the sagittal plane, i.e. orientations that are presented on the frontal plane) provide a memory advantage and decrease reaction time in detection tasks with respect to other symmetries (Cattaneo et al., 2017, 2010; Prather and Sathian, 2002; Rossi-Arnaud et al., 2012). Therefore, in order to investigate the effect of sensory transformation of different difficulties, we compared tests performed in the frontal and horizontal plane.

We hypothesized that sensory transformations would affect the uni-modal (visual or haptic) sensory processing, adding complexity: the re-encoding of the sensory signal imposed by the mirror task would negatively impact task performance, i.e. would show higher variability of performance compared to the parallel task. Consequently, we hypothesized that this added complexity in uni-modal sensory processing would affect the multi-sensory integration when both visual and haptic information are combined, by decreasing the sensory weight given to the transformed modality.

This opens to the second key question:

**Q2. Do sensory transformations affect the performance in uni-modal tasks (visual or haptic), and consequently influence multisensory visuo-haptic integration?**

### **1.5.3 Study 3 – Gravitational influence on sensory transformations**

Based on previous experiments of the research team, the third study consists in a set of experiments aiming at identifying the factors that can impact the efficiency of sensory (visuo-proprioceptive) transformations. Previous studies have shown that head tilt interferes with visuo-proprioceptive transformations (Burns and Blohm, 2010; Tagliabue et al., 2013; Tagliabue and McIntyre, 2011), but it is unclear whether this phenomenon is related to neck flexion (signals originating from the neck muscles and joints), or to the head-gravity misalignment (gravitational signals originating in the otolith system). The first option, “Neck Hypothesis”, would be consistent with the contribution of the neck flexion angle information to the kinematic chain linking the hand to the eyes which may be used to compute visuo-proprioceptive transformations (see section 1.2.2). The second option, “Gravity Hypothesis”, is related to the idea that gravity might play a fundamental role in the reciprocal calibration between visual and proprioceptive senses (see section 1.2.3).

To discriminate between these hypotheses, we performed a first virtual reality experiment in which healthy subjects had to align the hand to ‘grasp’ a visual target with the unseen hand (cross-modal task, necessitating sensory – visuo-proprioceptive – transformations) in a seated and in a supine position. To test the effect of the neck flexion, the subjects were asked to laterally tilt

## **Introduction: Goals and research questions**

the head between the target acquisition and the hand movement onset. In the seated position, the head-gravity misalignment and neck lateral flexion factors are confounded, whereas in the supine position the head-gravity misalignment is not dependent on neck lateral flexion. We hypothesized that the head-gravity misalignment, and not the neck lateral flexion, interferes with the sensory transformations: that will be supported by a decreased performance (precision) in the cross-modal task when supine, because in this position the head is constantly misaligned with respect to gravity. Two additional control experiments (uni-modal visual and uni-modal proprioceptive) were performed to test whether potential effects of posture observed in the cross-modal task could be due to an effect of posture on visual and/or proprioceptive perception, and not on the sensory transformations. To confirm our interpretation of the first set of results, we performed an additional experiment in which the subjects were tested seated and supine, but without lateral neck flexions. The goal was to specifically test the effect of the modulation of the gravitational information without interference from neck muscle-spindle signals.

The third key question of this thesis is thus:

**Q3. Which factors (head posture or head misalignment with gravity) affect the efficiency of sensory transformations?**

## **2 Methods**

### **2.1 Study 1 – Reinterpretation of the stroke literature on proprioceptive deficits**

The first study consists of a targeted review with qualitative and quantitative re-analysis of the literature aiming to provide a new classification of the sensory assessment tasks and an improved stratification of stroke patients with proprioceptive deficits.

Reviewed articles were first qualitatively analyzed in order to provide a new classification of the assessment tasks. Based on our new categorization, we then compared the quantitative assessment results of stroke patients with respect to experimental studies with healthy subjects performing similar tasks. Finally, we used the same categorization to review stroke lesion-behavior and functional brain imaging studies.

#### **2.1.1 Qualitative analysis of proprioceptive and visual compensation tasks**

Based on a non-systematic retrospective review, conducted through a PubMed database search, I collected studies on proprioceptive assessment methodologies in the clinical field as well as in stroke research. In addition to the PubMed search, the reference lists of included studies were screened for additional eligible studies that were not retrieved by the search. We included studies on proprioceptive assessment, on proprioceptive rehabilitation interventions, as well as studies that assessed visual compensation. We systematically excluded studies that treated other neurological diseases than stroke. A total of 44 studies were included for a qualitative comparison of their assessment methods. I presented the identified assessment technique in the introduction of this thesis (Table 1-1).

#### **2.1.2 Categorization of the assessment methodologies**

In order to analyze the diversity of clinical proprioceptive assessments (and visual compensation methods), we propose here a new task categorization. We differentiated four generic

## **Methods: Study 1 – Reinterpretation of the stroke literature on proprioceptive deficits**

assessment tasks (categories), which are characterized by specific (putative) sensory processing, (presence and type of sensory transformations). These four generic tasks are described in the following.

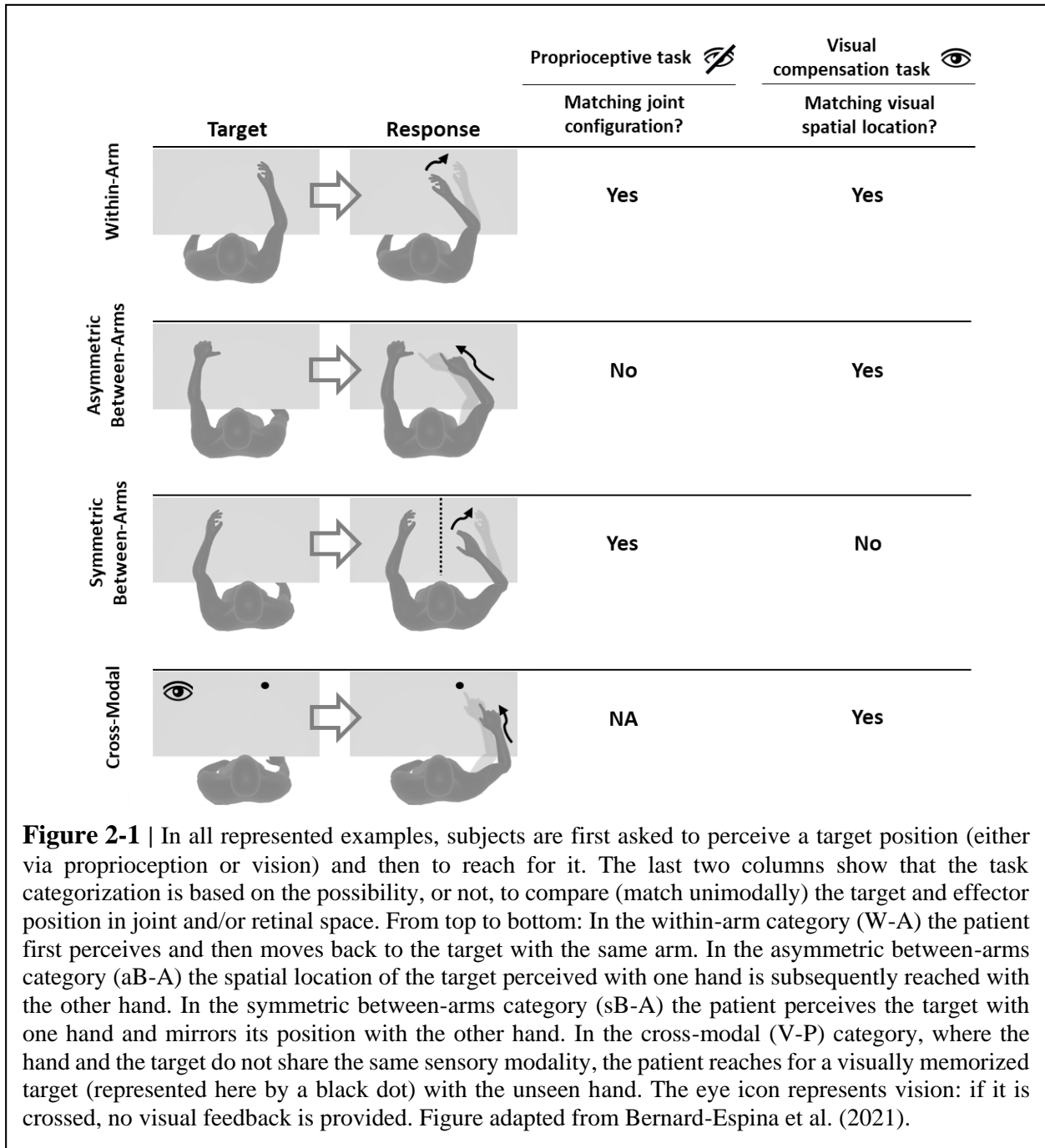
**Within-Arm task (W-A).** The W-A task for the assessment of proprioception (W-AP) requires one and the same articular chain to sense and to reproduce the target position. Thus, proprioceptive information to be remembered (target) and the feedback about the moving hand (effector) originate from the same joint receptors (Figure 2-1, W-AP). In this case, since target and effector position can be encoded in the same native reference frame, no sensory transformation is necessary to perform the task. Similarly, if both proprioceptive and visual cues are available, for visual compensation assessment (W-A<sub>VP</sub>), this task can also be performed by matching the target and effector position encoded in the retinal reference without the need of sensory transformation. W-A tasks are: Within-arm Position Test (WPT), Up or Down Test (UDT), Threshold Detection Test (TDT), and Bimanual Sagittal Matching Test (BSMT) (see Table 1-1).

**Asymmetric Between-Arms task (aB-A).** This involves two articular chains: the less-affected arm (effector) has to reach the target location perceived with the affected arm. For the assessment of proprioception (aB-AP), this task cannot be performed by matching the joint configuration of the affected arm (target) with that of the effector, since they differ at the endpoint of the movement (Figure 2-1, aB-AP). This would require a sensory transformation of the proprioceptive information. The visual compensation task (aB-A<sub>VP</sub>), however, can be accomplished by matching the target and effector location encoded in the retinal reference frame, without sensory transformations, since the task accomplishment consists in directly matching the target and effector spatial location. aB-A tasks are: Thumb Localization Test (TLT) and Motor Sequences Test (MS) (see Table 1-1).

**Symmetric Between-Arms task (sB-A).** This also involves two articular chains. “Symmetric” refers to the fact that the effector has to “mirror” the target configuration with respect to the sagittal plane. For the proprioceptive assessment (sB-AP), the joint configuration of the two articular chains is identical, allowing for direct matching of proprioceptive signals corresponding to the target and

**Methods: Study 1 – Reinterpretation of the stroke literature on proprioceptive deficits**

effector positions (Figure 2-1, sB-A<sub>P</sub>). Therefore, no sensory transformation of the proprioceptive signals is necessary. In contrast, the visual compensation task (sB-A<sub>V<sub>P</sub></sub>), cannot be performed in the retinal space, since the target and the effector do not share the same spatial location. Sensory transformation of the visual signals is necessary. sB-A tasks are: Mirror Position Test (MPT) and Finger Proprioception Test (FPT) (see Table 1-1).



**Cross-modal task (V-P).** This task differs from the others in that the target information is given visually (or remembered visually) whereas only proprioceptive information is provided for the effector (Figure 2-1, V-P). Thus, these tasks always require sensory transformations for both proprioceptive (V-P) and visual compensation (V-VP) tasks. For this reason, their categorization based on the direct encoding in the joint and/or retinal space is not fully applicable. V-P tasks are: Reaching Test (RT), Matching to a Visual image (MV), and Shape/Length Discrimination (SLD) (see Table 1-1).

### **2.1.3 Quantitative comparison between tasks**

Among the 44 studies that were used for the qualitative analysis, 18 studies could be included in this quantitative comparative analysis: 8 for stroke patients and 10 with healthy subjects. The selection criteria for the papers are the following: the use of quantitative measurements (such as robotic devices); the comparison of either (at least) two different categories of tasks, or of patients with healthy subjects.

In order to be able to quantitatively compare the performance (end point errors) in the different sensory assessment methods despite methodological differences among studies, we normalized the experimental data of the selected studies. For each category of proprioceptive task (and visual compensation task, i.e. same task performed using vision in addition to proprioception), we expressed the variable error of the end-point positions (for both stroke patients and control subjects) as a ratio of the variable error in the W-A<sub>p</sub> task performed by healthy subjects.

### **2.1.4 Correspondence with functional anatomy**

After a non-systematic PubMed screening, we reviewed 9 studies that used functional imaging (fMRI, PET and EEG) to analyze the neural networks involved in proprioceptive and visuo-proprioceptive tasks, as well as studies using imaging-based lesion-symptom mapping (LSM) which compared the performance of patients in at least two different types of tasks. The limited number of included studies comes from the fact that only few (2) lesion-symptom mapping studies provide a comparative approach with different types of tasks, and functional imaging studies analyzing proprioceptive assessment tasks are scarce (7 included).

## **2.2 Study 2 – Sensory transformations affecting visuo-proprioceptive integration**

The second study aims to determine whether and how unimodal (visual or proprioceptive) and multimodal (visuo-proprioceptive) processing is affected by the necessity of sensory transformations. The developed experimental tasks replicated the characteristics of the different clinical proprioceptive assessments (and visual compensation tasks) that are used in the stroke literature: using a virtual reality set-up combined with a motorized haptic feedback system, subjects had to reproduce the orientation of an object (parallel task), or mirror it relative to the sagittal plane (mirror task). The task was performed with haptic feedback only, visual feedback only, or with both.

Unlike the mirror proprioceptive assessment tasks that are described in Figure 2-1, in this study the haptic mirror task is performed with one arm. As a consequence, when mirroring the target orientation, the arm is not in the same joint configuration than during the target acquisition. We therefore made the assumption that mirroring the object orientation would require sensory transformations, that will be referred to as spatial mirror transformations.

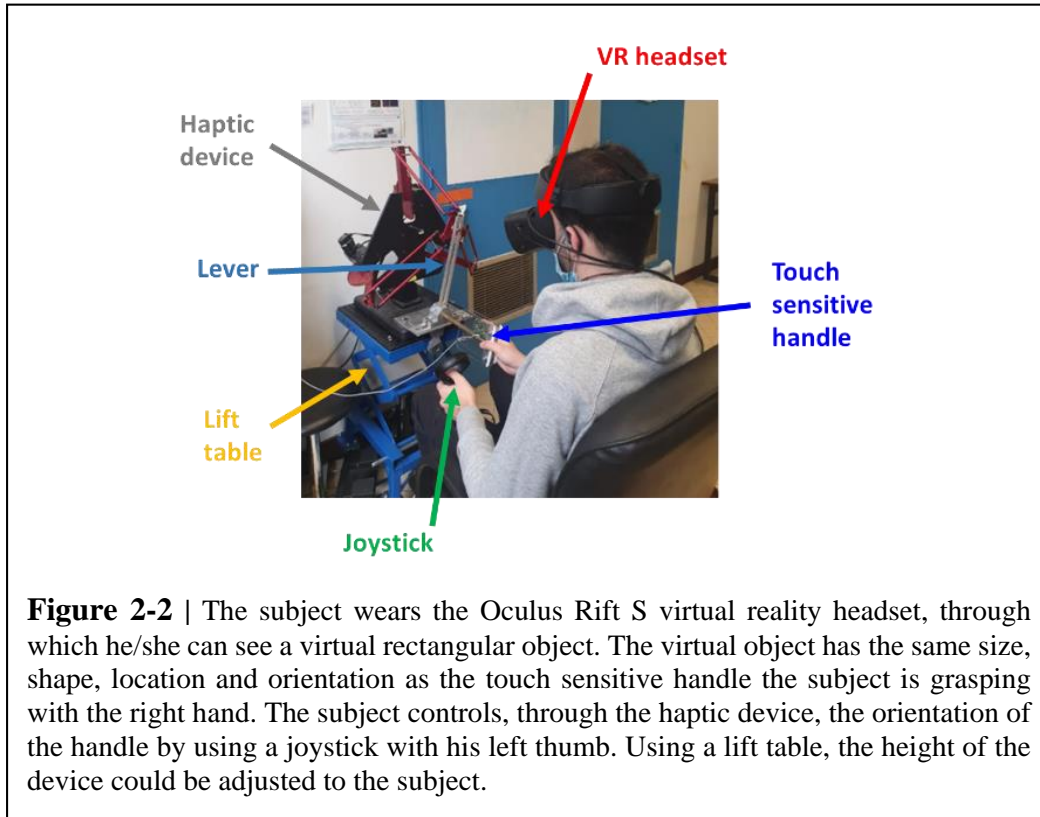
### **2.2.1 Experimental set-up**

As shown in Figure 2-2, the experimental setup mainly consists of a haptic device, used to rotate a rectangular handle, and a virtual reality (VR) headset that shows to the subject a virtual version of the handle. For the integration of the VR headset and the haptic device, I developed a custom real-time control program in C++ (see Appendix A for more details).

#### ***Virtual reality headset***

The Oculus Rift S (Oculus VR, Menlo Park, California, USA) used has a high resolution (1440x1280 pixels) display per eye with 80Hz frame rate, a 115° diagonal field of view, and a fixed interpupillary distance of 63.5mm. Information about the three-dimensional position and orientation of the subject's viewpoint (provided by the built-in cameras and inertial measurement

unit (IMU) of the Oculus Rift S) was used in real-time to update the images shown in the VR headset.



### ***Haptic device***

A haptic device (Delta Haptic Device, ForceDimension) was used to control the orientation of a handle (Figure 2-2). To convert the 3 translational degrees of freedom of the haptic device (translations along the x, y, and z-axis) into a single rotational degree of freedom for the handle, I designed a custom mechanical system: the handle was rotated by a lever which was operated by the haptic device. Depending on the phase of the experiment, the handle orientation was either driven by the computer, or by the subject through the joystick of the Oculus Touch Controller, therefore no active wrist rotations were required.

### 2.2.2 Experimental paradigm

Subjects sat comfortably in a chair with belts to avoid trunk movements. The haptic device height was adjusted so that subjects could grasp the handle with the elbow flexed at about 90° (Figure 2-3). Subjects had to look down at approximately 45° to see the handle through the VR headset. The virtual environment consisted of the virtual handle on a uniform gray background without external visual landmarks. This choice aims at removing all possible directional references with respect to which the handle orientation could be estimated.

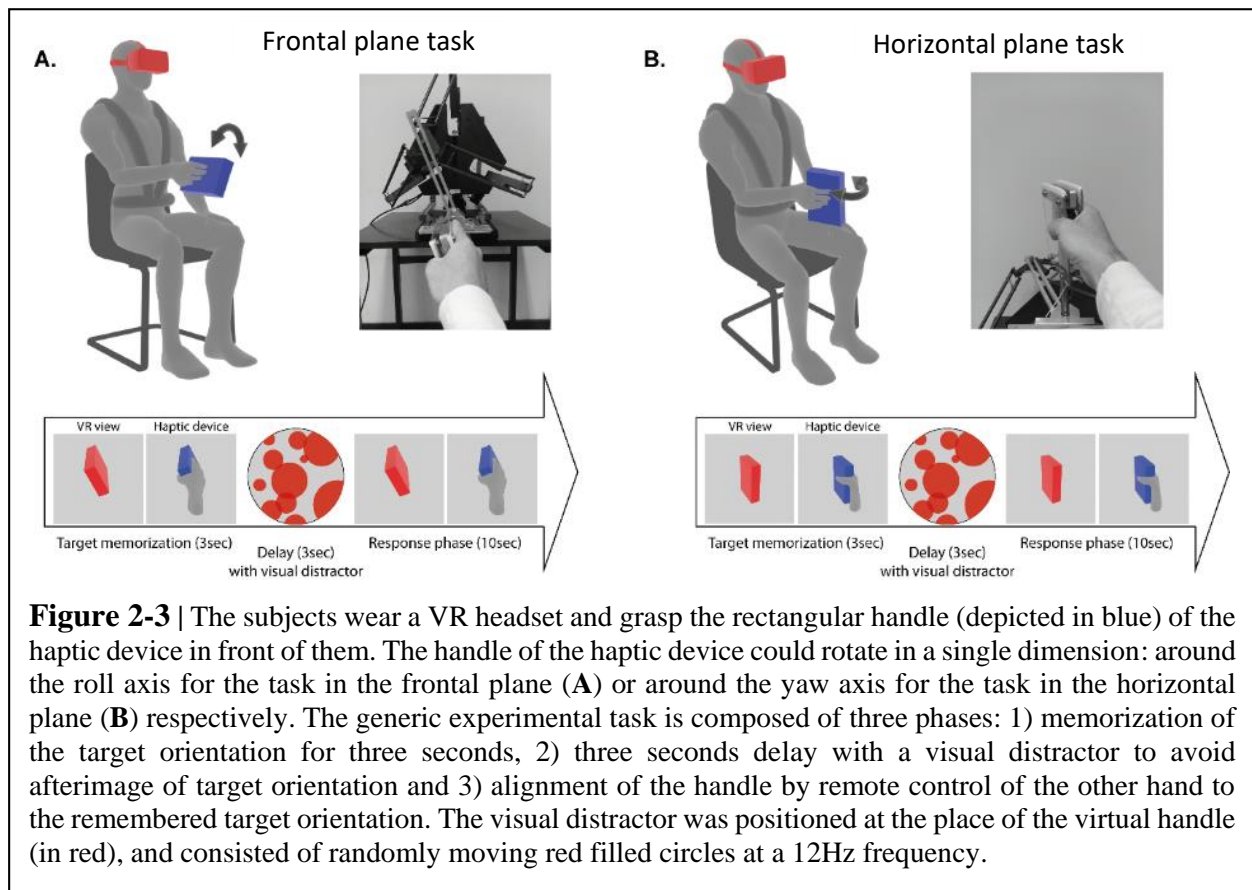


**Figure 2-3** | The subjects wear a VR headset and grasp the rectangular handle (depicted in blue) of the haptic device in front of them. The handle of the haptic device could rotate in a single dimension: around the roll axis for the task in the frontal plane (A) or around the yaw axis for the task in the horizontal plane (B) respectively. The generic experimental task is composed of three phases: 1) memorization of the target orientation for three seconds, 2) three seconds delay with a visual distractor to avoid afterimage of target orientation and 3) alignment of the handle by remote control of the other hand to the remembered target orientation. The visual distractor was positioned at the place of the virtual handle (in red), and consisted of randomly moving red filled circles at a 12Hz frequency.

Head movements were not constrained physically, but a warning was displayed when the head yaw or roll angle deviated from the straight-ahead direction by more than 15°, or when the lateral translation exceeded 10cm. For a first group of subjects the haptic device was positioned in the frontal working plane, and the movement of the handle constrained to the roll angle (Figure 2-3A), for a second group the device was placed in the horizontal working plane, and hence

the movement of the handle constrained to the yaw angle (Figure 2-3B). The subjects of each group performed the task in 12 conditions, which differed by the modality of the available sensory information, and the requirement to reproduce or mirror the target orientation.

The task consisted of three phases (see Figure 2-3): 1) memorization of the target orientation (sensed visually, haptically, or both) for three seconds, 2) a three seconds visual distraction to avoid a target afterimage in tasks involving vision, and 3) alignment of the handle to the memorized target orientation using the joystick. When the subjects considered that the handle was in the correct orientation, they validated their response by pressing an Oculus controller button. If the response was not provided after 10 seconds, an auditory prompt was given to the subject. The target orientations were  $-30^\circ$ ,  $-20^\circ$ ,  $-10^\circ$ ,  $0^\circ$ ,  $+10^\circ$ ,  $+20^\circ$  or  $+30^\circ$ , with respect to the sagittal plane.

In the following the experimental conditions are grouped in three sensory families (haptic, visual or visuo-haptic) and described in detail:

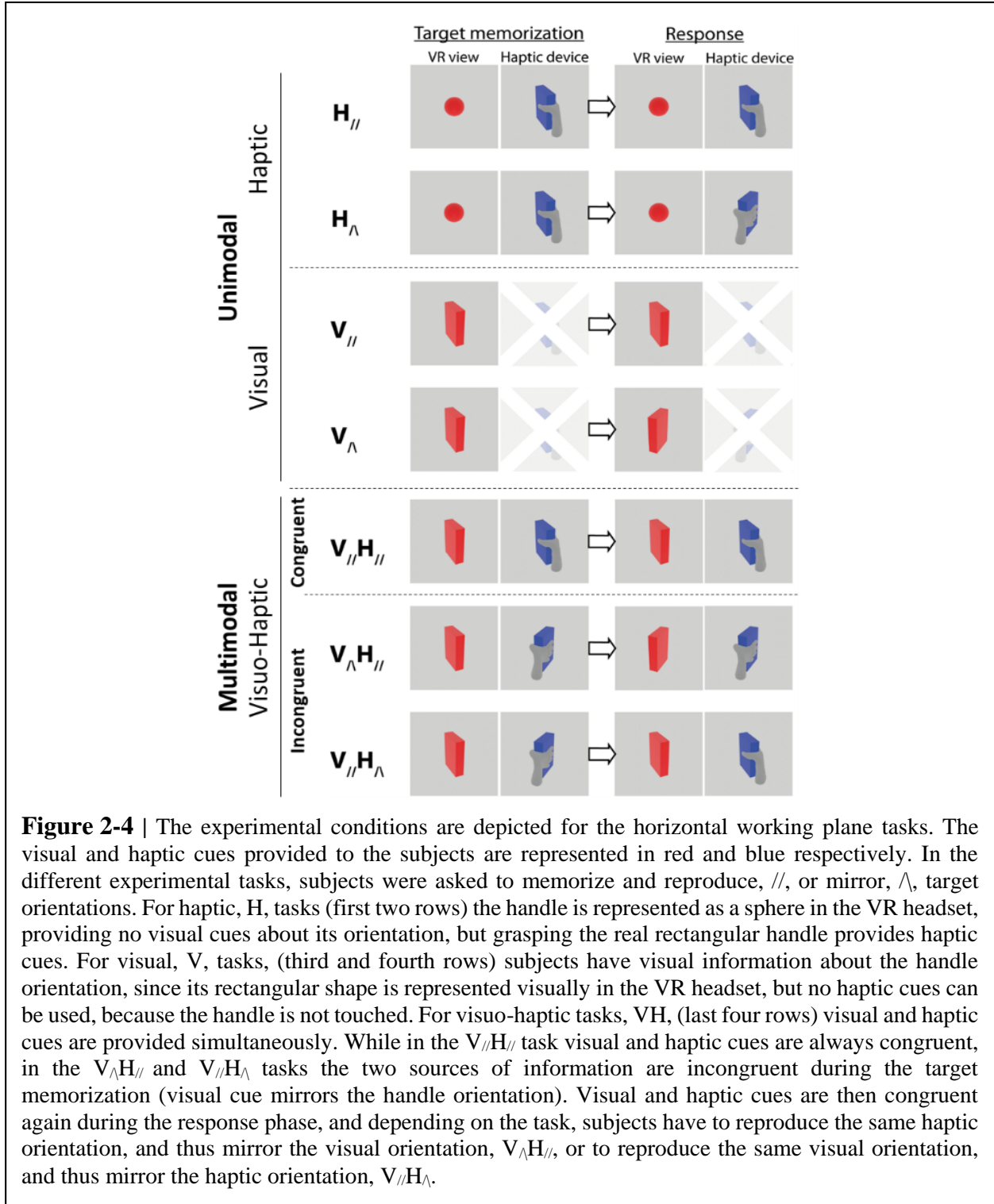
**Unimodal Haptic tasks.** Both target and response orientation cues were haptic only: perceived by grasping the handle. The subjects saw a spherical handle instead of the rectangular shape, which did not provide any visual orientation cue.

1. Unimodal *Haptic Parallel* task,  $\mathbf{H}_{//}$ : Subjects were asked to align their response to the memorized target orientation (Figure 2-4, top row);
2. Unimodal *Haptic Mirror* task,  $\mathbf{H}_{\wedge}$ : Subjects were asked to mirror the target orientation relative to the sagittal plane (Figure 2-4, second row).

**Unimodal Visual tasks.** Both target and response orientations were sensed through vision only: the subjects saw a virtual representation of the rectangular handle (same shape and dimensions), but did not grasp it.

1. Unimodal *Visual Parallel* task,  $\mathbf{V}_{//}$ : Subjects were asked to reproduce the target orientation (Figure 2-4, third row);
2. Unimodal *Visual Mirror task*,  $\mathbf{V}_{\wedge}$ : Subjects were asked to mirror the target orientation relative to the sagittal plane (fourth row of Figure 2-4).

The visual tasks were repeated with additional noise:  $\mathbf{Vn}_{//}$  and  $\mathbf{Vn}_{\wedge}$ . The visual noise consisted of random rotations of the handle image from its nominal orientation, following a normal distribution with  $0^\circ$  mean and  $4.5^\circ$  standard deviation.



**Multisensory Visuo-Haptic tasks.** Target and response orientation were sensed visually and haptically simultaneously: the subjects saw the same visual object as in the unimodal visual tasks while they grasped the handle as in the haptic tasks. To mimic the sensory processing characterizing the main clinical assessment categories (Figure 2.1), that is the necessity or absence of spatial sensory transformations in the visual or haptic channels, some tasks involved congruent or incongruent visuo-haptic signals: during the target acquisition phase, the handle and its virtual representation could have the same orientation (congruent) or they could mirror each other (incongruent); during the response phase, visuo-haptic information was always congruent.

*Congruent Visuo-Haptic task:*

1. *Visuo-Haptic Parallel* task,  $\mathbf{V}_{//}\mathbf{H}_{//}$ : Subjects were asked to reproduce the congruent visuo-haptic target orientation (Figure 2-4, fifth row);

*Incongruent Visuo-Haptic task:*

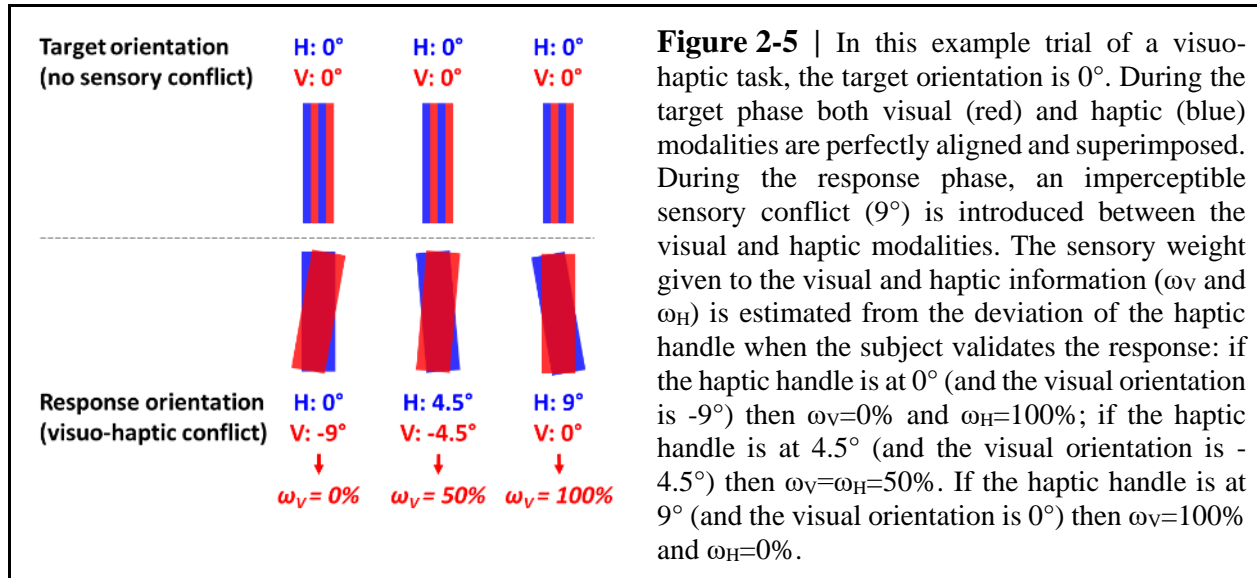
2. *Visual Mirror-Haptic Parallel* task,  $\mathbf{V}_{\wedge}\mathbf{H}_{//}$ : after the acquisition of incongruent visual and haptic targets, subjects were asked to reproduce the orientation of the haptic target and thus to mirror the orientation of the visual target (Figure 2-4, sixth row);
3. *Visual Parallel-Haptic Mirror* task,  $\mathbf{V}_{//}\mathbf{H}_{\wedge}$ : after the acquisition of incongruent visual and haptic targets (as in  $\mathbf{V}_{\wedge}\mathbf{H}_{//}$ ), the subjects were asked to mirror the haptic target and thus reproduce the orientation of the visual target (Figure 2-4, seventh row).

The visuo-haptic (VH) tasks were performed also with additional visual noise:  $\mathbf{Vn}_{//}\mathbf{H}_{//}$ ,  $\mathbf{Vn}_{\wedge}\mathbf{H}_{//}$  and  $\mathbf{Vn}_{//}\mathbf{H}_{\wedge}$ . The noise had the same characteristics as in the unimodal visual tasks,  $\mathbf{Vn}_{//}$  and  $\mathbf{Vn}_{\wedge}$ . The rationale for adding the visual noise was to decrease the visual precision relative to the haptic precision, such that the subject would give similar importance to haptic and visual cues in the multisensory integration (Ernst and Banks, 2002).

### **2.2.3 Sensory (visuo-haptic) conflict**

In the Visuo-Haptic tasks, in which the subject can combine two sources of information to estimate the object orientation, we wanted to quantify the relative importance given to the visual

and haptic signals. To this end, an imperceptible sensory conflict was artificially introduced during the response phase of half of the trials: orientation of the haptic handle (haptic cue) and its representation in the VR headset (the visual cue) were misaligned by  $9^\circ$  (see Figure 2-5).



We reasoned that if an average deviation of  $9^\circ$  of the haptic handle was observed between the trials with and without conflict, then the visual weight would be 100% (third column of Figure 2-5). Conversely if no deviation of the haptic handle due to the sensory conflict was observed, then the visual weight would be 0% (first column of Figure 2-5).

In order to verify that the conflict was not perceived by the subjects, and thus the natural multisensory integration preserved, the subjects were interviewed, at the end of the experiment, about the  $9^\circ$  visuo-haptic conflict. None of them reported to have noticed it.

#### 2.2.4 Experimental session structure

In each of the six unimodal tasks ( $\mathbf{H}_{//}$ ,  $\mathbf{H}_{\wedge}$ ,  $\mathbf{V}_{//}$ ,  $\mathbf{V}_{\wedge}$ ,  $\mathbf{Vn}_{//}$  and  $\mathbf{Vn}_{\wedge}$ ), the subjects performed four trials for each of the seven target orientations, for a total of 28 ( $=4 \times 7$ ) trials. In the six multisensory VH tasks ( $\mathbf{V}_{//}\mathbf{H}_{//}$ ,  $\mathbf{V}_{\wedge}\mathbf{H}_{//}$ ,  $\mathbf{V}_{//}\mathbf{H}_{\wedge}$ ,  $\mathbf{Vn}_{//}\mathbf{H}_{//}$ ,  $\mathbf{Vn}_{\wedge}\mathbf{H}_{//}$  and  $\mathbf{Vn}_{//}\mathbf{H}_{\wedge}$ ), for each target orientation four trials with sensory conflict were added with respect to the unimodal tasks, which led to 56 ( $=(4+4) \times 7$ )

trials per task. The order of the trials was randomized. To compensate for a possible order effect between the different experimental tasks all subjects performed the 12 tasks in a different sequence.

### **2.2.5 Participants**

36 healthy subjects participated in this study (18F, age:  $28.3 \pm 7.8$ y). Exclusion criteria were: history of neurological or vestibular disorder, history of seizure, orthopedic disorder affecting the upper limbs, and sight disorder (unless corrected). Participants could wear contact lenses or glasses for the experiment. Handedness was assessed with the Modified Edinburg Handedness Index (Milenkovic and Dragovic, 2013). 29 subjects were right-handed, 3 left-handed, and 4 ambidextrous. The subjects were balanced in two experimental groups: frontal plane (9F, 9M) and horizontal plane (9F, 9M). Participants in the two groups did not differ in age nor handedness.

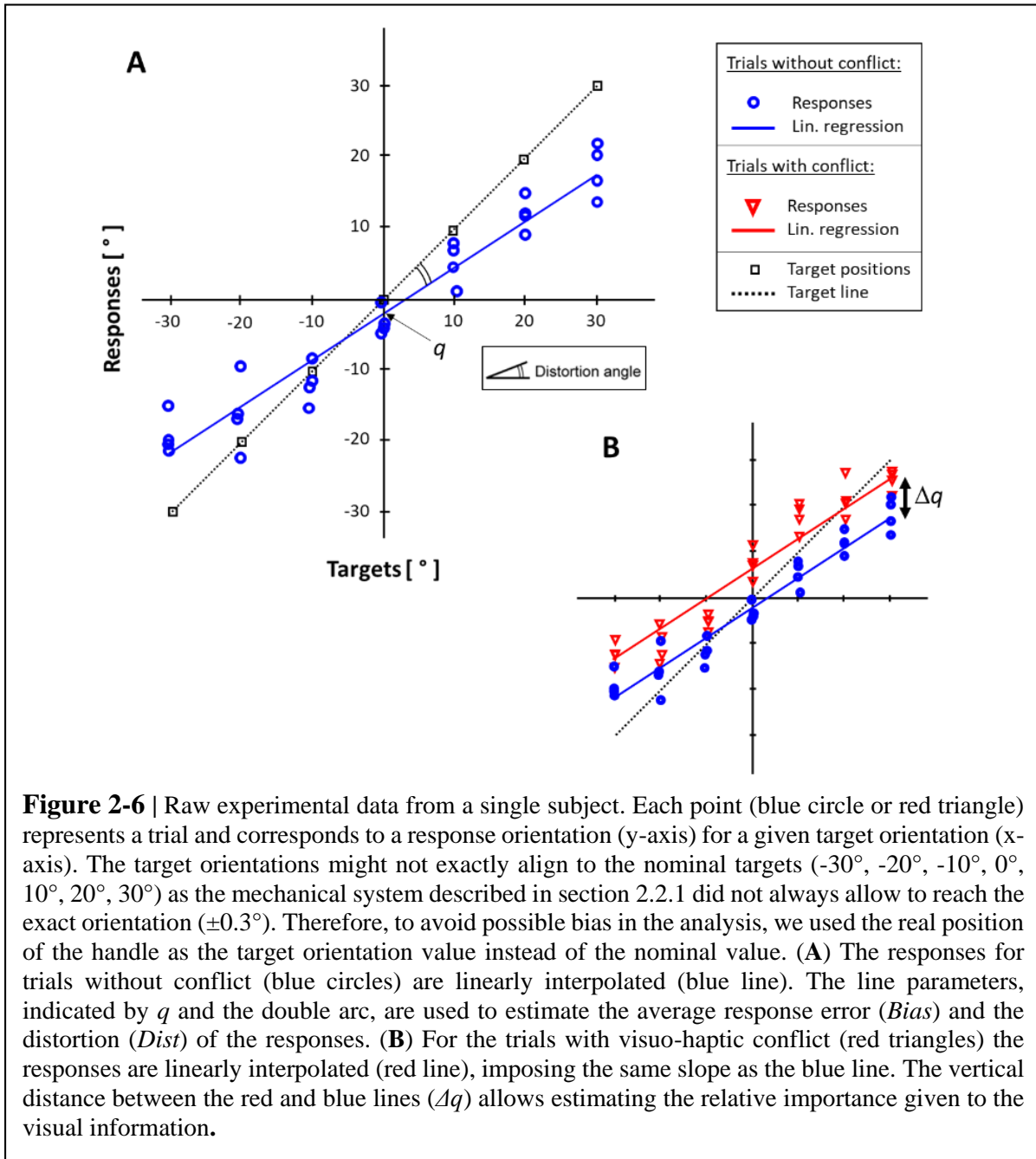
This experimental protocol was approved by the Ethics Committee of Université Paris Cité (N° IRB 2021-34 / 2022-3) and all participants gave written informed consent in line with the Declaration of Helsinki.

### **2.2.6 Data analysis**

The performance of each subject was analyzed using Matlab (MathWorks, RRID: SCR\_001622) in terms of the orientation of the responses. By convention, we considered the orientation of the response to be the orientation of the haptic handle (that could be different from the orientation of the virtual object when the visuo-haptic sensory conflict was introduced, as shown in Figure 2-5). To describe the characteristics of the average behavior of the subject, we used only the trials without the visuo-haptic sensory conflict. The trials with visuo-haptic conflict were only used to estimate the visual weight (see next section 2.2.7: “Sensory weighting quantification”).

To estimate the average error and the over/under-estimations of the response orientations, the linear regression line of the subjects’ responses were computed (blue line in Figure 2-6A). The regression line has the form  $\theta_r = m\theta_t + q$ , where  $\theta_r$  and  $\theta_t$  are the response and target orientation respectively, and it was used to quantify the following parameters:

- The average error (*Bias*), that is the average response-target distance, represented by the average distance across the 7 target directions between the regression line of the responses without conflict and the line passing through the target positions:  $Bias = q$  (y-intercept of the blue line in Figure 2-6A).



- The distortion (*Dist*), i.e. possible over/under-estimation of the distance between two target orientations (Tagliabue and McIntyre, 2008), represented by the angle between the regression line of the responses and the line passing through the target orientations (see Figure 2-6A):  $Dist = atan(m) - 45^\circ$ . Positive and negative values of *Dist* correspond to a global over- and under- estimation of the angular distances respectively.

The average number of control actions (*Nb Ctrl*) was recorded for each trial and averaged for each sensory task, representing how many times the subjects corrected the orientation of the handle with the oculus joystick before validating their response.

In order to robustly describe the variability of the responses (*Var*), I adapted a method proposed by McIntyre et al. (1997) to combine the responses associated to different targets: as described in Equation 11, we computed the square root of the combined variance  $\sigma_t^2$  of the responses obtained for each target  $t$ , weighted by  $\frac{n_t-1}{\sum_{t=1}^7(n_t-1)}$ , where  $n_t$  is the number of responses for each target.  $n_t = 4$ , unless a trial has been eliminated by the outlier detection procedure (Z-score > 3).

$$Var = \sqrt{\frac{\sum_{t=1}^7 \sigma_t^2 (n_t - 1)}{\sum_{t=1}^7 (n_t - 1)}} \quad \text{Equation 11}$$

### **2.2.7 Sensory weighting quantification**

To quantify the effect of the sensory conflict in each multisensory condition, we linearly interpolated the responses of the conflict-trials constraining the regression line (red line in Figure 2-6B) to be parallel to the regression line of the no-conflict-trials (blue line of Figure 2-6B). This procedure provides the intercept for the conflict trials ( $q_c$ ). The rationale for imposing two parallel regression lines was to estimate more robustly the average difference between the response orientations of the trials with and without conflict. The simpler approach, which consists in computing the difference of the mean responses with and without conflict, provides similar results but is less robust in the case of missing trials.

Subtracting the intercept value of the no-conflict and the conflict-trials we obtain the average deviation of the response due to the 9° visuo-haptic conflict:  $\Delta q = q_c - q$  (double-headed arrow in Figure 2-6B). The percentage weight given to the visual information,  $\omega_V$ , can then be computed as follows (Equation 12):

$$\omega_V = \frac{\Delta q}{9^\circ} \times 100\% \quad \text{Equation 12}$$

### **2.2.8 Statistical analysis**

We assessed the effect of the spatial mirror transformations on the individual subject performances in uni- and multi-sensory tasks, and on the sensory weighting in the multi-sensory tasks. We performed separate Repeated Measures ANOVA on the *Bias*, *Dist*, *Var*, *Nb Ctrl* and  $\omega_V$  dependent variables, with the *working plane* (*Plane*: frontal or horizontal) as between-subjects independent variable. For the unimodal tasks, the within-subjects factors were: the sensory modality (*Sense*: P, V and Vn), and the mirror spatial transformation (*Mirror*: // or ^). For the multisensory tasks, the within effect factors were: the absence/presence of visual noise (*Noise*: V or Vn) and the mirror spatial transformation (*Mirror*: V//H//, V^H// or V//H^). To achieve the normal distribution required to perform an ANOVA, values of *Var* were transformed by the function  $\log(x+1)$  (Luyat et al., 2005). We tested the normality assumption of the dependent variables with the Shapiro-Wilk test. To test whether *Bias*, *Dist*, *Var*, *Nb Ctrl* and  $\omega_V$  were significantly different for different values independent factors, post-hoc Student-Newman-Keuls (SNK) tests were used. In the following,  $p < 0.05$ ,  $p < 0.01$ , and  $p < 0.001$  will be indicated with \*, \*\*, and \*\*\* asterisks respectively. All statistical analyses were performed using the Statistica 8 software (Statsoft, SCR\_014213).

### **2.3 Study 3 – Gravitational influence on sensory transformations**

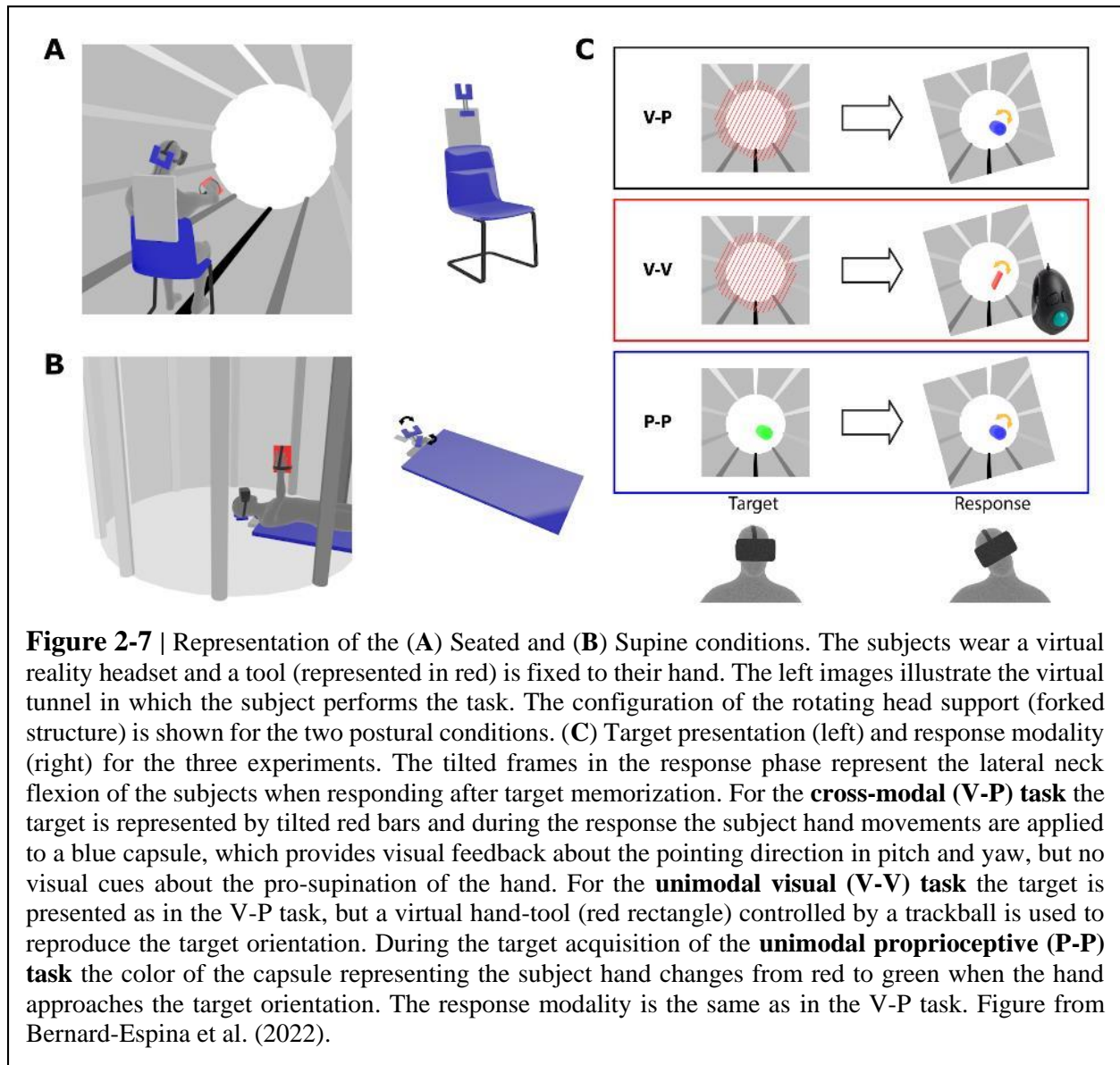
The third study aimed at determining whether head misalignment with respect to the vertical (gravitational signals) interferes with sensory transformations. We confronted the “Gravity Hypothesis” (*Gravity Hp*), with two alternative hypothesis that are two variations of the “Neck Hypothesis”: *Neck1 Hp*, wherein the lateral neck flexions *per se* (which is involved in the eye-hand kinematic chain) interferes with eye-hand transformation; and *Neck2 Hp*, wherein lateral flexions require an increase of neck muscle activations to support the weight of the head, resulting in increased signal-dependent noise that would interfere with eye-hand transformations (Abedi Khoozani and Blohm, 2018).

To discriminate between these three hypotheses, we asked healthy subjects to align their unseen hand to a visual target (cross-modal task, with the necessity of performing sensory transformations) in seated and supine postures. To test the effect of the neck flexion, the subjects had to laterally tilt their head between the target acquisition and the hand movement onset. If ‘Neck1 Hp’ is correct, task performance should not change notably between postures, because the tasks performed in the seated and supine condition do not significantly differ in terms of lateral neck flexion. On the other hand, ‘Neck2 Hp’ predicts an improvement of task performance (precision) when supine, because, thanks to a special head support, in this position the neck muscles never have to sustain the head weight, resulting in a reduction of muscle spindle noise (Abedi Khoozani and Blohm, 2018). Finally, ‘Gravity Hp’ will be supported by a decreased performance (precision) when supine, because in this position the head is constantly misaligned with respect to gravity.

#### **2.3.1 Experimental set-up**

The setup is similar to that used in the preceding study (see section 2.2.1), using virtual reality (VR), except that the haptic device was replaced by a hand-tool fixated to the hand. A 3D acquisition system (CODAmotion) was used for real time tracking of both VR headset and hand-tool position and orientation (for details, see Appendix D, methods section of Bernard-Espina et al. 2022).

The VR scene consisted of a cylindrical tunnel. Longitudinal marks (lines) parallel to the tunnel axis were added on the walls helping the subjects to perceive their own spatial orientation in the virtual world (Figure 2-7). The fact that these marks went from white in the ‘ceiling’ to black on the ‘floor’ facilitated the identification of the visual vertical. Since the main axis of the virtual tunnel always corresponded to the anterior-posterior subject direction, it was horizontal and vertical when the subject was seated and supine, respectively.



### **2.3.2 Experimental paradigm**

To dissociate the effects on the sensory transformations induced by neck lateral flexion and by head misalignment with respect to gravity, we performed a first VR experiment in which the subjects had to perform reaching movements in a Seated and in a Supine position (Figure 2-7A-B): in the seated position, neck lateral flexion and head misalignment with gravity are confounded, whereas in supine position, the head can be aligned with the body axis while remaining misaligned with respect to gravity. When the subjects performed the task in the supine position, they laid in a medical bed with their head supported by an articulated mechanical structure allowing for lateral neck flexions (Figure 2-7B). When the subjects performed the task in a seated position the same head support was fixed to the back of the chair to restrain the head movements similar to the supine condition (Figure 2-7A).

To specifically assess the sensory transformations, we performed a first cross-modal experiment where the subjects had to ‘grasp’ a visual target with the unseen hand (*V-P Experiment* in Figure 2-7C). Two additional control experiments were performed to test whether potential effect of posture observed in the cross-modal task could be due to an effect of posture on visual and/or proprioceptive perception, and not on the sensory transformations (Unimodal Visual, *V-V Experiment* and Proprioceptive, *P-P Experiment*). To confirm our interpretation of the first set of results, we performed an additional experiment in which the subjects were tested seated and supine, but without lateral neck flexion. The goal was to specifically test the effect of the modulation of the gravitational information without interferences from neck muscle-spindle signals (*Neck Straight Experiment*).

All experimental tasks consisted of three phases: 1) memorization of the target orientation, 2) lateral head tilt, and 3) alignment of the tool to the remembered target orientation. The target could be laterally tilted with respect to the virtual vertical of  $-45^\circ$ ,  $-30^\circ$ ,  $-15^\circ$ ,  $0^\circ$ ,  $+15^\circ$ ,  $+30^\circ$  or  $+45^\circ$ . The subjects had 2.5 seconds to memorize its orientation.

As in previous studies (Arnoux et al., 2017; Tagliabue et al., 2013; Tagliabue and McIntyre, 2013, 2012, 2011), we took advantage of the head rotation to introduce a sensory conflict which the subjects did not notice (see below section 2.3.3).

In all tests, except the Neck Straight Experiment, after the target disappeared, the subjects were guided to laterally tilt the head  $15^\circ$  to the right or to the left by a sound feedback with a left-right balance and a volume corresponding to the direction (left or right tilt) and the distance from the desired inclination. If they were unable to extinguish the sound within 5 seconds, the trial was interrupted and repeated later on, otherwise a go signal was given to indicate that they had to reproduce the target orientation with the hand tool (while holding the head tilted). After the go signal, the subjects aligned the tool to the memorized target and clicked on the trigger of a trackball held in their left hand to validate the response.

### **2.3.3 Sensory (visuo-vestibular) conflict**

Unlike the previous study (section 2.2.3), we could not generate a sensory conflict between visual and proprioceptive hand orientation cues because the two stimuli were not presented simultaneously. In order to quantify the sensory weighting in each experimental condition, a sensory conflict was artificially introduced (as in Tagliabue and McIntyre, 2011): tracking the VR goggles was normally used to hold the visual scene stable with respect to the real world during the head rotations, but in half of the trials, a gradual, imperceptible conflict was generated such that, when the head rotates, the subjects received visual information corresponding to a larger tilt. The amplitude of the angle between the visual vertical and subject body axis varied proportionally (by a factor of 0.6) with the actual head tilt, so that for a  $15^\circ$  lateral head roll a  $9^\circ$  conflict was generated. When, at the end of the experiment, the subjects were interviewed about the conflict perception, none of them reported to have noticed the tilt of the visual scene.

### **2.3.4 Experimental session structure**

In order to compensate for possible learning effects, half of the subjects were tested first seated and then supine, and the other half in the opposite order. For the Cross-modal, Uni-modal Visual and Uni-modal Proprioceptive Experiments, the subjects performed two trials for each combination of target orientation (7 different orientations), head inclination (right or left head tilt) and sensory conflict (with or without), for a total of 56 ( $=2 \times 7 \times 2 \times 2$ ) trials per posture. For the neck Straight Experiment, each target orientation was tested twice, for a total of 14 ( $=2 \times 7$ ) trials per posture. The order of the trials was randomized.

### **2.3.5 Participants**

In total 66 subjects were tested, 18 for each of the three experiments with the head tilted (9F, 9M, age: V-P  $26.5 \pm 9y$ ; V-V  $30 \pm 6y$ ; P-P  $24.5 \pm 6y$ ), and 12 for the additional experiment without head tilt (12M, age:  $38.5 \pm 8y$ ). Exclusion criteria were: history of neurological or vestibular disorder, history of seizure, orthopedic disorder affecting the upper limbs, and sight disorder (unless corrected). Participants could wear contact lenses or glasses for the experiment. Handedness was self-reported by the subjects: 17% of the subjects were left-handed.

This experimental protocol was approved by the Ethical Committee of the University of Paris (N° CER 2014-34 / 2018-115) and all participant gave written informed consent in line with the Declaration of Helsinki.

### **2.3.6 Data analysis**

The performance of each subject was analyzed in terms of the lateral inclination (roll) of the tool when they validated the response. We analyzed the data of this study using a similar approach to the one described for Study 2 “Sensory transformations affecting visuo-proprioceptive integration” (see section 2.2.6), but some modifications were necessary to adapt to the characteristics of the dataset. The main differences are:

- The Accuracy ( $Acc$ ), that is the average response-target distance, was represented by the average absolute distance between the target orientations and the response orientations.
- The Aubert-Muller effect ( $AMe$ ), corresponding to the global response bias due to the lateral head tilt (Guerraz et al., 1998), was quantified as half of the algebraic distance between the response orientations with right and left neck lateral flexion.
- The Visual weight ( $\omega_V$ ), that is the importance the subject gives to the visual landmarks for the encoding of the task in the trials with conflict, was estimated with the deviation of the response orientations due to the sensory (visuo-vestibular) conflict, compared to the theoretical deviation of the target orientations if they were assumed to move together with the visual scene.

Response distortions ( $Dist$ ) and variable error ( $Var$ ) was computed the same way as in the previous study (see section 2.2.6). All details about these methods are available in Appendix D (methods section of Bernard-Espina et al. 2022).

### **2.3.7 Statistical analysis**

For each experiment, we assessed the effect of posture on task performance using mixed model ANOVAs on the *AMe*, *Dist*, *Acc*, *Var* and  $\omega_v$  dependent variables, with the *Posture* (Seated, Supine) and *Order* (Seated-First and Supine-First) as within- and between-subjects independent variable respectively. No between-experiment comparisons were performed, because they do not correspond to the goal of this study. Since we performed three distinct experiments, we applied a Bonferroni correction ( $n=3$ ) for multiple comparisons to reduce the probability of type I errors (false positive). Therefore, in the following,  $p<0.05/3(\approx 0.0167)$ ,  $p<0.01/3(\approx 0.0033)$  and  $p<0.001/3(\approx 0.00033)$  will be indicated with \*, \*\*, \*\*\* respectively. For the straight-neck experiment, because we specifically wanted to test whether the Supine position increased the subjects' variable and constant errors, we performed one-tailed student t-tests on *Var* and *Acc*. All statistical analyses were performed using the Statistica 8 software (Statsoft, SCR\_014213).

## **3 Common theoretical approach**

*“All models are wrong, but some are useful.”*

*George Box (1978)*

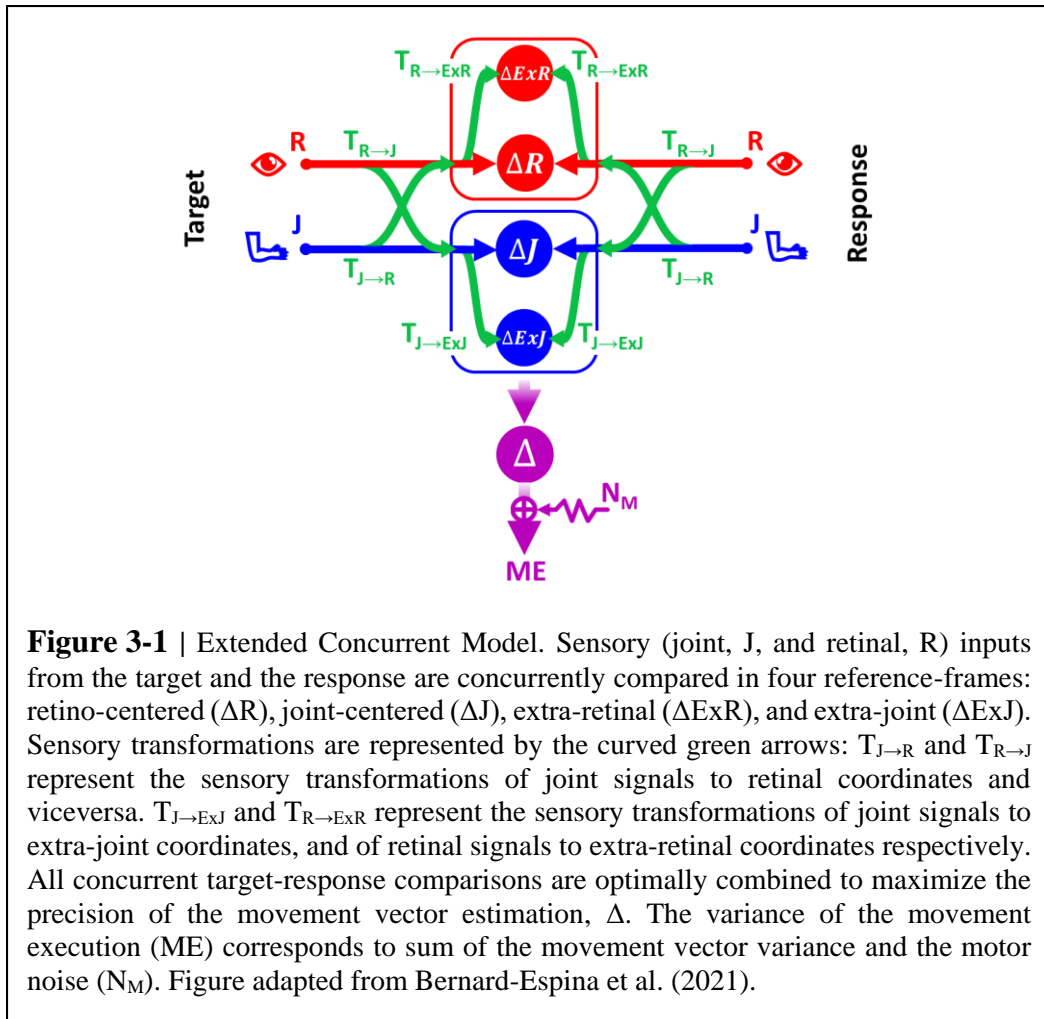
In order to provide a uniform conceptual framework, and compare our different hypotheses, in this thesis I used a common theoretical approach based on the statistical optimality of multisensory integration (see sections 1.3). The extended version of the “Concurrent Model” that I developed is indeed able to predict the statistically optimal sensory processing for each of the categories of proprioceptive and visual compensation assessments of section 2.1. The same model can also be used for the tasks of our experimental studies on the effect of sensory transformations on visuo-proprioceptive integration (section 2.2) and on the gravitational influence on sensory transformations (section 2.3). In this chapter, I will present the characteristics of the “Extended Concurrent Model” and its application to the three studies mentioned above.

### **3.1 Extended Concurrent Model**

The Extended Concurrent Model, represented in Figure 3-1, differs from the original version (section 1.3.2) by the fact that it explicitly distinguishes between the reference frames in which the sensory signals are natively encoded (the joint,  $J$ , and the retinal,  $R$ , reference frames for proprioception and vision respectively) and the reference frames which correspond to a combination of the original sensory signal about target and response position, with additional sensory information. For instance, the hand position perceived through joint receptors can be encoded with respect to different body parts or even with respect to external references, such as gravity or visual landmarks (Tagliabue and McIntyre, 2014), necessitating sensory transformations. To refer to this type of indirect sensory encodings we use the generic term “extra-joint”,  $ExJ$ , for proprioception and “extra-retinal”,  $ExR$ , for vision (see section 1.2.2).

Although both visual and proprioceptive information can potentially be encoded in multiple ‘extra-’ reference frames, we have reduced the model formulation to its simplest version allowing

an accurate description of the sensory processing underlying the analyzed tasks. A more complex model, such as the fully concurrent model proposed by Tagliabue and McIntyre (2014) (Figure 6 of the article) could have been more accurate, but computational and numerical constraints imposed the use of this simplified, yet useful, formulation.



As shown in Figure 3-1, the Extended Concurrent Model includes four target-response comparisons:  $\Delta J$ ,  $\Delta R$ ,  $\Delta ExJ$ ,  $\Delta ExR$ . The variability associated with these four concurrent comparisons is a function of the sensory noise of the joint (J) and/or the retinal (R) signals and of the potential sensory transformations  $T_{J \rightarrow R}$ ,  $T_{R \rightarrow J}$ ,  $T_{J \rightarrow ExJ}$ ,  $T_{R \rightarrow ExR}$ .

The optimal movement vector  $\Delta$  corresponds to the weighted sum of the four target-response comparisons ( $\Delta J$ ,  $\Delta R$ ,  $\Delta ExJ$ , and  $\Delta ExR$ ) with the sensory weights  $w_{\Delta J}$ ,  $w_{\Delta ExJ}$ ,  $w_{\Delta R}$ , and  $w_{\Delta ExR}$ , which are determined to minimize the variance of the movement vector  $\sigma_{\Delta}^2$ . For all tasks, once the movement vector is estimated, the motor system generates the muscle activations necessary to displace the hand (or activate the joystick to control the haptic handle) in the defined direction and distance. This step introduces some additional noise, that we will call motor noise,  $\sigma_{NM}^2$ , so that the variance of the movement execution is  $\sigma_{ME}^2 = \sigma_{\Delta}^2 + \sigma_{NM}^2$ . There might be additional factors, such as working memory, concentration, and fatigue, that can contribute to the movement execution variability. For sake of simplicity, the present version of the model does not include them separately and they are all combined together in the  $\sigma_{NM}^2$  term.

Our statistical model will predict the optimal set of four weights and the resulting variance for each of sensory tasks that will be investigated in this thesis. In the following sections, to improve readability, I will only use graphical representations of the model predictions representing the information flow theoretically associated with each experimental task. The analytical equations of the sensory weights and variability of the optimal movement vector, as well as computational details are reported in Appendix D (see Supplementary Materials of Bernard-Espina et al., 2021).

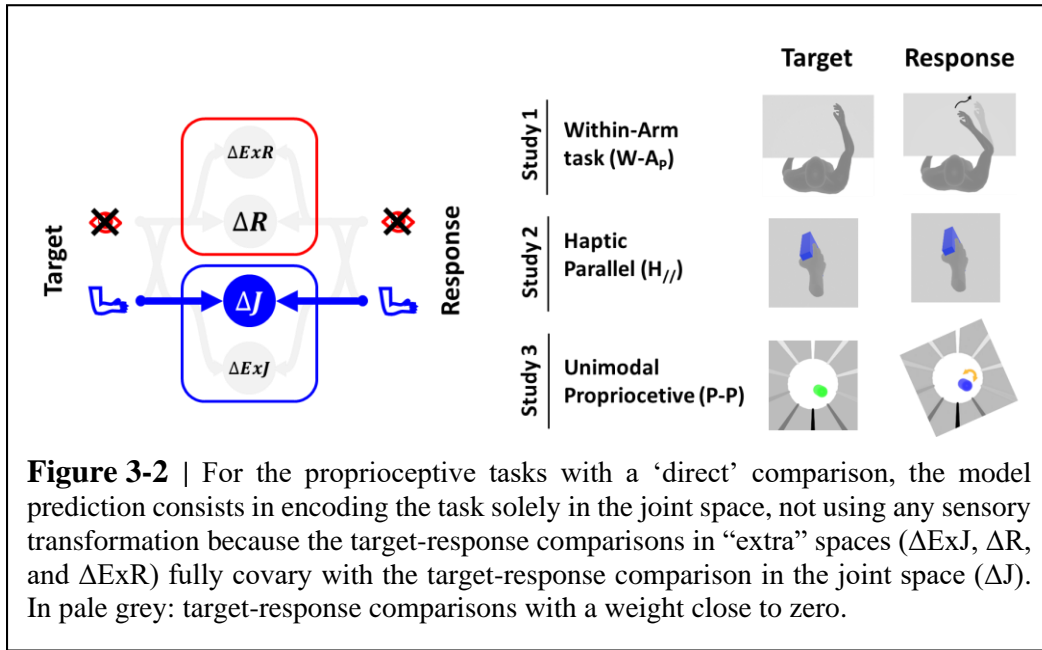
### **3.2 Application of the model for proprioceptive tasks**

We distinguish here two main types of uni-modal proprioceptive tasks: tasks in which the joint signals from the target and the response can be compared in the native “Joint” reference, and tasks in which the target-response comparison necessitates the re-encoding of the joint signals in “Extra-Joint” reference frames.

#### ***Uni-modal proprioceptive tasks without the necessity of sensory transformations***

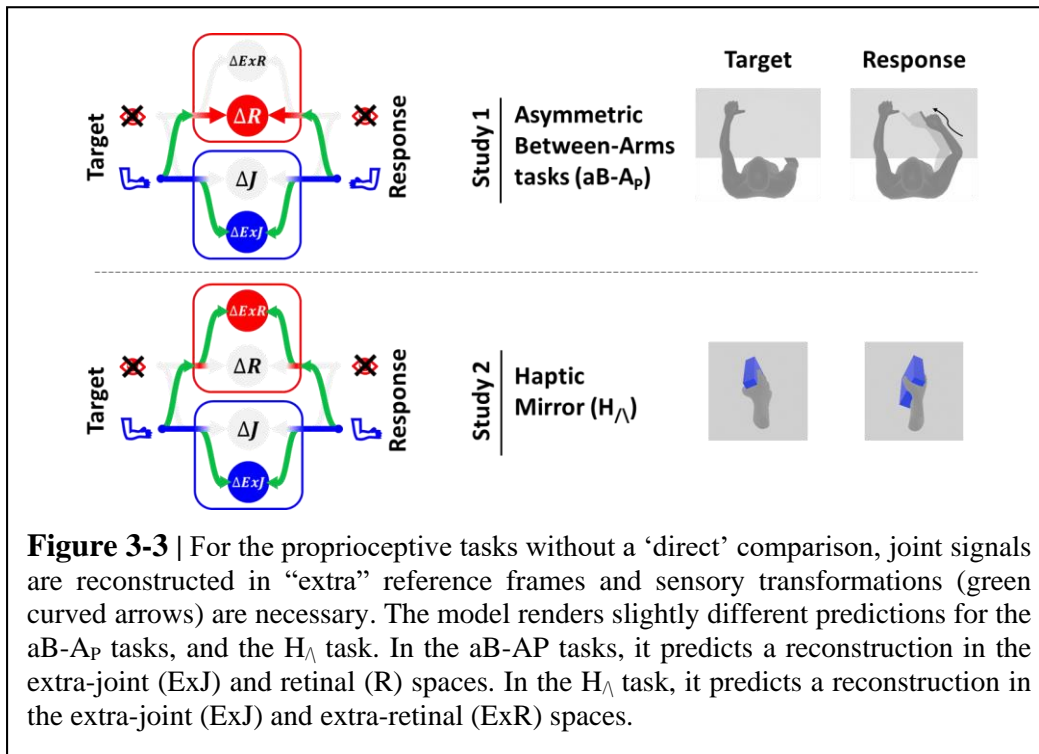
These tasks include the within-arm proprioceptive, W-AP assessment tasks (section 2.1.2), the uni-modal haptic parallel, H// task (section 2.2.2) and the uni-modal proprioceptive, P-P task (section 2.3.2). In these tests, because the target and the response positions/orientations correspond to the same joints' configuration, and hence to the same joint signals (Arnoux et al., 2017; Tagliabue

and McIntyre, 2013, 2011), they can be compared ‘directly’ in the joint space  $J$ , without sensory transformations. The optimal information flow predicted is represented in Figure 3-2.



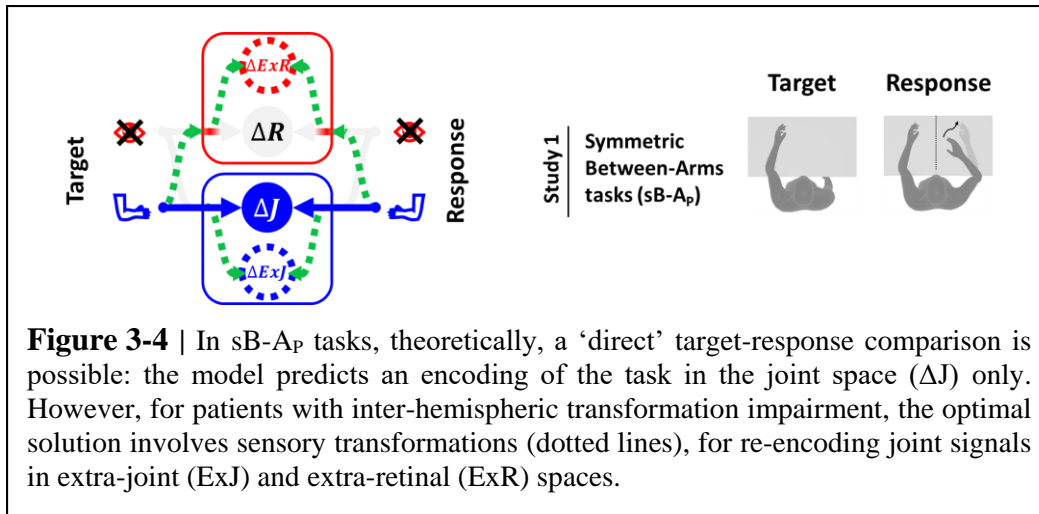
***Uni-modal proprioceptive tasks with the necessity of sensory transformations***

These tasks include the asymmetric between-arms proprioceptive assessment, aB-A<sub>p</sub> tasks (section 2.1.2), and the uni-modal haptic mirror, H<sub>∧</sub> task (section 2.2.2). In these tests the target and the response position/orientation do not correspond to the same joint signals. In the aB-A<sub>p</sub> tasks, the left and right arms are not in the same configuration. In the H<sub>∧</sub> task, even though this is a within-arm test, the hand orientation during target memorization and the response phase are different (mirrored). Thus, the target and the response position/orientation cannot be compared ‘directly’ in the joint space  $J$ . The optimal sensory weighting predicted by our model consists in encoding the target and response position/orientation perceived through proprioception in alternative reference frames, rather than in joint space (see Figure 3-3). As a result, the predicted variability of the response is higher than for the proprioceptive tasks without sensory transformations represented in Figure 3-2. As shown in Figure 3-3, the model predicts two different ‘visual reconstruction’ for the aB-A<sub>p</sub> and H<sub>∧</sub> tasks. This is due to the fact that only in the former target and response have the same spatial location/orientation.



***Uni-modal proprioceptive tasks with potential sensory transformations***

These tasks include the symmetric between-arms proprioceptive, sB-A<sub>p</sub>, assessment tasks (section 2.1.2). As shown in Figure 3-4, the model predicts a signal flow very similar to the one predicted for the proprioceptive tasks without sensory transformations (Figure 3-2). These similarities appear to be due to the same joint configuration of the arm holding the target and the arm performing the movement when achieving sB-A<sub>p</sub> tasks. Hence, the movement can be controlled by a ‘direct’ comparison between proprioceptive signals from homologous joints of the two limbs. Figure 3-4 reports also the information flow predicted by our model for patients with difficulties in performing inter-hemispheric transformations (dashed lines): an encoding of the information also in extra-joint and extra-retinal spaces. The encoding of the information in the retinal reference is not used, because target and response do not have the same spatial location.

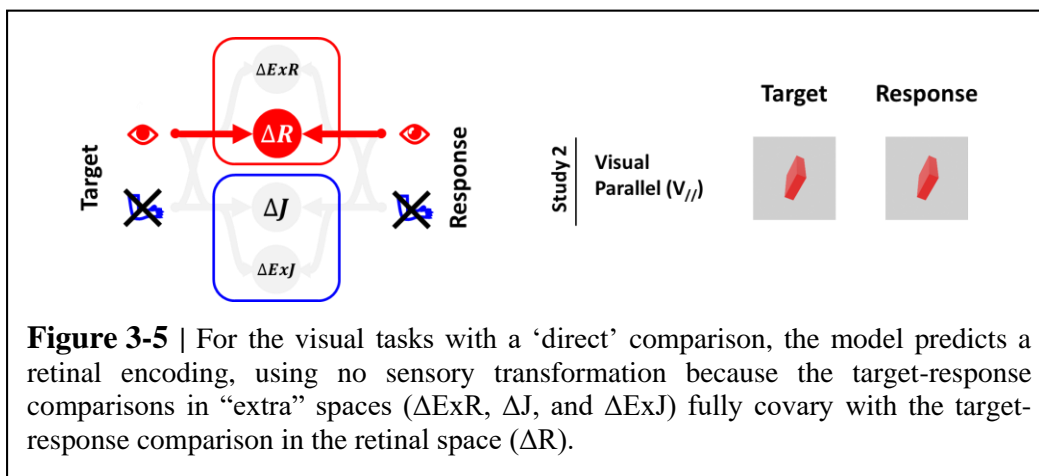


### 3.3 Application of the model for visual tasks

We distinguish here two main types of uni-modal visual tasks: tasks in which the visual signals of the target and the response can be compared in the native “Retinal” reference, and tasks in which the target-response comparison necessitate the re-encoding of the visual signals in “Extra-Retinal” reference frames.

#### *Uni-modal visual tasks without the necessity of sensory transformations*

These include the uni-modal visual parallel,  $V_{//}$  task (section 2.2.2), in which the target and response images on the retina can be compared directly. The optimal information flow predicted by the model is represented in Figure 3-5.

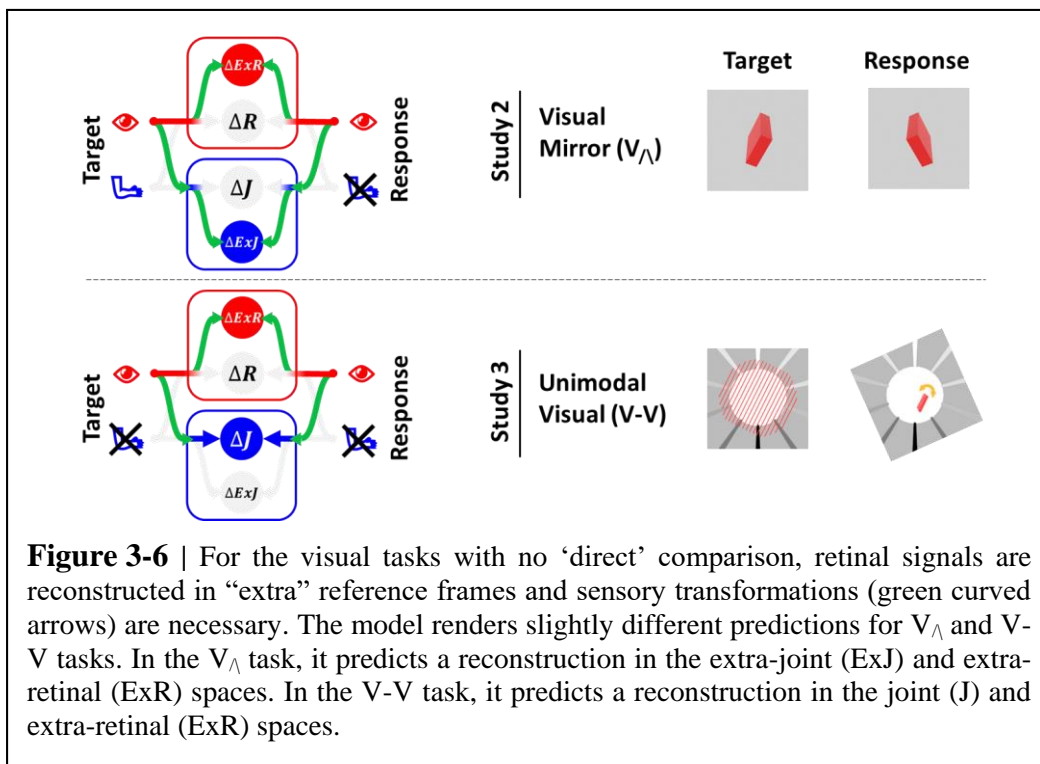


*Uni-modal visual tasks with the necessity of sensory transformations*

These tasks include the uni-modal visual mirror,  $V_{\wedge}$  task (section 2.2.2), and the uni-modal visual, V-V task (section 2.3.2). In these tests, the target and response images on the retina cannot be compared directly (see Figure 3-6) because:

- In the  $V_{\wedge}$  task, the mirror spatial transformation results in a different orientation of target and response on the retina.
- In the V-V task, due to the head rotation after target acquisition, the orientation of the response and of the memorized target do not have the same orientation on the retina.

Therefore, the model predicts that the target and response position/orientation is encoded in alternative reference frames, rather than in the retinal space (see Figure 3-6). As a result, the predicted variability of the response is higher than for the visual tasks without sensory transformations represented in Figure 3-5.

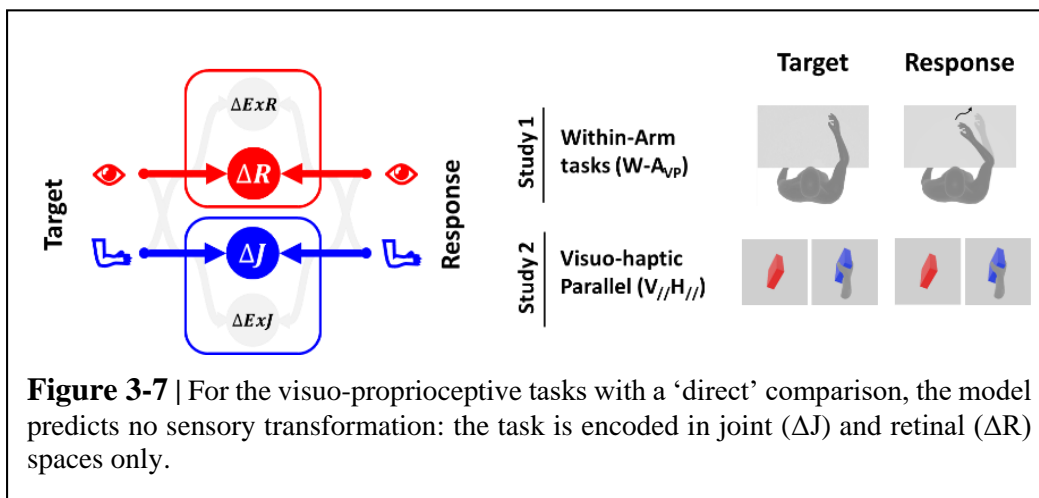


### 3.4 Application of the model for visuo-proprioceptive tasks

We distinguish here three main types of multi-modal visuo-proprioceptive tasks: 1) tasks in which both proprioceptive and visual signals of the target and the response can be compared in the native “Joint” and “Retinal” reference frames respectively, 2) tasks necessitating the re-encoding of the visual signals in “Extra-Retinal” reference frames, and 3) tasks necessitating the re-encoding of the joint signals in “Extra-Joint” reference frames.

#### *Multi-modal visuo-proprioceptive tasks without the necessity of sensory transformations*

These tasks include the within-arm visuo-proprioceptive, W-A<sub>VP</sub> tasks (section 2.1.2), and the visuo-haptic parallel, V//H// task (section 2.2.2). In these tests the target and the response have the same position/orientation. Therefore, they can be compared ‘directly’ in both joint, *J*, and retinal, *R*, space. The optimal information flow predicted by the model is represented in Figure 3-7 and it results in a variance of the movement vector smaller than both proprioceptive and visual unimodal tasks (Figure 3-2 and Figure 3-5 respectively).

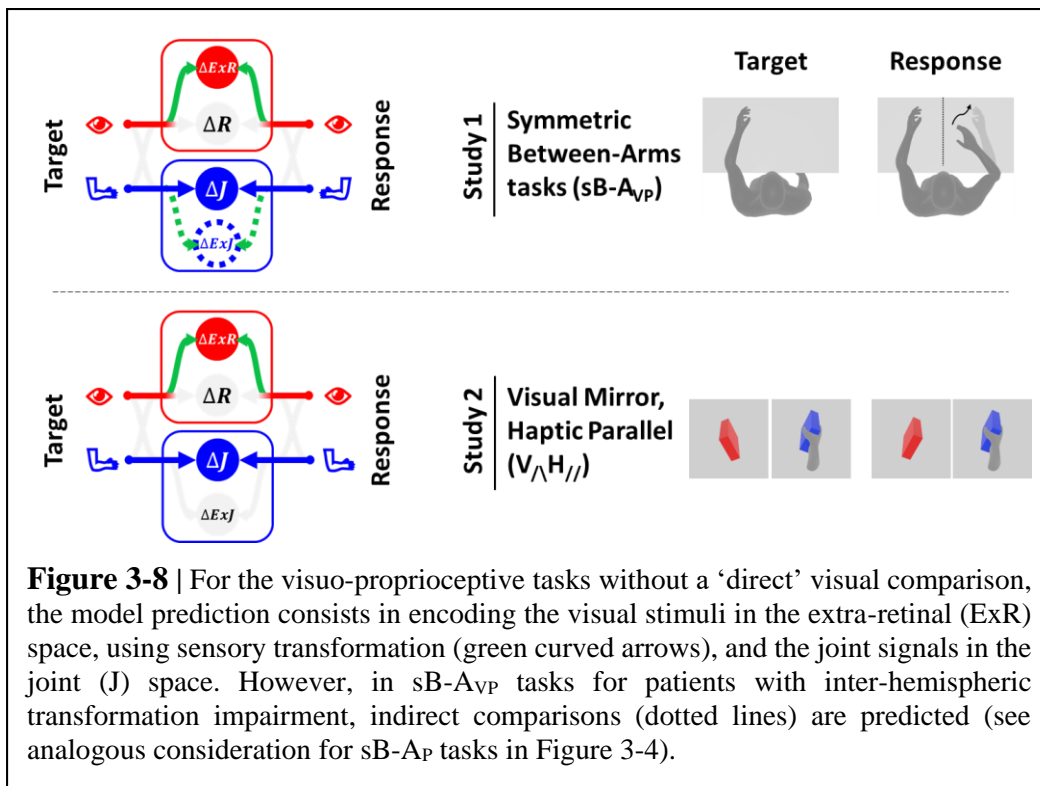


#### *Multi-modal visuo-proprioceptive tasks with the necessity of sensory transformations for the retinal signals*

These tasks include the symmetric between-arms visuo-proprioceptive, sB-A<sub>VP</sub> tasks (section 2.1.2), and the multisensory visuo-haptic mirror visual, V<sup>^</sup>H// task (section 2.2.2). In these

**Common theoretical approach: Application of the model for visuo-proprioceptive tasks**

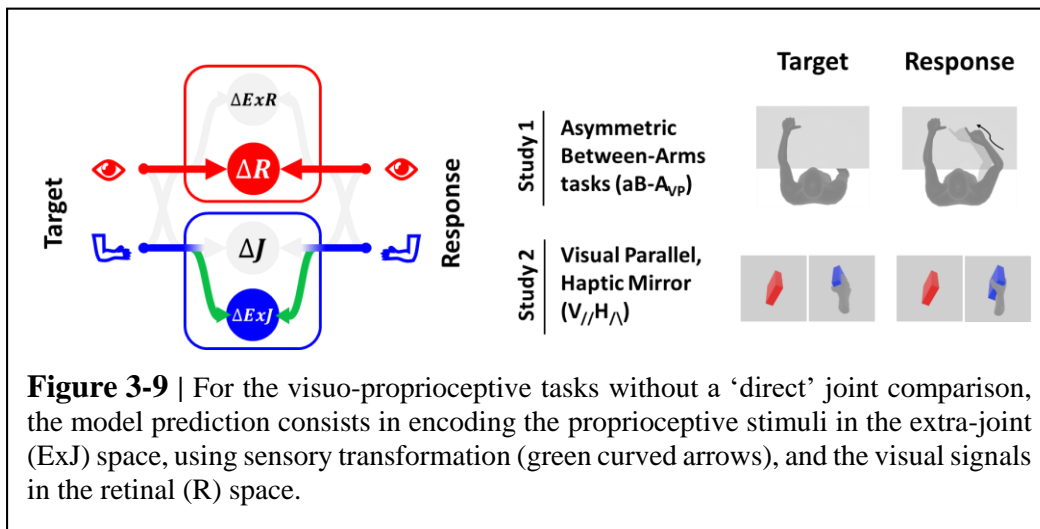
tests the target and the response do not have the same visual position/orientation, hence their position/orientation cannot be compared ‘directly’ in the retinal space  $R$ . Regarding the joint signals, the memorized target and the response positions/orientations are perceived through homologous (for sB-A<sub>VP</sub>) or the same set of joint sensors (for V<sub>//</sub>H<sub>//</sub>). Thus, their position/orientation can be compared ‘directly’ in the joint space  $J$  (Figure 3-8). Due to the visual sensory transformation, the model predicts a larger variability of the visual comparison compared to the visuo-proprioceptive tasks without sensory transformations (see Figure 3-7). This has two consequences: first, the variability of the movement vector increases; second, the visual weight decreases.



**Multi-modal visuo-proprioceptive tasks with the necessity of sensory transformations for the joint signals**

These tasks include the asymmetric between-arms visuo-proprioceptive, aB-A<sub>VP</sub> tasks (section 2.1.2), and the visuo-haptic mirror haptic, V<sub>//</sub>H<sub>//</sub> task (section 2.2.2). In these tests the target

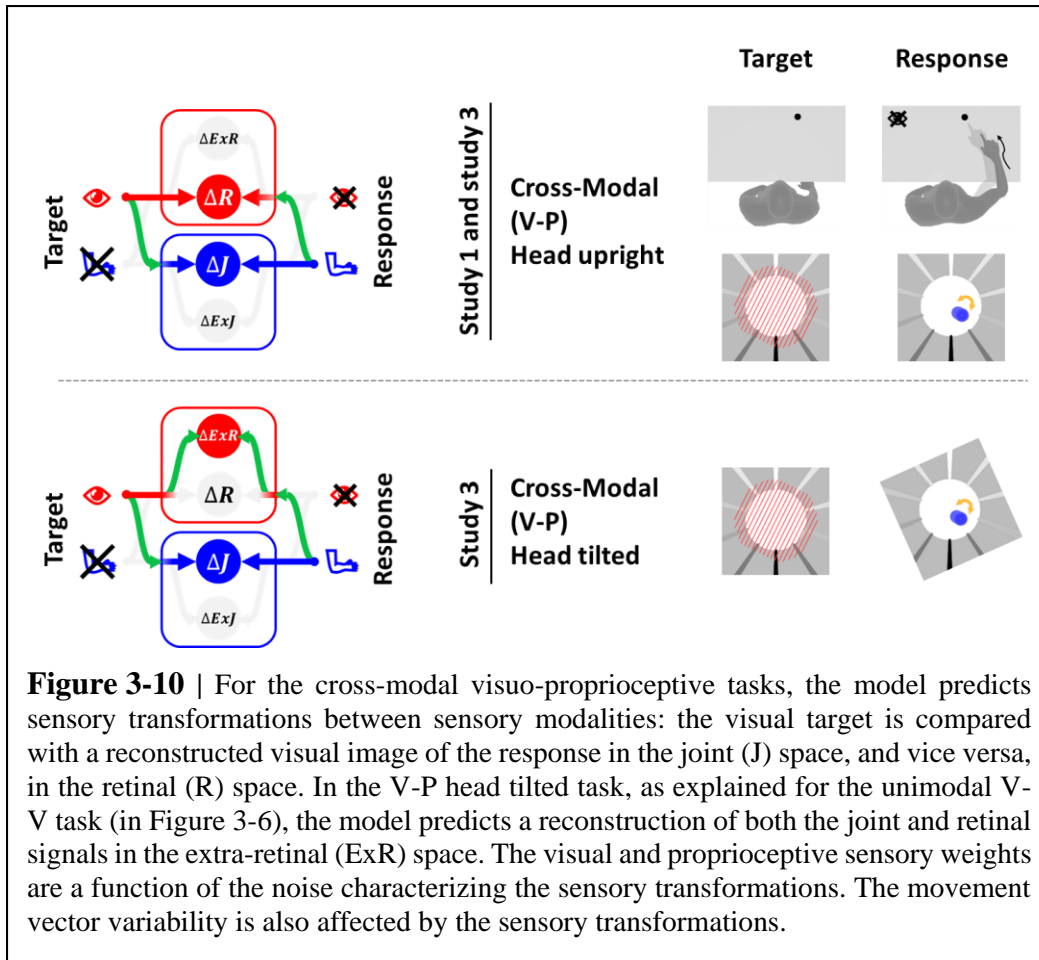
and the response have the same position/orientation in the retinal space  $R$ . However, the target and the response position/orientation do not correspond to the same joint configuration. As explained for the proprioceptive tasks involving sensory transformations, their position/orientation cannot be compared ‘directly’ in the joint space  $J$  (Figure 3-9). Due to the proprioceptive transformation the model predicts a larger variability of the proprioceptive comparison compared to the visuo-propriceptive task without sensory transformations (see Figure 3-7). This has two consequences: an increase of the variability of the movement vector, and an increase of the visual weight.



### 3.5 Application of the model for cross-modal tasks

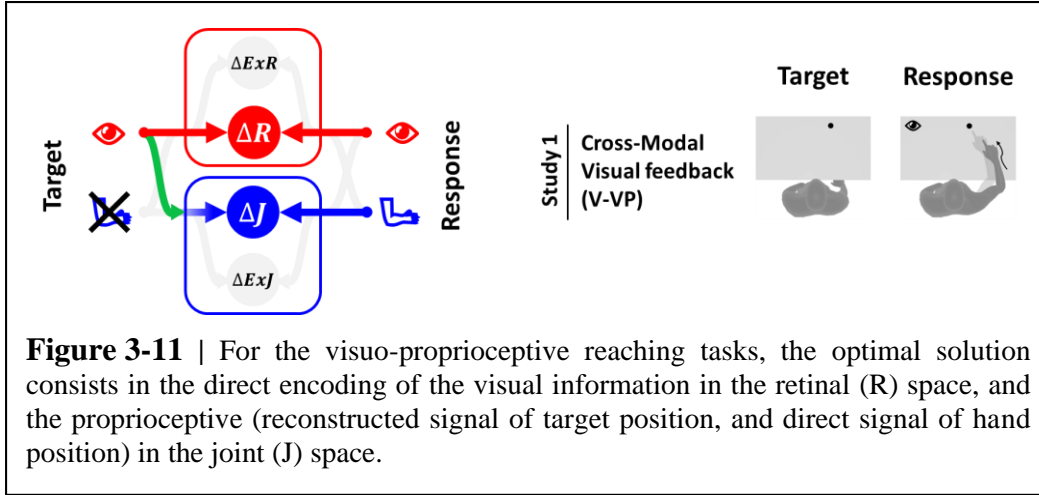
#### *Cross-modal visuo-propriceptive tasks (proprioceptive reaching of a visual target)*

This category of tasks includes the cross-modal visuo-propriceptive, V-P tasks (sections 2.1.2 and 2.3.2). These tasks involve a visually memorized target which the patient/subject has to match with the unseen hand: no direct comparison is possible between the target and the response. The model predictions are shown in Figure 3-10.



***Visuo-proprioceptive reaching of a visual target***

The V-VP tasks are investigated in the first study “Reinterpretation of the stroke literature on proprioceptive deficits” (section 2.1.2). Both visual and proprioceptive inputs are available while positioning/orienting the hand with respect to the visually acquired target. A direct comparison is possible between the target and response in the retinal space, but no direct comparison is possible in joint space (Figure 3-11). As a consequence, the visual sensory weight increases, and the variability of the movement vector decreases compared to the cross-modal V-P task (Figure 3-10)



### 3.6 Description of the model fitting procedures

We assessed the ability of the model to describe our experimental data. For this purpose, we fitted the model results to the experimental data, using Matlab® built-in “fmincon” function (R2019b, with the Optimization Toolbox) to minimize the *l2-norm* of the fitting errors, represented by the following cost function *cf*:

$$cf = \sum_{i=1}^n (\sigma_{exp_i}^2 - \sigma_{th_i}^2)^2 + \sum_{i=1}^m (\omega_{Vexp_i} - \omega_{Vth_i})^2 \quad \text{Equation 13}$$

where *n* is the number of tasks under consideration for which we have both experimental values and a model predictions of the variance ( $\sigma_{exp_i}^2$  and  $\sigma_{th_i}^2$  respectively). *m* is the number of tasks for which both experimental value and model prediction of the visual weight are available ( $\omega_{Vexp_i}$  and  $\omega_{Vth_i}$ ). For each experimental task,  $\sigma_{exp_i}^2$  and  $\omega_{Vexp_i}$  were averaged across all subjects, to filter the noise of the data due to experimental variability, and thus avoiding individual noise fitting.

In order to avoid data overfitting, the number of independent variables in the model was reduced to the lowest possible number to test the specific hypothesis of the three studies.

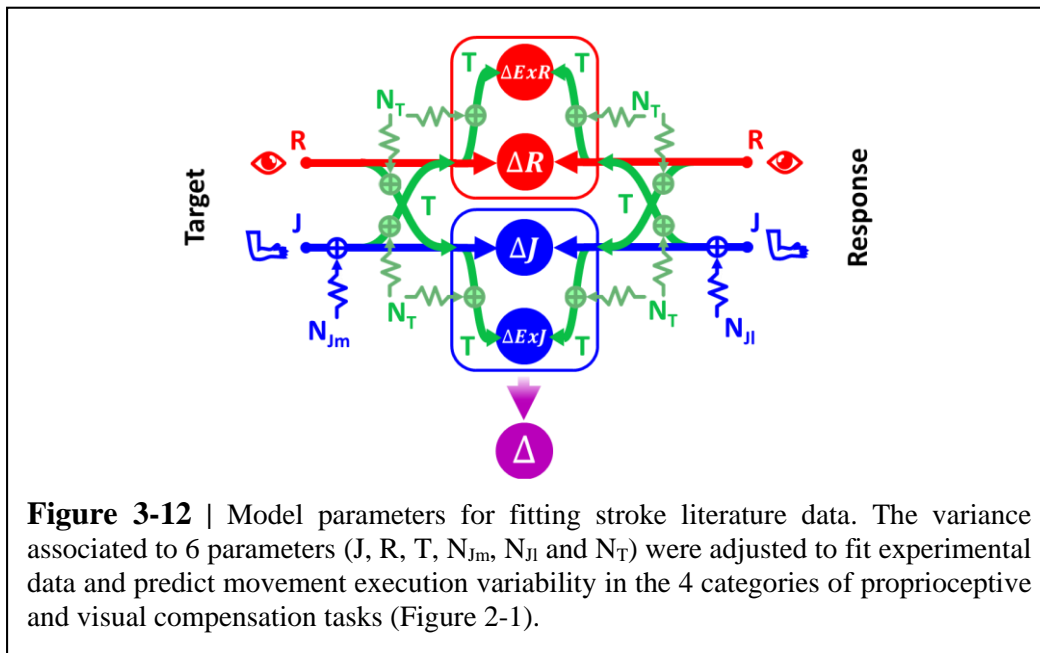
When different hypothesis were tested (see sections 3.6.2 and 3.6.3), in order to statistically test whether the predictions of the various hypotheses differed from the experimental data, a multivariate Hotelling’s  $T^2$  test was performed.

**3.6.1 Fitting quantitative data from the stroke literature (Study 1)**

The following parameters were used to predict the performance of healthy subjects and stroke patients in the proprioceptive and visual compensation assessment tasks (Figure 3-12):

- $\sigma_J^2$ : variability of joint signals,  $J$ .
- $\sigma_R^2$ : variability of retinal signals,  $R$ .
- $\sigma_T^2$ : noise introduced by sensory transformations,  $T$ .
- $\sigma_{N_{J_m}}^2$ : additional noise in the more affected arm due to stroke,  $N_{J_m}$ .
- $\sigma_{N_{J_l}}^2$ : additional noise in the less affected arm due to stroke,  $N_{J_l}$ .
- $\sigma_{N_T}^2$ : additional noise associated to sensory transformation due to stroke,  $N_T$ .

Even though the motor noise plays a role in many of the analyzed stroke assessments, the diversity of the assessment methods that were included (with some that are purely perceptive, without motor nor memory components), made impossible to use the parameter  $\sigma_{N_M}^2$  to systematically account for the motor noise (see section 3.1).



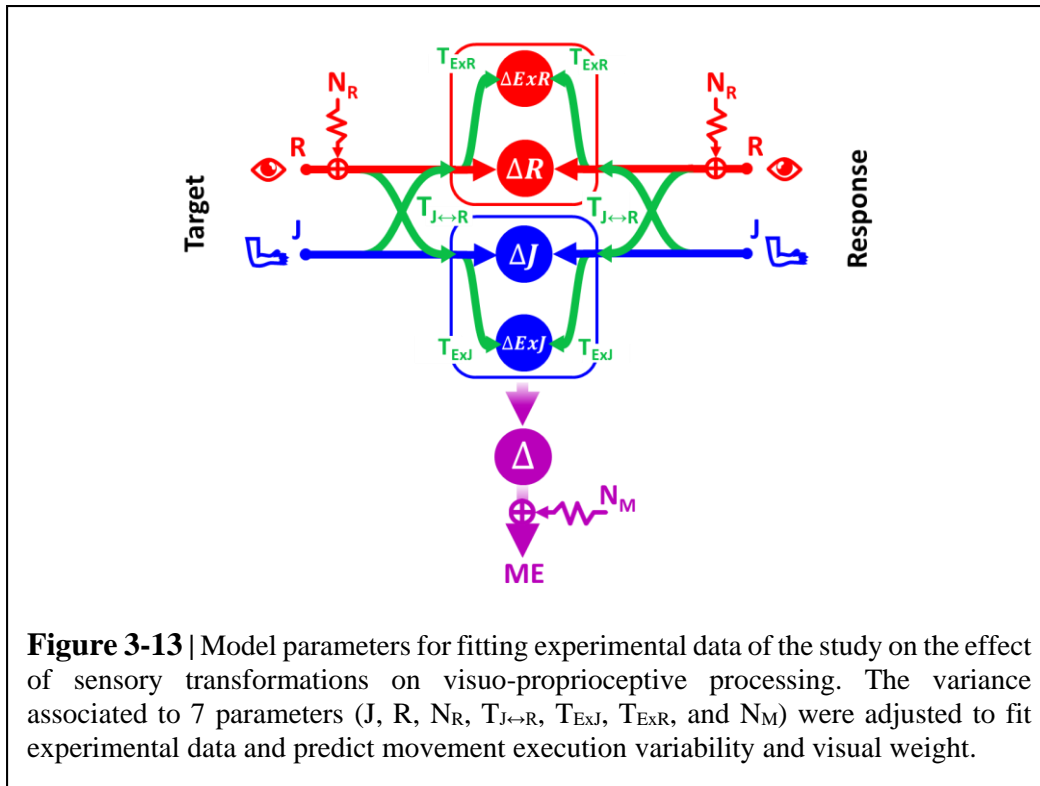
This model aims to test the hypothesis that, while some patients have proprioceptive deficits only ( $\sigma_{N_{Jm}}^2$  and  $\sigma_{N_{Jl}}^2 > 0$  and  $\sigma_{N_T}^2 = 0$ ), other patients might have sensory deficits affecting the sensory transformations specifically ( $\sigma_{N_{Jm}}^2 = \sigma_{N_{Jl}}^2 = 0$  and  $\sigma_{N_T}^2 > 0$ ), or might have combined proprioceptive and sensory transformations deficits ( $\sigma_{N_{Jm}}^2, \sigma_{N_{Jl}}^2$  and  $\sigma_{N_T}^2 > 0$ ).

Given that in our quantitative analysis of the data from the stroke literature we included the variance of 17 different assessment tasks, and none for the sensory weight ( $n=17$  and  $m=0$  in Equation 13), for this study 17 experimental data were fitted by adjusting 7 model parameters.

### **3.6.2 Fitting experimental data of the study on the effect of sensory transformations on visuo-proprioceptive processing (Study 2)**

To predict the effect of sensory transformations in the unimodal haptic and visual tasks, and in the multisensory visuo-haptic tasks, the following parameters were used (Figure 3-13):

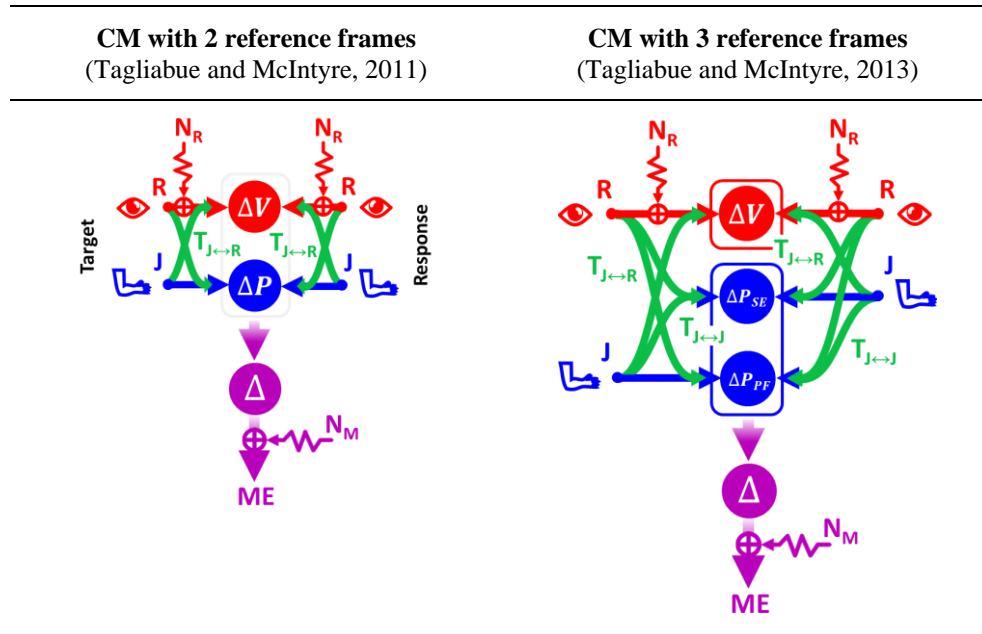
- $\sigma_J^2$ : variability of joint signals,  $J$ .
- $\sigma_R^2$ : variability of retinal signals,  $R$ .
- $\sigma_{N_R}^2$ : variability of the artificial noise  $N_R$  added to the retinal signals.
- $\sigma_{T_{J \leftrightarrow R}}^2$ : noise due to sensory transformations,  $T_{J \leftrightarrow R}$ , between the joint and retinal spaces.
- $\sigma_{T_{ExR}}^2$ : noise due to sensory transformations,  $T_{ExR}$ , from retinal to extra-retinal space.
- $\sigma_{T_{ExJ}}^2$ : noise due to sensory transformations,  $T_{ExJ}$ , from joint to the extra-joint space.
- $\sigma_{N_M}^2$ : motor noise.



The cost function for the fitting procedure took into consideration both response variability and visual weight estimations (see Equation 13): the variance was assessed for all unimodal visual and haptic and multisensory visuo-haptic tasks ( $n=12$  data points), and the visual sensory weight for the multisensory visuo-haptic tasks only ( $m=6$ ). It follows that 7 parameters of the model were optimized to fit 18 experimental data.

In order to appreciate the effectiveness of the extended concurrent model (with four reference frames) and the necessity of using it, we compared its predictions to those of two alternative models: the ‘original’ concurrent model as described in section 1.3.2 (Tagliabue and McIntyre, 2011) which has two reference frames (for visual and proprioceptive target-response comparisons), and a slightly more complex concurrent model with three reference frames (for visual, proprioceptive ‘direct’ and proprioceptive ‘indirect’ target-response comparisons) (see Figure 7 of Tagliabue and McIntyre, 2013). These two alternative models are described in Table 3-1. Details about their predictions for each experimental task are presented in Appendix B.

**Table 3-1** | Representation of the two alternative Concurrent Models (CM). The CM with 2 reference frames does not take into account the mirror symmetry in the proprioceptive and visual target-response comparison in the tasks under investigation here: the sensory transformations  $T_{J \leftrightarrow R}$  were not present in the final equations (see Appendix B). The variance associated to 4 parameters (J, R,  $N_R$ , and  $N_M$ ) were adjusted to fit experimental data. The CM with 3 reference frames takes into account the mirror symmetry only for the proprioceptive target-response comparison. The variance associated to 6 parameters (J, R,  $N_R$ ,  $T_{J \leftrightarrow R}$ ,  $T_{J \leftrightarrow J}$  and  $N_M$ ) were adjusted to fit experimental data.

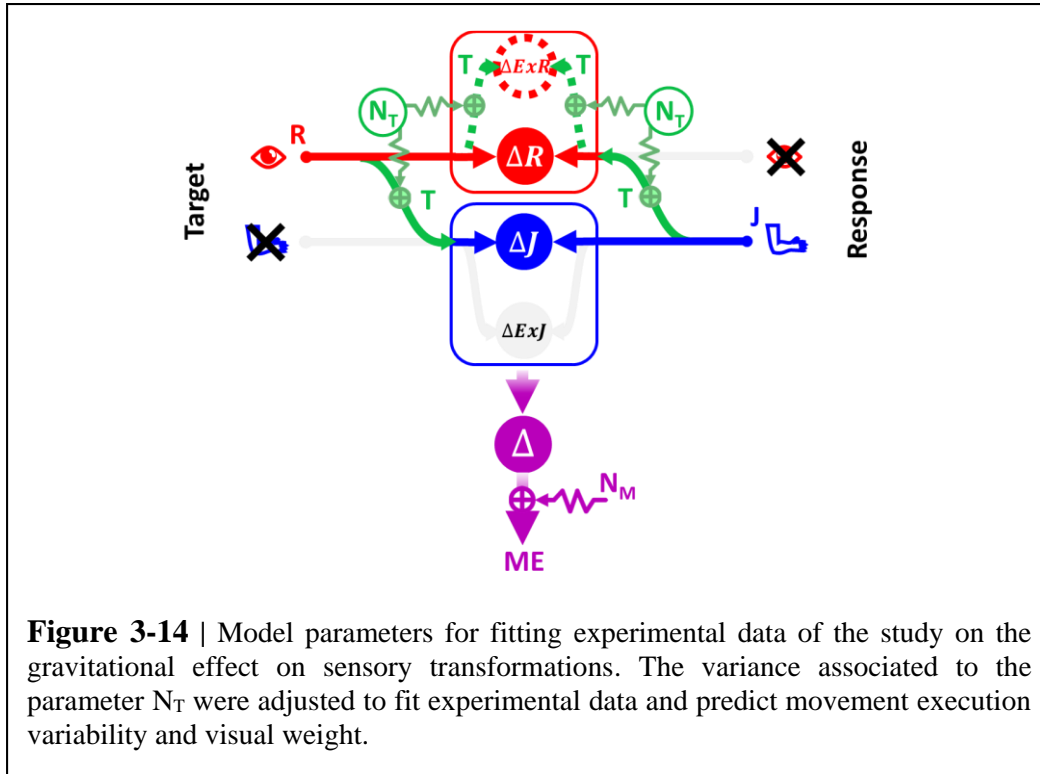


### 3.6.3 Fitting experimental data of the study on gravitational influence on sensory transformations (Study 3)

To simulate the effect of head inclination with respect to gravity or of neck flexion on the information processing, the following parameters was used (see Figure 3-14):

- $\sigma_{N_T}^2$  : additional noise associated to the cross-modal sensory transformations.

The value of the other model parameters was determined from the literature, or did not affect the predictions.



In order to specifically test the effect of posture on sensory transformations, with the three hypothesis (Neck1 Hp, Neck2 Hp and Gravity Hp detailed in section 2.3), we compared the observed effect of posture on the response variability,  $\Delta Var^2 = Var_{Supine}^2 - Var_{Seated}^2$ , and on the response deviation due to visual scene rotation,  $\Delta \omega_V = \omega_{V,Supine} - \omega_{V,Seated}$ , with corresponding equations of the model for the movement execution variability,  $\Delta \sigma_{ME}^2 = \sigma_{ME,Supine}^2 - \sigma_{ME,Seated}^2$ , and for the weight associated with visual representation of the task.

In fact, using  $\Delta \sigma_{ME}^2$  allows to reduce the number of parameters to two:  $\sigma_M^2$ ,  $\sigma_R^2$  and  $\sigma_J^2$  are simplified in the subtraction, and only the parameters  $\sigma_T^2$  and  $\sigma_{N_T}^2$  remain. To reduce further the number of parameters, and thus the possibility of overfitting the experimental data, the value of  $\sigma_T^2$  is set to  $23.19^{o^2}$ : a variance (in degrees squared) that is computed from the results of Tagliabue and McIntyre (2011). Therefore, for each of the three hypotheses only the parameter  $\sigma_{N_T}^2$  was adjusted to try to fit the modulation of the response variability and of visual weighting due to the posture in the 3 experimental conditions (6 data points). Computational details, with the detailed equations for the three hypothesis, are available in Appendix D (see Supplementary Materials of Bernard-Espina et al., 2022).

## **4 Results**

### **4.1 Study 1 – Reinterpretation of the stroke literature on proprioceptive deficits**

The first study aimed to provide a new classification of the sensory assessment tasks and an improved stratification of stroke patients with proprioceptive deficits. We compared quantitative data from the literature on stroke proprioceptive assessments, and, based on our theoretical approach described in the previous section 3.6.1, we predicted the performance of stroke patients in various assessment methods based on the nature of their sensory deficits (that is purely proprioceptive or affecting sensory transformations). Finally, we related the different types of sensory deficits to the location of brain lesions.

#### **4.1.1 Categorization of proprioceptive and visual compensation assessments**

As described in the methods (section 2.1.3), in order to be able to compare the experimental data and present the results from different studies on the same plots, among the numerous studies that can be found in the literature, only experiments that compared at least two of the four categories of tasks (Within-arm, Asymmetric between-arms, Symmetric between-arms and Cross-modal), or performance of patients and healthy subjects could be included.

Table 4-1 shows the normalized variance (see section 2.1.3) associated with each category of tasks for healthy subjects. The results show that, in the proprioceptive tasks, the precision in the Symmetric Between-Arms tasks (sB-A<sub>P</sub>) is similar to the Within-Arm tasks (W-A<sub>P</sub>). Both Asymmetric Between-Arms tasks (aB-A<sub>P</sub>) and Cross-Modal tasks (V-P) appear less precise compared to the Within-Arm tasks. Regarding the visuo-proprioceptive (visual compensation) tasks, all are more precise compared to the Within-Arm proprioceptive tasks, although for the Symmetric Between-Arms visuo-proprioceptive tasks (sB-A<sub>VP</sub>) the addition of vision does not increase precision as much as in the other visual compensation tasks.

**Results: Study 1 – Reinterpretation of the stroke literature on proprioceptive deficits**

**Table 4-1** | Performance variability reported in studies involving healthy subjects. W-A: Within-Arm, aB-A: Asymmetric Between-Arms, sB-A: Symmetric Between-Arms, V-P: Cross-Modal task (visual target-proprioceptive response). P and VP subscripts refer to proprioceptive and visuo-proprioceptive (that is visual compensation) assessments respectively.

| Study \ Task     | W-A <sub>P</sub> | aB-A <sub>P</sub> | sB-A <sub>P</sub> | V-P            | W-A <sub>VP</sub> | aB-A <sub>VP</sub> | sB-A <sub>VP</sub> | V-VP           |
|------------------|------------------|-------------------|-------------------|----------------|-------------------|--------------------|--------------------|----------------|
| Van Beers 1996   |                  |                   |                   | 1.6            |                   |                    |                    |                |
| Ernst 2002       | 1                |                   |                   |                | 0.2               |                    |                    |                |
| Butler 2004      | 1                | 1.1               |                   | 1.2            |                   |                    |                    |                |
| Monaco 2010      |                  | 1.9               |                   |                |                   | 0.4                |                    | 0.4            |
| Tagliabue 2011   | 1                |                   |                   | 1.1            |                   |                    |                    | 0.6            |
| Torre 2013       | 1                |                   |                   |                | 1                 |                    |                    |                |
| Khanafar 2014    |                  |                   |                   | 1.5            |                   |                    |                    |                |
| Cameron 2015     |                  |                   |                   |                |                   |                    |                    | 0.8            |
| Arnoux 2017      | 1                | 2.3               | 1.1               |                |                   |                    |                    |                |
| Herter 2019      |                  |                   |                   |                |                   |                    | 0.9                |                |
| Marini 2019      | 1                |                   |                   |                | 0.4               |                    |                    |                |
| <b>mean(±SD)</b> | <b>1</b>         | <b>1.8±0.6</b>    | <b>1.1</b>        | <b>1.3±0.2</b> | <b>0.5±0.4</b>    | <b>0.4</b>         | <b>0.9</b>         | <b>0.6±0.2</b> |

Table 4-2 reports the performance of stroke patients in the same assessment tasks, normalized with respect to the W-A<sub>P</sub> task performance of healthy subjects. The results reported in this table allow to distinguish between 3 types of stroke patients:

- (P) Patients with proprioceptive deficits only. In these patients only the noise of the proprioceptive joint signals is increased with respect to healthy subjects. Although their performances in all proprioceptive tasks should be affected compared to healthy subjects, they should have no difficulties to visually compensate for their proprioceptive deficits in any type of tasks, even in the Symmetric Between-Arms visual compensation tasks (sB-A<sub>VP</sub>): as shown in section 3.4 (Figure 3-8), the sB-A<sub>VP</sub> involves the (mirror) transformation of the visual signals, therefore, the visual compensation in this task relies on the patient’s sensory transformations abilities (which are preserved if the deficit is purely proprioceptive).
- (T) Patients with sensory transformation deficits only, for which only the noise associated to the sensory transformation is increased with respect to healthy subjects. Therefore, these patients should have no proprioceptive deficits in the Within-Arm tasks (W-A<sub>P</sub>), which do not require sensory transformations (section 3.2, Figure 3-2). However, they should have

**Results: Study 1 – Reinterpretation of the stroke literature on proprioceptive deficits**

difficulties in performing the other proprioceptive tasks (that involve sensory transformations: see section 3.2, Figure 3-3), and they should not be able to fully visually compensate in sB-A<sub>VP</sub> tasks (see section 3.4, Figure 3-8).

**(P+T)** For patients with combined proprioceptive and sensory transformations deficits. In these patients the noise is increased for both proprioception tasks and sensory transformations. Therefore, their performances should be affected in all proprioceptive assessment tasks as well as in sB-A<sub>VP</sub> visual compensation tasks (because they involve sensory transformations: see section 3.4, Figure 3-8).

**Table 4-2** | Performance variability reported in studies involving stroke patients. The symbols “<1” and “>1” represent qualitative results (improvement or deterioration of performance compared to control subjects, respectively) that were not used for the quantitative analysis. The column “Deficit?” proposes a possible type of deficit (or several) that would match the performance of patients in the different categories of tasks: proprioceptive deficit only (P), sensory transformation deficit only (T) and combined proprioceptive and sensory transformations deficit (P+T).

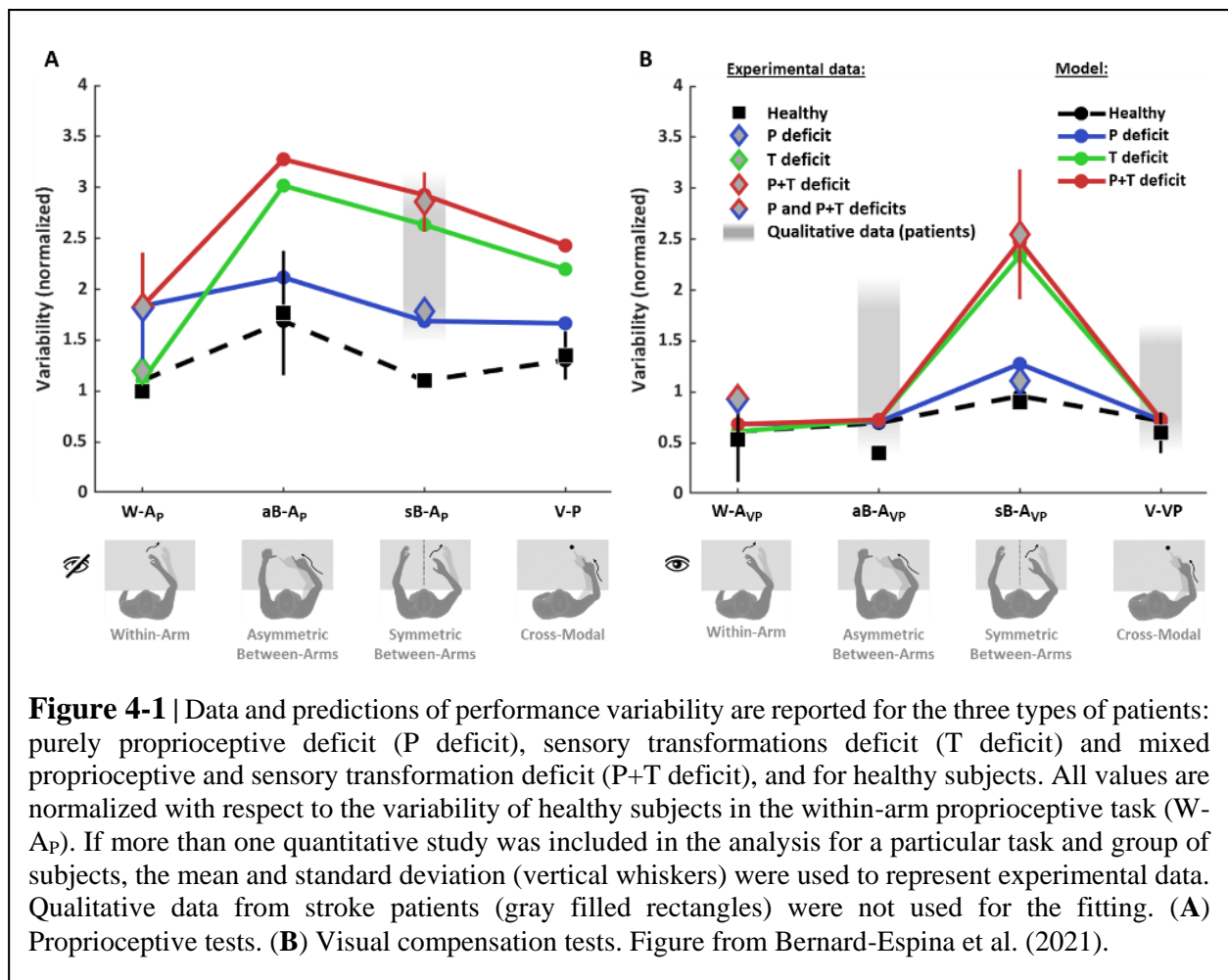
| Study             | Task | Proprioceptive Tasks |                   |                   |     | Visual Compensation Tasks |                    |                    |      | Deficit? |
|-------------------|------|----------------------|-------------------|-------------------|-----|---------------------------|--------------------|--------------------|------|----------|
|                   |      | W-A <sub>P</sub>     | aB-A <sub>P</sub> | sB-A <sub>P</sub> | V-P | W-A <sub>VP</sub>         | aB-A <sub>VP</sub> | sB-A <sub>VP</sub> | V-VP |          |
| Scalha 2011       |      |                      |                   |                   |     |                           |                    |                    |      | P/T/P+T  |
| Torre 2013        |      | 1.4                  |                   |                   |     | 0.9                       |                    |                    |      | P/P+T    |
| Dos Santos 2015   |      | 2.5                  |                   |                   |     |                           |                    |                    |      | P/P+T    |
| Contu 2017        |      | 1.4                  |                   |                   |     |                           |                    |                    |      | P/P+T    |
| Gurari 2017       |      | 1.2                  |                   | >1                |     |                           |                    |                    |      | T        |
| Rinderknecht 2019 |      | 1.9                  |                   |                   |     |                           |                    |                    |      | P/P+T    |
| Herter 2019 (a)   |      |                      |                   | 1.8               |     |                           |                    | 1.1                |      | P        |
| Herter 2019 (b)   |      |                      |                   | 3.0               |     |                           |                    | 3.0                |      | T/P+T    |
| Herter 2019 (c)   |      |                      |                   | 3.0               |     |                           |                    | 2.1                |      | T/P+T    |
| Ingemanson 2019   |      |                      |                   | 2.5               |     |                           |                    |                    |      | T/P+T    |

With the proposed categorization of proprioceptive (and visual compensation) tasks, the stratification of stroke patients based on the performance level in each category of tasks provides a new perspective for the comprehension of sensory deficits post-stroke. In the following sections, we analyze the faculty of our model to predict patient performance in the different types of tasks depending on the sensory deficit (section 4.1.2) and the correspondence between our predictions and functional anatomy studies (section 4.1.3).

**4.1.2 Reinterpretation of experimental observations based on our categorization**

Based on the described theoretical sensory information processing underlying the four categories of assessment tasks (see section 3 “Common theoretical approach”), we assess the ability of the model to capture the relevant experimental findings described in the previous section.

Figure 4-1 shows the comparison between the quantitative experimental data found in the literature and the prediction of the model for the four categories of proprioceptive tasks (Figure 4-1A) and for the same four tasks performed using vision to compensate for proprioceptive deficits (Figure 4-1B). The model predicts very different results for healthy subjects and for the three type of patients (P, T and P+T), depending on the task category.



## **Results: Study 1 – Reinterpretation of the stroke literature on proprioceptive deficits**

---

For healthy subjects, our model reproduces well the experimentally observed modulations of the precision among the eight tasks. In particular, the model correctly predicts that the asymmetric between-arms proprioceptive tasks (aB-AP) are the least precise (largest variability) among the proprioceptive tasks (Figure 4-1A) and that the symmetric between-arms visuo-proprioceptive tasks (sB-AVP) are the less precise among the tasks using vision (Figure 4-1B).

For stroke patients, the results of Figure 4-1A show that the model seems to capture the different experimental data for the within-arm proprioceptive tasks (W-AP) suggesting that the heterogeneity of the results would be partially explained by differentiating patients with “pure” sensory transformations (T) deficits (Gurari et al., 2017: green diamond in Figure 4-1A) from patients with “pure” proprioceptive (P) and mixed (P+T) deficits (Contu et al., 2017; Rinderknecht et al., 2018; dos Santos et al., 2015: bicolor (red/blue) diamond in Figure 4-1A). For the asymmetric between-arms proprioceptive tasks (aB-AP) the model predicts a very high variability for the T and P+T patients while the increase with respect to the within-arm proprioceptive tasks (W-AP) is moderate for P patients, but unfortunately we do not have experimental data to validate this prediction. For the symmetric between-arms proprioceptive tasks (sA-BP), the model captures the heterogeneity of the patient dataset well by distinguishing P patients (Herter et al., 2019) from T and P+T patients (Herter et al., 2019; Ingemanson et al., 2019) (blue and red diamonds respectively in Figure 4-1A). The prediction for the sB-AP task is also consistent with qualitative observations of Gurari et al. (2017) that the same patients that performed without difficulties the W-AP task (classified as T patients) showed significant deficits in a symmetric task (grey rectangle in Figure 4-1A). For the cross-modal tasks (V-P), the model predicts that performances of T and P+T patients would be characterized by a variability significantly larger than that of P patients, similarly to the sB-AP task, but we have no data to validate this this prediction.

Concerning the patients’ ability to visually compensate for their proprioceptive deficits (Figure 4-1B), the model predicts that in the within-arm visual compensation tasks (W-AVP) all three types of patients (P, T and P+T) should be able to use visual information to improve performance to that of healthy subjects. This prediction is consistent with the experimental observation of Torre et al. (2013) that stroke patients can fully compensate with vision when performing this kind of task (bicolor (red/blue) diamond in Figure 4-1B), where the information about the target and the effector could be compared directly in both joint and retinal space. For the

## **Results: Study 1 – Reinterpretation of the stroke literature on proprioceptive deficits**

asymmetric between-arms visual compensation tasks (aB-A<sub>VP</sub>), the model predicts the same full visual compensation as for the within-arm tasks. Although we could not find any quantitative experimental results for patients in this type of tasks, the model prediction is coherent with the qualitative observation of Scalha et al. (2011) that patients can significantly improve their performances with vision (shaded grey rectangle in Figure 4-1B). For the symmetric between-arms visual compensation tasks (sB-A<sub>VP</sub>), the model prediction is very different from the other tasks and it matches the different results obtained by Herter et al. (2019) for patients with low and high levels of visual compensation (red and blue diamond respectively in Figure 4-1B). The model predictions for this task suggests that the group of patients showing low visual compensation (higher variability) could confound T and P+T patients, although the patients with the ability to visually compensate (lower variability) are probably of type P. For the cross-modal visual compensation tasks (V-VP), the same considerations apply as for the aB-A<sub>VP</sub> tasks, in terms of model predictions and of matching with qualitative observations: patients can significantly improve their performances with vision (shaded grey rectangle in Figure 4-1B).

Altogether, these results suggest that only the within-arm proprioceptive tasks (W-A<sub>P</sub>) can be considered as “pure proprioception tests”. This expression here refers to those tests whose outcome is affected only by deficits of the proprioceptive system, and not by other factors, such as the inability to perform sensory transformations. In contrast, between-arms (sB-A<sub>P</sub>, aB-A<sub>P</sub>) and cross-modal (V-P) proprioceptive tasks appear to confound proprioceptive deficits and sensory transformation deficits, since they are affected by P, T or P+T deficits. These results also suggest that the visual compensation tests for symmetric between-arms (sB-A<sub>VP</sub>) tasks can assess the patients’ ability to perform sensory transformations. The reinterpretation of the data of the literature through the model framework represented in Figure 4-1 additionally suggests that most of the tested stroke patients have mixed P+T deficits (Contu et al., 2017; Herter et al., 2019; Rinderknecht et al., 2018; dos Santos et al., 2015), but that there are also clear occurrences of T deficits (Gurari et al., 2017) and P deficits (Herter et al., 2019) as hypothesized.

In conclusion, the proposed stratification of patients presented here based on their deficits (P, T and P+T) appears to explain, and at least partially reconcile, the apparently contradictory experimental outcomes of various assessments currently in use in clinical research.

### **4.1.3 Insights from brain lesions and functional anatomy studies**

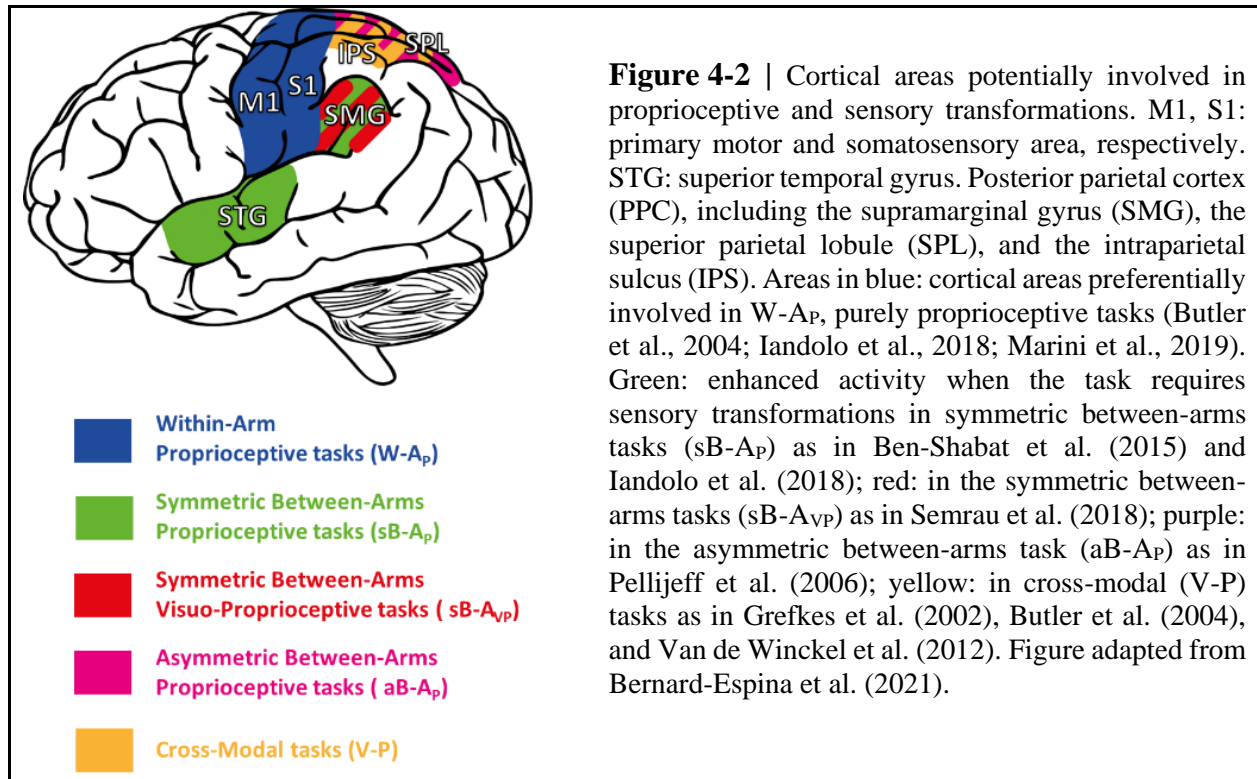
According to our model predictions (described in section 3), we consider within-arm proprioceptive (W-AP) assessments to be “purely” proprioceptive (Figure 3-2) in contrast to other proprioceptive assessments which involve sensory transformations (aB-AP, sB-AP, V-P: see Figure 3-3, Figure 3-4, and Figure 3-10). We therefore attempted to classify the reviewed functional brain imaging studies accordingly and to probe whether this categorization might result in a processing-specific topological cerebral organization.

“Pure” proprioceptive processing, assessed with a within-arm proprioceptive (W-AP) task seemed to entail primarily the activation of M1 and S1 (Butler et al., 2004; Marini et al., 2019: blue areas in Figure 4-2). The W-AP tasks, the simplest tasks in terms of computational load, are presumably based on simpler networks. In contrast, the mirror task (a symmetric between-arms, sB-AP task) seem to involve sensory transformations. Consistent with this theoretical difference, fMRI revealed that a larger brain network was involved compared to W-AP tasks, with higher activation of the supramarginal gyrus (SMG) and superior temporal gyrus (STG) (Ben-Shabat et al., 2015; Iandolo et al., 2018: green areas in Figure 4-2). In theory, the same mirror task with visual feedback (sB-A<sub>VP</sub>) also involves sensory transformations. A lesion-symptom mapping study showed that patients with lesions to the SMG did not improve their performance when adding visual feedback in the mirror test (sB-AP vs. sB-A<sub>VP</sub>), a result presumably related to sensory transformation deficit (Semrau et al., 2018: red area in Figure 4-2). Patients that improved to normal performance with vision, i.e. presumably patients with “pure” proprioceptive deficit (Figure 4-1), had smaller lesions that primarily affected white-matter tracts carrying proprioceptive information rather than lesions in parietal association areas (Semrau et al., 2018). This result is therefore consistent with a specific role of the parietal association areas in sensory transformations.

Other proprioceptive tasks such as asymmetric between-arms (aB-AP) and cross-modal (V-P) tasks, known for the visual encoding of proprioceptive information, and thus requiring sensory transformations, have also been associated to posterior parietal activation. Pellijeff et al. (2006) showed that the fMRI response was specifically enhanced in the superior parietal lobule (SPL) and Precuneus (medial part of the posterior parietal cortex, PPC) in a thumb and chin pointing task (purple area in Figure 4-2). Similarly, using Positron emission tomography (PET), Butler et al. (2004) showed a greater activity in the SPL in the V-P reaching task compared to a

## Results: Study 1 – Reinterpretation of the stroke literature on proprioceptive deficits

W- $A_P$  task (orange area in Figure 4-2). Within the PPC, Grefkes et al. (2002) showed that the activity in the anterior intraparietal sulcus (IPS) was specifically enhanced during tactile object recognition. This task, requiring cross-modal visuo-tactile information transfer, involved the anterior IPS in stroke patients (Van de Winckel et al., 2012: orange area in Figure 4-2).



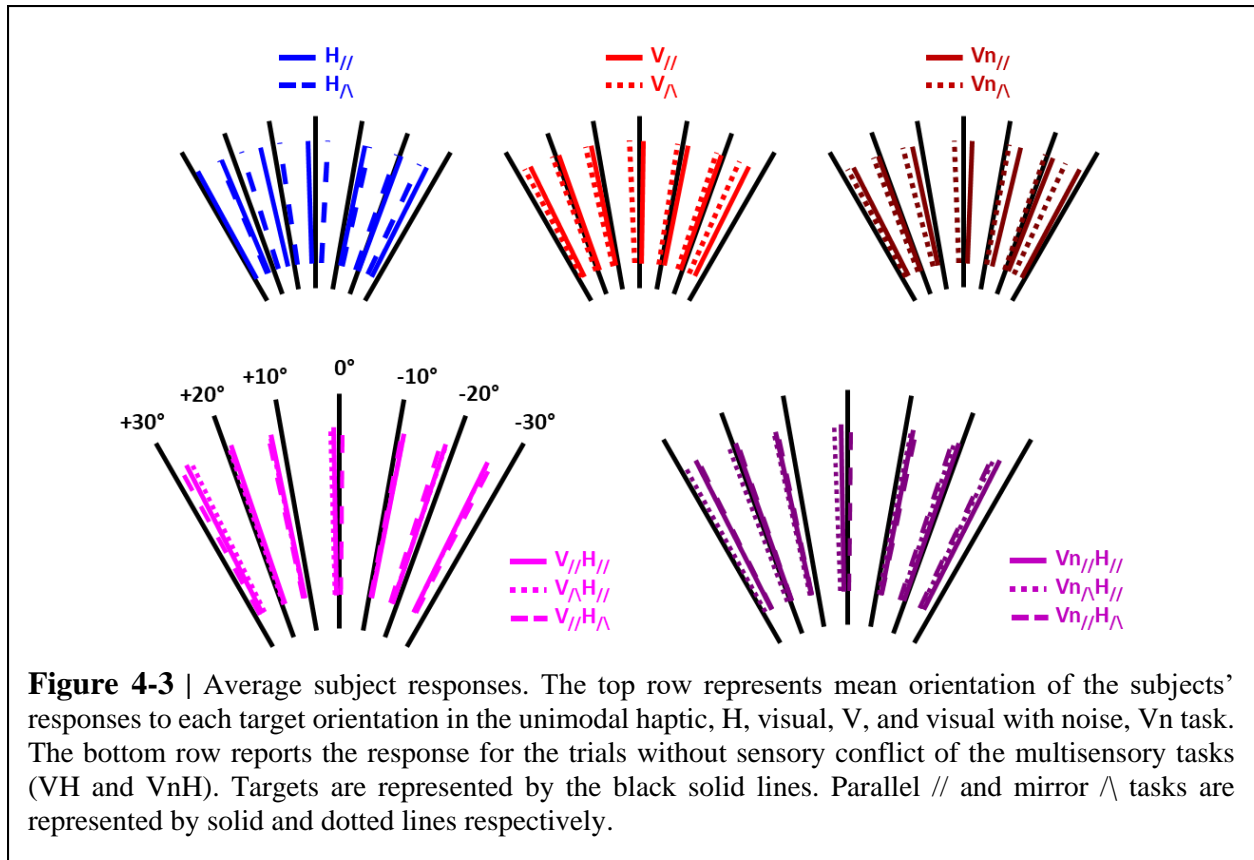
Overall, these studies tend to show that “pure” proprioceptive processing involves mainly S1, whereas sensory transformation processing recruits specifically the parietal associative cortex. Figure 4-2 shows the main trends for task-specific involvement that might be read out as: (i) Tasks excluding visual inputs and that do not require sensory transformations (W- $A_P$ ) showed a trend for activating preferentially frontal (M1) and anterior parietal areas (S1). (ii) Tasks excluding visual inputs but requiring sensory transformations (sB- $A_P$ ), or for which visual spatial processing requires sensory transformations (sB- $A_{VP}$ ), seemed to entail additional activation of superior temporal and inferior-lateral PPC areas. (iii) Tasks that impose cross-modal processing, for which a visual encoding of the proprioceptive information has been reported in healthy subjects (aB- $A_P$ , V-P) tended to activate the superior-medial PPC areas.

## **4.2 Study 2 – Sensory transformations affecting visuo-proprioceptive integration**

The second study aims to experimentally determine whether and how the necessity of sensory spatial transformation affects unimodal (visual or haptic) and multimodal (visuo-haptic) processing. The experimental paradigm examined whether movements in different working planes would affect spatial transformations. Subjects had to reproduce the orientation of an object (parallel task: //), or mirror it relative to the sagittal plane (mirror task: ^). The task was performed in two different working planes (frontal and horizontal) with haptic feedback only, visual feedback only or both (see section 2.2.2). The mirror (but not the parallel) task was supposed to require spatial transformations. After having analyzed the response patterns and the multisensory integration of visual and haptic signals, we then compared our model predictions to the experimental data as described in section 3.6.2.

### **4.2.1 Response patterns**

Average responses in the unimodal haptic only (H), visual only (V), and visual with noise (Vn) condition, as well as the responses in the multisensory visuo-haptic condition without (VH) and with noise (VnH) are depicted in Figure 4-3. Specific response deviations from the target can be seen for each sensory condition. Responses of all subjects for both *frontal plane* (roll target orientations) and *horizontal plane* (yaw target orientation) groups are depicted together as they do not differ qualitatively. Response patterns seem affected by the spatial mirror transformations, with deviations of the responses in the mirror (^) conditions compared to the parallel conditions (//). Responses seem biased in opposite direction in the H^ and V^ conditions, and response deviations seem less pronounced in the multisensory VH tasks.



We first examined haptic, visual and visuo-haptic integration by quantifying: the average error (*Bias*), the over/under-estimation of the angular distance between targets (*Dist*), the average number of control actions (*Nb Ctrl*), and the variability of the responses (*Var*).

#### *Unimodal sensory, visual and haptic, tasks*

As shown in Figure 4-4A, the spatial mirror transformation appears to affect the *Bias* in opposite directions for the haptic mirror ( $H_{\setminus}$ ) and visual mirror tasks (without and with visual noise:  $V_{\setminus}$  and  $Vn_{\setminus}$ ), with the same pattern in the frontal and horizontal working planes. These observations are supported by the absence of *Mirror*, *Sense*, and *Plane* main effects, and by the presence of *Sense\*Mirror* interaction (Table 4-3). The average responses were deviated towards the wrist supination/extension in the frontal/horizontal working planes for the  $H_{\setminus}$  task ( $p=0.006$ ), and towards the wrist pronation/flexion in the  $V_{\setminus}$  (*ns*) and  $Vn_{\setminus}$  (tendency,  $p=0.056$ ) tasks, in both working planes.

## Results: Study 2 – Sensory transformations affecting visuo-proprioceptive integration

In contrast, perceptive distortions (*Dist*) showed *Sense*, *Mirror*, and *Plane* main effects (Table 4-3):

- *Sense*: *Dist* is less pronounced in Vn compared to H ( $p=0.04$ ) and V ( $p=0.02$ ),
- *Mirror*: on average, *Dist* is more important (negative) in the mirror compared to the parallel conditions ( $p=0.0001$ ), revealing a larger under-estimation of the target orientation with the mirror spatial transformation,
- *Plane*: *Dist* is more important (larger under-estimation of the target orientation) in the frontal compared to the horizontal plane ( $p=0.04$ ).

The *Sense*\**Mirror* interaction shows that the global effect of the mirror spatial transformation on *Dist* is mainly due to the haptic modality ( $H_{\wedge}$  vs  $H_{//}$ ,  $p=0.0001$ , see negative value of *Dist* in Figure 4-4B), whereas no difference was observed in the unimodal visual tasks ( $V_{//}$  vs  $V_{\wedge}$  and  $Vn_{//}$  vs  $Vn_{\wedge}$ ). The effect of the mirror transformation and its specificity to the haptic modality, appears to be similar for both working planes (no *Mirror*\**Plane*, nor *Sense*\**Mirror*\**Plane* interaction: see Table 4-3).

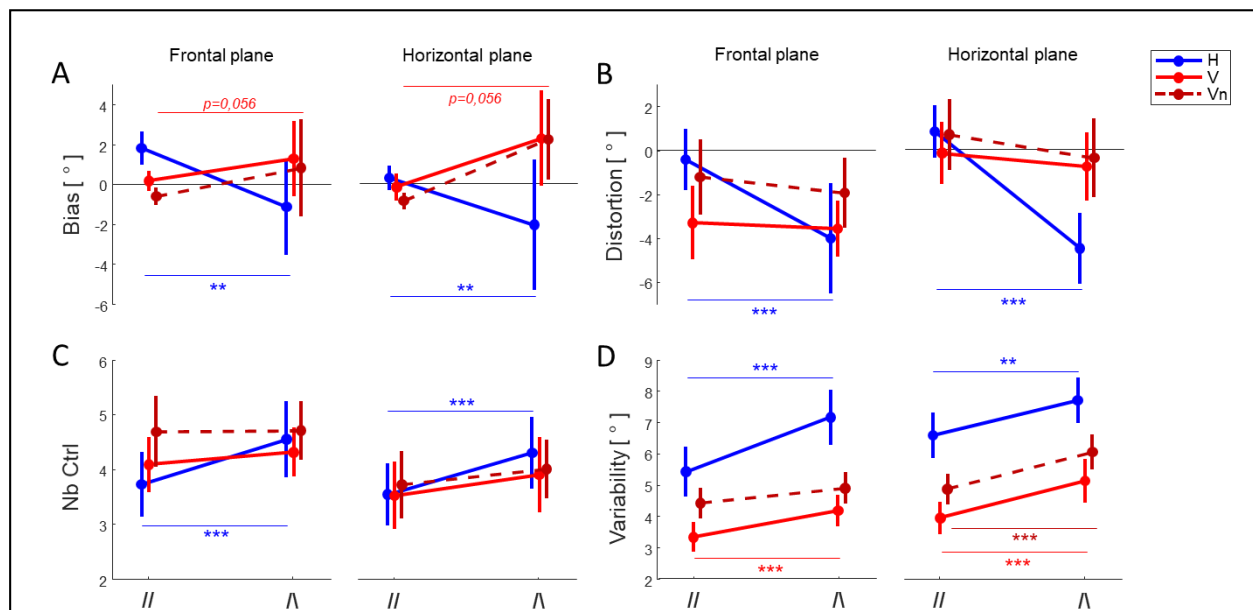


**Figure 4-4** | Response patterns for unimodal tasks, in the two working planes: (A) average error of responses (*Bias*), (B) responses distortion (*Dist*), (C) number of control actions (*Nb Ctrl*), and (D) responses variability (*Var*). Dotted lines represent the visual noise. Vertical whiskers correspond to 95% CI. \*, \*\* and \*\*\* represent  $p<0.05$ ,  $p<0.01$  and  $p<0.001$  respectively, and their colour represents the sensory condition to which they refer to. **Legend:** H: Haptic tasks; V: Visual tasks; Vn: Visual tasks with visual noise; //: Unimodal parallel tasks;  $\wedge$ : Unimodal mirror tasks.

**Table 4-3** | ANOVA main and interaction effects for the unimodal tasks. The Repeated Measures ANOVA main effects of the mirror spatial transformation (*Mirror*: // or  $\wedge$ ) are reported for the average response (*Bias*), distortion (*Dist*), average number of control actions (*Nb Ctrl*), and variability (*Var*). To assess how the sensory modality (*Sense*: H, V or Vn) and the working plane (*Plane*: frontal or horizontal) affects the sensory combinations specifically, we measured the interactions effects: *Sense\*Mirror*, *Mirror\*Plane*, and *Sense\*Mirror\*Plane*. The significant results ( $p < 0.05$ ) are highlighted in bold font.

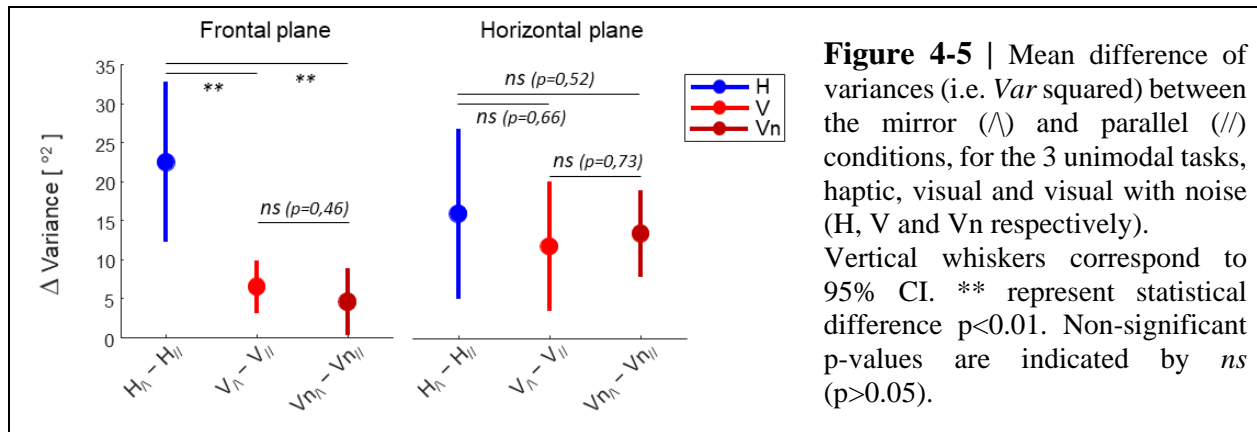
| Unimodal Haptic (H) and Visual (V, and Vn) tasks |   |  |  |  |                                    |                                    |
|--|---|--|--|--|------------------------------------|------------------------------------|
| Param.   | <i>Sense</i>  | <i>Mirror</i>  | <i>Plane</i>                                     | <i>Sense*Mirror</i>  | <i>Mirror*Plane</i>                | <i>Sense*Mirror*Plane</i>          |
| <i>Bias</i>                                      | F <sub>(2,68)</sub> =2.1<br>p=0.14                            | F <sub>(1,34)</sub> =0.5<br>p=0.50                           | F <sub>(1,34)</sub> =0.1<br>p=0.80               | <b>F<sub>(2,68)</sub>=11.2</b><br><b>p=0.00006</b>           | F <sub>(1,34)</sub> =1.3<br>p=0.27 | F <sub>(2,68)</sub> =0.2<br>p=0.84 |
| <i>Dist</i>                                      | <b>F<sub>(2,68)</sub>=3.7</b><br><b>p=0.03</b>                | <b>F<sub>(1,34)</sub>=33.8</b><br><b>p=2*10<sup>-6</sup></b> | <b>F<sub>(1,34)</sub>=4.5</b><br><b>p=0.04</b>   | <b>F<sub>(2,68)</sub>=16.8</b><br><b>p=1*10<sup>-6</sup></b> | F <sub>(1,34)</sub> =1.3<br>p=0.24 | F <sub>(2,68)</sub> =0.5<br>p=0.60 |
| <i>Nb Ctrl</i>                                   | F <sub>(2,68)</sub> =2.3<br>p=0.1                             | <b>F<sub>(1,34)</sub>=12.4</b><br><b>p=0.001</b>             | F <sub>(1,34)</sub> =3.1<br>p=0.09               | <b>F<sub>(2,68)</sub>=4.3</b><br><b>p=0.02</b>               | F <sub>(1,34)</sub> =0.3<br>p=0.59 | F <sub>(2,68)</sub> =0.3<br>p=0.76 |
| <i>Var</i>                                       | <b>F<sub>(2,68)</sub>=81.7</b><br><b>p&lt;10<sup>-9</sup></b> | <b>F<sub>(1,34)</sub>=65.3</b><br><b>p=2*10<sup>-9</sup></b> | <b>F<sub>(1,34)</sub>=10.1</b><br><b>p=0.003</b> | F <sub>(2,68)</sub> =1.3<br>p=0.28                           | F <sub>(1,34)</sub> =0.0<br>p=0.87 | F <sub>(2,68)</sub> =2.7<br>p=0.07 |

The number of control actions (*Nb Ctrl*) was similar between sensory conditions and between working planes (no *Sense*, nor *Plane* main effect), but significantly increased with the necessity of performing a mirror transformation (Figure 4-4C) with a significant *Mirror* main effect ( $\wedge > //$ ,  $p=0.001$ ). The *Sense\*Mirror* interaction however suggests that the mirror effect is stronger for the Haptic task: *Nb Ctrl* increased in  $H_{\wedge}$  with respect to  $H_{//}$  ( $p=0.0001$ ), and in  $V_{\wedge}$  with respect to  $V_{//}$  (tendency,  $p=0.055$ ) but not in the presence of visual noise ( $Vn_{\wedge}$  was no different to  $Vn_{//}$ ,  $p=0.22$ ). The effect of the mirror transformation appears to be similar in both working planes (no *Mirror\*Plane*, nor *Sense\*Mirror\*Plane* interaction: see Table 4-3).

Finally, we observed that the response variability (*Var*) strongly depends on the sensory conditions (Figure 4-4D): *Sense* main effect, with the V condition significantly less variable (more precise) than the Vn condition (post-hoc  $p=0.0001$ ) which is significantly less variable than H (post-hoc  $p=0.0001$ ). Spatial transformation increased the response variability in all 3 unimodal tasks, with no difference between sensory conditions (significant *Mirror* main effect, but no significant *Sense\*Mirror* interaction effect: see Table 4-3). The working plane orientation also significantly affect *Var* (*Plane* main effect: Horizontal > Frontal,  $p=0.003$ ). Although not statistically significant, the tendency to a *Sense\*Mirror\*Plane* interaction ( $p=0.07$ ) suggests that the spatial mirror transformation could affect differently the haptic and visual modalities depending on the working plane orientation.

## Results: Study 2 – Sensory transformations affecting visuo-proprioceptive integration

Figure 4-5 shows that the mirror transformation in the frontal working plane clearly increases the response variance in the haptic modality ( $\Delta=22.5^{\circ 2}$ ), whereas it affects less the visual modality (with,  $\Delta=6.5^{\circ 2}$ , and without visual noise,  $\Delta=4.5^{\circ 2}$ ). But the mirror transformation in the horizontal working plane affects the haptic ( $\Delta=15.9^{\circ 2}$ ) and visual modalities (with,  $\Delta=11.7^{\circ 2}$ , and without visual noise,  $\Delta=13.4^{\circ 2}$ ) to a similar extent (right part of Figure 4-5).



Together, these results support the hypothesis that the spatial transformation adds complexity in the unimodal tasks which is reflected by a global increase of *Var* and *Nb Ctrl*, as well as specific *Bias* and *Dist* patterns. And that the effect of the mirror transformation on the response variability appears similar among sensory conditions in the horizontal, but not in the frontal plane.

### Multisensory (visuo- haptic) tasks

Figure 4-6A shows the average error (*Bias*) in the multisensory visuo-haptic tasks is larger on average in the frontal compared to the horizontal plane (*Plane* main effect, see Table 4-4). This increase of *Bias* appears to be due to the spatial transformation affecting the visual modality (*Mirror\*Plane* interaction:  $V_{\wedge}H_{//} > V_{//}H_{//}$  and  $V_{//}H_{\wedge}$ ,  $p=0.02$ ). *Bias* also tends to be more sensitive to the spatial transformation affecting the visual modality in the presence of visual noise (*Noise\*Mirror* interaction) (see dotted lines in Figure 4-6A).

The under-estimation of the target orientations (negative value of *Dist* in Figure 4-6B) also increased in the frontal compared to the horizontal plane (*Plane* main effect, Table 4-4). The

## **Results: Study 2 – Sensory transformations affecting visuo-proprioceptive integration**

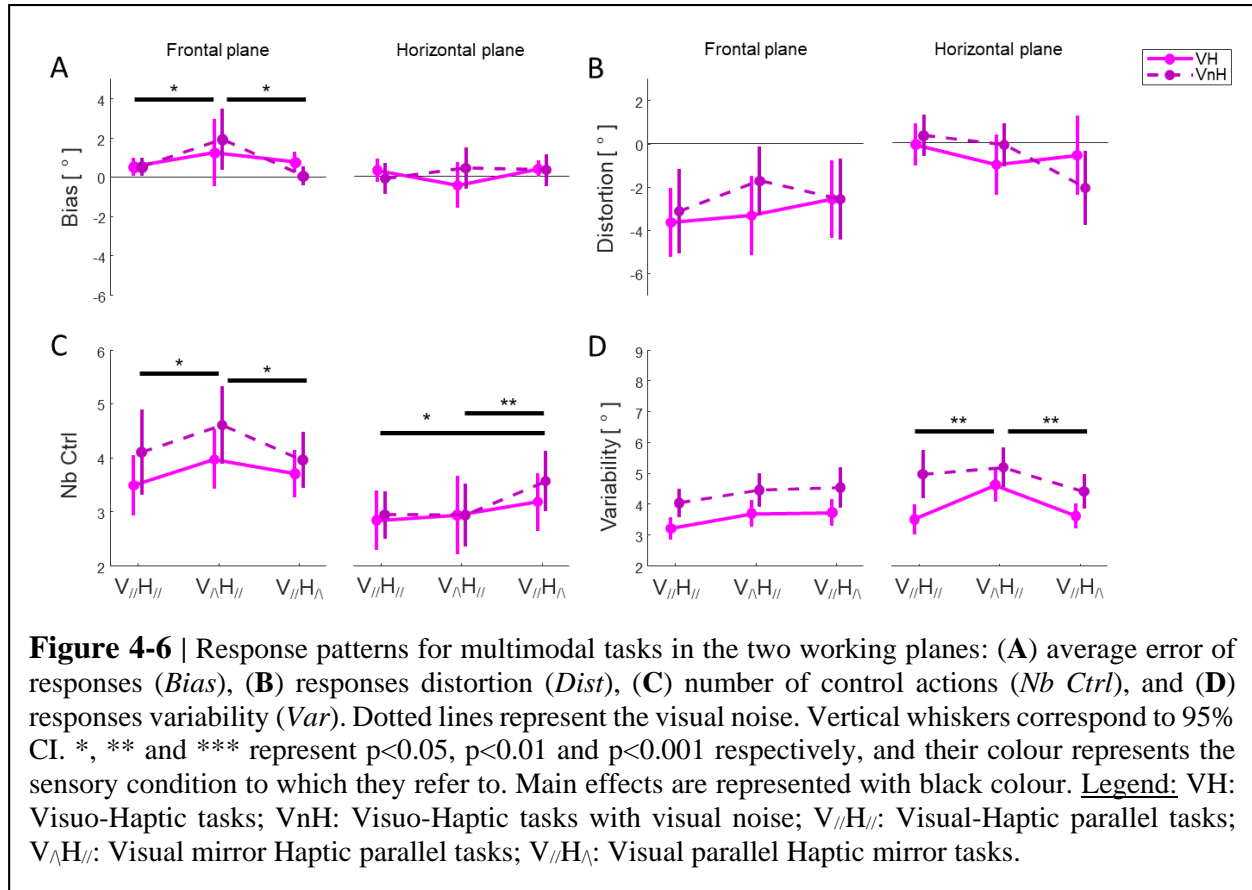
*Mirror\*Plane* and *Noise\*Mirror* interactions show that the effect of the mirror spatial transformation on *Dist* tends to be different in both working plane orientations and with respect to the presence of visual noise.

Responses *Nb Ctrl* (Figure 4-6C) was affected by the presence of visual noise ( $VnH > VH$ ), working plane orientation (frontal > horizontal) and mirror spatial transformation ( $V_{\wedge}H_{//} > V_{//}H_{//}$ ,  $p=0.057$ , and  $V_{//}H_{\wedge} > V_{//}H_{//}$ ,  $p=0.03$ ): *Noise*, *Mirror* and *Plane* main effects are reported in Table 4-4. The *Mirror\*Plane* interaction shows that the effect of the mirror spatial transformation is not the same in both working plane orientations (in the frontal plane, *Nb Ctrl* is larger in  $V_{\wedge}H_{//}$  compared to  $V_{//}H_{//}$ ,  $p=0.02$ , and  $V_{//}H_{\wedge}$ ,  $p=0.03$ ; in the horizontal plane, *Nb Ctrl* is larger in  $V_{//}H_{\wedge}$  compared to  $V_{//}H_{//}$ ,  $p=0.004$ , and  $V_{\wedge}H_{//}$ ,  $p=0.01$ ).

The response variability (*Var*, Figure 4-6D) was also affected by the presence of visual noise ( $VnH > VH$ ), by working plane orientation (horizontal > frontal) and mirror spatial transformation: *Noise*, *Plane* and *Mirror* main effects are reported in Table 4-4. For the *Mirror* effect, in particular,  $V_{\wedge}H_{//} > V_{//}H_{//}$  ( $p=0.0006$ ) and  $V_{\wedge}H_{//} > V_{//}H_{\wedge}$  ( $p=0.008$ ). The *Mirror\*Plane* interaction shows that the *Mirror* main effect is mainly due to the spatial transformations performed in the horizontal plane (Figure 4-6D).

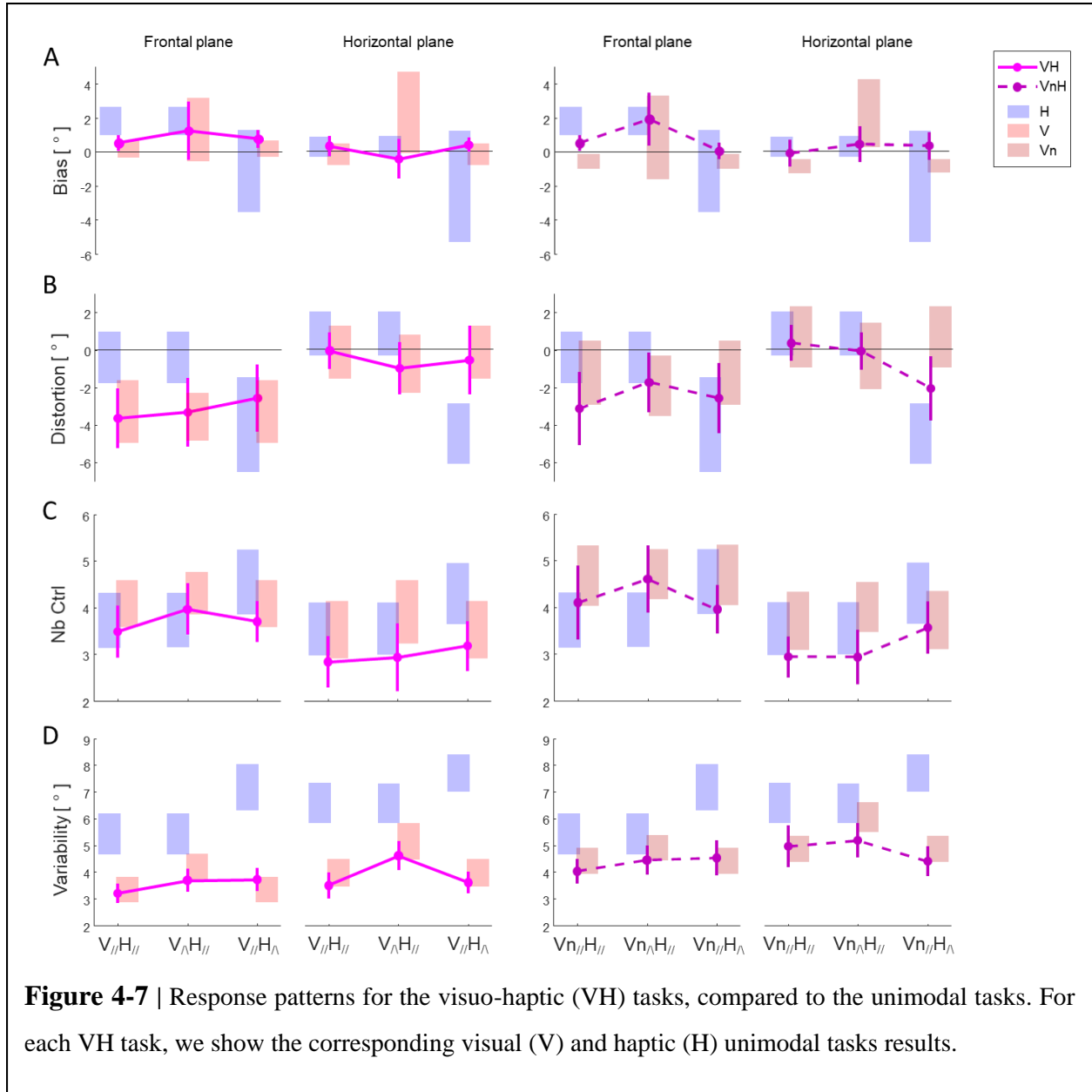
**Table 4-4** | ANOVA main and interaction effects for the multisensory tasks. The Repeated Measures ANOVA main effects of the visual noise (*Noise*: VH and VnH) and the spatial mirror transformation (*Mirror*:  $V_{//}H_{//}$ ,  $V_{\wedge}H_{//}$ , and  $V_{//}H_{\wedge}$ ) are reported for the average response, *Bias*, distortion, *Dist*, average number of control actions, *Nb Ctrl*, and variability, *Var*. To assess how the visual noise (*Noise*) and the working plane (*Plane*) affects the spatial mirror transformation specifically, we measured the interaction effects: *Noise\*Mirror*, *Mirror\*Plane* and *Noise\*Mirror\*Plane*. The significant results ( $p < 0.05$ ) are highlighted in bold font.

| Param.         | Multisensory Visuo-Haptic tasks  |  |   |   |   |                              |
|----------------|--|--|---|---|---|------------------------------|
|                | <i>Noise</i>   | <i>Mirror</i>  | <i>Plane</i>  | <i>Noise*Mirror</i>   | <i>Mirror*Plane</i>   | <i>Noise*Mirror*Plane</i>    |
| <i>Bias</i>    | $F_{(1,34)}=1.7$<br>$p=0.21$   | $F_{(2,68)}=1.2$<br>$p=0.30$                                       | <b><math>F_{(1,34)}=4.6</math></b><br><b><math>p=0.04</math></b>  | $F_{(2,68)}=2.9$<br>$p=0.06$                                      | <b><math>F_{(2,68)}=3.3</math></b><br><b><math>p=0.04</math></b>  | $F_{(2,68)}=0.4$<br>$p=0.68$ |
| <i>Dist</i>    | $F_{(1,34)}=1.4$<br>$p=0.24$   | $F_{(2,68)}=0.6$<br>$p=0.58$                                       | <b><math>F_{(1,34)}=6.9</math></b><br><b><math>p=0.01</math></b>  | <b><math>F_{(2,68)}=6.7</math></b><br><b><math>p=0.002</math></b> | $F_{(2,68)}=2.9$<br>$p=0.06$                                      | $F_{(2,68)}=1.5$<br>$p=0.23$ |
| <i>Nb Ctrl</i> | <b><math>F_{(1,34)}=1.2</math></b><br><b><math>p=0.002</math></b>      | <b><math>F_{(2,68)}=3.6</math></b><br><b><math>p=0.03</math></b>   | <b><math>F_{(1,34)}=8.3</math></b><br><b><math>p=0.007</math></b> | $F_{(2,68)}=0.1$<br>$p=0.90$                                      | <b><math>F_{(2,68)}=6.4</math></b><br><b><math>p=0.003</math></b> | $F_{(2,68)}=2.7$<br>$p=0.08$ |
| <i>Var</i>     | <b><math>F_{(1,34)}=49.0</math></b><br><b><math>p=4*10^{-8}</math></b> | <b><math>F_{(2,68)}=8.2</math></b><br><b><math>p=0.0006</math></b> | $F_{(1,34)}=3.2$<br>$p=0.08$                                      | $F_{(2,68)}=1.7$<br>$p=0.18$                                      | <b><math>F_{(2,68)}=4.8</math></b><br><b><math>p=0.01</math></b>  | $F_{(2,68)}=0.9$<br>$p=0.41$ |



### 4.2.2 Multisensory integration

Qualitatively, in order to assess how visual and haptic cues are integrated in the visuo-haptic tasks, we compare the response patterns in the unimodal (visual and haptic) tasks with the multisensory tasks. The *Bias* in the VH tasks tends to be intermediate between the *Bias* of the unimodal V and H tasks, suggesting that both visual and haptic cues are integrated to reduce *Bias* (Figure 4-7A). For responses distortion, it seems that without visual noise, *Dist* in VH tasks is similar to *Dist* in the unimodal visual task. In contrast, in the presence of visual noise, *Dist* in VH tasks tends to be balanced between both unimodal visual and haptic tasks (Figure 4-7B). The responses *Nb Ctrl* tend to be smaller on average in the VH tasks compared to the unimodal tasks, for the horizontal plane (Figure 4-7C). Finally, *Var* seems smaller on average in VH tasks, compared to both unimodal visual and haptic tasks (Figure 4-7D), suggesting that multisensory integration could be optimal, expressed by reduced response errors (Ernst and Banks, 2002).



***Effect of the multisensory integration on the response variability***

In order to quantitatively assess whether multisensory integration reduces response variability (*Var*) with respect to unimodal conditions, as theoretically expected (see section 1.3.2), we performed multiple statistical comparisons (one-tailed t-test) between haptic and visuo-haptic tasks (H-VH), and between visual and visuo-haptic tasks (V-VH) for all combinations of spatial transformations and visual noise, in both working plane orientations. Table 4-5 shows the results of these tests.

## Results: Study 2 – Sensory transformations affecting visuo-proprioceptive integration

**Table 4-5** | Difference in response variability between VH tasks (columns) and the corresponding unimodal H, V tasks (row). Significance level of the t-test comparisons for *Var*. *ns*,  $\sim$ , \*, \*\*, and \*\*\* represent  $p > 0.10$ ,  $0.05 < p < 0.10$ ,  $p < 0.05$ ,  $p < 0.01$  and  $p < 0.001$  respectively, after Benjamini-Hochberg correction for multiple (12) comparisons.

| Frontal working plane             |                                      |                                      | Horizontal working plane           |                                     |                                       |
|-----------------------------------|--------------------------------------|--------------------------------------|------------------------------------|-------------------------------------|---------------------------------------|
| $V_{//}H_{//}$                    | $V_{\wedge}H_{//}$                   | $V_{//}H_{\wedge}$                   | $V_{//}H_{//}$                     | $V_{\wedge}H_{//}$                  | $V_{//}H_{\wedge}$                    |
| $V_{//}$<br><i>ns</i><br>$p=0.42$ | $V_{\wedge}$<br>*<br>$p=0.028$       | $V_{//}$<br><i>ns</i><br>$p=0.93$    | $V_{//}$<br>$\sim$<br>$p=0.038$    | $V_{\wedge}$<br>$\sim$<br>$p=0.055$ | $V_{//}$<br>$\sim$<br>$p=0.094$       |
| $H_{//}$<br>***<br>$p=1.10^{-5}$  | $H_{//}$<br>***<br>$p=2.10^{-4}$     | $H_{\wedge}$<br>***<br>$p=1.10^{-8}$ | $H_{//}$<br>***<br>$p=7.10^{-7}$   | $H_{//}$<br>***<br>$p=5.10^{-5}$    | $H_{\wedge}$<br>***<br>$p=5.10^{-11}$ |
| $Vn_{//}H_{//}$                   | $Vn_{\wedge}H_{//}$                  | $Vn_{//}H_{\wedge}$                  | $Vn_{//}H_{//}$                    | $Vn_{\wedge}H_{//}$                 | $Vn_{//}H_{\wedge}$                   |
| $Vn_{//}$<br>$\sim$<br>$p=0.081$  | $Vn_{\wedge}$<br>$\sim$<br>$p=0.075$ | $Vn_{//}$<br><i>ns</i><br>$p=0.60$   | $Vn_{//}$<br><i>ns</i><br>$p=0.48$ | $Vn_{\wedge}$<br>**<br>$p=0.005$    | $Vn_{//}$<br>$\sim$<br>$p=0.071$      |
| $H_{//}$<br>**<br>$p=0.003$       | $H_{//}$<br>*<br>$p=0.025$           | $H_{\wedge}$<br>***<br>$p=7.10^{-7}$ | $H_{//}$<br>***<br>$p=3.10^{-5}$   | $H_{//}$<br>***<br>$p=4.10^{-4}$    | $H_{\wedge}$<br>***<br>$p=9.10^{-7}$  |

Overall in visuo-haptic tasks, *Var* was significantly lower compared to haptic tasks (see Figure 4-7D and Table 4-5), showing a clear advantage of multisensory processing with respect to purely haptic processing in terms of response variability. When compared to visual tasks, *Var* in visuo-haptic tasks is also numerically lower (see Figure 4-7D), and the difference is (or tends to be) statistically significant for both  $V_{\wedge}H_{//}$  and  $Vn_{\wedge}H_{//}$  tasks, and in both frontal and horizontal planes. The variability tends to be smaller than in the visual tasks also in the  $V_{//}H_{//}$ ,  $V_{//}H_{\wedge}$  and  $Vn_{//}H_{\wedge}$ , but only in the horizontal plane.

These results suggest that multisensory integration tends to improve the response precision with respect to the use of haptic or visual information alone. However, our data might not be sufficiently precise to clearly show the improvement with respect to the unimodal visual conditions, which is relatively small. Indeed, visual perception is overall more precise compared to haptic perception, therefore, the improvement in precision to be expected with the multisensory integration is small (Ernst and Banks, 2002).

Importantly, the decrease of variable error in multisensory conditions, predicted by the optimal sensory integration theory occurs when visual and haptic cues are incongruent (in the  $V_{\wedge}H_{//}$  and  $V_{//}H_{\wedge}$  tasks): the subjects do not choose to follow one and neglect the other (visual or haptic) sensory cue, but use both to achieve the task despite the unnatural aspect of the visuo-haptic incongruence.

*Visual sensory weighting*

In order to describe the multisensory integration in the visuo-haptic (VH) tasks, we estimated the visual sensory weight (that is the importance given to the visual cues, over the haptic cues) as described in section 2.2.7. We found that the visual sensory weight ( $\omega_V$ ) was sensitive to the level of visual noise (*Noise* main effect, see Table 4-6): as we introduced noise in the visual signals, we observed a global reduction of  $\omega_V$  in the VH tasks (see Figure 4-8), consistent with the increased variability of the responses in the unimodal visual tasks with the addition of visual noise (V vs. Vn, in Figure 4-4D). As described in section 1.3.2, the relative weight of visual and haptic cues in a visuo-haptic task is expected to depend on their relative precision.

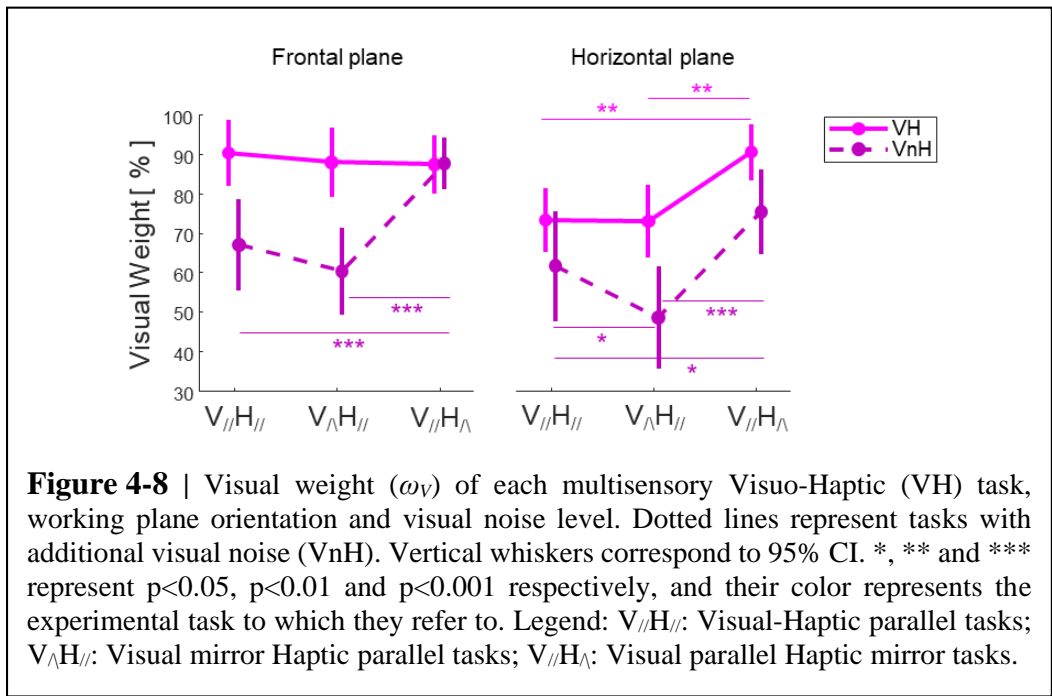


**Table 4-6** | ANOVA main and interaction effects for the visual weight in the multisensory tasks. The Repeated Measures ANOVA main effects of the visual noise (*Noise*: VH and VnH) and the spatial mirror transformation (*Mirror*:  $V_{//}H_{//}$ ,  $V^H H_{//}$ , and  $V_{//}H^H$ ) are reported for the relative weight associated to visual information,  $\omega_V$ . To assess how the visual noise (*Noise*) and the working plane (*Plane*) affects the spatial mirror transformation specifically, we measured the interaction effects: *Noise\*Mirror*, *Mirror\*Plane* and *Noise\*Mirror\*Plane*. Significant results ( $p < 0.05$ ) are highlighted in bold font.

| Param.     | Multisensory VH tasks  |  |  |   |                             |  |
|------------|--|--|--|---|-----------------------------|--|
|            | <i>Noise</i>   | <i>Mirror</i>  | <i>Plane</i>   | <i>Noise*Mirror</i>   | <i>Mirror*Plane</i>         | <i>Noise*Mirror*Plane</i>  |
| $\omega_V$ | <b><math>F_{(1,34)}=51.3</math></b><br><b><math>p=3*10^{-8}</math></b> | <b><math>F_{(2,68)}=19.2</math></b><br><b><math>p=2*10^{-7}</math></b> | <b><math>F_{(1,34)}=4.8</math></b><br><b><math>p=0.03</math></b> | <b><math>F_{(2,68)}=7.6</math></b><br><b><math>p=0.001</math></b> | $F_{(2,68)}=1.2$<br>$p=0.3$ | <b><math>F_{(2,68)}=4.3</math></b><br><b><math>p=0.02</math></b> |

## **Results: Study 2 – Sensory transformations affecting visuo-proprioceptive integration**

Next, we found a significant *Plane* effect (frontal > horizontal,  $p=0.03$ ), and *Mirror* effect ( $V_{//}H_{\wedge} > V_{//}H_{//}$ ,  $p=0.0002$ ;  $V_{//}H_{\wedge} > V_{\wedge}H_{//}$ ,  $p=0.0001$ ;  $V_{//}H_{//} > V_{\wedge}H_{//}$ ,  $p=0.059$ ). The *Noise\*Mirror* and *Noise\*Mirror\*Plane* interactions suggest that the effect of mirror transformations depends on the level of noise and the working plane orientation (see Table 4-6 and Figure 4-8):

- In the frontal plane, in the absence of visual noise (left column of Figure 4-8, solid line), our results do not show any modulation of the visual weight with respect to the spatial transformation;
- In the frontal plane, with visual noise (left column of Figure 4-8, dashed line), and in the horizontal plane without visual noise (right column of Figure 4-8, solid line), we observe a difference between  $V_{//}H_{\wedge}$  and the other two conditions ( $V_{//}H_{//}$  and  $V_{\wedge}H_{//}$ ) which are characterized by similar visual weight;
- In the horizontal plane, with visual noise (right column of Figure 4-8, dashed line), we observe stronger effect of spatial transformations:  $\omega_V$  is higher in the  $V_{//}H_{\wedge}$  task with respect to  $V_{//}H_{//}$  and  $V_{\wedge}H_{//}$ , and  $\omega_V$  is lower in the  $V_{\wedge}H_{//}$  task with respect to  $V_{//}H_{//}$  and  $V_{//}H_{\wedge}$ .

As we expected an increase of  $\omega_V$  for the  $V_{//}H_{\wedge}$  tasks with respect to  $V_{//}H_{//}$ , we expected a decrease of  $\omega_V$  for the  $V_{\wedge}H_{//}$  tasks with respect to  $V_{//}H_{//}$ . Indeed,  $V_{\wedge}H_{//}$  tasks involve a spatial mirror transformation of the visual signals, thus reducing visual precision compared to haptic precision. However, we observed the expected decrease of  $\omega_V$  only on the horizontal plane and in the presence of visual noise. This apparently negative result, however, is consistent with the observation that the mirror transformation significantly increased the response variability in the unimodal visual tasks,  $V$  and  $V_n$ , in the horizontal plane, but less in the frontal plane (Figure 4-5).

### **4.2.3 Model predictions**

Finally, we compared the experimental results with the predictions of our model (the “Extended Concurrent Model” presented in section 3.1). In order to test the robustness of its predictions, we compared the Extended Concurrent Model with two previous formulations of the Concurrent Model as described in section 3.6.2. The main difference between the Extended Concurrent Model (ECM) and the two alternative formulations resides in the number of reference

**Results: Study 2 – Sensory transformations affecting visuo-proprioceptive integration**

frames it uses (4 in the ECM, against 3 and 2 for the alternative models). The fact of having less reference frames to compare the target-response orientations implies that there are less possibilities of performing sensory transformations (re-encoding sensory signals in other reference frames) (see the details of the two alternative model predictions for each experimental task in Appendix B).

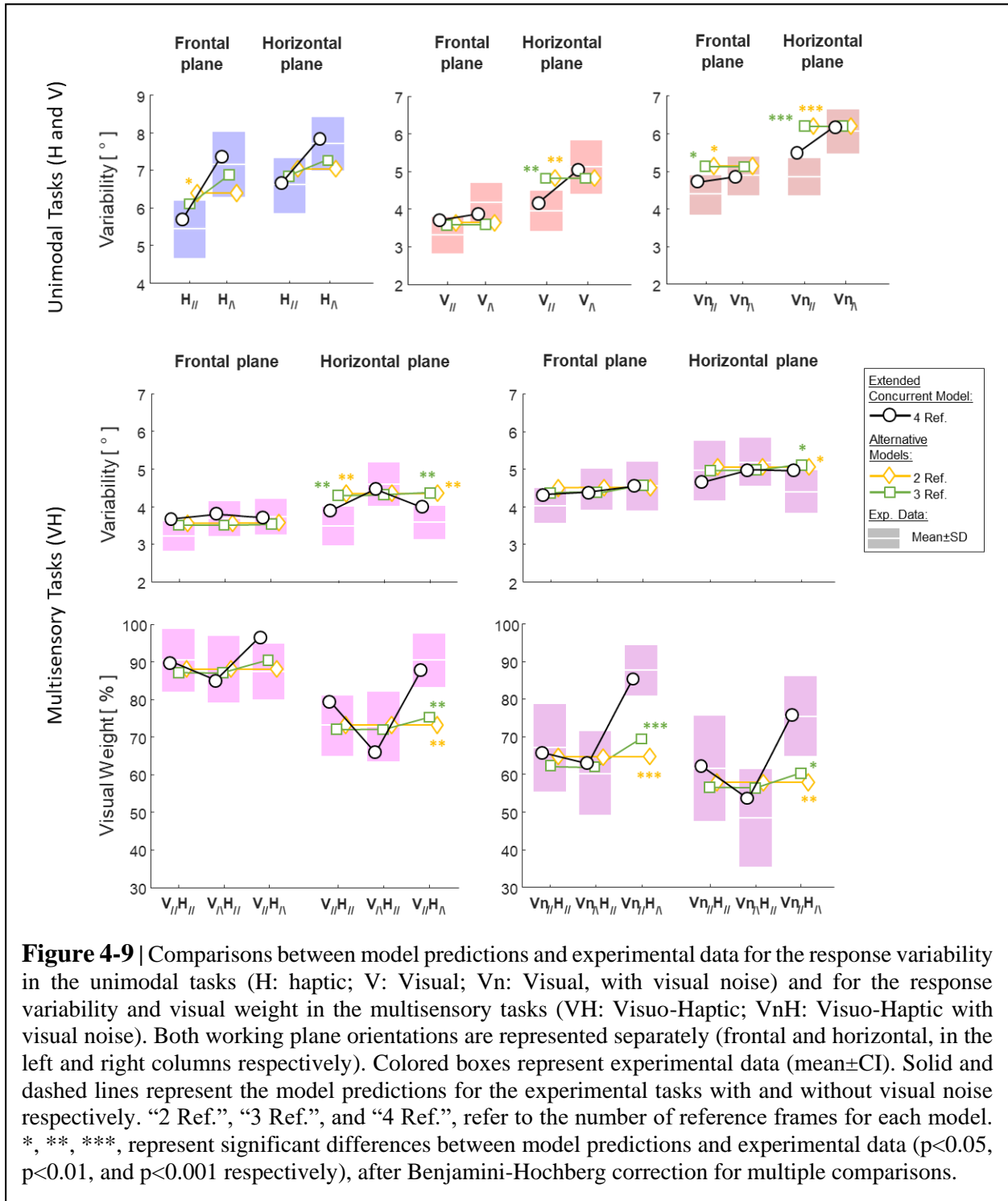
With an optimization procedure, we adjusted the parameters of the three models to try to fit the unimodal tasks variance, the multisensory tasks variance and visual weights (Figure 4-9).

Qualitatively, we observe for the unimodal tasks that only the Extended Concurrent Model (ECM) renders the increase of *Var* in the mirror conditions ( $H_{\wedge}$  vs  $H_{//}$ , and  $V_{\wedge}$  vs  $V_{//}$ ), whereas the model with 3 reference frames only renders the increase of *Var* in  $H_{\wedge}$  (and not  $V_{\wedge}$ ), and the model with 2 reference frames predicts no effect of spatial transformations. For the multisensory tasks, the ECM is the only model to predict the increase of  $\omega_V$  in  $V_{//}H_{\wedge}$  compared to  $V_{\wedge}H_{//}$  and  $V_{//}H_{//}$  that is observed in the experimental data.

To statistically test whether the predictions of the three models differed from the experimental data, we used the Hotelling’s  $T^2$  test (see statistics reported in Table 4-7): only the Extended Concurrent Model showed no significant differences between prediction and empirical data, suggesting that it captures well the effect of spatial mirror transformations of the unimodal (visual and haptic) tasks, and of multisensory visuo-haptic tasks, in both working (horizontal and frontal) planes.

**Table 4-7** | Hotelling T-Squared value (and associated p-value) between the model predictions and experimental data for the unimodal and multisensory tasks, in the Frontal and Horizontal working planes. Statistical differences ( $p < 0.05$ ) are highlighted in bold font. “2 ref.” and “3 ref.” refers to the number of reference frames included in the two alternative concurrent models.

|                                      |                    | <b>Frontal Plane</b>               |   | <b>Horizontal Plane</b>                                |  |  |
|--------------------------------------|--------------------|------------------------------------|---|--|--|--|
| <b>Extended Concurrent Model</b>     | Unimodal tasks     | $T^2=12.3, F_{(6,12)}=1.5, p=0.27$ | $T^2=14.7, F_{(6,12)}=1.7, p=0.19$                    |  |  |  |
|                                      | Multisensory tasks | $T^2=39.4, F_{(12,6)}=1.1, p=0.45$ | $T^2=106.3, F_{(12,6)}=3.1, p=0.09$                   |  |  |  |
| <b>Alternative Concurrent Models</b> | <b>2 ref.</b>      | Unimodal tasks                     | <b><math>T^2=42.1, F_{(6,12)}=4.9, p=0.009</math></b> | <b><math>T^2=84.6, F_{(6,12)}=9.9, p=0.0004</math></b> |  |  |
|                                      |                    | Multisensory tasks                 | <b><math>T^2=155.3, F_{(12,6)}=4.6, p=0.03</math></b> | <b><math>T^2=141.4, F_{(12,6)}=4.1, p=0.04</math></b>  |  |  |
|                                      | <b>3 ref.</b>      | Unimodal tasks                     | <b><math>T^2=29.8, F_{(6,12)}=3.5, p=0.03</math></b>  | <b><math>T^2=78.7, F_{(6,12)}=9.2, p=0.0006</math></b> |  |  |
|                                      |                    | Multisensory tasks                 | $T^2=108.8, F_{(12,6)}=3.2, p=0.08$                   | <b><math>T^2=139.6, F_{(12,6)}=4.1, p=0.04</math></b>  |  |  |



## Results: Study 3 – Gravitational influence on sensory transformations

The best fit of the experimental data by the Extended Concurrent Model predictions was obtained with the parameter values reported in Table 4-8 for each working plane orientation: overall, joint signals ( $\sigma_J^2$ ) are noisier compared to retinal signals ( $\sigma_R^2$ ), and the addition of visual noise in the experimental tasks ( $\sigma_{N_R}^2$ ) substantially increases noise. The sensory transformations between joint and retinal reference frames ( $\sigma_{T_{J \leftrightarrow R}}^2$ ), and sensory transformation from joint to extra-joint reference frames ( $\sigma_{T_{ExJ}}^2$ ) also add substantial noise. However, sensory transformations from retinal to extra-retinal reference frames ( $\sigma_{T_{ExR}}^2$ ) is close to 0 for the frontal plane, but larger for the horizontal plane. This result suggests that the cost of sensory transformations of retinal signals to extra-retinal coordinates (for mirror visual transformation) is negligible in the frontal, but not in the horizontal plane, consistent with the different finding observed for the two working planes.

| <u>Frontal plane</u>                                  | <u>Horizontal plane</u>                               | <b>Table 4-8</b>   Model parameter values for the Extended Concurrent Model that best fits the experimental data in both frontal and horizontal working planes. The model parameters are: the noise of the joint signal ( $\sigma_J^2$ ) and of the retinal signals ( $\sigma_R^2$ ), the additional variance due to the visual noise ( $\sigma_{N_R}^2$ ), the noise of the sensory transformations between the joint and retinal reference frames ( $\sigma_{T_{J \leftrightarrow R}}^2$ ), from the joint to the extra-joint reference frame ( $\sigma_{T_{ExJ}}^2$ ) and from the retinal to the extra-retinal reference frame ( $\sigma_{T_{ExR}}^2$ ). See method section 3.1 for parameters description. |
|---|---|---|
| $\sigma_J^2 = 10.5^{\circ 2}$                         | $\sigma_J^2 = 18.4^{\circ 2}$                         |   |
| $\sigma_R^2 = 1.2^{\circ 2}$                          | $\sigma_R^2 = 4.7^{\circ 2}$                          |   |
| $\sigma_{N_R}^2 = 4.3^{\circ 2}$                      | $\sigma_{N_R}^2 = 6.5^{\circ 2}$                      |   |
| $\sigma_{T_{J \leftrightarrow R}}^2 = 21.5^{\circ 2}$ | $\sigma_{T_{J \leftrightarrow R}}^2 = 13.2^{\circ 2}$ |   |
| $\sigma_{T_{ExJ}}^2 = 21.6^{\circ 2}$                 | $\sigma_{T_{ExJ}}^2 = 16.5^{\circ 2}$                 |   |
| $\sigma_{T_{ExR}}^2 = 0.6^{\circ 2}$                  | $\sigma_{T_{ExR}}^2 = 4.7^{\circ 2}$                  |   |
| $\sigma_M^2 = 11.3^{\circ 2}$                         | $\sigma_M^2 = 7.8^{\circ 2}$                          |   |

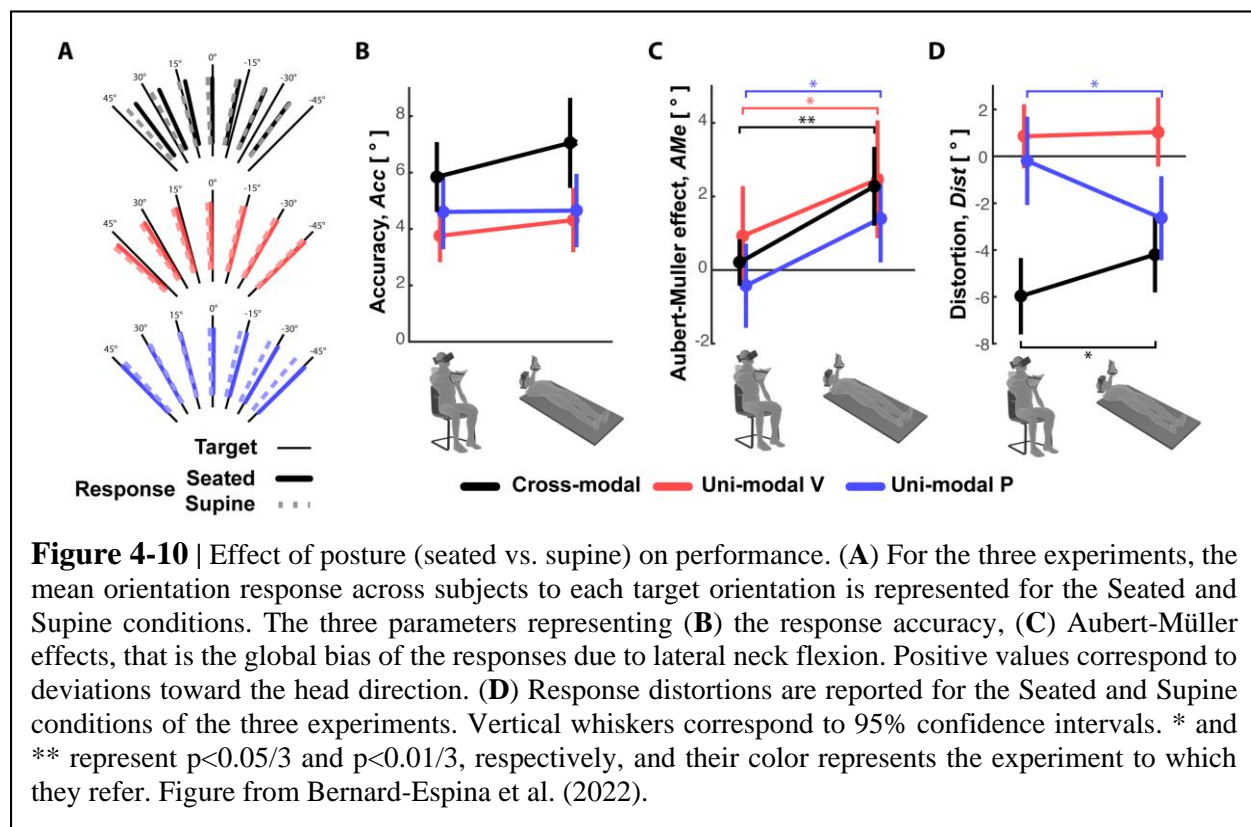
### 4.3 Study 3 – Gravitational influence on sensory transformations

The third study aimed to experimentally determine whether head misalignment with respect to the vertical (gravitational signals) interferes with sensory transformations. We asked subjects to align their unseen hand to a visual target (cross-modal task, with the necessity of performing sensory transformations) in seated and supine postures. After analyzing the response patterns, in

comparison to the response patterns observed in control experiments, we confronted the “Gravity Hypothesis” (*Gravity Hp*) with the two variations of the “Neck Hypothesis” (see section 2.3) using the model described in section 3.6.3.

### 4.3.1 Response patterns

The subjects’ average responses in the three main experiments (Cross-modal (V-P), Unimodal Visual (V-V) and Unimodal Proprioceptive (P-P) tasks) for the two tested postures (Seated and Supine) are depicted in Figure 4-10A where specific deviations of the responses away from the target can be seen for each task and each posture. Statistical analyses showed that none of the analyzed parameters were significantly affected by the posture *Order* and that the *Order* did not significantly interact with the *Posture* effect. Neither did *Posture* have a significant effect on the average error (accuracy) in any of three experiments (Figure 4-10B).



## Results: Study 3 – Gravitational influence on sensory transformations

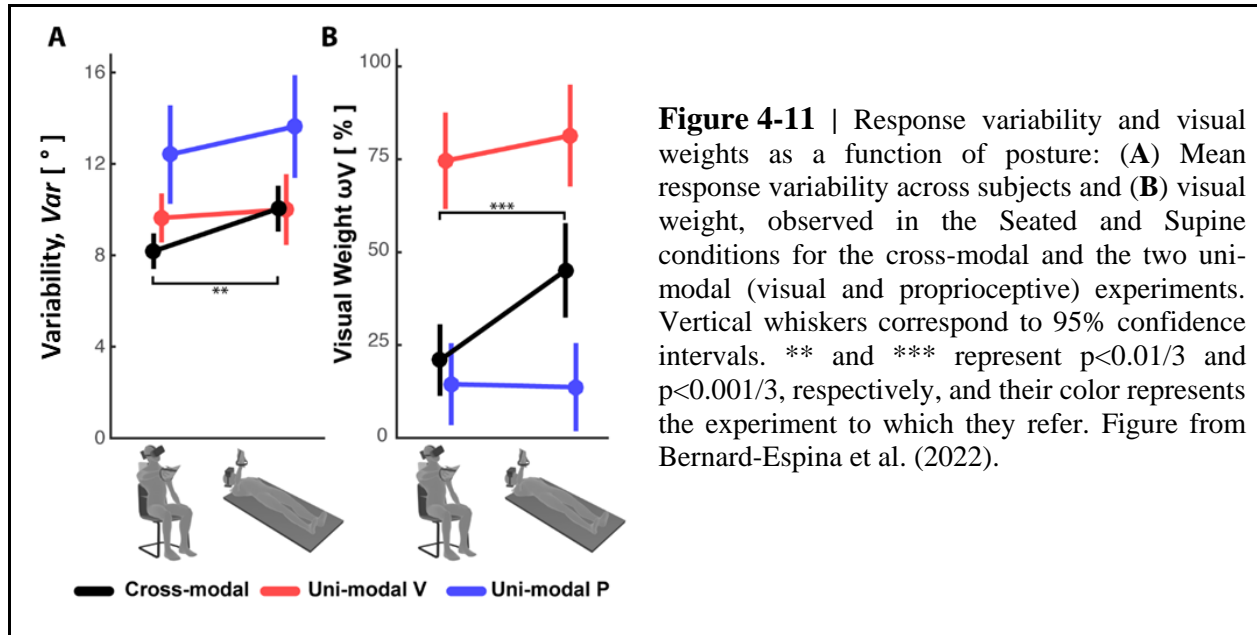
More specific analyses of the pattern of errors, however, revealed some specific effects of *Posture* (see statistics reported in Table 4-9). More precisely, the global response deviation in relation with the lateral head tilt, close to zero in the Seated condition, significantly increased in all three experiments when the subjects were Supine (Aubert-Muller effect in Figure 4-10C). The effect of posture on the perceptive distortion differed among the three experiments (Figure 4-10D): a significant modulation, in opposite directions, for cross-modal (V-P) and unimodal proprioceptive (P-P) tasks, but no difference for the unimodal visual experiment (V-V). In conclusion, seated or supine posture appeared to affect specific aspects of average response patterns, but the average error (accuracy) did not significantly change when supine.

**Table 4-9** | ANOVA main and interaction effects. For each of the experiments (cross-modal, V-P; unimodal visual V-V; unimodal proprioceptive, P-P) the two-factor ANOVA main effect of *Posture*, posture *Order* and the interaction between these two factors are reported for the Aubert-Müller effect (*AMe*), the response distortion (*Dist*), accuracy (*Acc*), and variability (*Var*), as well as for the relative weight associated to visual information,  $\omega_V$ . The significant results after the Bonferroni correction ( $p < 0.05/3$ ) are reported in bold fonts.

| Exp | Param.     | <i>Posture</i>   | <i>Order</i>                 | <i>Posture</i> × <i>Order</i> |
|-----|------------|--|------------------------------|-------------------------------|
| V-P | AMe        | $F_{(1,16)}=12.7$ , <b><math>p=0.0026</math></b>           | $F_{(1,16)}=0.18$ , $p=0.67$ | $F_{(1,16)}=0.01$ , $p=0.89$  |
|     | Dist       | $F_{(1,16)}=10.6$ , <b><math>p=0.0049</math></b>           | $F_{(1,16)}=0.23$ , $p=0.63$ | $F_{(1,16)}=0.61$ , $p=0.44$  |
|     | Acc        | $F_{(1,16)}=0.97$ , $p=0.34$                               | $F_{(1,16)}=0.97$ , $p=0.33$ | $F_{(1,16)}=0.34$ , $p=0.57$  |
|     | Var        | $F_{(1,16)}=15.3$ , <b><math>p=0.0012</math></b>           | $F_{(1,16)}=0.01$ , $p=0.91$ | $F_{(1,16)}=1.41$ , $p=0.25$  |
|     | $\omega_V$ | $F_{(1,16)}=23.9$ , <b><math>p=16 \cdot 10^{-5}</math></b> | $F_{(1,16)}=0.00$ , $p=0.97$ | $F_{(1,16)}=0.57$ , $p=0.46$  |
| V-V | AMe        | $F_{(1,16)}=9.16$ , <b><math>p=0.0080</math></b>           | $F_{(1,16)}=0.19$ , $p=0.67$ | $F_{(1,16)}=2.91$ , $p=0.11$  |
|     | Dist       | $F_{(1,16)}=0.01$ , $p=0.93$                               | $F_{(1,16)}=0.20$ , $p=0.65$ | $F_{(1,16)}=2.49$ , $p=0.13$  |
|     | Acc        | $F_{(1,16)}=1.63$ , $p=0.22$                               | $F_{(1,16)}=0.42$ , $p=0.52$ | $F_{(1,16)}=0.86$ , $p=0.37$  |
|     | Var        | $F_{(1,16)}=0.10$ , $p=0.76$                               | $F_{(1,16)}=0.07$ , $p=0.79$ | $F_{(1,16)}=0.85$ , $p=0.37$  |
|     | $\omega_V$ | $F_{(1,16)}=2.36$ , $p=0.14$                               | $F_{(1,16)}=0.25$ , $p=0.62$ | $F_{(1,16)}=3.54$ , $p=0.08$  |
| P-P | AMe        | $F_{(1,16)}=10.9$ , <b><math>p=0.0044</math></b>           | $F_{(1,16)}=0.98$ , $p=0.34$ | $F_{(1,16)}=2.11$ , $p=0.16$  |
|     | Dist       | $F_{(1,16)}=10.7$ , <b><math>p=0.0048</math></b>           | $F_{(1,16)}=0.01$ , $p=0.92$ | $F_{(1,16)}=6.93$ , $p=0.018$ |
|     | Acc        | $F_{(1,16)}=0.01$ , $p=0.93$                               | $F_{(1,16)}=4.94$ , $p=0.04$ | $F_{(1,16)}=0.04$ , $p=0.83$  |
|     | Var        | $F_{(1,16)}=0.85$ , $p=0.37$                               | $F_{(1,16)}=2.89$ , $p=0.11$ | $F_{(1,16)}=0.98$ , $p=0.33$  |
|     | $\omega_V$ | $F_{(1,16)}=0.02$ , $p=0.89$                               | $F_{(1,16)}=0.71$ , $p=0.41$ | $F_{(1,16)}=4.31$ , $p=0.054$ |

On the other hand, the variability of the responses *Var*, reported in Figure 4-11A, was affected by the posture: in the cross-modal experiment (V-P) the subjects were significantly less precise when supine, but this was not the case in the unimodal visual (V-V) and proprioceptive

experiments (P-P). The change, or lack thereof, in response variability was accompanied by a similar modulation of the sensory weighting shown in Figure 4-11B: only in the cross-modal task did the visual weight significantly increase in the supine posture.



Overall, these results suggest that the use of sensory information during the cross-modal paradigm differs from that of unimodal tasks, and that this weighted processing is significantly affected by posture.

### 4.3.2 Analysis of between-subject differences

To go beyond average responses, we then assessed whether inter-individual variability can provide more insight on the sensory processing underlying the three experiments.

For the Seated condition of the unimodal visual (V-V) and proprioceptive (P-P) experiments, the concurrent model predicts respectively a negative and positive correlation between the visual weighting and the variability of the motor vector estimation. In fact, a visual weight which is not close to 100% in the V-V task (because the cost of the sensory transformation from retinal to extra-retinal coordinates is negligible, as shown by the previous study, in

## **Results: Study 3 – Gravitational influence on sensory transformations**

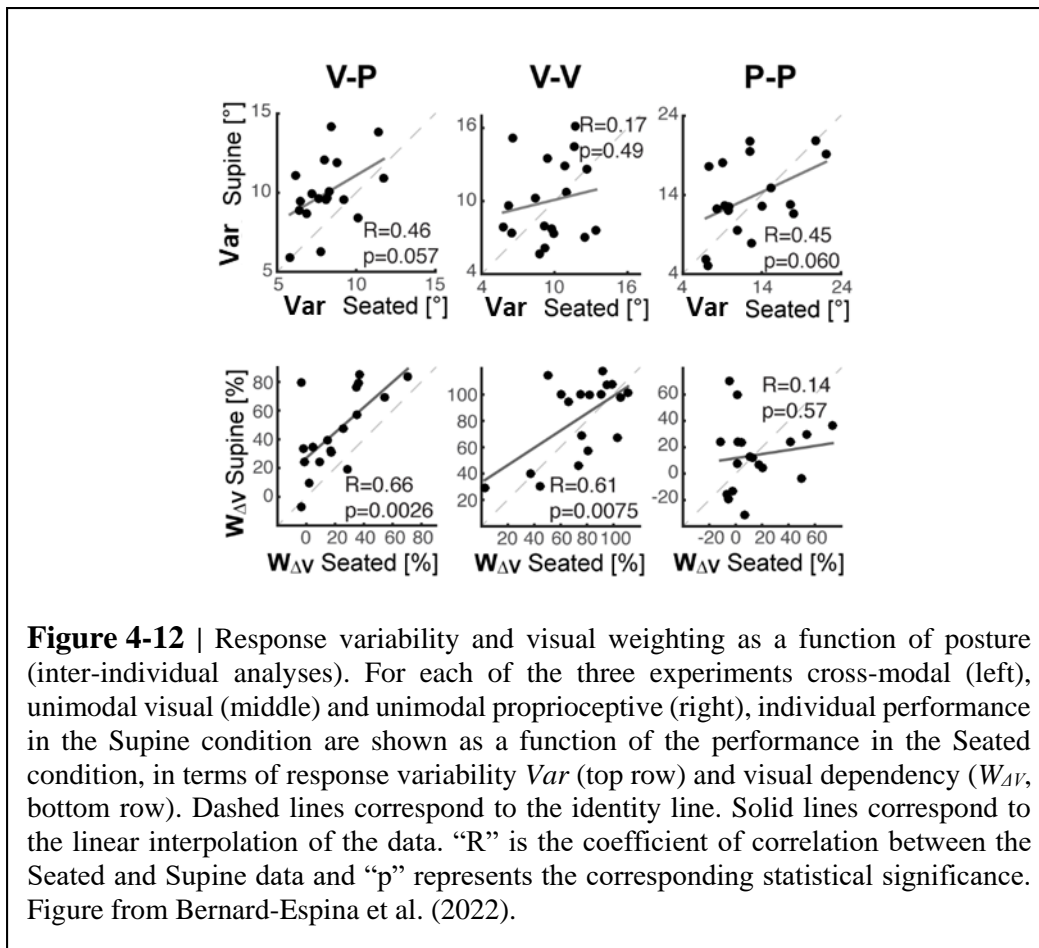
section 4.2.3), or higher than 0% in the P-P task (because we expect the proprioceptive signals to be encoded in joint coordinates in this case), both would correspond to suboptimal solutions and thus to an increase of the variability of the motor vector estimation (see sections 3.2 and 3.3). The correlation between inter-individual visual weighting and the variability of the motor vector estimation is reported in Table 4-10.

| <b>Exp.</b> | <b>R</b> | <b><i>p</i></b> | <b>Table 4-10</b>   Coefficient of correlation R (and associated <i>p</i> -value) between the variability ( <i>Var</i> ), and visual dependency ( $\omega_v$ ), in the Seated condition of the three experiments (Exp). |
|-------------|----------|-----------------|---|
| <b>V-P</b>  | 0.11     | 0.65            |   |
| <b>V-V</b>  | -0.41    | 0.09            |   |
| <b>P-P</b>  | 0.17     | 0.51            |   |

Although not statistically significant, the tendency to a negative correlation in the unimodal visual task reported in Table 4-10, is consistent with the model prediction, while the absence of correlation in the P-P experiment is not. This could be due to a significant contribution of motor noise to performance variability (*Var*) in this task, because both memorization and response require active hand movements. Motor noise affects the response variability but not the sensory weight, thus it might hide an existing correlation between the variability of motor vector estimation and the sensory weighting. The potential influence of motor noise is supported by the fact that the expected correlation seems to exist for the V-V task, where the motor component should be irrelevant. At least, we can expect that the motor noise in the V-V task, coming from the joystick actuation, is less important, and more similar between subjects, compared to the motor noise in the P-P task which involves a whole arm movement.

For the V-P task no clear correlation between weight  $\omega_v$  and response variability *Var* is to be expected, because, as explained in section 3.5 “*Cross-modal visuo-proprioceptive tasks (proprioceptive reaching of a visual target)*”, the sensory weight theoretically depends only on the noise attributed to the cross-modal sensory transformations, while the response variability depends also on the subject's visual and proprioceptive acuity. Moreover, motor noise could play a role, as in the P-P task.

In order to understand whether between-subject differences while seated would affect the individual performance when supine, we evaluated the correlation between the individual performance in the Seated and Supine conditions. As shown in Figure 4-12, we evaluated the performance in terms of response variability  $Var$ , and visual weight  $wv$ .



The top part of Figure 4-12 shows that the ranking of the subject in terms of response precision in the Seated condition tends to be preserved when Supine, but only in the tasks with relevant proprioceptive and motor components (V-P and P-P). Consistent with the results of Table 4-10, this finding suggests that the individual motor noise contributes to the observed response variability and tends to be preserved between postures. The bottom part of Figure 4-12 shows that in the tasks with a relevant visual component (V-P, V-V), the subjects that are most

visuo-dependent when seated, remain the most visuo-dependent when supine. These correlations suggest that, although different levels of visual-dependency can be observed among the subjects, their visual-dependency ranking was not altered by posture. It follows that the effect of the postural change in the cross-modal task was quite consistent among all participants.

### **4.3.3 Model predictions**

Figure 4-13A graphically represents the model predictions associated with the hypotheses that the lateral neck flexion per se (Neck1 Hp), the increase of the noise in the neck muscle-spindles (Neck2 Hp) or the head misalignment with respect to gravity (Gravity Hp), interferes with the ability to perform cross-modal transformation (detailed model equations are presented in Appendix D: see Supplementary Materials of Bernard-Espina et al., 2022). Their quantitative comparison with the experimental results is shown in Figure 4-13B in terms of differences between the Seated and Supine condition. Focusing these predictions on the effect of the postural change has two main advantages: first, it compensates for a possible role of individual motor precision or sensory acuity that, as we have shown above, might increase between-subject variability. Second, it simplifies the model by allowing a significant reduction of the number of estimated parameters (see section 3.6.3).

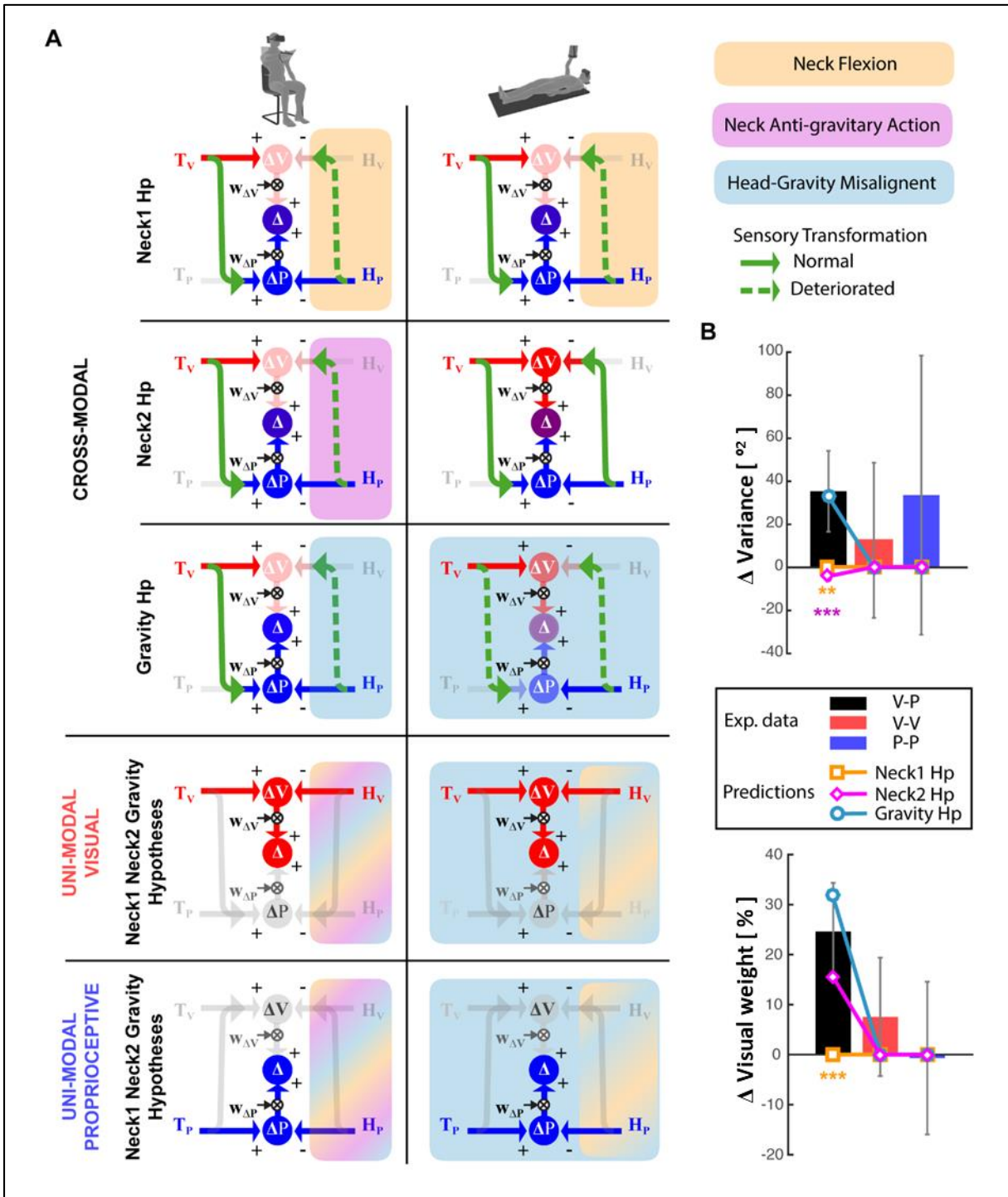
We simplified here the model presented in section 3.6.3, based on the hypothesis that, as suggested by the results of the previous study (section 4.2.3), the sensory transformation of retinal signals in extra-retinal coordinates does not substantially add noise the visual processing. Therefore, the retinal and extra-retinal reference frames are represented as a unique visual reference frame. Similarly, the joint and extra-joint reference frames are represented as a unique proprioceptive reference frame. In fact, in the three experimental tasks of this study (P-P, V-V, and V-P), the “extra-joint” reference frame has a sensory weight close to zero (see sections 3.2, 3.3 and 3.5). Therefore, the simplified model has only two reference frames that are sufficient to describe these tasks.

Figure 4-13B show that the first neck hypothesis (Neck1 Hp), which predicts no changes between Seated and Supine postures for all three, Cross-Modal, Unimodal Visual and Unimodal Proprioceptive tasks, is significantly different from the experimental observations (Hotelling’s test:

$T^2=93.0$ ,  $F_{(6,12)}=10.9$ ,  $p=0.0003$ ). The second neck hypothesis (Neck2 Hp) prediction also significantly differs from the experimental observations (Hotelling's test:  $T^2=34.93$ ,  $F_{(6,12)}=4.11$ ,  $p=0.017$ ). Indeed, although this hypothesis appears to better match the increase of the visual weight when supine, it cannot account for the increase in response variability; since in the Supine posture the neck muscles never act against gravity the model must predict a decrease of the response variability with respect to the Seated posture, which requires a neck muscle activation during the response phase to support the tilted head.

The gravity hypothesis (Gravity Hp), in contrast, appears to well capture the fact that the Supine posture increases both the response variability and the visual weight in the cross-modal task only (Hotelling's test:  $T^2= 9.65$ ,  $F_{(6,12)}=1.13$ ,  $p=0.40$ ). The matching between the Gravity Hp prediction and the experimental data is obtained with  $\sigma_N^2 = 81^{\circ 2}$ , which means that the variance associated with the cross-modal transformation would increase by about 3.5 times when the head is not aligned with gravity.

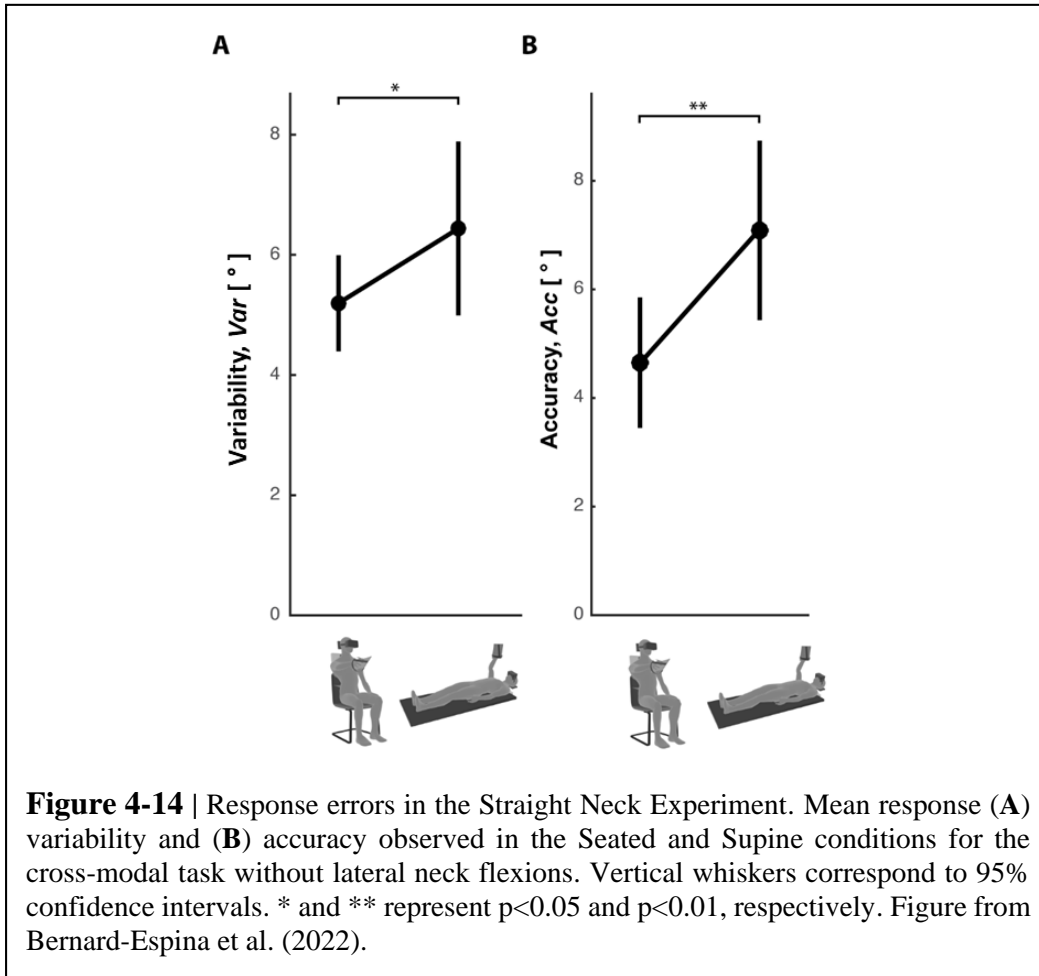
**Results: Study 3 – Gravitational influence on sensory transformations**



**Figure 4-13** | Model predictions as a function of seated vs. supine posture. **(A)** Graphical representation of the sensory information flow in the Seated (left) and Supine (right) conditions for the cross-modal, unimodal visual and unimodal proprioceptive experiments. For the cross-modal task the predictions for the Neck1, Neck2, and Gravity hypotheses are represented separately. For the unimodal visual and proprioceptive tasks, the three hypotheses are identical and thus represented together. The model structures and the graphical conventions are the same as in Figure 3-1, with a focus on the 2 reference frames that are used as predicted by the model. In addition, dashed green arrows represent perturbed cross-modal sensory transformations; faded arrows and circles are associated with a noisy information. For each tested theory the colored rectangular areas include the cross-modal transformations perturbed by the hypothesized disrupting factor: orange, violet and cyan represent the neck flexion, the neck muscles action against gravity and the head-gravity misalignment, respectively. Since for the unimodal tasks the three hypotheses are represented together, multicolor areas illustrate the cross-modal transformations affected by more than one disrupting factor. **(B)** Comparison between the experimental results and the predictions of the three hypotheses, in terms of modulation of the response variance (upper panel) and visual weight (lower panel) due to postural change (Supine-Seated). Vertical whiskers represent the 95% confidence interval of the experimental data. \*\* and \*\*\* represent statistical difference ( $p < 0.01$  and  $p < 0.001$ ) between the model predictions and the empirical results for each experiment and each parameter separately. The color of the stars indicates the tested hypothesis. Figure from Bernard-Espina et al. (2022).

### 4.3.4 Straight-Neck Experiment

To confirm the role of the head-gravity misalignment on the noise of visuo-proprioceptive transformations (experimental results and the model predictions of Figure 4-13) the response variability and accuracy was compared between the Seated and Supine conditions of a cross-modal task (V-P) performed without lateral neck movements. Figure 4-14 shows that, similar to the previous experiments, when supine the subjects are significantly less precise (one-tailed  $t$ -test  $t_{(11)}=3.42, p=0.04$ ) and less accurate (one-tailed  $t$ -test:  $t_{(11)}=2.79, p=0.009$ ) than when seated.



## **5 Discussion**

The main goal of this thesis is to provide new insights for the comprehension of proprioceptive deficits post-stroke, we further asked to which extent these deficits can be compensated with vision. We designed three studies focusing on the central processing of proprioceptive and visual information when using the upper limb, in the context of stroke and of healthy subjects. The experimental results of each study were interpreted through the prism of a common theoretical approach which describes the optimal fusion of visual and proprioceptive signals that are represented in multiple, concurrent reference frames (see the common theoretical framework presented in section 3). This concept allows distinguishing between “pure” proprioceptive processing (i.e. encoding of proprioceptive signals in native joint coordinates) and sensory transformations (i.e. re-encoding of the proprioceptive signals in non-native reference frames).

The three research questions, for the three studies, were:

- Q1. How does sensory transformation processing interact with proprioceptive deficits post-stroke, and how does it affect the patients’ ability to visually compensate for these deficits?
- Q2. Do sensory transformations affect the performance in uni-modal tasks (visual or haptic), and consequently influence multisensory visuo-haptic integration?
- Q3. Does head posture (head-gravity misalignment) affect the efficiency of sensory transformations?

In the following, I will summarize the main findings for each study, and will then justify how these results, together, contribute to a better understanding of sensory upper limb deficits that may be beneficial for stroke patients’ sensory assessment and rehabilitation.

### **5.1 Study 1 – Reinterpretation of the stroke literature on proprioceptive deficits**

In the first study, we presented a reinterpretation of proprioceptive post-stroke deficits affecting manual control, and of the ability of patients to compensate for these deficits using vision.

Our theoretical analysis uses a new “Extended Concurrent Model” for multisensory integration (see section 3). The rationale for this work hinges on the conceptual approach that the sensory space in which the information is encoded is not limited to the sensory system from which the signal originates. This concept is supported by evidence that retinal encoding of purely proprioceptive task-contingent stimuli (i.e., in absence of vision) occurs in some pointing tasks (Arnoux et al., 2017; Jones and Henriques, 2010; McGuire and Sabes, 2009; Pouget et al., 2002; Sarlegna and Sainburg, 2007; Tagliabue and McIntyre, 2013). Hence, it is questionable whether some tasks, traditionally classified as being proprioceptive, can be considered as relying on proprioceptive information only. Moreover, there is evidence that the efficacy of visual compensation is task-dependent (Herter et al., 2019; Scalha et al., 2011; Semrau et al., 2018; Torre et al., 2013). Therefore, it is also questionable whether different visual compensation tasks imply similar visual sensory processing.

### **5.1.1 A useful categorization of proprioceptive assessments**

Applying this concept to clinical proprioceptive deficits and visual compensation tests, we attempted to dissociate purely proprioceptive deficits from those affecting sensory transformations. We were able to show that tasks described as proprioceptive in clinical practice are likely to involve sensory transformations. As a consequence, task performances in patients may not specifically depend on a strictly proprioceptive deficit, but may also depend on deficits in performing these sensory transformations. Clinical and nonclinical methods as well as tasks that assess proprioceptive function and visual compensation have been reviewed and compared through this new conceptual framework. This led to a new classification of methods for proprioceptive assessments into four categories, which differ by the possibility or impossibility of performing a task by encoding sensory information directly in the reference frame associated with proprioception (joint receptors) and vision (retinal receptors). In the first category (within-arm assessments) both visual and proprioceptive information can be encoded in the primary sensory space, and the encoding of the information in additional reference frames does not lead a better task performance (precision). The second category (asymmetric between-arms assessments) includes those tasks in which visual, but not proprioceptive, information can be encoded in the primary sensory space. In the tasks of the third category (symmetric between-arms assessments), proprioceptive, but not

visual, information can be encoded in the primary sensory space. The tasks of the fourth category (cross-modal assessments) require encoding of retinal visual signals into a proprioceptive joint space and, vice-versa.

The present analysis suggests that only assessments using a within-arm task represent a “pure” proprioceptive test, because their execution does not require any sensory transformation of proprioceptive information. On the contrary, tasks including a between-arms condition, and in particular those that are asymmetric with respect to the body-midline, likely require sensory transformations, among which a reconstruction of the task in visual space. As a consequence, these tests do not specifically assess proprioceptive integrity per se, but also the ability to perform sensory transformations. Lesion-symptom and functional imaging studies support this hypothesis (Ben-Shabat et al., 2015; Butler et al., 2004; Grefkes et al., 2002; Iandolo et al., 2018; Pellijeff et al., 2006; Semrau et al., 2018; Van de Winckel et al., 2012). The neural network involved in between-arms tasks is wider compared to the network involved in simpler, within-arm, proprioceptive tasks (Ben-Shabat et al., 2015; Iandolo et al., 2018) and includes the PPC which is known to be involved in cross-modal (visuo-proprioceptive) transformation processing (Grefkes et al., 2002; Yau et al., 2015). Moreover, the use of visual information in between-arms mirror (symmetric) tasks might be dependent on the ability to perform sensory transformations (Herter et al., 2019; Semrau et al., 2018). Hence, the common practice in neurorehabilitation, to encourage the use of vision for guiding limb movements poststroke (Pumpa et al., 2015), might be effective when using only one arm or a between-arms asymmetric configuration, but not in the mirror configuration, unless the target is on the body midline (Torre et al., 2013). Since activities of daily living usually involve objects (e.g., grasping), visual feedback of hand position and orientation can often be used to compensate for proprioceptive deficits, as previously suggested (Scalha et al., 2011).

### **5.1.2 An enhanced patient stratification**

According to the present reasoning, the commonly interpreted proprioceptive deficits might often encompass a larger and in part multi-modal spectrum of dysfunctions. Taking sensory transformation processing into account in the assessment may potentially provide a more detailed patient stratification. The deficits may be reclassified into three distinct categories: (P) pure

**Discussion: Study 1 – Reinterpretation of the stroke literature on proprioceptive deficits**

proprioceptive deficits, (T) pure sensory transformation deficits, and (P+T) mixed proprioceptive and sensory transformation deficits. Table 5-1 lists the expected test performance as a function of assessment type and deficit category: although no single test can potentially differentiate these three clinical groups, the different combination of these tests could. This model, though more adequate, also has limits, since it focuses on stroke deficits in terms of sensory processing. Other factors can interfere with post-stroke performance in the different type of assessments, which are not taken into account by our model, such as age, hand dominance, target memorization, task workspace (Goble, 2010), active or passive reaching (Gurari et al., 2017), position or movement sense (Semrau et al., 2018). However, it provides a framework which reconciles apparently contradictory results from proprioceptive assessments (Contu et al., 2017; Gurari et al., 2017; Herter et al., 2019; Ingemanson et al., 2019; Rinderknecht et al., 2018; dos Santos et al., 2015; Torre et al., 2013) and from visual compensation tests (Darling et al., 2008a; Herter et al., 2019; Scalha et al., 2011; Semrau et al., 2018; Torre et al., 2013), and it adequately predicts the tendencies of experimental data (see Figure 4-1).

|                                 |                          | <b>P</b> | <b>T</b> | <b>P+T</b> |
|---------------------------------|--------------------------|----------|----------|------------|
| Proprioceptive assessments      | <b>W-A<sub>P</sub></b>   | x        |          | x          |
|                                 | <b>aB-A<sub>P</sub></b>  | x        | x        | x          |
|                                 | <b>sB-A<sub>P</sub></b>  | x        | x        | x          |
|                                 | <b>V-P</b>               | x        | x        | x          |
| Visual-compensation assessments | <b>W-A<sub>VP</sub></b>  |          |          |            |
|                                 | <b>aB-A<sub>VP</sub></b> |          |          |            |
|                                 | <b>sB-A<sub>VP</sub></b> |          | x        | x          |
|                                 | <b>V-VP</b>              |          |          |            |

**Table 5-1** | Tasks for which the model predicts an impairment (x) depending on the type of deficit present in patients: (P) deficit of purely proprioceptive origin, (T) sensory transformations deficit only, and (P+T) combined deficits.

W-A: within-arm assessments; aB-A: asymmetric between-arms assessments; sB-A: symmetric between-arms assessments; V-P/V-VP: cross-modal tasks. P and VP subscripts refer to proprioceptive and visuo-proprioceptive assessments (that is visual compensation) respectively.

According to the predicted effect of the three type of deficits (P, T, and P+T) on the test results (Table 5-1 and Figure 4-1), the best candidates for stratifying patients, among the assessments that are currently used, would be the combined use of the W-A<sub>P</sub> task (eyes closed) and a sB-A<sub>VP</sub> task (mirror, with visual feedback). Together, these two complementary assessments may help to better stratify patients. In addition to these two methods, adding visual feedback in common proprioceptive tasks (Herter et al., 2019; Marini et al., 2019; Scalha et al., 2011; Semrau et al., 2018; Torre et al., 2013), or using graphesthesia, shape or length discrimination (de Diego et al.,

2013; Turville et al., 2017; Van de Winckel et al., 2012) or reaching to visual targets with the unseen hand (Elangovan et al., 2019; Tagliabue and McIntyre, 2011) could help to further explore the complexity of sensorimotor deficits. In the future, to help explore this diversity, robot assisted tests may enter clinical routine (Contu et al., 2017; Rinderknecht et al., 2018). Robotic devices can overcome major limits of current clinical assessment: a quantitative measurement, without ceiling or floor effect, allowing for a more reliable, precise and reproducible evaluation of proprioceptive deficits (Contu et al., 2017; Deblock-Bellamy et al., 2018; Dukelow et al., 2010; Ingemanson et al., 2019; Lambercy et al., 2011; Rinderknecht et al., 2018; dos Santos et al., 2015; Semrau et al., 2017; Simo et al., 2014). The proposed stratification of patients may also provide insights about the neural correlates. We would expect that lesions of different brain areas would correspond to the three different categories of deficits. Hypothetically, and informed by the reviewed brain-mapping literature (section 4.1.3), injury affecting S1 may primarily relate to purely proprioceptive deficits, whereas lesions in the PPC and STG may cause deficits in the ability of performing sensory transformations. Patients with mixed deficits would likely tend to have larger lesions affecting both proprioceptive and associative areas.

### **5.2 Study 2 – Sensory transformations affecting visuo-proprioceptive integration**

In the second study, we investigated how sensory transformations affect visual, proprioceptive, and visuo-proprioceptive processing to further understand how it could influence functional performance of stroke patients. For this purpose, using a virtual reality set-up combined with a haptic feedback device, we have replicated the characteristics of the different clinical proprioceptive, and visual-compensation, assessments identified in my stroke literature analysis (section 2.1.2). Healthy subjects were asked to reproduce the same orientation (parallel task), or the mirror orientation (mirror task) of an object relative to the sagittal plane. In the mirror condition, but not in the parallel, we assume that sensory transformations are necessary to encode the visual or proprioceptive signals in extra-retinal or extra-joint reference frames.

## **Discussion: Study 2 – Sensory transformations affecting visuo-proprioceptive integration**

The unimodal visual tasks in this study (parallel,  $V_{//}$ , and mirror,  $V_{\wedge}$ ) do not have a clinical assessment equivalent, but were needed in order to study the multisensory integration in the visuo-haptic tasks.

It should be noted that the haptic and visuo-haptic tasks used in this experiment were all unimanual tasks, so we could study sensory transformations without considerations of interhemispheric transfer: the different tasks only differ by the mirror spatial transformation. Therefore, the comparison with proprioceptive clinical between-arms assessments need to account for this difference. From the visual point of view, the effect of mirroring the target position/orientation is the same for both our experimental tasks and the clinical between-arms assessments. But from the proprioceptive point of view, mirroring a target orientation with the same hand results in different joint signals, whereas mirroring a target position in a between-arm task result in the same joint configuration in both arms. Therefore, we compare our experimental tasks with the clinical assessments depending on the presence or absence of sensory transformations in the different tasks (and not on the use of one or two arms):

1. The Haptic Parallel task ( $H_{//}$ ) is equivalent to the Within-Arm proprioceptive assessments ( $W-A_P$ ), because the optimal execution of these tasks does not require sensory transformation of the joint signals (first row of Figure 5-1);
2. The Haptic Mirror task ( $H_{\wedge}$ ) is equivalent to the Asymmetric Between-Arms proprioceptive assessments ( $aB-A_P$ ), because these tasks cannot be performed by matching the joint configuration between the target and the response position/orientation, since they differ at the endpoint/orientation of the movement (second row of Figure 5-1);
3. The Visuo-Haptic Parallel task ( $V_{//}H_{//}$ ) is equivalent to the Within-Arm visual compensation assessments ( $W-A_{VP}$ ), because the optimal execution of these tasks does not require sensory transformation of neither the joint nor the retinal signals (third row of Figure 5-1);
4. The Visual Mirror-Haptic Parallel task ( $V_{\wedge}H_{//}$ ) is equivalent to the Symmetric Between-Arms visual compensation assessments ( $sB-A_{VP}$ ), because in these tasks the joint signals between target and response position/orientation can be directly compared, but not the visual signals (fourth row of Figure 5-1);
5. The Visual Parallel-Haptic Mirror task ( $V_{//}H_{\wedge}$ ) is equivalent to the Asymmetric Between-Arms visual compensation assessments ( $aB-A_{VP}$ ), because in these tasks the visual (retinal) signals

**Discussion: Study 2 – Sensory transformations affecting visuo-proprioceptive integration**

between target position/orientation can be directly compared with the response, but not the proprioceptive signals (fifth row of Figure 5-1).

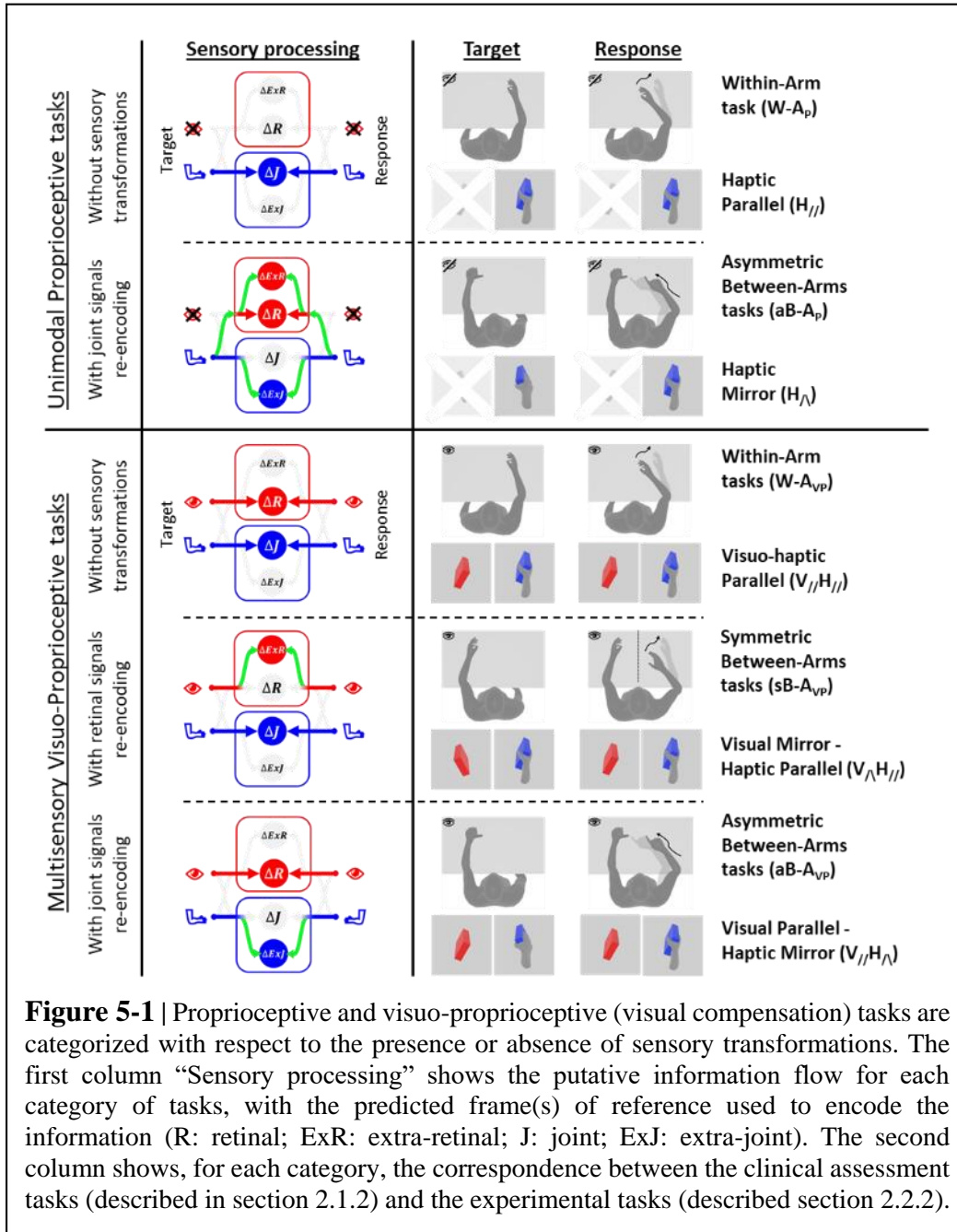


**Figure 5-1** | Proprioceptive and visuo-proprioceptive (visual compensation) tasks are categorized with respect to the presence or absence of sensory transformations. The first column “Sensory processing” shows the putative information flow for each category of tasks, with the predicted frame(s) of reference used to encode the information (R: retinal; ExR: extra-retinal; J: joint; ExJ: extra-joint). The second column shows, for each category, the correspondence between the clinical assessment tasks (described in section 2.1.2) and the experimental tasks (described section 2.2.2).

### **5.2.1 Evidence that sensory transformations affect sensory processing**

Our results support the idea that sensory transformations affect sensory processing in both visual and proprioceptive unimodal tasks. The increase of response variability, of response bias distortions, and of number of response adjustments, in the haptic mirror task with respect to the haptic parallel task is in line with experimental findings of studies using similar tests (Arnoux et al., 2017; Tagliabue and McIntyre, 2013), as well as with proprioceptive assessments results (see the results section 4.1.2 of the study on stroke proprioceptive assessments). Compared to “pure” proprioceptive tasks (i.e. without the necessity of transforming joint signals, see first row of Figure 5-1), the response precision in proprioceptive tasks involving the re-encoding of joint signals is worse (Arnoux et al., 2017; Bernard-Espina et al., 2021; Tagliabue and McIntyre, 2013), and a visual encoding of joint signals can be observed (Arnoux et al., 2017; Jones and Henriques, 2010; McGuire and Sabes, 2009; Pouget et al., 2002; Sarlegna and Sainburg, 2007; Tagliabue and McIntyre, 2013) (see second row of Figure 5-1). We found similar results for the unimodal visual tasks, in the horizontal working plane, which supports the idea that sensory transformations affect both proprioceptive and visual perception. This provides new insights into visuo-proprioceptive multisensory processing (and also into visual compensation post-stroke).

We clearly show that the increase of response variability in unimodal visual and unimodal haptic tasks, due to the necessity of sensory transformations, affects the relative importance associated to visual and haptic cues in multisensory fusion. In the  $V \wedge H //$  tasks (see fourth row of Figure 5-1), the decreased visual precision due to the sensory transformation of the retinal signals causes the visual sensory weight to decrease (as we observed in the horizontal plane, in the presence of visual noise). This experimental result is consistent with the results of Semrau et al. (2018) and Herter et al. (2019) showing that the majority of stroke patients have difficulties to compensate for their proprioceptive deficits using vision in this type of tasks: the potential advantage of the visual feedback is counterbalanced by the noise that the sensory transformation adds to the visual perception, especially for patients with posterior parietal cortex (PPC) lesions, which is likely involved in functional deficits in the ability to perform sensory transformations (see section 4.1.3). In contrast, in the  $V // H \wedge$  tasks (see last row of Figure 5-1), we found an increase of the visual weight, consistent with the decreased precision of the haptic perception (which involved a sensory transformation). Therefore, in this type of tasks, healthy subjects tend to rely more on vision for

which the target-response comparison is direct. As predicted by our model, the most efficient strategy is to mainly encode the task in the retinal reference frame, and reduce the proprioceptive sensory weight. This result supports the observations made with stroke patients that, even in the presence of a proprioceptive deficit, or sensory transformation deficit (or both), visual feedback (compensation) always provides a significant advantage (Bernard-Espina et al., 2021; Pampa et al., 2015; Scalha et al., 2011; Torre et al., 2013) due to a small proprioceptive weight and a high visual weight (close to 100%).

These results (the visual weight decreases in the  $V \wedge H //$  and increases in  $V // H \wedge$  task) appear to correspond to an optimal sensory fusion, and not to the neglect of visual or proprioceptive information. For the healthy subjects in our study, we observed a tendency for the variable error to decrease with respect to the unimodal tasks, suggesting that the multisensory integration of visual and haptic (proprioceptive) information is operated in a statistical optimal fashion, adjusting the sensory weights to minimize the variability of the responses. This optimal fusion of visual and haptic signals has been reported in previous research (Ernst and Banks, 2002).

### **5.2.2 Working plane orientation acts on the noise of sensory transformations**

Interestingly, we observed a visual weight decrease in the visuo-haptic  $V \wedge H //$  task (as predicted by our model) only in the horizontal working plane, that is for yaw orientations relative to the antero-posterior axis, and not in the frontal plane, that is for roll orientations relative to the vertical (gravity) axis (see Figure 4-8 in section 4.2.2). This result, together with those relative to unimodal tasks (Figure 4-5) indicate that the spatial mirror transformation of visual signals performed in the horizontal working plane decrease performances more than mirroring orientations in the frontal working plane. This is in line with studies on visual symmetries and mental rotations, suggesting that visual vertical symmetries provide a memory advantage and decrease reaction time in detection tasks with respect to other symmetries (Cattaneo et al., 2017, 2010; Prather and Sathian, 2002; Rossi-Arnaud et al., 2012). Using transcranial magnetic stimulation (TMS), Cattaneo et al. (2017) investigated two brain regions within the occipital cortex that might be involved in these visual symmetries. They found that the lateral occipital complex (LOC) was involved in detection of both vertical and horizontal symmetries, and that vertical symmetries rely also on other occipital regions. This suggests that our brain has developed specialized networks for

## **Discussion: Study 3 – Gravitational influence on sensory transformations**

the processing of vertical (over other types of) symmetries. Indeed, the vertical symmetry is omnipresent in our visual environment and in the spatial organization of visual shapes (Cattaneo et al., 2010; Wenderoth, 1994). Another factor, which could explain why the spatial mirror transformation are more efficient in the frontal plane, compared to the horizontal plane, is that gravity can be used as reference frame for the former but not the latter. As described in 1.2.3, the gravity vertical is hypothesized to play an important role in sensory transformations. More precisely, it is used as a reference to encode visual orientations in the frontal plane (roll orientations, similar to our experiment in the frontal plane) in the absence of external visual landmarks (Niehof et al., 2017).

Because most clinical proprioceptive (and visual compensation) assessments take place in the horizontal plane, our results in this working plane provide the best model to infer the sensory processing in clinical assessment tasks. All together, these experimental results provide a justification to our theoretical reinterpretation of proprioceptive post-stroke deficits. More specifically, we confirmed previous results showing sensory transformations affect unimodal proprioceptive perception (Arnoux et al., 2017; Tagliabue and McIntyre, 2013), and we provided the first experimental evidence (to our knowledge) of how visual sensory transformations can affect the ability to compensate for a proprioceptive deficit with vision.

### **5.3 Study 3 – Gravitational influence on sensory transformations**

In the third study, we have performed experiments to try to understand why lateral neck flexions appear to interfere with the sensory transformations used during reaching/grasping movements (Burns and Blohm, 2010; Tagliabue et al., 2013; Tagliabue and McIntyre, 2014, 2011). We asked volunteers to perform a virtual-reality task, that involved matching with an unseen hand a memorized visual target orientation, as if to grab it, after a lateral neck flexion. The subjects performed this task both in a Seated and Supine position. This cross-modal visuo-proprioceptive task requires sensory transformations which consist in encoding visual signals (of hand position/orientation) into proprioceptive joint space, and vice-versa.

### **5.3.1 Evidence for the gravitational influence on sensory transformations**

Our experimental data, together with our model of optimal multi-sensory integration, supported the hypothesis that head misalignment with respect to gravity, and not lateral neck flexion on its own, mainly interferes with the cross-modal visuo-proprioceptive transformations. Our model allowed to compute the effects of changing posture (seated or supine) in terms of response variability and in terms of the relative importance given to the visual and proprioceptive encoding. The “Gravity Hp” predicts an increase of both response variability and weight associated to the visual encoding in the cross-modal task, because when supine the head of the subject is always misaligned with respect to gravity, continuously perturbing sensory transformations. In contrast, it does not predict any change in response variability, nor sensory weighting, in unimodal tasks without the necessity of sensory transformations.

First, the results of the “Cross-Modal Experiment” (section 4.3.3) show a significant increase of the response variability and visual weight when supine, so that the “Gravity Hp” prediction is the closest to the experimental observations. With the “Straight-Neck Experiment” (section 4.3.4), which does not involve lateral head rotations, we were able to disentangle even further the role of gravitational afferences from those generated by neck movements, such as neck muscle spindle and semi-circular canal signals. The persistence, in this experiment as in the task with head rotations, of an increase of performance errors in the supine posture confirms and reinforces the importance of the gravity-head alignment. Overall, these results clearly support the hypothesis of a fundamental role of gravity in the ability to perform sensory transformations by reciprocal calibration of retinal and proprioceptive reference frames (see section 1.2.3), and is also consistent with our results from the study on multisensory integration which suggest a computational advantage of the sensory transformation when it is possible to use the gravity vertical as a reference frame (for spatial mirror transformations in the frontal working plane).

Second, to be able to exclude the hypothesis that the observed effect of posture in the cross-modal task could be ascribed to a degradation of the visual or proprioceptive acuity per se and not of the sensory transformations, we added two control experiments in which the subjects performed visual and proprioceptive tasks not requiring sensory transformations. The lack of significant differences between the seated and supine condition in terms of response variability and sensory weighting in these uni-modal experiments suggests that the head misalignment with respect to

gravity does not significantly alter the unimodal sensory precision per se, and thus supports the idea of a specific effect of posture/gravity on the sensory transformations.

The differential effects of posture on response precision between the cross-modal and unimodal tasks are perfectly in line with the results of McIntyre and Lipshits (2008). They showed that lateral tilting of the whole body by  $22.5^\circ$  clearly increases response (orientation) errors in a cross-modal (haptic-visual) task, but not so in two unimodal tasks (visual-visual and haptic-haptic). The consistency with the present results also suggests that the head tilt effects are independent of the tilt axis (pitch or roll).

In the three experimental tasks of this study (cross-modal visuo-proprioceptive, unimodal visual, and unimodal proprioceptive) we observed that posture also influences some features of the average response patterns. Although our theoretical framework does not provide predictions on this aspect of the subjects' performance, it is interesting to note that the response shifts due to the lateral neck flexion (Aubert-Müller effect) significantly increased when supine. This result suggests that gravity direction contributes to the encoding of target and response orientation, no independent of the modality. This is consistent with the study of Darling and Gilchrist (1991) on hand orientation reproduction showing that gravitational information influences the encoding of hand roll. Similarly, the disappearance of the oblique effect when the whole body is laterally tilted in purely visual (McIntyre et al., 2001) and cross-modal (McIntyre and Lipshits, 2008) orientation reproduction tasks was interpreted as evidence of the use of gravity as a reference to encode orientation cues.

### **5.3.2 Vestibular pathways to cortical networks involved in visuo-proprioceptive transformations**

That the brain performs cross-modal sensory transformations is well supported by several electrophysiological and brain imaging studies in healthy subjects (see sections 1.2.2 and 1.2.3), and also in stroke patients during specific proprioceptive assessment tasks (see section 4.1.3).

A brain area which appears to be a good candidate for performing cross-modal sensory transformations is the Intra-Parietal Sulcus (IPS) which has been shown to have neural activations compatible with the computation of visuo-tactile transformations in monkeys (Avillac et al., 2005)

and which is known to be involved in visuo-motor transformations performed during grasp movements (Janssen and Scherberger, 2015; McGuire and Sabes, 2011), as well as in proprioceptive assessment tasks requiring transformation of joint signals (see section 4.1.3). Experiments in monkeys have shown that, in this brain area, the information can be reencoded from retinal space to somatosensory space, and vice-versa, thanks to recurrent neural networks (Pouget et al., 2002) which would use the sensory signals relative to the eye-body kinematic chain to “connect” the two sensory spaces. In humans, the anterior part of IPS is strongly activated when comparing visual to haptic objects, and vice-versa (Grefkes et al., 2002) or when reaching a visual target without visual feedback of the hand (Beurze et al., 2010). Virtual lesions of this area through TMS interfere with visuo-tactile transformations, but not with uni-modal, visual and tactile, tasks (Buelte et al., 2008). The planning of cross-modal tasks, such as reach-and-grasp visual objects with an unseen hand, also appears affected by TMS of the anterior IPS (Verhagen et al., 2012).

Focusing on the main finding of the present study, one can ask through which neural pathway the head-gravity misalignment can affect the visuo-proprioceptive transformations occurring in the IPS. At the peripheral level, the information about the head orientation with respect to gravity is mainly provided by a complex integration of otolithic signals (Chartrand et al., 2016) arising from both the left and right organs (Uchino and Kushiro, 2011). Semicircular canal and neck proprioception, combined with otolithic information at the level of the vestibular nuclei (Dickman and Angelaki, 2002; Gdowski and McCrea, 2000), can also contribute to estimation of head orientation. However, since in the Straight Neck Experiment the posture effect was also observed when no head rotations, nor neck flexions, occurred, we can conclude that the otolithic signals are sufficient to affect visuo-proprioceptive transformations. At the central level, it is known that vestibular-otolithic information can reach the posterior parietal cortex through the posterior vestibular thalamocortical pathway, and also through the primary somatosensory (S1) and medial superior temporal cortices (Cullen, 2019; Hitier et al., 2014) which are all involved in sensory processing required in some proprioceptive assessments (see section 4.1.3). Specific otolithic afferences have been indeed observed in the IPS: otolithic stimulations activate neurons of Ventral IPS in monkeys (Chen et al., 2011; Schlack et al., 2002), with half of the neurons in this area which receive vestibular inputs (Bremmer, 2005), and human fMRI studies also show IPS activations resulting from saccular stimulations (Miyamoto et al., 2007; Schlindwein et al., 2008). Electrical stimulations of the anterior IPS have also been reported to elicit linear vestibular

---

## **Discussion: Common theoretical approach**

sensations in a patient (Blanke et al., 2000). Since head-gravity misalignment modulates the otolithic inputs and the otolithic system projects to the IPS, it is plausible that gravitational information would be integrated in the network of these brain areas (Avillac et al., 2005; Pouget et al., 2002) to “connect” the visual and the proprioceptive space. As a consequence, it is reasonable that an alteration of the otolithic gravitational input due to head tilt can alter sensory transformations.

It was suggested that we develop, through our sensory experiences, specialized networks for the processing of vertical symmetries (see section 5.2.2). That the Intra-Parietal Sulcus (IPS) is optimized to function with the head aligned with gravity appears consistent with its recurrent neural network structure (Pouget et al., 2002) in which the synaptic weights, necessary to perform visuo-proprioceptive transformations, are learnt through experience. Since the upright position is the most common head orientation in our everyday life, it is possible that these neural networks become “optimized” for this head position, and become significantly less effective when otolithic afferences signal a head tilt for which we have limited experience.

### **5.4 Common theoretical approach**

To describe and predict the sensory processing involved in all assessment and experimental tasks under investigation in this thesis, I developed an extended version of the “Concurrent Model” originally proposed to quantify optimal visuo-proprioceptive integration in the context of upper limb reaching tasks (Tagliabue and McIntyre, 2013, 2011). The “Extended Concurrent Model” (ECM) introduces additional reference frames for sensory encoding (4 in total, against 2 and 3 in the previous formulations, see Figure 3-13 and Table 3-1): it accounts for the possibility of re-encoding joint signals in “Extra-Joint” reference frames, as well as retinal signals in “Extra-Retinal” reference frames. The novelty of the ECM resides in this latter feature (extra-reference frames) providing a simple mathematical formulation to account for sensory transformations that occur in visual and proprioceptive spaces.

With this new theoretical approach, we were able to predict the performance of stroke patients accurately in various clinical sensory assessments (section 4.1.2). This conceptual framework was also consistent with neuroimaging studies (section 4.1.3), suggesting it may be

useful to represent cerebral aspects of visuo-proprioceptive processing. Furthermore, the ECM accurately predicted our experimental results in the study on multisensory visuo-haptic integration (section 4.2.3). Most importantly, the previous formulations of the concurrent model (with 2 and 3 reference frames) were unsuccessful in predicting our experimental results, which supports the necessity of using the ECM for a more comprehensive view of visuo-proprioceptive transformations.

Further results obtained from the data fitting procedure in our multisensory integration study (section 4.2.3) provide interesting insights, suggesting an asymmetry in sensory transformations, such that sensory transformations from joint to extra-joint space ( $T_{\text{ExJ}}$ ) are more noisy compared to retinal to extra-retinal transformations ( $T_{\text{ExR}}$ ), especially in the frontal plane (for roll orientations). Therefore, the encoding of visual information in retinal or extra-retinal spaces should be equivalent in terms of variability for tasks that are executed in the frontal plane: the previous formulations of the concurrent model with 2 or 3 reference frames would be adequate in this context. This is consistent with the findings of our study on gravitational influence on sensory transformations, in which the simpler model version was sufficient to describe accurately the sensory processing involved in the experimental tasks.

In contrast, in the horizontal working plane, as is the case for most clinical assessments, transformation of visual signals from retinal to extra-retinal space cannot be ignored. This is consistent with the reported results in the stroke literature and with our study on multisensory integration (as discussed in the previous paragraphs). Taking into account the  $T_{\text{ExR}}$  transformation is also consistent with the results from (Iandolo et al., 2015) who reported that, in the horizontal working plane, healthy subjects were more precise in a proprioceptive task where joint signals could be reconstructed in retinal coordinates (compared to a proprioceptive task not allowing visual reconstruction of joint signals in retinal coordinates).

Overall the ECM encompasses the two previous formulations of the concurrent model (Tagliabue and McIntyre, 2013, 2011), and provides accurate predictions where the latter failed.

As mentioned, our model does not intent to provide an exhaustive description of sensorimotor control. In particular, the ECM is based on the assumption that the main factors determining the modulation of task performance (precision) are of sensory (and not motor) origin. Although this choice appears appropriate for the tasks investigated here, which involve passive

## **Discussion: From assessment to rehabilitation**

and/or slow movements (with negligible dynamics), many other control theories focus on the optimization of biomechanical costs (Berret et al., 2011; Flash and Hogan, 1985; Nakano et al., 1999; Uno et al., 1989). Still other models linked movement variability to the level of muscle activation and motor noise (Harris and Wolpert, 1998; Todorov and Jordan, 2002). For movements at higher velocities, it has been shown: first, that the minimized movement costs depend on sensory and motor aspects (Berret et al., 2021); second, that modality-specific sensory delays determine how multiple feedback signals are combined (Crevecoeur et al., 2016). It follows that, if we want to predict performances for faster executions of the considered assessment tasks, and if we want to take into account redundant degrees of freedom of the arm (Levin et al., 2002), the ECM would need to be modified by including biomechanical and time related factors.

Other aspects not included in our theoretical framework are the role of prior knowledge, as implemented by Bayesian theory (Körding and Wolpert, 2004, 2006), and internal models which encompass the previously cited aspects (McNamee and Wolpert, 2019). Our decision is based on the hypothesis that little or no learning is involved during proprioceptive assessments (and our experimental paradigms). However, especially for our experiments involving ‘unusual’ postural configurations (section 4.3), this choice may be questionable: the role of gravity in the internal model (Assaiante et al., 2011; Chabeauti et al., 2012; Crevecoeur et al., 2009) may be linked to sensory transformations.

### **5.5 From assessment to rehabilitation**

Together, our three studies provide a novel framework to better understand sensory upper limb deficits. We learned from our reinterpretation of the stroke literature (study 1) that we can classify the different proprioceptive assessments based on the nature of the sensory processing involved. This finding allowed us to propose an improved stratification of post-stroke patients, which distinguishes between patients with deficits of the proprioceptive system per se, patients with deficits of the sensory transformation processing, and patients with the combined deficits of the former two. With the second study on multisensory visuo-haptic integration (study 2), we were able to confirm experimentally that the different assessment methods commonly used in clinical practice for post-stroke rehabilitation are characterized by different sensory processing. More

precisely, we showed that sensory transformations affect performance in unimodal proprioceptive tasks, and affect the ability to use vision to improve the performance in assessments of visual compensation. These experimental results were accurately predicted by our theoretical model developed in the context of the first study. This provides an additional justification for our new post-stroke stratification: since we precisely determined the sensory processing underlying the task execution for each type of assessment, we can therefore infer the patient-specific type of sensory deficit based on the functional performance of the patient. Finally, we learned from our study on the gravitational influence on sensory transformations (study 3) that gravity plays a fundamental role in the ability to perform sensory transformations, which provides a plausible interpretation for the different test results depending on the working plane orientation. A possible explanation for the gravity vertical acting as a common reference for the respective calibration of the different reference frames that we use for movement planning, as Paillard (1991) hypothesized, is that brain areas which are specifically involved in visuo-proprioceptive transformations receive otolithic afferences. In particular, otolithic pathways project to the posterior parietal and superior temporal cortices, that were both linked with the ability to perform proprioceptive tasks necessitating a re-encoding of the joint signals, which was reported in our stroke literature reinterpretation (study1).

The sum of these findings highlights that proprioceptive control of the hand may be strongly affected by the inability to perform sensory transformations. It is therefore crucial to assess sensory transformation capacities in stroke patients. In order to develop an accurate and robust clinical assessment of proprioception for stroke patients, we need to overcome substantial challenges. Even though our experimental results provide evidence that we can distinguish proprioception from sensory transformations, a major limit for the clinical translation of our approach is that we have so far studied behavior at the population level, but not at the single subject level. Given the high inter-individual variability in our two experimental studies, drawing conclusions at the individual level remains difficult.

Our results also suggest that knowing the brain lesion site could provide a first clue to know whether or not a sensory transformation deficit is to be expected, and therefore should not be overlooked in the clinical assessment. However, this consideration must be taken with care because discrepancies between the clinical assessments and the imaging reports are sometimes observed (Baudoin, 1996; Duyff et al., 1996; Healy et al., 2017). This may in part be explained by the

## **Discussion: From assessment to rehabilitation**

misidentification of the type of sensory deficits because of the lack of adequate assessment methods. Further lesion symptom studies examining the correlation of brain lesions in different categories of tasks may offer better identification of brain structures in relation to proprioception or sensory transformations.

Our new stratification of stroke patients may also result in more personalized rehabilitation plans. Given that sensory recovery is a predictor for motor and functional recovery (Bolognini et al., 2016), training of proprioception and sensory transformation processing may be key to improve motor recovery. However, sensory training, in contrast to motor training, is often neglected in neurorehabilitation. One of the main reasons for the neglected sensory rehabilitation in clinical practice is the lack of evidence demonstrating the benefits of somatosensory interventions on stroke recovery. The effectiveness of sensory rehabilitation is rather weak (Doyle et al., 2010; Findlater and Dukelow, 2017), in part due to heterogeneity in interventions, in outcomes measures (Doyle et al., 2010), and in the precision and reliability of the assessment (Findlater and Dukelow, 2017). A more accurate assessment of proprioceptive functions is key as it would potentially allow for sensory rehabilitation interventions targeting either proprioception alone, sensory transformations alone, or both of them. This would also allow adequate tracking of progress and effectiveness of a given rehabilitation protocol.

Some evidence of the effectiveness of sensory retraining, reinterpreted through the novel framework developed in this thesis, provides interesting perspectives for future research. Cross-modal training (reaching toward visual targets with the unseen hand) can improve cross-modal function in stroke patients, that is visuo-proprioceptive sensory transformations (Elangovan et al., 2019; Valdes et al., 2019), but does not specifically improve task performance in symmetric between-arms assessment (Sallés et al., 2017), which relies on different neural networks (see section 4.1.3, Figure 4-2). Within-arm proprioceptive training, without visual feedback (not requiring sensory transformations), improves performance in a within-arm (purely proprioceptive), but not in an asymmetric between arm assessment task requiring transformations (He et al., 2022). In contrast, patients with similar training with visual feedback appear to improve performance in an asymmetric between arm assessment (He et al., 2022).

These results, together with our theoretical approach and our experimental findings, suggest that adequate training needs to match the symptoms: training restricted to the proprioceptive

modality may not address dysfunction in sensory transformation processing, and vice versa. Using the concepts developed in this thesis, it seems possible to develop new and innovative rehabilitation strategies, using virtual reality for instance, which has been shown to be effective for upper-limb rehabilitation (Corbetta et al., 2015; Yates et al., 2016).

## **6 Perspectives**

In this last chapter, I will show some possible developments for the continuation of this thesis project, with a specific clinical application for the assessment of proprioception and sensory transformation.

### **6.1 A new paradigm for the assessment of proprioception**

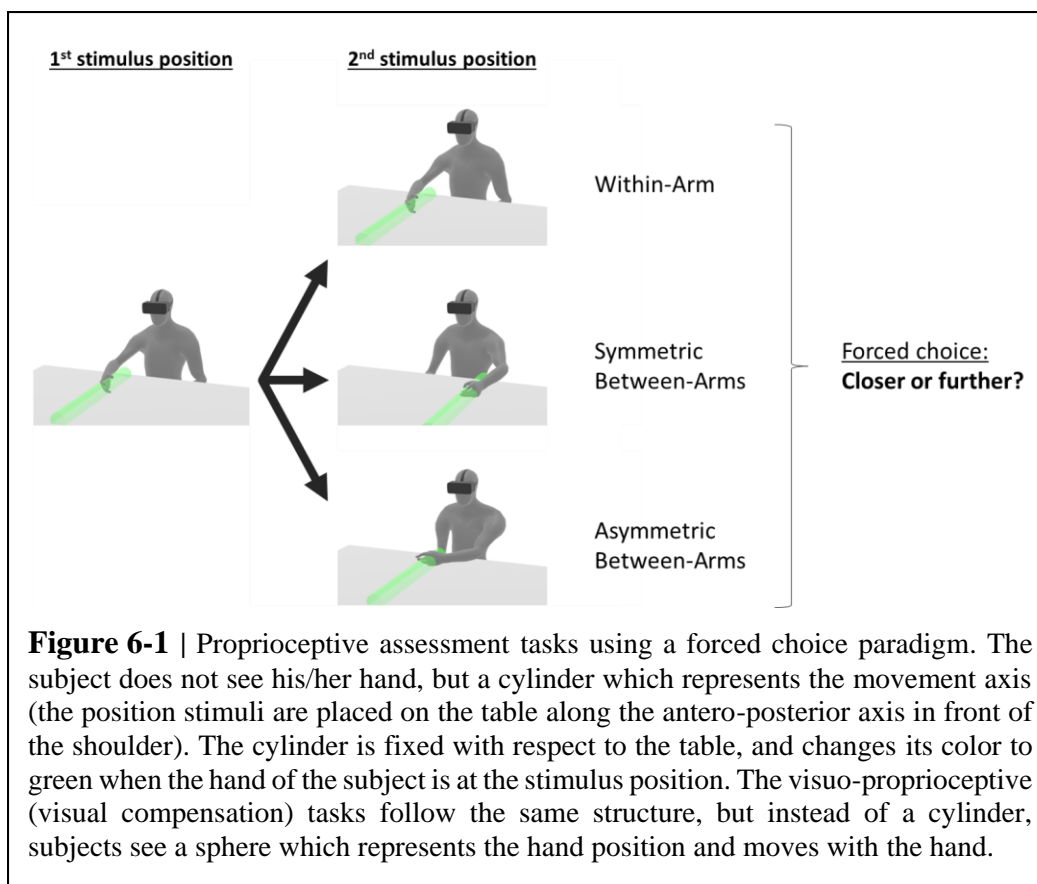
Applying our findings to the clinic may lead to new paradigms and guidelines for the development of new clinical assessment techniques of proprioception:

1. It seems fundamental to use several assessment methods to disentangle proprioceptive from sensory transformation deficits.
2. Proprioceptive and visuo-proprioceptive assessments that involve sensory transformations (as defined by our categorization of assessment tasks) should be executed in the horizontal working plan, to avoid interference of gravity.

Potential obstacles to the application of our findings for clinical assessments are the long duration of the experimental tasks (fatigue), and individual cognitive differences, such as in attention, working memory, and executive functions.

We currently are in the process of developing an assessment protocol that is intended to account for these limitations, and offer a reliable measurement at the single subject level with sufficient precision to detect small changes/improvements in task performance. We aim at developing an ecological task, that can be performed by most post-stroke patients (with motor deficits, spasticity, as well as attentional and working memory deficits). The assessment set-up should be light and portable in order to be easily used in the clinic.

This assessment protocol consists, for the first testing phase, of three proprioceptive tasks, and the corresponding three visuo-proprioceptive (compensation) tasks. The proprioceptive tasks mimic classical clinical assessments, performed in the horizontal plane (on a table) (see Figure 6-1).

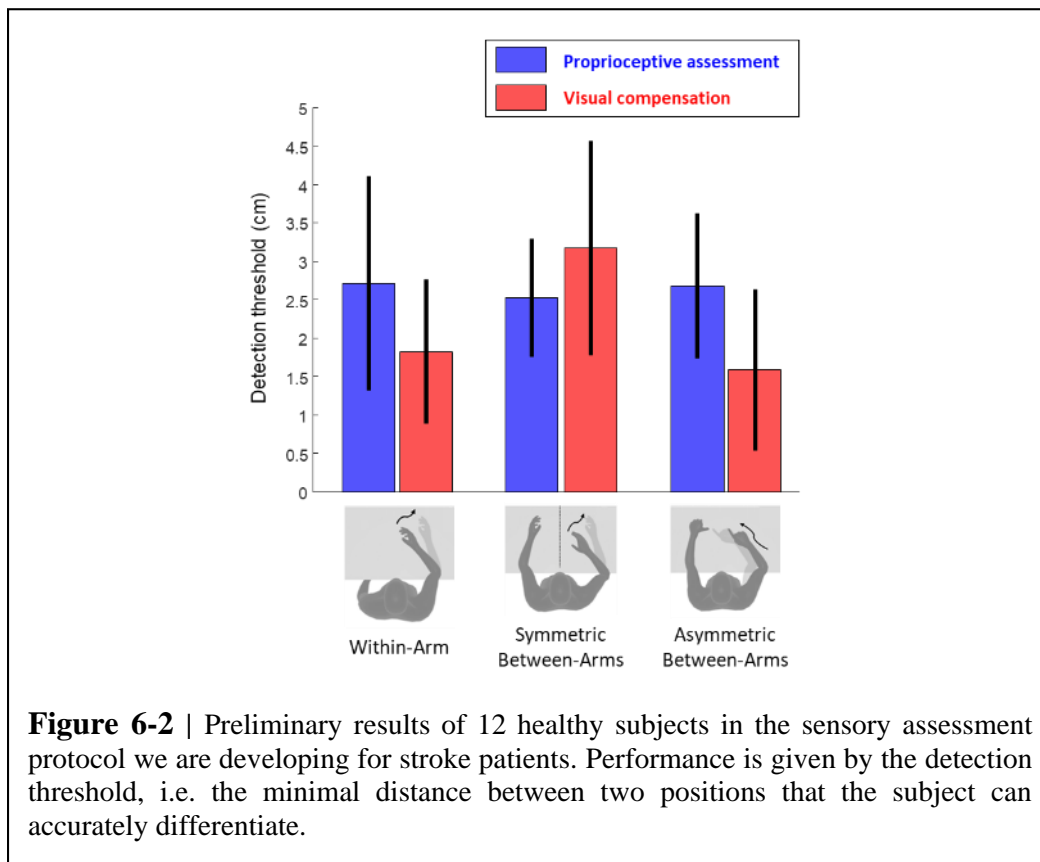


For each category of task (Within-arm, Between-arms symmetric and asymmetric), the proprioceptive or visual compensation conditions vary only by the presence or absence of a visual rendering of the virtual hand (as a small sphere). All tasks consist in sensing two different hand positions on the table (depth), and subjects are asked to report if the second position is farther or closer from the first (forced choice paradigm). No indications are provided concerning the reference frame to be used. The tasks are passive: the experimenter passively guides the subject's hand to the desired positions thanks to a feedback monitor. These tasks do not require active movement, thus reducing fatigue and allowing for testing of severely affected patients. Moreover, passive tasks seem to be more sensitive than active tasks to detect proprioceptive deficits (Goble, 2010).

Performance is measured with the detection threshold, i.e. the minimal distance between the two stimuli positions which are correctly perceived with 84% probability (Ernst and Banks, 2002). Preliminary results, obtained with 12 healthy subjects, show expected tendencies for the visual compensation tasks (see Figure 6-2): the visual feedback decreases the detection threshold

## Perspectives: A new paradigm for the assessment of proprioception

(i.e. improves performance) in the within-arm and between-arm asymmetric tasks, but not in the between-arms symmetric task. However, for the proprioceptive tasks, we cannot observe the expected modulation of precision between proprioceptive conditions, that is the higher variability in the asymmetric between-arms task with respect to the two other proprioceptive tasks. This is inconsistent with our experimental results of the study on multisensory visuo-haptic performance, where we showed that the necessity of re-encoding the joint signals in extra-joint reference frames (as in the asymmetric between-arm task) increases response errors.



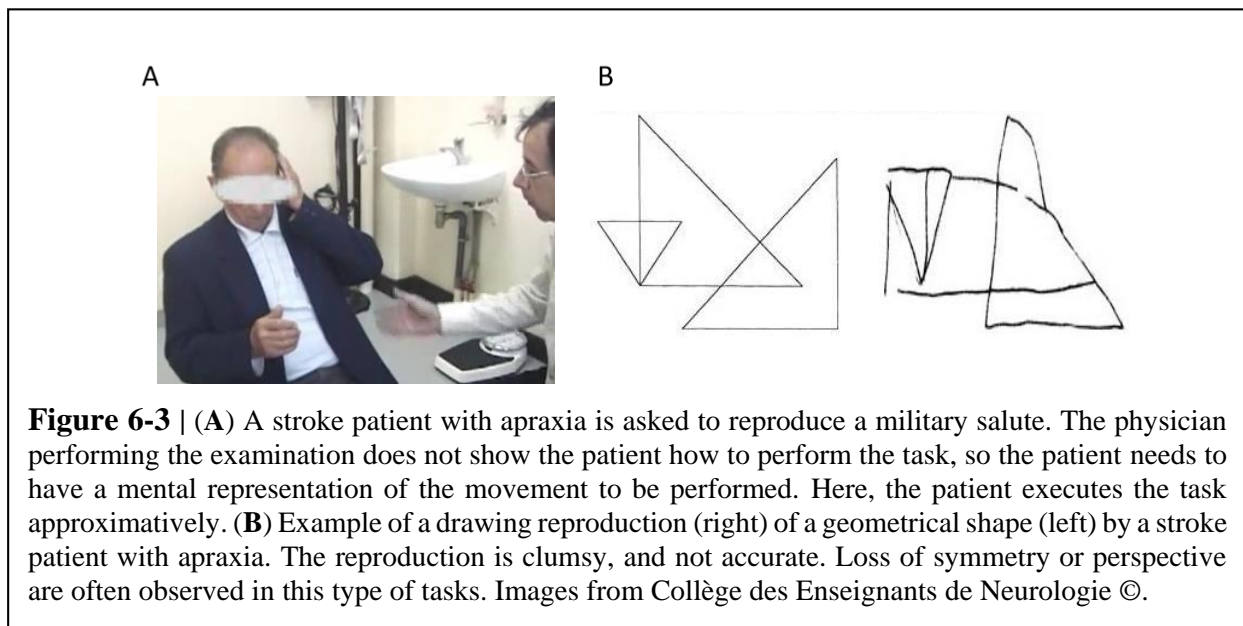
This result may be explained by the fact that this preliminary version of the protocol shows ceiling and floor effects. We expect that implementing a psychometric adaptive staircase procedure will provide the individual detection thresholds more precisely, rapidly, and with good reliability (Hoseini et al., 2015). After validation of this assessment protocol, we aim at simplifying and optimizing the experimental paradigm for stratifying the patients.

## **6.2 Possible applications for the assessment of other neurological deficits**

Knowing now that sensory transformation processing mainly involves the posterior parietal cortex (PPC), and that it is affected by gravity perception, we can have a new look on neurological deficits such as apraxia and hemispatial neglect which are both caused by PPC lesions, and vestibular disorders which can impact gravity perception.

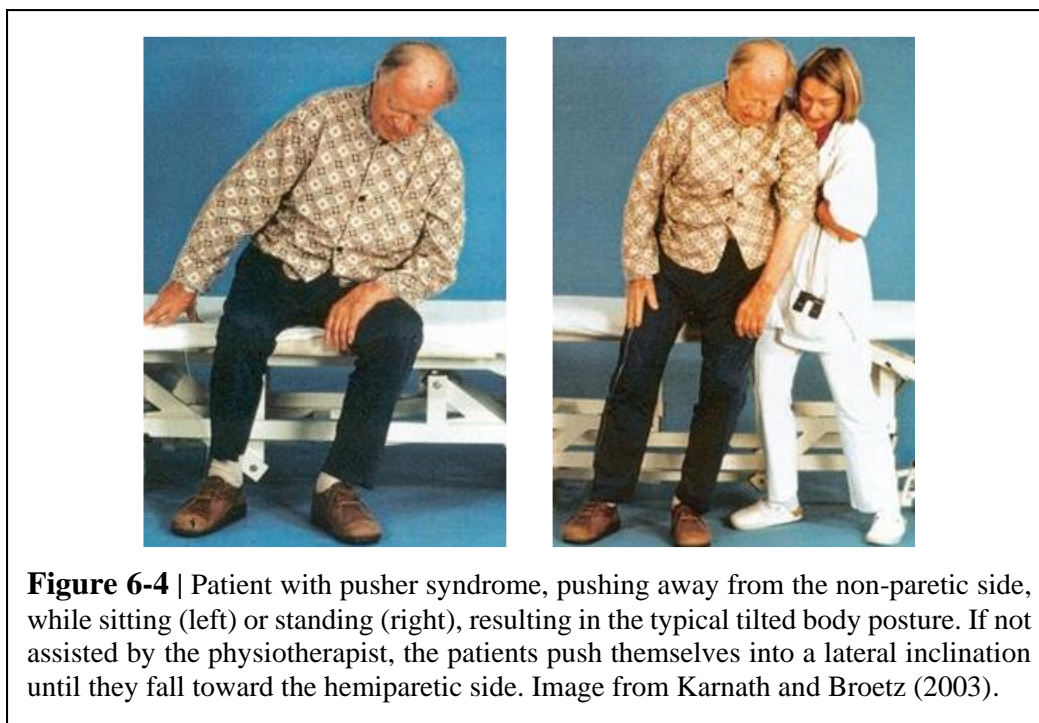
### ***Apraxia***

Apraxia is a disorder of movement programming which cannot be explained by weakness, sensory loss, abnormalities of posture/tone/movement, or a lack of understanding/cooperation. Patients with apraxia can have difficulty manipulating and using objects as well as copying/visualizing movements and complex geometric shapes (Foundas, 2013; Trojano and Grossi, 1998). This neurological disorder is poorly understood, underdiagnosed and very few therapeutic options are available (Foundas and Duncan, 2019). The systematic assessment of the ability to perform sensory transformations, and its rehabilitation, could enter the clinical routine for apraxia. It may explain in part movement abnormalities (Figure 6-3A) and poor shape reproduction (Figure 6-3B), where the patients have to transform a visual/mental representation to a movement.



***Hemispatial neglect***

Hemispatial neglect is characterized by a deficit in attention and awareness towards the side opposite to the brain lesion (contralesional space). It was shown that patients with hemispatial neglect display systematic deviations of the subjective vertical (Funk et al., 2011), which is a highly multisensory process relying on visual, proprioceptive and otolithic signals (Fraser et al., 2015). This deviation is consistent with the fact that some patients can experience their body as oriented "upright" when the body is actually tilted to the side of the brain lesion (to the ipsilesional side), which can cause the *pusher syndrome* (Karnath and Broetz, 2003). This is a clinical disorder in which patients actively push away from the non-hemiparetic side, leading to a loss of postural balance (see Figure 6-4). Interestingly, it was reported that manipulating the gravitational-otolithic information, as we did in our experimental study by placing the subject in a supine posture, significantly improved hemispatial neglect (Onaka et al., 2022; Pizzamiglio et al., 1997, 1995). Assessing and treating potential sensory transformation deficits could be relevant in this case, as a way to realign the different sensory percepts (visual, proprioceptive and vestibular), which do not appear to be affected individually (Karnath and Broetz, 2003).



*Vestibular disorders*

The assessment of sensory transformations processing could also be important in non-stroke neurological disorders, such as pathologies of the vestibular system. Indeed, the results from our experiment on the effect of posture (see section 5.3) suggests that vestibular pathologies might perturb not only equilibrium and eye movements, but also the eye-hand coordination, which is rarely assessed in these patients.

## 7 Conclusion

Proprioception is a prerequisite for normal hand function, in particular for reaching, grasping and object manipulation. Using a theoretical approach, based on statistical models of optimal multi-sensory integration, we have reinterpreted post-stroke proprioceptive deficits, as well as the ability of patients to visually compensate for their deficit. We successfully reconciled the apparently contradictory results of a large number of clinical studies, providing a novel rationale for an improved stratification of stroke patients according to their sensory deficits (either of purely proprioceptive origin, or of sensory transformations). This new stratification was supported by lesion-behavior studies: patients with lesions in the posterior parietal cortex, which is known to be involved in visuo-proprioceptive transformations, appear to show specific functional deficits in the proprioceptive and visual compensation assessment tasks requiring sensory transformations. Using virtual reality and a haptic device, we designed behavioral experiments with healthy participants to reproduce the characteristics of post-stroke assessment tasks in the laboratory. Our results confirmed our reinterpretation of the stroke literature: we found that sensory transformations affect visuo-proprioceptive integration, supporting that proprioceptive control of the hand may be largely affected by the inability to perform sensory transformations in stroke patients, and that visual compensation in some cases may also be perturbed. In a second virtual reality experiment, we showed that head-gravity misalignment interferes with sensory transformations, supporting the theorized central role of gravity in spatial perception. This suggests that the neural networks in the posterior parietal cortex involved in visuo-proprioceptive sensory transformations are dependent on otolithic afferences. Altogether, these results provide a novel framework to better understand sensory deficits and allow us to propose an improved classification of post-stroke deficits with a new stratification of patients, and a new innovative sensory assessment protocol. This may result, in the long term, in more personalized and more effective sensory rehabilitation plans.

# References

- Abedi Khoozani P, Blohm G. Neck muscle spindle noise biases reaches in a multisensory integration task. *Journal of Neurophysiology* 2018;120:893–909. <https://doi.org/10.1152/jn.00643.2017>.
- Alawieh A, Zhao J, Feng W. Factors affecting post-stroke motor recovery: Implications on neurotherapy after brain injury. *Behav Brain Res* 2018;340:94–101. <https://doi.org/10.1016/j.bbr.2016.08.029>.
- Armenta Salas M, Bashford L, Kellis S, Jafari M, Jo H, Kramer D, et al. Proprioceptive and cutaneous sensations in humans elicited by intracortical microstimulation. *ELife* 2018;7:e32904. <https://doi.org/10.7554/eLife.32904>.
- Arnoux L, Fromentin S, Farotto D, Beranek M, McIntyre J, Tagliabue M. The visual encoding of purely proprioceptive intermanual tasks is due to the need of transforming joint signals, not to their interhemispheric transfer. *Journal of Neurophysiology* 2017;118:1598–608. <https://doi.org/10.1152/jn.00140.2017>.
- Assaiante C, Chabeauti P-Y, Sveistrup H, Vaugoyeau M. Updating process of internal model of action as assessed from motor and postural strategies in young adults. *Hum Mov Sci* 2011;30:227–37. <https://doi.org/10.1016/j.humov.2010.05.007>.
- Avillac M, Denève S, Olivier E, Pouget A, Duhamel J-R. Reference frames for representing visual and tactile locations in parietal cortex. *Nat Neurosci* 2005;8:941–9. <https://doi.org/10.1038/nn1480>.
- Azañón E, Longo MR. Tactile Perception: Beyond the Somatotopy of the Somatosensory Cortex. *Curr Biol* 2019;29:R322–4. <https://doi.org/10.1016/j.cub.2019.03.037>.
- Azañón E, Longo MR, Soto-Faraco S, Haggard P. The Posterior Parietal Cortex Remaps Touch into External Space. *Current Biology* 2010;20:1304–9. <https://doi.org/10.1016/j.cub.2010.05.063>.
- Bastian HC. The “muscular sense”; its nature and localization. *Brain* 1887;10:1–89. <https://doi.org/10.1093/brain/10.1.1>.
- Baudoin D. Curious dissociation between cerebral imaging and clinical findings. *Lancet* 1996;347:965. [https://doi.org/10.1016/s0140-6736\(96\)91447-6](https://doi.org/10.1016/s0140-6736(96)91447-6).
- van Beers RJ, Sittig AC, van der Gon Denier JJ. How humans combine simultaneous proprioceptive and visual position information. *Exp Brain Res* 1996;111:253–61. <https://doi.org/10.1007/BF00227302>.
- Ben-Shabat E, Matyas TA, Pell GS, Brodtmann A, Carey LM. The Right Supramarginal Gyrus Is Important for Proprioception in Healthy and Stroke-Affected Participants: A Functional MRI Study. *Front Neurol* 2015;6. <https://doi.org/10.3389/fneur.2015.00248>.

- Bernard-Espina J, Beraneck M, Maier MA, Tagliabue M. Multisensory Integration in Stroke Patients: A Theoretical Approach to Reinterpret Upper-Limb Proprioceptive Deficits and Visual Compensation. *Front Neurosci* 2021;15:646698. <https://doi.org/10.3389/fnins.2021.646698>.
- Bernard-Espina J, Dal Canto D, Beraneck M, McIntyre J, Tagliabue M. How Tilting the Head Interferes With Eye-Hand Coordination: The Role of Gravity in Visuo-Proprioceptive, Cross-Modal Sensory Transformations. *Front Integr Neurosci* 2022;16:788905. <https://doi.org/10.3389/fnint.2022.788905>.
- Berret B, Chiovetto E, Nori F, Pozzo T. Evidence for Composite Cost Functions in Arm Movement Planning: An Inverse Optimal Control Approach. *PLOS Computational Biology* 2011;7:e1002183. <https://doi.org/10.1371/journal.pcbi.1002183>.
- Berret B, Conessa A, Schweighofer N, Burdet E. Stochastic optimal feedforward-feedback control determines timing and variability of arm movements with or without vision. *PLoS Comput Biol* 2021;17:e1009047. <https://doi.org/10.1371/journal.pcbi.1009047>.
- Beurze SM, Toni I, Pisella L, Medendorp WP. Reference Frames for Reach Planning in Human Parietofrontal Cortex. *Journal of Neurophysiology* 2010;104:1736–45. <https://doi.org/10.1152/jn.01044.2009>.
- Birchenall J, Térémetz M, Roca P, Lamy J-C, Oppenheim C, Maier MA, et al. Individual recovery profiles of manual dexterity, and relation to corticospinal lesion load and excitability after stroke –a longitudinal pilot study. *Neurophysiologie Clinique* 2019;49:149–64. <https://doi.org/10.1016/j.neucli.2018.10.065>.
- Blanke O, Perrig S, Thut G, Landis T, Seeck M. Simple and complex vestibular responses induced by electrical cortical stimulation of the parietal cortex in humans. *Journal of Neurology, Neurosurgery & Psychiatry* 2000;69:553–6. <https://doi.org/10.1136/jnnp.69.4.553>.
- Bolognini N, Russo C, Edwards DJ. The sensory side of post-stroke motor rehabilitation. *RNN* 2016;34:571–86. <https://doi.org/10.3233/RNN-150606>.
- Bottini R, Doeller CF. Knowledge Across Reference Frames: Cognitive Maps and Image Spaces. *Trends in Cognitive Sciences* 2020;24:606–19. <https://doi.org/10.1016/j.tics.2020.05.008>.
- Bremmer F. Navigation in space – the role of the macaque ventral intraparietal area. *The Journal of Physiology* 2005;566:29–35. <https://doi.org/10.1113/jphysiol.2005.082552>.
- Brindley GS, Lewin WS. The sensations produced by electrical stimulation of the visual cortex. *The Journal of Physiology* 1968;196:479–93. <https://doi.org/10.1113/jphysiol.1968.sp008519>.
- Buelte D, Meister IG, Staedtgen M, Dambeck N, Sparing R, Grefkes C, et al. The role of the anterior intraparietal sulcus in crossmodal processing of object features in humans: An rTMS study. *Brain Research* 2008;1217:110–8. <https://doi.org/10.1016/j.brainres.2008.03.075>.
- Buneo CA, Andersen RA. Integration of target and hand position signals in the posterior parietal cortex: effects of workspace and hand vision. *J Neurophysiol* 2012;108:187–99. <https://doi.org/10.1152/jn.00137.2011>.
- Burgess N. Spatial cognition and the brain. *Ann N Y Acad Sci* 2008;1124:77–97. <https://doi.org/10.1196/annals.1440.002>.

- Burns JK, Blohm G. Multi-sensory weights depend on contextual noise in reference frame transformations. *Front Hum Neurosci* 2010;4:221. <https://doi.org/10.3389/fnhum.2010.00221>.
- Butler AJ, Fink GR, Dohle C, Wunderlich G, Tellmann L, Seitz RJ, et al. Neural mechanisms underlying reaching for remembered targets cued kinesthetically or visually in left or right hemispace. *Hum Brain Mapp* 2004;21:165–77. <https://doi.org/10.1002/hbm.20001>.
- Büttner-Ennever JA. A review of otolith pathways to brainstem and cerebellum. *Ann N Y Acad Sci* 1999;871:51–64. <https://doi.org/10.1111/j.1749-6632.1999.tb09175.x>.
- Carlsson H, Ekstrand E, Brogårdh C. Sensory Function, Measured as Active Discriminative Touch, is Associated With Dexterity after Stroke. *PM&R* 2019;11:821–7. <https://doi.org/10.1002/pmrj.12044>.
- Cattaneo Z, Bona S, Silvanto J. Not all visual symmetry is equal: Partially distinct neural bases for vertical and horizontal symmetry. *Neuropsychologia* 2017;104:126–32. <https://doi.org/10.1016/j.neuropsychologia.2017.08.002>.
- Cattaneo Z, Fantino M, Silvanto J, Tinti C, Pascual-Leone A, Vecchi T. Symmetry perception in the blind. *Acta Psychol (Amst)* 2010;134:398–402. <https://doi.org/10.1016/j.actpsy.2010.04.002>.
- Chabeauti PY, Assaiante C, Vaugoyeau M. Extreme short-term environmental constraints do not update internal models of action as assessed from motor imagery in adults. *Neuroscience* 2012;222:69–74. <https://doi.org/10.1016/j.neuroscience.2012.07.002>.
- Chafee MV, Averbeck BB, Crowe DA. Representing Spatial Relationships in Posterior Parietal Cortex: Single Neurons Code Object-Referenced Position. *Cerebral Cortex* 2007;17:2914–32. <https://doi.org/10.1093/cercor/bhm017>.
- Chartrand T, McCollum G, Hanes DA, Boyle RD. Symmetries of a generic utricular projection: neural connectivity and the distribution of utricular information. *J Math Biol* 2016;72:727–53. <https://doi.org/10.1007/s00285-015-0900-5>.
- Chen A, DeAngelis GC, Angelaki DE. Representation of Vestibular and Visual Cues to Self-Motion in Ventral Intraparietal Cortex. *J Neurosci* 2011;31:12036–52. <https://doi.org/10.1523/JNEUROSCI.0395-11.2011>.
- Chen X, DeAngelis GC, Angelaki DE. Flexible egocentric and allocentric representations of heading signals in parietal cortex. *Proc Natl Acad Sci U S A* 2018;115:E3305–12. <https://doi.org/10.1073/pnas.1715625115>.
- Cluff T, Crevecoeur F, Scott SH. A perspective on multisensory integration and rapid perturbation responses. *Vision Research* 2015;110:215–22. <https://doi.org/10.1016/j.visres.2014.06.011>.
- Collins DF. Proprioception: Role of Cutaneous Receptors. In: Binder MD, Hirokawa N, Windhorst U, editors. *Encyclopedia of Neuroscience*, Berlin, Heidelberg: Springer; 2009, p. 3311–5. [https://doi.org/10.1007/978-3-540-29678-2\\_4825](https://doi.org/10.1007/978-3-540-29678-2_4825).
- Connell L, Lincoln N, Radford K. Somatosensory impairment after stroke: frequency of different deficits and their recovery. *Clin Rehabil* 2008;22:758–67. <https://doi.org/10.1177/0269215508090674>.

- Contu S, Hussain A, Kager S, Budhota A, Deshmukh VA, Kuah CWK, et al. Proprioceptive assessment in clinical settings: Evaluation of joint position sense in upper limb post-stroke using a robotic manipulator. *PLoS One* 2017;12. <https://doi.org/10.1371/journal.pone.0183257>.
- Corbetta D, Imeri F, Gatti R. Rehabilitation that incorporates virtual reality is more effective than standard rehabilitation for improving walking speed, balance and mobility after stroke: a systematic review. *J Physiother* 2015;61:117–24. <https://doi.org/10.1016/j.jphys.2015.05.017>.
- Crevecoeur F, Munoz DP, Scott SH. Dynamic Multisensory Integration: Somatosensory Speed Trumps Visual Accuracy during Feedback Control. *J Neurosci* 2016;36:8598–611. <https://doi.org/10.1523/JNEUROSCI.0184-16.2016>.
- Crevecoeur F, Thonnard J-L, Lefèvre P. Optimal integration of gravity in trajectory planning of vertical pointing movements. *J Neurophysiol* 2009;102:786–96. <https://doi.org/10.1152/jn.00113.2009>.
- Cullen KE. Vestibular processing during natural self-motion: implications for perception and action. *Nat Rev Neurosci* 2019;20:346–63. <https://doi.org/10.1038/s41583-019-0153-1>.
- Darling WG, Bartelt R, Pizzimenti MA, Rizzo M. Spatial perception errors do not predict pointing errors by individuals with brain lesions. *J Clin Exp Neuropsychol* 2008a;30:102–19. <https://doi.org/10.1080/13803390701249036>.
- Darling WG, Gilchrist L. Is there a preferred coordinate system for perception of hand orientation in three-dimensional space? *Exp Brain Res* 1991;85:405–16. <https://doi.org/10.1007/BF00229417>.
- Darling WG, Viaene AN, Peterson CR, Schmiedeler JP. Perception of hand motion direction uses a gravitational reference. *Exp Brain Res* 2008b;186:237–48. <https://doi.org/10.1007/s00221-007-1227-2>.
- De Santis D, Zenzeri J, Casadio M, Masia L, Riva A, Morasso P, et al. Robot-Assisted Training of the Kinesthetic Sense: Enhancing Proprioception after Stroke. *Front Hum Neurosci* 2015;8. <https://doi.org/10.3389/fnhum.2014.01037>.
- Deblock-Bellamy A, Batcho CS, Mercier C, Blanchette AK. Quantification of upper limb position sense using an exoskeleton and a virtual reality display. *J NeuroEngineering Rehabil* 2018;15:24. <https://doi.org/10.1186/s12984-018-0367-x>.
- Delhaye BP, Long KH, Bensmaia SJ. Neural Basis of Touch and Proprioception in Primate Cortex. In: Pollock DM, editor. *Comprehensive Physiology*, Hoboken, NJ, USA: John Wiley & Sons, Inc.; 2018, p. 1575–602. <https://doi.org/10.1002/cphy.c170033>.
- Dickman JD, Angelaki DE. Vestibular Convergence Patterns in Vestibular Nuclei Neurons of Alert Primates. *Journal of Neurophysiology* 2002;88:3518–33. <https://doi.org/10.1152/jn.00518.2002>.
- de Diego C, Puig S, Navarro X. A sensorimotor stimulation program for rehabilitation of chronic stroke patients. *Restorative Neurology and Neuroscience* 2013;31:361–71. <https://doi.org/10.3233/RNN-120250>.

- Donkor ES. Stroke in the 21st Century: A Snapshot of the Burden, Epidemiology, and Quality of Life. *Stroke Res Treat* 2018;2018:3238165. <https://doi.org/10.1155/2018/3238165>.
- Doyle S, Bennett S, Fasoli SE, McKenna KT. Interventions for sensory impairment in the upper limb after stroke. *Cochrane Database of Systematic Reviews* 2010. <https://doi.org/10.1002/14651858.CD006331.pub2>.
- Duhamel J-R, Bremmer F, Ben Hamed S, Graf W. Spatial invariance of visual receptive fields in parietal cortex neurons. *Nature* 1997;389:845–8. <https://doi.org/10.1038/39865>.
- Duhamel JR, Colby CL, Goldberg ME. The updating of the representation of visual space in parietal cortex by intended eye movements. *Science* 1992;255:90–2. <https://doi.org/10.1126/science.1553535>.
- Dukelow SP, Herter TM, Bagg SD, Scott SH. The independence of deficits in position sense and visually guided reaching following stroke. *J Neuroeng Rehabil* 2012;9:72. <https://doi.org/10.1186/1743-0003-9-72>.
- Dukelow SP, Herter TM, Moore KD, Demers MJ, Glasgow JI, Bagg SD, et al. Quantitative Assessment of Limb Position Sense Following Stroke. *Neurorehabil Neural Repair* 2010;24:178–87. <https://doi.org/10.1177/1545968309345267>.
- Duyff RF, Davies G, Vos J. Dissociation between cerebral imaging and clinical picture. *The Lancet* 1996;347:1829–30. [https://doi.org/10.1016/S0140-6736\(96\)91649-9](https://doi.org/10.1016/S0140-6736(96)91649-9).
- Elangovan N, Yeh I-L, Holst-Wolf J, Konczak J. A robot-assisted sensorimotor training program can improve proprioception and motor function in stroke survivors. 2019 IEEE 16th International Conference on Rehabilitation Robotics (ICORR), Toronto, ON, Canada: IEEE; 2019, p. 660–4. <https://doi.org/10.1109/ICORR.2019.8779409>.
- Engel KC, Flanders M, Soechting JF. Oculocentric frames of reference for limb movement. *Arch Ital Biol* 2002;140:211–9.
- Ernst MO, Banks MS. Humans integrate visual and haptic information in a statistically optimal fashion. *Nature* 2002;415:429–33. <https://doi.org/10.1038/415429a>.
- Faisal AA, Selen LPJ, Wolpert DM. Noise in the nervous system. *Nat Rev Neurosci* 2008;9:292–303. <https://doi.org/10.1038/nrn2258>.
- Findlater SE, Dukelow SP. Upper Extremity Proprioception After Stroke: Bridging the Gap Between Neuroscience and Rehabilitation. *Journal of Motor Behavior* 2017;49:27–34. <https://doi.org/10.1080/00222895.2016.1219303>.
- Findlater SE, Hawe RL, Semrau JA, Kenzie JM, Yu AY, Scott SH, et al. Lesion locations associated with persistent proprioceptive impairment in the upper limbs after stroke. *NeuroImage: Clinical* 2018;20:955–71. <https://doi.org/10.1016/j.nicl.2018.10.003>.
- Finlayson NJ, Zhang X, Golomb JD. Differential patterns of 2D location versus depth decoding along the visual hierarchy. *NeuroImage* 2017;147:507–16. <https://doi.org/10.1016/j.neuroimage.2016.12.039>.
- Fishman RS. Gordon Holmes, the cortical retina, and the wounds of war. The seventh Charles B. Snyder Lecture. *Doc Ophthalmol* 1997;93:9–28. <https://doi.org/10.1007/BF02569044>.

- Flash T, Hogan N. The coordination of arm movements: an experimentally confirmed mathematical model. *J Neurosci* 1985;5:1688–703. <https://doi.org/10.1523/JNEUROSCI.05-07-01688.1985>.
- Foundas AL. Apraxia: neural mechanisms and functional recovery. *Handb Clin Neurol* 2013;110:335–45. <https://doi.org/10.1016/B978-0-444-52901-5.00028-9>.
- Foundas AL, Duncan ES. Limb Apraxia: a Disorder of Learned Skilled Movement. *Curr Neurol Neurosci Rep* 2019;19:82. <https://doi.org/10.1007/s11910-019-0989-9>.
- Fraser LE, Makooie B, Harris LR. The Subjective Visual Vertical and the Subjective Haptic Vertical Access Different Gravity Estimates. *PLoS One* 2015;10:e0145528. <https://doi.org/10.1371/journal.pone.0145528>.
- Frenkel-Toledo S, Fridberg G, Ofir S, Bartur G, Lowenthal-Raz J, Granot O, et al. Lesion location impact on functional recovery of the hemiparetic upper limb. *PLoS ONE* 2019;14:e0219738. <https://doi.org/10.1371/journal.pone.0219738>.
- Funk J, Finke K, Müller HJ, Utz KS, Kerkhoff G. Visual context modulates the subjective vertical in neglect: evidence for an increased rod-and-frame-effect. *Neuroscience* 2011;173:124–34. <https://doi.org/10.1016/j.neuroscience.2010.10.067>.
- Gdowski GT, McCrea RA. Neck proprioceptive inputs to primate vestibular nucleus neurons. *Exp Brain Res* 2000;135:511–26. <https://doi.org/10.1007/s002210000542>.
- Ghahramani Z, Wolpert DM, Jordan MI. Computational models of sensorimotor integration. In: Morasso P, Sanguineti V, editors. *Advances in Psychology*, vol. 119, North-Holland; 1997, p. 117–47. [https://doi.org/10.1016/S0166-4115\(97\)80006-4](https://doi.org/10.1016/S0166-4115(97)80006-4).
- Go AS, Mozaffarian D, Roger VL, Benjamin EJ, Berry JD, Blaha MJ, et al. Heart disease and stroke statistics--2014 update: a report from the American Heart Association. *Circulation* 2014;129:e28–292. <https://doi.org/10.1161/01.cir.0000441139.02102.80>.
- Goble DJ. Proprioceptive Acuity Assessment Via Joint Position Matching: From Basic Science to General Practice. *Physical Therapy* 2010;90:1176–84. <https://doi.org/10.2522/ptj.20090399>.
- Grefkes C, Weiss PH, Zilles K, Fink GR. Crossmodal processing of object features in human anterior intraparietal cortex: an fMRI study implies equivalencies between humans and monkeys. *Neuron* 2002;35:173–84. [https://doi.org/10.1016/s0896-6273\(02\)00741-9](https://doi.org/10.1016/s0896-6273(02)00741-9).
- Guerraz M, Poquin D, Ohlmann T. The role of head-centric spatial reference with a static and kinetic visual disturbance. *Perception & Psychophysics* 1998;60:287–95. <https://doi.org/10.3758/BF03206037>.
- Gurari N, Drogos JM, Dewald JPA. Individuals with chronic hemiparetic stroke can correctly match forearm positions within a single arm. *Clinical Neurophysiology* 2017;128:18–30. <https://doi.org/10.1016/j.clinph.2016.10.009>.
- Hain TC. Neurophysiology of vestibular rehabilitation. *NeuroRehabilitation* 2011;29:127–41. <https://doi.org/10.3233/NRE-2011-0687>.
- Han J, Waddington G, Adams R, Anson J, Liu Y. Assessing proprioception: A critical review of methods. *Journal of Sport and Health Science* 2016;5:80–90. <https://doi.org/10.1016/j.jshs.2014.10.004>.

- Harris CM, Wolpert DM. Signal-dependent noise determines motor planning. *Nature* 1998;394:780–4. <https://doi.org/10.1038/29528>.
- He J, Li C, Lin J, Shu B, Ye B, Wang J, et al. Proprioceptive Training with Visual Feedback Improves Upper Limb Function in Stroke Patients: A Pilot Study. *Neural Plasticity* 2022;2022:e1588090. <https://doi.org/10.1155/2022/1588090>.
- Healy BC, Buckle GJ, Ali EN, Egorova S, Khalid F, Tauhid S, et al. Characterizing Clinical and MRI Dissociation in Patients with Multiple Sclerosis. *J Neuroimaging* 2017;27:481–5. <https://doi.org/10.1111/jon.12433>.
- Herter TM, Scott SH, Dukelow SP. Vision does not always help stroke survivors compensate for impaired limb position sense. *J Neuroeng Rehabil* 2019;16:129. <https://doi.org/10.1186/s12984-019-0596-7>.
- Hirayama K, Fukutake T, Kawamura M. “Thumb localizing test” for detecting a lesion in the posterior column-medial lemniscal system. *J Neurol Sci* 1999;167:45–9. [https://doi.org/10.1016/s0022-510x\(99\)00136-7](https://doi.org/10.1016/s0022-510x(99)00136-7).
- Hitier M, Besnard S, Smith PF. Vestibular pathways involved in cognition. *Front Integr Neurosci* 2014;8:59. <https://doi.org/10.3389/fnint.2014.00059>.
- Hoseini N, Sexton BM, Kurtz K, Liu Y, Block HJ. Adaptive Staircase Measurement of Hand Proprioception. *PLoS One* 2015;10:e0135757. <https://doi.org/10.1371/journal.pone.0135757>.
- Huang R-S, Sereno MI. Multisensory and sensorimotor maps. *Handb Clin Neurol* 2018;151:141–61. <https://doi.org/10.1016/B978-0-444-63622-5.00007-3>.
- Iandolo R, Bellini A, Saiote C, Marre I, Bommarito G, Oesingmann N, et al. Neural correlates of lower limbs proprioception: An fMRI study of foot position matching. *Hum Brain Mapp* 2018;39:1929–44. <https://doi.org/10.1002/hbm.23972>.
- Iandolo R, Squeri V, De Santis D, Giannoni P, Morasso P, Casadio M. Proprioceptive Bimanual Test in Intrinsic and Extrinsic Coordinates. *Front Hum Neurosci* 2015;9. <https://doi.org/10.3389/fnhum.2015.00072>.
- Iandolo R, Squeri V, De Santis D, Giannoni P, Morasso P, Casadio M. Testing proprioception in intrinsic and extrinsic coordinate systems: Is there a difference? 2014 36th Annual International Conference of the IEEE Engineering in Medicine and Biology Society, Chicago, IL: IEEE; 2014, p. 6961–4. <https://doi.org/10.1109/EMBC.2014.6945229>.
- Ingemanson ML, Rowe JR, Chan V, Riley J, Wolbrecht ET, Reinkensmeyer DJ, et al. Neural Correlates of Passive Position Finger Sense After Stroke. *Neurorehabil Neural Repair* 2019;33:740–50. <https://doi.org/10.1177/1545968319862556>.
- Janssen P, Scherberger H. Visual Guidance in Control of Grasping. *Annual Review of Neuroscience* 2015;38:69–86. <https://doi.org/10.1146/annurev-neuro-071714-034028>.
- Johansson RS, Vallbo AB. Tactile sensibility in the human hand: relative and absolute densities of four types of mechanoreceptive units in glabrous skin. *J Physiol* 1979;286:283–300.
- Jones SAH, Henriques DYP. Memory for proprioceptive and multisensory targets is partially coded relative to gaze. *Neuropsychologia* 2010;48:3782–92. <https://doi.org/10.1016/j.neuropsychologia.2010.10.001>.

- Karnath H-O, Broetz D. Understanding and treating “pusher syndrome.” *Phys Ther* 2003;83:1119–25.
- Kenzie JM, Semrau JA, Hill MD, Scott SH, Dukelow SP. A composite robotic-based measure of upper limb proprioception. *J Neuroeng Rehabil* 2017;14:114. <https://doi.org/10.1186/s12984-017-0329-8>.
- Kessner SS, Bingel U, Thomalla G. Somatosensory deficits after stroke: a scoping review. *Topics in Stroke Rehabilitation* 2016;23:136–46. <https://doi.org/10.1080/10749357.2015.1116822>.
- Kessner SS, Schlemm E, Cheng B, Bingel U, Fiehler J, Gerloff C, et al. Somatosensory Deficits After Ischemic Stroke: Time Course and Association With Infarct Location. *Stroke* 2019;50:1116–23. <https://doi.org/10.1161/STROKEAHA.118.023750>.
- Khan S, Chang R. Anatomy of the vestibular system: a review. *NeuroRehabilitation* 2013;32:437–43. <https://doi.org/10.3233/NRE-130866>.
- Körding KP, Wolpert DM. Bayesian decision theory in sensorimotor control. *Trends Cogn Sci* 2006;10:319–26. <https://doi.org/10.1016/j.tics.2006.05.003>.
- Körding KP, Wolpert DM. Bayesian integration in sensorimotor learning. *Nature* 2004;427:244–7. <https://doi.org/10.1038/nature02169>.
- Lacquaniti F, Bosco G, Gravano S, Indovina I, La Scaleia B, Maffei V, et al. Gravity in the Brain as a Reference for Space and Time Perception. *Multisens Res* 2015;28:397–426.
- Lambercy O, Robles AJ, Yeongmi Kim, Gassert R. Design of a robotic device for assessment and rehabilitation of hand sensory function. 2011 IEEE International Conference on Rehabilitation Robotics, Zurich: IEEE; 2011, p. 1–6. <https://doi.org/10.1109/ICORR.2011.5975436>.
- Lanska DJ, Kryscio R. “Thumb localizing test” for detecting a lesion in the posterior column-medial lemniscal system. *J Neurol Sci* 2000;174:152–4. [https://doi.org/10.1016/s0022-510x\(99\)00321-4](https://doi.org/10.1016/s0022-510x(99)00321-4).
- Levin MF, Michaelsen SM, Cirstea CM, Roby-Brami A. Use of the trunk for reaching targets placed within and beyond the reach in adult hemiparesis. *Exp Brain Res* 2002;143:171–80. <https://doi.org/10.1007/s00221-001-0976-6>.
- London BM, Jordan LR, Jackson CR, Miller LE. Electrical stimulation of the proprioceptive cortex (area 3a) used to instruct a behaving monkey. *IEEE Trans Neural Syst Rehabil Eng* 2008;16:32–6. <https://doi.org/10.1109/TNSRE.2007.907544>.
- Luyat M, Mobarek S, Leconte C, Gentaz E. The plasticity of gravitational reference frame and the subjective vertical: peripheral visual information affects the oblique effect. *Neurosci Lett* 2005;385:215–9. <https://doi.org/10.1016/j.neulet.2005.05.044>.
- Marini F, Zenzeri J, Pippo V, Morasso P, Campus C. Neural correlates of proprioceptive upper limb position matching. *Hum Brain Mapp* 2019;40:4813–26. <https://doi.org/10.1002/hbm.24739>.
- Masland RH. The Neuronal Organization of the Retina. *Neuron* 2012;76:266–80. <https://doi.org/10.1016/j.neuron.2012.10.002>.

- Matsuda K, Satoh M, Tabei K, Ueda Y, Itoh A, Ishikawa H, et al. Subregional heterogeneity of somatosensory dysfunction in the insula. *J Neurol Neurosurg Psychiatry* 2019;90:957–8. <https://doi.org/10.1136/jnnp-2018-319174>.
- McGuire LMM, Sabes PN. Heterogeneous representations in the superior parietal lobule are common across reaches to visual and proprioceptive targets. *J Neurosci* 2011;31:6661–73. <https://doi.org/10.1523/JNEUROSCI.2921-10.2011>.
- McGuire LMM, Sabes PN. Sensory transformations and the use of multiple reference frames for reach planning. *Nat Neurosci* 2009;12:1056–61. <https://doi.org/10.1038/nn.2357>.
- McIntyre J, Lipshits M. Central processes amplify and transform anisotropies of the visual system in a test of visual-haptic coordination. *The Journal of Neuroscience* 2008;28:1246–61. <https://doi.org/10.1523/JNEUROSCI.2066-07.2008>.
- McIntyre J, Lipshits M, Zaoui M, Berthoz A, Gurfinkel V. Internal reference frames for representation and storage of visual information: the role of gravity. *Acta Astronautica* 2001;49:111–21. [https://doi.org/10.1016/S0094-5765\(01\)00087-X](https://doi.org/10.1016/S0094-5765(01)00087-X).
- McIntyre J, Stratta F, Lacquaniti F. Viewer-centered frame of reference for pointing to memorized targets in three-dimensional space. *J Neurophysiol* 1997;78:1601–18. <https://doi.org/10.1152/jn.1997.78.3.1601>.
- McNamee D, Wolpert DM. Internal Models in Biological Control. *Annu Rev Control Robot Auton Syst* 2019;2:339–64. <https://doi.org/10.1146/annurev-control-060117-105206>.
- Metzger J-C, Lambercy O, Califfi A, Conti FM, Gassert R. Neurocognitive Robot-Assisted Therapy of Hand Function. *IEEE Trans Haptics* 2014;7:140–9. <https://doi.org/10.1109/TOH.2013.72>.
- Meyer S, De Bruyn N, Lafosse C, Van Dijk M, Michielsen M, Thijs L, et al. Somatosensory Impairments in the Upper Limb Poststroke: Distribution and Association With Motor Function and Visuospatial Neglect. *Neurorehabil Neural Repair* 2016;30:731–42. <https://doi.org/10.1177/1545968315624779>.
- Meyer S, Karttunen AH, Thijs V, Feys H, Verheyden G. How Do Somatosensory Deficits in the Arm and Hand Relate to Upper Limb Impairment, Activity, and Participation Problems After Stroke? A Systematic Review. *Physical Therapy* 2014;94:1220–31. <https://doi.org/10.2522/ptj.20130271>.
- Milenkovic S, Dragovic M. Modification of the Edinburgh Handedness Inventory: a replication study. *Laterality* 2013;18:340–8. <https://doi.org/10.1080/1357650X.2012.683196>.
- Miyamoto T, Fukushima K, Takada T, de Waele C, Vidal P-P. Saccular stimulation of the human cortex: A functional magnetic resonance imaging study. *Neuroscience Letters* 2007;423:68–72. <https://doi.org/10.1016/j.neulet.2007.06.036>.
- Nakano E, Imamizu H, Osu R, Uno Y, Gomi H, Yoshioka T, et al. Quantitative examinations of internal representations for arm trajectory planning: minimum commanded torque change model. *J Neurophysiol* 1999;81:2140–55. <https://doi.org/10.1152/jn.1999.81.5.2140>.
- Niehof N, Tramper JJ, Doeller CF, Medendorp WP. Updating of visual orientation in a gravity-based reference frame. *J Vis* 2017;17:4. <https://doi.org/10.1167/17.12.4>.

- Olson CR. Brain representation of object-centered space in monkeys and humans. *Annu Rev Neurosci* 2003;26:331–54. <https://doi.org/10.1146/annurev.neuro.26.041002.131405>.
- Onaka H, Kouda K, Nishimura Y, Tojo H, Umemoto Y, Kubo T, et al. Standing and supine positions are better than sitting in improving rightward deviation in right-hemispheric stroke patients with unilateral spatial neglect: A randomized trial. *Medicine (Baltimore)* 2022;101:e31571. <https://doi.org/10.1097/MD.00000000000031571>.
- O'Reilly JX, Jbabdi S, Behrens TEJ. How can a Bayesian approach inform neuroscience? *Eur J Neurosci* 2012;35:1169–79. <https://doi.org/10.1111/j.1460-9568.2012.08010.x>.
- Otaka E, Otaka Y, Kasuga S, Nishimoto A, Yamazaki K, Kawakami M, et al. Reliability of the thumb localizing test and its validity against quantitative measures with a robotic device in patients with hemiparetic stroke. *PLOS ONE* 2020;15:e0236437. <https://doi.org/10.1371/journal.pone.0236437>.
- Paillard J. Knowing where and knowing how to get there. *Brain and space*, New York, NY, US: Oxford University Press; 1991, p. 461–81.
- Paulun L, Wendt A, Kasabov N. A Retinotopic Spiking Neural Network System for Accurate Recognition of Moving Objects Using NeuCube and Dynamic Vision Sensors. *Frontiers in Computational Neuroscience* 2018;12.
- Pellijeff A, Bonilha L, Morgan PS, McKenzie K, Jackson SR. Parietal updating of limb posture: an event-related fMRI study. *Neuropsychologia* 2006;44:2685–90. <https://doi.org/10.1016/j.neuropsychologia.2006.01.009>.
- Penfield W, Boldrey E. Somatic motor and sensory representation in the cerebral cortex of man as studied by electrical stimulation. *Brain: A Journal of Neurology* 1937;60:389–443. <https://doi.org/10.1093/brain/60.4.389>.
- Pennati GV, Plantin J, Carment L, Roca P, Baron J-C, Pavlova E, et al. Recovery and Prediction of Dynamic Precision Grip Force Control After Stroke. *Stroke* 2020;51:944–51. <https://doi.org/10.1161/STROKEAHA.119.026205>.
- Pizzamiglio L, Vallar G, Doricchi F. Gravitational inputs modulate visuospatial neglect. *Exp Brain Res* 1997;117:341–5. <https://doi.org/10.1007/s002210050227>.
- Pizzamiglio L, Vallar G, Doricchi F. Gravity and hemineglect. *Neuroreport* 1995;7:370–1.
- Pouget A, Ducom J, Torri J, Bavelier D. Multisensory spatial representations in eye-centered coordinates for reaching. *Cognition* 2002;83:B1–11. [https://doi.org/10.1016/S0010-0277\(01\)00163-9](https://doi.org/10.1016/S0010-0277(01)00163-9).
- Prather SC, Sathian K. Mental rotation of tactile stimuli. *Cognitive Brain Research* 2002;14:91–8. [https://doi.org/10.1016/S0926-6410\(02\)00063-0](https://doi.org/10.1016/S0926-6410(02)00063-0).
- Proske U, Gandevia SC. The Proprioceptive Senses: Their Roles in Signaling Body Shape, Body Position and Movement, and Muscle Force. *Physiological Reviews* 2012;92:1651–97. <https://doi.org/10.1152/physrev.00048.2011>.
- Pumpa LU, Cahill LS, Carey LM. Somatosensory assessment and treatment after stroke: An evidence-practice gap. *Aust Occup Ther J* 2015;62:93–104. <https://doi.org/10.1111/1440-1630.12170>.

- Rand D. Proprioception deficits in chronic stroke—Upper extremity function and daily living. *PLoS ONE* 2018;13:e0195043. <https://doi.org/10.1371/journal.pone.0195043>.
- Rinderknecht MD, Lambercy O, Raible V, Büsching I, Sehle A, Liepert J, et al. Reliability, validity, and clinical feasibility of a rapid and objective assessment of post-stroke deficits in hand proprioception. *J NeuroEngineering Rehabil* 2018;15:47. <https://doi.org/10.1186/s12984-018-0387-6>.
- Rosenberg A, Angelaki DE. Gravity influences the visual representation of object tilt in parietal cortex. *J Neurosci* 2014;34:14170–80. <https://doi.org/10.1523/JNEUROSCI.2030-14.2014>.
- Rosker J, Sarabon N. Kinaesthesia and Methods for its Assessment: Literature Review. *Sport Science Review* 2010;XIX. <https://doi.org/10.2478/v10237-011-0037-4>.
- Rossi-Arnaud C, Pieroni L, Spataro P, Baddeley A. Working memory and individual differences in the encoding of vertical, horizontal and diagonal symmetry. *Acta Psychol (Amst)* 2012;141:122–32. <https://doi.org/10.1016/j.actpsy.2012.06.007>.
- Saeyns W, Vereeck L, Truijten S, Lafosse C, Wuyts FP, Van de Heyning P. Influence of sensory loss on the perception of verticality in stroke patients. *Disability and Rehabilitation* 2012;34:1965–70. <https://doi.org/10.3109/09638288.2012.671883>.
- Saini V, Guada L, Yavagal DR. Global Epidemiology of Stroke and Access to Acute Ischemic Stroke Interventions. *Neurology* 2021;97:S6–16. <https://doi.org/10.1212/WNL.0000000000012781>.
- Sallés L, Martín-Casas P, Gironès X, Durà MJ, Lafuente JV, Perfetti C. A neurocognitive approach for recovering upper extremity movement following subacute stroke: a randomized controlled pilot study. *J Phys Ther Sci* 2017;29:665–72. <https://doi.org/10.1589/jpts.29.665>.
- Santisteban L, Térémetz M, Bleton J-P, Baron J-C, Maier MA, Lindberg PG. Upper Limb Outcome Measures Used in Stroke Rehabilitation Studies: A Systematic Literature Review. *PLoS ONE* 2016;11:e0154792. <https://doi.org/10.1371/journal.pone.0154792>.
- dos Santos GL, Salazar LFG, Lazarin AC, de Russo TL. Joint position sense is bilaterally reduced for shoulder abduction and flexion in chronic hemiparetic individuals. *Topics in Stroke Rehabilitation* 2015;22:271–80. <https://doi.org/10.1179/1074935714Z.0000000014>.
- Sarlegna FR, Przybyla A, Sainburg RL. The influence of target sensory modality on motor planning may reflect errors in sensori-motor transformations. *Neuroscience* 2009;164:597–610. <https://doi.org/10.1016/j.neuroscience.2009.07.057>.
- Sarlegna FR, Sainburg RL. The roles of vision and proprioception in the planning of reaching movements. *Adv Exp Med Biol* 2009;629:317–35. [https://doi.org/10.1007/978-0-387-77064-2\\_16](https://doi.org/10.1007/978-0-387-77064-2_16).
- Sarlegna FR, Sainburg RL. The effect of target modality on visual and proprioceptive contributions to the control of movement distance. *Exp Brain Res* 2007;176:267–80. <https://doi.org/10.1007/s00221-006-0613-5>.
- Scalha TB, Miyasaki E, Lima NMFV, Borges G. Correlations between motor and sensory functions in upper limb chronic hemiparetics after stroke. *Arq Neuro-Psiquiatr* 2011;69:624–9. <https://doi.org/10.1590/S0004-282X2011000500010>.

- Schlack A, Hoffmann K-P, Bremmer F. Interaction of linear vestibular and visual stimulation in the macaque ventral intraparietal area (VIP). *European Journal of Neuroscience* 2002;16:1877–86. <https://doi.org/10.1046/j.1460-9568.2002.02251.x>.
- Schlindwein P, Mueller M, Bauermann T, Brandt T, Stoeter P, Dieterich M. Cortical representation of saccular vestibular stimulation: VEMPs in fMRI. *NeuroImage* 2008;39:19–31. <https://doi.org/10.1016/j.neuroimage.2007.08.016>.
- Scotto Di Cesare C, Sarlegna FR, Bourdin C, Mestre DR, Bringoux L. Combined influence of visual scene and body tilt on arm pointing movements: gravity matters! *PLoS ONE* 2014;9:e99866. <https://doi.org/10.1371/journal.pone.0099866>.
- Semrau JA, Herter TM, Scott SH, Dukelow SP. Vision of the upper limb fails to compensate for kinesthetic impairments in subacute stroke. *Cortex* 2018;109:245–59. <https://doi.org/10.1016/j.cortex.2018.09.022>.
- Semrau JA, Herter TM, Scott SH, Dukelow SP. Inter-rater reliability of kinesthetic measurements with the KINARM robotic exoskeleton. *J NeuroEngineering Rehabil* 2017;14:42. <https://doi.org/10.1186/s12984-017-0260-z>.
- Sereno MI, Huang R-S. Multisensory maps in parietal cortex. *Current Opinion in Neurobiology* 2014;24:39–46. <https://doi.org/10.1016/j.conb.2013.08.014>.
- Sherrington CS. On the proprioceptive system, especially in its reflex aspects. *Brain* 1907;29:467–82. <https://doi.org/10.1093/brain/29.4.467>.
- Simo L, Botzer L, Ghez C, Scheidt RA. A robotic test of proprioception within the hemiparetic arm post-stroke. *J NeuroEngineering Rehabil* 2014;11:77. <https://doi.org/10.1186/1743-0003-11-77>.
- Snyder LH, Grieve KL, Brotchie P, Andersen RA. Separate body- and world-referenced representations of visual space in parietal cortex. *Nature* 1998;394:887–91. <https://doi.org/10.1038/29777>.
- Sober SJ, Sabes PN. Flexible strategies for sensory integration during motor planning. *Nat Neurosci* 2005;8:490–7. <https://doi.org/10.1038/nn1427>.
- Stillman BC. Making Sense of Proprioception: The meaning of proprioception, kinaesthesia and related terms. *Physiotherapy* 2002;88:667–76. [https://doi.org/10.1016/S0031-9406\(05\)60109-5](https://doi.org/10.1016/S0031-9406(05)60109-5).
- Stinear CM, Lang CE, Zeiler S, Byblow WD. Advances and challenges in stroke rehabilitation. *Lancet Neurol* 2020;19:348–60. [https://doi.org/10.1016/S1474-4422\(19\)30415-6](https://doi.org/10.1016/S1474-4422(19)30415-6).
- Tagliabue M, Arnoux L, McIntyre J. Keep your head on straight: facilitating sensori-motor transformations for eye-hand coordination. *Neuroscience* 2013;248:88–94. <https://doi.org/10.1016/j.neuroscience.2013.05.051>.
- Tagliabue M, McIntyre J. A modular theory of multisensory integration for motor control. *Front Comput Neurosci* 2014;8. <https://doi.org/10.3389/fncom.2014.00001>.
- Tagliabue M, McIntyre J. When Kinesthesia Becomes Visual: A Theoretical Justification for Executing Motor Tasks in Visual Space. *PLoS ONE* 2013;8:e68438. <https://doi.org/10.1371/journal.pone.0068438>.

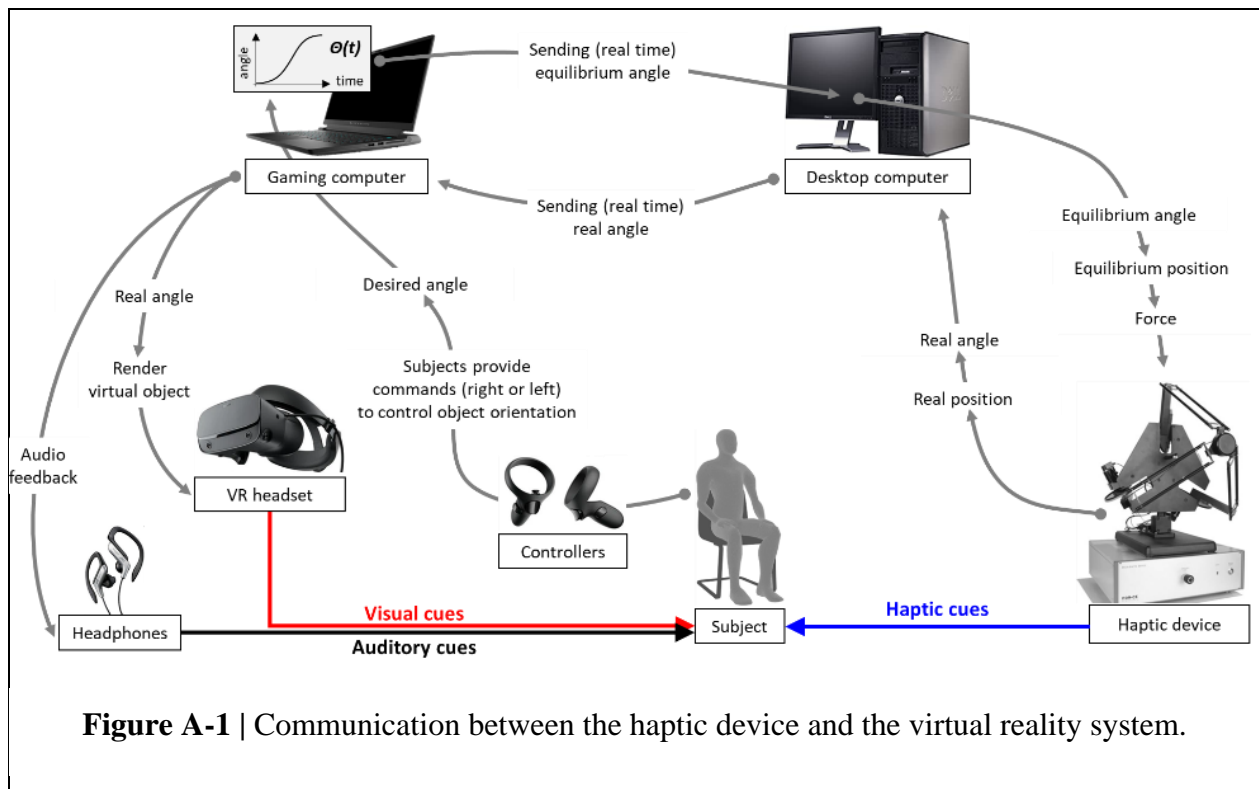
- Tagliabue M, McIntyre J. Eye-hand coordination when the body moves: dynamic egocentric and exocentric sensory encoding. *Neurosci Lett* 2012;513:78–83. <https://doi.org/10.1016/j.neulet.2012.02.011>.
- Tagliabue M, McIntyre J. Necessity is the mother of invention: reconstructing missing sensory information in multiple, concurrent reference frames for eye-hand coordination. *J Neurosci* 2011;31:1397–409. <https://doi.org/10.1523/JNEUROSCI.0623-10.2011>.
- Tagliabue M, McIntyre J. Multiple and Multimodal Reference Frames for Eye-Hand Coordination. Program Neuroscience Meeting. Washington, DC: Society for Neuroscience 2008.
- Tamè L, Moles A, Holmes NP. Within, but not between hands interactions in vibrotactile detection thresholds reflect somatosensory receptive field organization. *Front Psychol* 2014;5:174. <https://doi.org/10.3389/fpsyg.2014.00174>.
- Tamè L, Wühle A, Petri CD, Pavani F, Braun C. Concurrent use of somatotopic and external reference frames in a tactile mislocalization task. *Brain and Cognition* 2017;111:25–33. <https://doi.org/10.1016/j.bandc.2016.10.005>.
- Tarnutzer AA, Bockisch CJ, Olasagasti I, Straumann D. Egocentric and allocentric alignment tasks are affected by otolith input. *J Neurophysiol* 2012;107:3095–106. <https://doi.org/10.1152/jn.00724.2010>.
- Tarnutzer AA, Bockisch CJ, Straumann D. Roll-dependent modulation of the subjective visual vertical: contributions of head- and trunk-based signals. *J Neurophysiol* 2010;103:934–41. <https://doi.org/10.1152/jn.00407.2009>.
- Tasseel-Ponche S, Yelnik AP, Bonan IV. Motor strategies of postural control after hemispheric stroke. *Neurophysiol Clin* 2015;45:327–33. <https://doi.org/10.1016/j.neucli.2015.09.003>.
- Todorov E, Jordan MI. Optimal feedback control as a theory of motor coordination. *Nat Neurosci* 2002;5:1226–35. <https://doi.org/10.1038/nn963>.
- Torre K, Hammami N, Metrot J, van Dokkum L, Coroian F, Mottet D, et al. Somatosensory-Related Limitations for Bimanual Coordination After Stroke. *Neurorehabil Neural Repair* 2013;27:507–15. <https://doi.org/10.1177/1545968313478483>.
- Trojano L, Grossi D. ‘Pure’ Constructional Apraxia—A Cognitive Analysis of a Single Case. *Behavioural Neurology* 1998;11:43–9. <https://doi.org/10.1155/1998/614728>.
- Turville M, Carey LM, Matyas TA, Blennerhassett J. Change in Functional Arm Use Is Associated With Somatosensory Skills After Sensory Retraining Poststroke. *Am J Occup Ther* 2017;71:7103190070p1–9. <https://doi.org/10.5014/ajot.2017.024950>.
- Uchino Y, Kushiro K. Differences between otolith- and semicircular canal-activated neural circuitry in the vestibular system. *Neuroscience Research* 2011;71:315–27. <https://doi.org/10.1016/j.neures.2011.09.001>.
- Uno Y, Kawato M, Suzuki R. Formation and control of optimal trajectory in human multijoint arm movement. Minimum torque-change model. *Biol Cybern* 1989;61:89–101. <https://doi.org/10.1007/BF00204593>.

- Usrey WM, Alitto HJ. Visual Functions of the Thalamus. *Annu Rev Vis Sci* 2015;1:351–71.  
<https://doi.org/10.1146/annurev-vision-082114-035920>.
- Valdes BA, Khoshnam M, Neva JL, Menon C. Robot-Aided Upper-limb Proprioceptive Training in Three-Dimensional Space. *IEEE Int Conf Rehabil Robot* 2019;2019:121–6.  
<https://doi.org/10.1109/ICORR.2019.8779529>.
- Vallar G. Spatial frames of reference and somatosensory processing: a neuropsychological perspective. *Philos Trans R Soc Lond B Biol Sci* 1997;352:1401–9.  
<https://doi.org/10.1098/rstb.1997.0126>.
- Van de Winckel A, Wenderoth N, De Weerd W, Sunaert S, Peeters R, Van Hecke W, et al. Frontoparietal involvement in passively guided shape and length discrimination: a comparison between subcortical stroke patients and healthy controls. *Exp Brain Res* 2012;220:179–89.  
<https://doi.org/10.1007/s00221-012-3128-2>.
- Verhagen L, Dijkerman HC, Medendorp WP, Toni I. Cortical Dynamics of Sensorimotor Integration during Grasp Planning. *J Neurosci* 2012;32:4508–19.  
<https://doi.org/10.1523/JNEUROSCI.5451-11.2012>.
- Wenderoth P. The salience of vertical symmetry. *Perception* 1994;23:221–36.  
<https://doi.org/10.1068/p230221>.
- Yates M, Kelemen A, Sik Lanyi C. Virtual reality gaming in the rehabilitation of the upper extremities post-stroke. *Brain Inj* 2016;30:855–63.  
<https://doi.org/10.3109/02699052.2016.1144146>.
- Yau JM, DeAngelis GC, Angelaki DE. Dissecting neural circuits for multisensory integration and crossmodal processing. *Phil Trans R Soc B* 2015;370:20140203.  
<https://doi.org/10.1098/rstb.2014.0203>.
- Zackowski KM. How do strength, sensation, spasticity and joint individuation relate to the reaching deficits of people with chronic hemiparesis? *Brain* 2004;127:1035–46.  
<https://doi.org/10.1093/brain/awh116>.
- Zandvliet SB, Kwakkel G, Nijland RHM, van Wegen EEH, Meskers CGM. Is Recovery of Somatosensory Impairment Conditional for Upper-Limb Motor Recovery Early After Stroke? *Neurorehabil Neural Repair* 2020;34:403–16. <https://doi.org/10.1177/1545968320907075>.

# Appendix

## A. Software development for our study on multisensory integration

For the experimental study “Sensory transformations affecting visuo-proprioceptive integration” (Study 2, see section 2.2), I developed two interacting custom programs to control the following aspects of the experimental setup in real-time (see Figure A-1):



1. Real-time communication (TCP/IP protocol) between a desktop computer (Transtec, Windows XP) controlling the haptic device, and a gaming laptop (Alienware M15, Windows 10) rendering the VR environment.

2. To control the angular position of the handle, the VR laptop computes the angular trajectory from the initial to the desired angle following a jerk-minimizing function  $\theta(t)$  to provide a smooth movement, with angular speed  $< 15^\circ/\text{sec}$ . In real-time, the VR laptop sends the equilibrium angle to the desktop computer, such that the angular position of the handle follows the trajectory  $\theta(t)$ . In return, the VR laptop receives in real-time the real angle of the handle from the desktop computer (read from the encoders). Based on this real-time orientation, the VR laptop continuously renders the visual scene (virtual object) in the VR headset. Audio feedback is provided to the subject to increase ergonomics and facilitate the interaction with the VR system (go signals, grasp/release handle signals, error signals, movement feedback).
  
3. The desktop computer converts the received equilibrium angle into a 3D (x, y, z) equilibrium (endpoint) position for the haptic device. Then, the endpoint force is computed using a spring-mass model which moves the handle into the new equilibrium position. Because of independent factors (such as the viscosity of the mechanical system) the real position can be different from the equilibrium position ( $\pm 1\text{mm}$ ). Therefore, the real angle of the handle serves as input for VR rendering, and for data analysis.

## B. Previous models of optimal multisensory integration

In order to quantify the accuracy of the Extended Concurrent Model (ECM, described in section 3) to predict our experimental data, we compared its predictions to those of two alternative concurrent models (Tagliabue and McIntyre, 2011, 2013). As done for the ECM in sections 3.2, 3.3, and 3.4, I will detail here the two alternative model predictions for our experimental tasks. Further mathematical details for these two models are available in Tagliabue and McIntyre (2013).

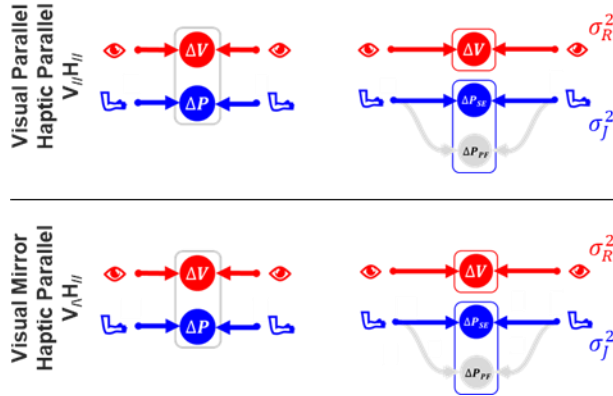
### Unimodal (haptic and visual) tasks

|                             |                               | Previous concurrent models |  |  |   |
|-----------------------------|-------------------------------|----------------------------|--|--|---|
|                             |                               | 2 reference frames         | 3 reference frames   |  |   |
| Haptic Parallel<br>$H_{//}$ |                               |                            | Both models provide the same prediction: the task is encoded in proprioceptive space, and the movement vector variance only depends on the precision of joint signals: | $\sigma_{\Delta}^2 = 2\sigma_j^2$  |   |
|                             | Haptic Mirror<br>$H_{\wedge}$ |                            |  | The model with 2 reference frames predicts an identical sensory processing for the $H_{//}$ and $H_{\wedge}$ tasks.<br>The model with 3 reference frames predicts a partial visual encoding of the task, the variance of the movement vector is affected by the sensory transformations: | $\sigma_{\Delta}^2 = 2\sigma_j^2 + \frac{2\sigma_{T_{J \to J}}^2 \sigma_{T_{J \to R}}^2}{\sigma_{T_{J \to J}}^2 + 4\sigma_{T_{J \to R}}^2}$ |
| Visual Parallel<br>$V_{//}$ |                               |                            |  | Both models provide the same prediction for the two unimodal visual tasks ( $V_{//}$ and $V_{\wedge}$ ): the task is encoded in visual space, and the movement vector variance only depends on the precision of retinal signals:   | $\sigma_{\Delta}^2 = 2\sigma_R^2$   |
|                             | Visual Mirror<br>$V_{\wedge}$ |                            |  |  |   |

## Multimodal (visuo-haptic) tasks

### Previous concurrent models

2 reference frames      3 reference frames

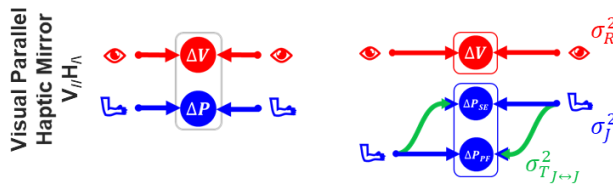


Both models provide the same prediction: the task is encoded in proprioceptive and visual space, and the movement vector variance only depends on the precision of joint and retinal signals:

$$\sigma_{\Delta}^2 = \frac{2\sigma_J^2\sigma_R^2}{\sigma_J^2 + \sigma_R^2}$$

The optimal visual weight is:

$$\omega_V = \frac{\sigma_J^2}{\sigma_J^2 + \sigma_R^2}$$



The model with 2 reference frames predicts the same sensory processing for the  $V_{//}H_{//}$  and  $V_{//}H_{\wedge}$  tasks.

The model with 3 reference frames predicts a sensory transformation of the proprioceptive (joint) signals, which affects the movement vector variance:

$$\sigma_{\Delta}^2 = \frac{2\sigma_R^2(4\sigma_J^2 + \sigma_{T_{J \leftrightarrow J}}^2)}{4\sigma_R^2 + 4\sigma_J^2 + \sigma_{T_{J \leftrightarrow J}}^2}$$

The optimal visual weight is:

$$\omega_V = \frac{4\sigma_J^2 + \sigma_{T_{J \leftrightarrow J}}^2}{4\sigma_R^2 + 4\sigma_J^2 + \sigma_{T_{J \leftrightarrow J}}^2}$$

## C. Scientific contribution

### Communications in international congresses

#### *FENS Forum 2022.*

**Bernard-Espina J**, Beraneck M, Maier MA, Tagliabue M. Multisensory integration in stroke patients: a theoretical approach to reinterpret upper-limb proprioceptive deficits and visual compensation. Poster presentation, FENS Forum 2022, Paris, France.

#### *ENCODS 2022.*

**Bernard-Espina J**, Dal Canto D, Beraneck M, McIntyre J and Tagliabue M. How tilting the head interferes with eye-hand coordination: the role of gravity in visuo-proprioceptive, cross-modal sensory transformations. Oral presentation, ENCODS 2022, Paris, France.

#### *World Congress of Physiotherapy 2017.*

**Bernard J**, Beldame J, Lecuyer M, Brunel H, Van Driessche S, Masse M, Matsoukis J, Billuart F. Electromyographic analysis of hip muscles involved in total hip arthroplasty during bipedal and unipedal stance among asymptomatic and operated participants. Oral presentation, World Congress of Physiotherapy 2017, Cape Town, South Africa.

### Peer-reviewed publications

**Bernard-Espina J**, Dal Canto D, Beraneck M, McIntyre J, Tagliabue M. How Tilting the Head Interferes With Eye-Hand Coordination: The Role of Gravity in Visuo-Proprioceptive, Cross-Modal Sensory Transformations. *Front Integr Neurosci.* 2022 Mar; 16:788905.

**Bernard-Espina J**, Beraneck M, Maier MA, Tagliabue M. Multisensory integration in stroke patients: a theoretical approach to reinterpret upper-limb proprioceptive deficits and visual compensation. *Front Neurosci.* 2021 Apr; 15:646698.

**Bernard J**, Razanabola F, Beldame J, Van Driessche S, Brunel H, Poirier T, Matsoukis J, Billuart F. Electromyographic study of hip muscles involved in total hip arthroplasty: Surprising results using the direct anterior minimally invasive approach. *Orthop Traumatol Surg Res.* 2018 Dec;104(8):1137-1142.

**Bernard J**, Beldame J, Lecuyer M, Poirier T, Brunel H, Guiffault P, Van Driessche S, Matsoukis J, Billuart F. Does hip joint positioning affects the maximal voluntary contraction of Gluteus Maximus, Gluteus Medius, TFL and Sartorius muscles? *Orthop Traumatol Surg Res.* 2017 Nov;103(7): 999-1004.

**Bernard J**, Gadioux C. “Wii-habilitation” in Parkinson's disease and multiple sclerosis. *Kinésithérapie.* 2015 Jun;15(162): 63-69.

## **D. Articles published in the context of the thesis**

Copy of the two articles published in peer-reviewed journals in the context of this thesis:

1. **Bernard-Espina J**, Dal Canto D, Beraneck M, McIntyre J, Tagliabue M.

*How Tilting the Head Interferes With Eye-Hand Coordination: The Role of Gravity in Visuo-Proprioceptive, Cross-Modal Sensory Transformations.*

Frontiers in Integrative Neuroscience. 2022 March; 16:788905.

2. **Bernard-Espina J**, Beraneck M, Maier MA, Tagliabue M.

*Multisensory integration in stroke patients: a theoretical approach to reinterpret upper-limb proprioceptive deficits and visual compensation.*

Frontiers in Neuroscience. 2021 April; 15:646698.



# Multisensory Integration in Stroke Patients: A Theoretical Approach to Reinterpret Upper-Limb Proprioceptive Deficits and Visual Compensation

Jules Bernard-Espina\*, Mathieu Beraneck, Marc A. Maier and Michele Tagliabue

Université de Paris, INCC UMR 8002, CNRS, Paris, France

## OPEN ACCESS

### Edited by:

Luigi F. Cuturi,  
Italian Institute of Technology (IIT), Italy

### Reviewed by:

Jacopo Zenzeri,  
Italian Institute of Technology (IIT), Italy  
Laura Mikula,  
York University, Canada

### \*Correspondence:

Jules Bernard-Espina  
jules.bernard@parisdescartes.fr

### Specialty section:

This article was submitted to  
Perception Science,  
a section of the journal  
Frontiers in Neuroscience

**Received:** 27 December 2020

**Accepted:** 04 March 2021

**Published:** 07 April 2021

### Citation:

Bernard-Espina J, Beraneck M,  
Maier MA and Tagliabue M (2021)  
Multisensory Integration in Stroke  
Patients: A Theoretical Approach  
to Reinterpret Upper-Limb  
Proprioceptive Deficits and Visual  
Compensation.  
Front. Neurosci. 15:646698.  
doi: 10.3389/fnins.2021.646698

For reaching and grasping, as well as for manipulating objects, optimal hand motor control arises from the integration of multiple sources of sensory information, such as proprioception and vision. For this reason, proprioceptive deficits often observed in stroke patients have a significant impact on the integrity of motor functions. The present targeted review attempts to reanalyze previous findings about proprioceptive upper-limb deficits in stroke patients, as well as their ability to compensate for these deficits using vision. Our theoretical approach is based on two concepts: first, the description of multi-sensory integration using statistical optimization models; second, on the insight that sensory information is not only encoded in the reference frame of origin (e.g., retinal and joint space for vision and proprioception, respectively), but also in higher-order sensory spaces. Combining these two concepts within a single framework appears to account for the heterogeneity of experimental findings reported in the literature. The present analysis suggests that functional upper limb post-stroke deficits could not only be due to an impairment of the proprioceptive system per se, but also due to deficiencies of cross-references processing; that is of the ability to encode proprioceptive information in a non-joint space. The distinction between purely proprioceptive or cross-reference-related deficits can account for two experimental observations: first, one and the same patient can perform differently depending on specific proprioceptive assessments; and a given behavioral assessment results in large variability across patients. The distinction between sensory and cross-reference deficits is also supported by a targeted literature review on the relation between cerebral structure and proprioceptive function. This theoretical framework has the potential to lead to a new stratification of patients with proprioceptive deficits, and may offer a novel approach to post-stroke rehabilitation.

**Keywords:** stroke, eye-hand coordination, maximum likelihood principle, visual compensation, proprioception assessment, multisensory integration

## INTRODUCTION

Manual dexterity is highly specialized in humans (Lemon, 2008). Multimodal information from different sensory systems need to be combined to optimally control hand movements. Among them are vision, proprioception, touch, audition and graviception. Goal-oriented upper limb movements are planned and controlled using mainly vision and proprioception, which allow comparison of hand position with the location/orientation of the object to be reached and/or grasped.

In the context of brain lesions, such as in stroke, proprioceptive deficits are common (Connell et al., 2008; Kessner et al., 2016). These deficits significantly contribute to the patients' motor disability and largely determine their degree of recovery (Turville et al., 2017; Zandvliet et al., 2020). Despite the clinical relevance, no consensus exists regarding the neurological assessment of proprioceptive deficits, nor on the rehabilitation strategies (Findlater and Dukelow, 2017). Clinical research studies that investigated and compared various techniques for the assessment of proprioception observed inconsistencies (Dukelow et al., 2012; Gurari et al., 2017; Ingemanson et al., 2019). Attempts to quantify the patients' ability to use vision to compensate for proprioceptive deficits also provided contrasting results depending on the task and on the brain lesion (Darling et al., 2008; Scalha et al., 2011; Semrau et al., 2018; Herter et al., 2019).

In the present non-systematic review, we propose a new analysis and re-classification of assessment techniques commonly used in clinical practice and stroke research. This reinterpretation is based on the theoretical framework provided by the Maximum Likelihood Principle (MLP) and its application in the field of perception and sensorimotor control (Van Beers et al., 1996; Ernst and Banks, 2002; Körding et al., 2007). This theory describes how sensory inputs are optimally combined to generate a coherent movement representation and statistically maximize its precision. Experimental evidence, and its interpretation through this statistical model, suggests that the central nervous system (CNS) reconstructs multiple concurrent representations of the task (Tagliabue and McIntyre, 2008; McGuire and Sabes, 2009; Tagliabue and McIntyre, 2011, 2014). Each of these concurrent representations encodes the information in a specific reference frame, which can be directly associated to a sensory system (e.g., the retinal reference for vision and the joint reference for proprioception) or to a combination of sensory signals (i.e., body-centered, gravito-centered and allocentric references). As a consequence, the information acquired through a sensory channel can be encoded in a reference frame not directly associated to the originating sensory system. This information processing is commonly termed "cross-modal" when the transformations involves two reference frames associated to two different sensory modalities. In the following we will privilege the more generic "cross-reference" term, which accounts for both between-modalities transformations (e.g., proprioceptive to visual) and within-modality transformations (e.g., proprioceptive transformation between different reference frames as the hand or the trunk, or even with respect to external references).

Cross-reference processing appears to take place even when the constraints of the task leaves only one sensory input modality available (Pouget et al., 2002; Sarlegna and Sainburg, 2007; McGuire and Sabes, 2009; Jones and Henriques, 2010; Tagliabue and McIntyre, 2013; Arnoux et al., 2017). It is therefore critical to distinguish between the modality of the sensory inputs provided by the task, and the potential cross-reference sensory processing that ensues during task performance.

The present reinterpretation of the contrasting results reported in the stroke literature is founded on the hypothesis that altered cross-reference processing could form an essential part of what has (perhaps misleadingly) been termed proprioceptive post-stroke deficits.

In the next section, we will describe the standard methods used for the assessment of proprioceptive deficits and visual compensation mechanisms post-stroke. In the following section we will present the multisensory integration theory based on MLP and its application to the most representative clinical tests. Based on the MLP theoretical predictions, in section "Reinterpretation of Experimental Observations About Proprioceptive Deficits and Visual Compensation" we will propose a new stratification for stroke patients which is based on their sensory deficits. In section "Insights From Brain Lesions and Functional Anatomy Studies," we will review lesion-behavior and brain imaging studies in the framework of this novel classification and attempt to relate brain structures to either purely proprioceptive functions or cross-reference processing. In the final section, we will summarize the contribution of this review to neuroscientific and clinical research and describe some specific applications for post-stroke sensory assessment and rehabilitation.

## UPPER LIMB PROPRIOCEPTIVE DEFICITS POST-STROKE

Stroke can affect not only motor abilities, but also sensory functions. In particular, proprioceptive deficits can be observed in a large percentage, up to 60%, of individuals following stroke (Connell et al., 2008; Kessner et al., 2016). These impairments are clearly correlated with functional deficits (Scalha et al., 2011; Meyer et al., 2014, 2016; Rand, 2018). In particular, reaching (Zackowski et al., 2004), dexterity (Carlsson et al., 2019), and inter-limb coordination (Torre et al., 2013) appear to be negatively affected by proprioceptive deficits. Moreover, sensory recovery is a predictive factor for functional recovery (Turville et al., 2017; Zandvliet et al., 2020).

Yet, no consensus seems to have emerged regarding proprioceptive assessment methods (Saeys et al., 2012; Simo et al., 2014; Pumpa et al., 2015; Santisteban et al., 2016). For the assessment of upper-limb function, no less than 48 different clinically validated (standardized) measures are used in clinical research (Santisteban et al., 2016). A high discrepancy between studies was found, as only 15 of the 48 outcome measures are used in more than 5% of the studies. In particular, only few studies specifically assess proprioceptive function: the NSA<sup>1</sup>, one

<sup>1</sup>Nottingham Sensory Assessment.

of the most commonly used standardized scales, was applied in only 0.6% of studies reviewed (Santisteban et al., 2016). Moreover, current clinical practice does not systematically use standardized scales (Saeys et al., 2012; Simo et al., 2014; Pampa et al., 2015; Santisteban et al., 2016; Matsuda et al., 2019). This lack of consensus is a major shortcoming for meta-analysis of recovery of upper limb function after stroke (Findlater and Dukelow, 2017). Similarly, research examining the ability of patients to compensate for a proprioceptive deficit using vision lack homogeneity. Although empirical evidence suggests that vision is helpful to compensate a proprioceptive deficit (Pampa et al., 2015), the studies addressing this question are scarce and their methodologies are hardly comparable (Darling et al., 2008; Scalha et al., 2011; Torre et al., 2013; Semrau et al., 2018; Herter et al., 2019).

In the following subsections we will review the assessment techniques currently used in stroke for proprioceptive function, as well as for visual compensation. We will then discuss several studies showing that some of these proprioception and visual compensation tests might lead to different diagnostics. Finally, in the last subsection we will propose a new categorization of these tests with the aim of better understanding the origin of their different outcomes.

## Proprioceptive Tests in the Clinical Practice

All existing proprioceptive assessment methods are relevant from a functional point of view, but their differences pose a challenge for their comparability. The commonly used tests, both in clinical practice (Pampa et al., 2015) and in clinical research are described below:

- **Thumb Localization Test (TLT):** Assesses the ability of a subject to localize a body part (thumb). The physiotherapist positions the affected arm of the patient who then has to point, without vision, to the affected thumb with the other, less-affected hand (Dukelow et al., 2012; Meyer et al., 2016; Rand, 2018).
- **Up or Down Test (UDT):** Assesses the ability of a subject to detect joint displacement direction. The physiotherapist moves a joint of the patient whose vision is occluded. The subject is then asked to report the up or down movement direction. This test is part of the FMA-UE<sup>2</sup> and the RASP<sup>3</sup> (Scalha et al., 2011; Saeys et al., 2012; Simo et al., 2014; Rand, 2018; Birchenall et al., 2019; Carlsson et al., 2019; Frenkel-Toledo et al., 2019; Kessner et al., 2019; Pennati et al., 2020; Zandvliet et al., 2020).
- **Mirror Position Test (MPT):** Assesses the ability of a subject to perceive the angular configuration of a particular joint. The physiotherapist positions a joint of the patient's affected arm in the absence of vision. The patient is then asked to mirror the position with the other, less-affected arm. This task can also be performed using a robotic device. This test is part of the NSA (Connell et al., 2008;

Dukelow et al., 2010; Scalha et al., 2011; Iandolo et al., 2014; Ben-Shabat et al., 2015; Meyer et al., 2016; Gurari et al., 2017; Sallés et al., 2017; Findlater et al., 2018; Rinderknecht et al., 2018; Semrau et al., 2018; Herter et al., 2019; Zandvliet et al., 2020).

- **Bimanual Sagittal Matching Test (BSMT):** Assesses the ability of the patients to reproduce with their free hand the trajectory/position of the affected hand which is passively driven by a robotic device along the sagittal plane (Torre et al., 2013).
- **Within-arm Position Test (WPT):** Assesses the ability of a subject to perceive the angular configuration of one joint. A robot moves the arm of the patient to a position to be memorized and then back to the initial configuration. Subsequently, the subject is asked to move his/her arm to the remembered position (Dos Santos et al., 2015; Contu et al., 2017; Gurari et al., 2017).
- **Matching to a Visual Image (MV):** Assesses the ability of a subject to localize in space his/her unseen arm or hand relative to a visual reference. A visual image, that could be a lever or a virtual hand with a given orientation, is shown to the subject. The subject is then asked, without visual feedback, to reproduce the same orientation with his/her hand. The vision of the hand can be occluded by a box covering the hand, or by wearing a virtual reality headset that leaves the subject's hand non-rendered (Turville et al., 2017; Deblock-Bellamy et al., 2018).
- **Threshold Detection Test (TDT):** Assesses the patient's ability to detect hand displacements of various magnitudes. Using a robotic device, a joint (elbow, wrist, metacarpophalangeal) is first moved from a starting to a reference position. Then, a second movement from the starting position in the same direction, but not with the same amplitude, is operated by the robot. The subject is asked to assess whether the second movement was larger or smaller than first one. The threshold detection value is measured (Simo et al., 2014; De Santis et al., 2015; Rinderknecht et al., 2018; Ingemanson et al., 2019).
- **Finger Proprioception Test (FPT):** Assesses the patient's ability to detect whether the index finger is aligned (in flexion/extension) with the middle finger. The two fingers are passively moved by a robotic device in a crossing flexion/extension movement. For each finger-crossing movement, the patient is asked to report when the two fingers are directly aligned relative to each other (Ingemanson et al., 2019).
- **Motor Sequences Test (MS):** Assesses the patient's ability to localize a body part (fingers). The subject is asked to touch with the thumb pad (I) the other finger pads (II, III, IV, V) with eyes closed. Motor sequences with alternating movements between the thumb and the other fingers are used: for example, touching in the following order: I with II, I with III, I with IV, I with V (Scalha et al., 2011).
- **Reaching Test (RT):** Assesses the patient's ability to localize in space his/her unseen arm relative to a visual reference. A visual target (real or on a screen) is shown and the subject asked to reach to the memorized target, without

<sup>2</sup>Fugl-Meyer Assessment for the Upper Extremity.

<sup>3</sup>Rivermead Assessment of Somatosensory Performance.

visual feedback of the reaching hand (Scalha et al., 2011; Elangovan et al., 2019; Valdes et al., 2019).

- **Shape or Length Discrimination (SLD):** Assesses the patient's ability to discriminate object shapes and dimensions without vision. Different objects of familiar geometric shapes, everyday objects or segments of different lengths are presented to the patient whose vision is occluded. Either with passive movements (operated by a robotic device or a physiotherapist) or active movements, the patient interacts with the different objects. The subject is asked to report the perceived shape, object or length (Van de Winkel et al., 2012; De Diego et al., 2013; Metzger et al., 2014; Sallés et al., 2017; Turville et al., 2017; Matsuda et al., 2019; Carlsson et al., 2019).

Although each one of these tests involves proprioception, they are clearly different. For instance, some tests involve one articular chain only (UDT, TDT, WPT), whereas others involve two distinct articular chains (two arms for MPT and TLT or two fingers for FPT and MS). When two articular chains are involved, the patient is either asked to mirror the joint configuration (MPT, FPT), or to point to a body part (e.g., thumb of the affected arm: TLT and MS). It is noteworthy that some other tests do not rely on proprioceptive inputs only, but use visually remembered references (MV, RT, SLD).

## Different Proprioceptive Assessments, Different Outcomes

Experimental observations suggest that methodological differences between these tests can lead to different diagnostics (Hirayama et al., 1999; Dukelow et al., 2012; Gurari et al., 2017; Ingemanson et al., 2019). Similarly, the ability of patients to compensate the proprioceptive deficit with vision depends on the task considered (Darling et al., 2008; Scalha et al., 2011; Torre et al., 2013; Semrau et al., 2018; Herter et al., 2019). In the following we will detail and discuss some of the studies reporting differences between proprioceptive assessment techniques for stroke patients.

### Within-Arm Position Test (WPT) vs. Mirror Position Test (MPT)

Gurari et al. (2017) characterized the ability of chronic stroke patients and healthy controls to match elbow flexion/extension positions using two approaches: the **MPT** performed with a physiotherapist vs. the **WPT** under robotic control. The large majority of stroke patients showed impairments in the mirror task, but no difference with the control group in the within-arm task. These different outcomes could be due to lateralized sensory deficits observed after stroke (Connell et al., 2008; Kessner et al., 2016) resulting in asymmetries that may affect the between-arms comparison in the mirror task, but not the unilateral within-arm task. A non-exclusive alternative explanation for the difference in performances may reside in stroke lesions that could have damaged brain networks specifically involved in the mirror but not in the within-arm task (Iandolo et al., 2018). This second hypothesis appears

supported by the results of Torre et al. (2013), where stroke patients performed the bimanual sagittal matching tests (BSMT). The accomplishment of BSMT does not require mirroring with respect to the body midline of the hand position, because both hands moved along the sagittal plane, close to each other. The precision of the patients in this study is similar to that observed in within-arm tasks (Dos Santos et al., 2015; Contu et al., 2017; Rinderknecht et al., 2018) and appears better than for the MPT (Herter et al., 2019; Ingemanson et al., 2019), suggesting that stroke lesions can affect the sensory processing necessary to mirror the hand position with respect to the body midline without affecting the between-arms communication *per se*.

### Mirror Position Test (MPT) vs. Thumb Localization Test (TLT)

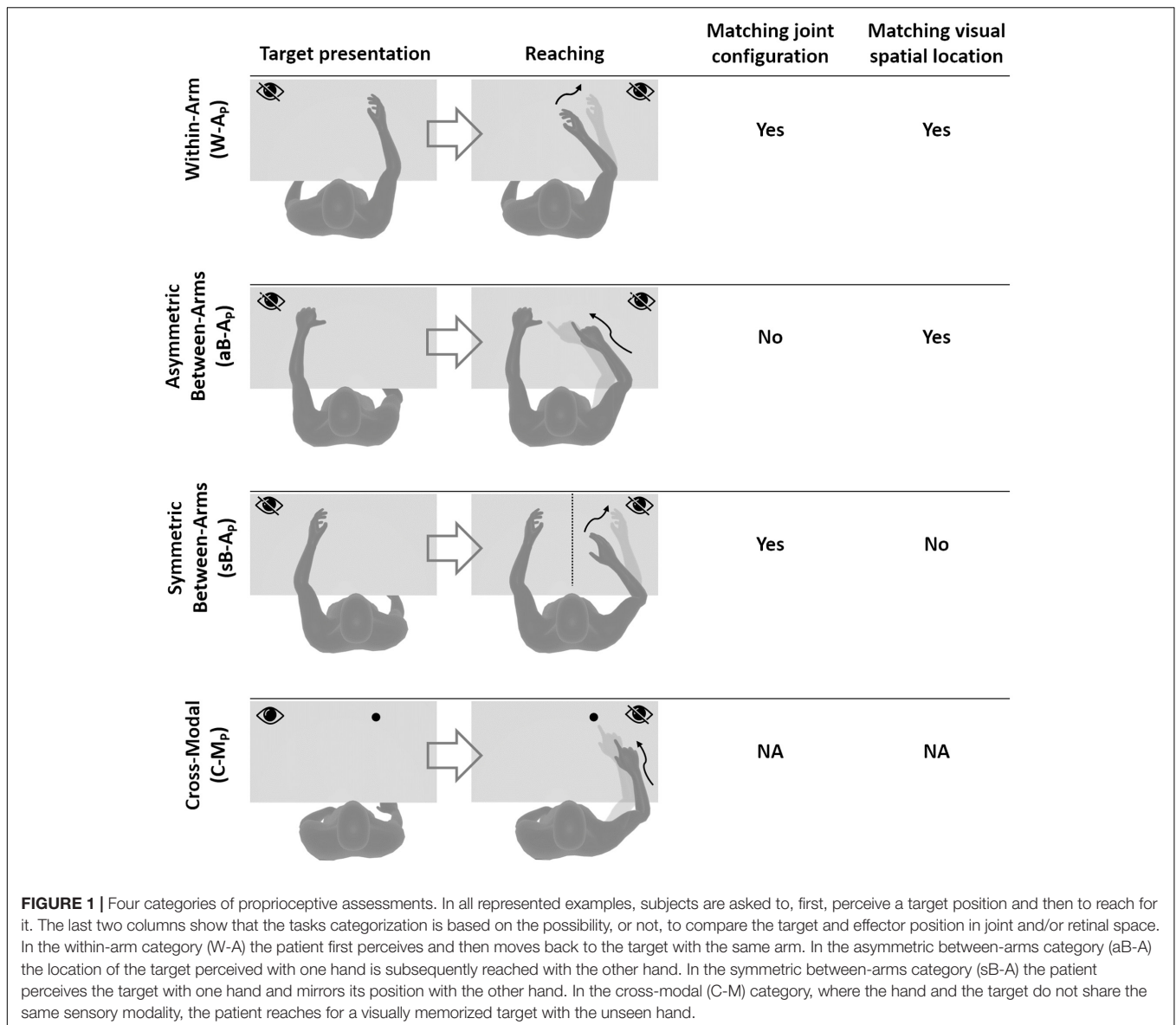
Outcomes of these two tests were only poorly correlated (Kenzie et al., 2017) and could not reliably identify a proprioceptive deficit within the same patients (Dukelow et al., 2012). Estimated prevalence of proprioceptive deficits using these two tests varied by a factor of two (Meyer et al., 2016). A clear difference between the two tasks, which might explain the different outcomes, is the use of a left/right symmetric (MPT) vs. an asymmetric joint configuration in the TLT. Studies on healthy subjects comparing analogous symmetric and asymmetric inter-manual proprioceptive tasks suggest that these tests differ by the way the joint information from the two arms is processed (Arnoux et al., 2017). Stroke lesions may differentially damage brain areas involved in the specific sensory processing characterizing symmetric and asymmetric tasks.

### Thumb Localization Test (TLT) and Finger Proprioception Test (FPT) vs. Up or Down Test (UDT)

These comparisons showed poor correlations (Lanska and Kryscio, 2000; Ingemanson et al., 2019), and prevalence of proprioceptive deficits varied by a factor of three (Hirayama et al., 1999). The difference between the unimanual UDT and both the inter-manual TLT and FPT, which uses two fingers of the affected hand, suggests that the different outcomes do not originate from involving only the affected limb. A key difference between these tasks resides in using a single (UDT) vs. two articular chains (TLT and FPT). Research on healthy subjects, comparing analogous proprioceptive tasks, supports differential proprioceptive processing in these two situations (Tagliabue and McIntyre, 2013).

### Within-Arm Position Test (WPT) vs. Reaching Test (RT)

Performance errors in the WPT were only poorly correlated with errors in the RT (Darling et al., 2008). This result is most likely due to the obvious difference in sensory modality: the target position is either memorized through proprioception (WPT) or through vision (RT). These tasks have been studied in healthy subjects and been shown to require different sensory processing (Tagliabue and McIntyre, 2011; Tagliabue et al., 2013).



## Different Visual Compensation Assessments, Different Outcomes

Several studies tested whether stroke patients could compensate for their proprioceptive deficits by using visual information. The results appear to be very different depending on the task under investigation.

Visual feedback of the hand appears to improve the patient's performance in some tasks, such as the **Motor Sequences Test** (Scalha et al., 2011), and the **Reaching Test** (Darling et al., 2008). On the other hand, in a large-scale study where patients were assessed using a **Mirror Position Test**, up to 80% of patients with proprioceptive deficits were not able to improve their performance when visual feedback of both arms was available (Semrau et al., 2018; Herter et al., 2019). The important difference between Mirror Position Test and both Motor Sequences Test and Reaching Test, is the different way

visual information can be used. In both tasks where vision significantly improves performance in patients, the hand (or finger) reaches the same spatial position of the target: the tasks can hence be accomplished by simply matching the visually acquired target position and the visual feedback of the hand (or finger). In the Mirror Position Test in contrast, the patient does not have to reach the spatial location of the target, but its mirror position: the patient must thus “flip,” relative to the body midline, the image of the arms to evaluate the task accomplishment. It follows that the ability to use visual information to compensate for proprioceptive deficits in reaching, but not in mirror tasks, could be due to specific difficulties in performing “mirroring” of visual information. Consistent with this interpretation, patients were shown to be able to significantly improve their performance with vision in the Bimanual Sagittal Matching Test which does not require the “mirroring” of visual information, because their

hands moved parallel to the sagittal plane and close to each other (Torre et al., 2013).

## Categorization of Proprioceptive Assessments

Based on the above observations, we propose here a new categorization of these various proprioceptive tests. We group them into four distinct categories (**within-arm** tasks, **asymmetric between-arms** tasks, **symmetric between-arms**<sup>4</sup> tasks, and **cross-modal** tasks). This categorization is based on the possibility to achieve the tasks by reproducing the joint configuration memorized during the target acquisition and/or by matching the target position in retinal coordinates (Figure 1).

**Within-Arm tasks** require one and the same articular chain to perceive and to reproduce the target position. Thus, proprioceptive information to be remembered (target) and the feedback about the moving hand (effector) originate from the same joints (Figure 1, W-A). These tasks can be performed by directly matching the proprioceptive signals corresponding to the target and effector positions (Within-arm Position Test) or by directly comparing two movement signals originating from the same joints (Up or Down Test, Threshold Detection Test). These tasks can also be performed by matching the target and effector position encoded in the retinal reference. Bi-manual matching tests performed along the mid-sagittal plane (BSMT) are also associated to this category, because, as described in sections “Different Proprioceptive Assessments, Different Outcomes” and “Different Visual Compensation Assessments, Different Outcomes,” although involving two arms, the experimental results suggest that they are performed by a direct encoding of the information in joint and retinal coordinates, similarly to the within-arm tasks.

**Asymmetric Between-Arms tasks** involve two articular chains. Typically, the less-affected arm (effector) has to reach the target location perceived with the affected arm (Thumb Location Test, see Figure 1, aB-A). These tasks cannot be performed by matching the joint configuration of the affected arm (target) with that of the effector, since they differ at the end of the movement. They can be accomplished, however, by matching the target and effector location encoded in the retinal reference frame. The Motor Sequences test (involving only one arm), as well as the Thumb Location Test, can also be classified in this category since they involve different articular chains (fingers) to perceive the target position and to match it.

**Symmetric Between-Arms tasks** also involve two articular chains. “Symmetric” refers to the fact that the effector has to “mirror” the target configuration. The articular chains can be the arms (Mirror Position Test, see Figure 1, sB-A) or the index and middle fingers (Finger Proprioception Test). At task achievement, the joint configuration of the two articular chains is identical, allowing for direct matching of proprioceptive signals corresponding to the target and effector positions. In

<sup>4</sup>We choose here to refer to this group of tasks as “between-arms,” and not bimanual, as the two arms are not used together to sense and move to the target. In contrast, tasks involving only one arm will be referred as “within-arm.”

**TABLE 1** | Categorization of proprioceptive assessments.

| Category                       | Test  |
|--------------------------------|---|
| Within-arm (W-A)               | Within-arm Position Test (WPT)<br>Up or Down Test (UDT)<br>Threshold Detection Test (TDT)<br>Bimanual Sagittal Matching Test (BSMT) |
| Asymmetric between-arms (aB-A) | Thumb Localization Test (TLT)<br>Motor Sequences Test (MS)  |
| Symmetric between-arms (sB-A)  | Mirror Position Test (MPT)<br>Finger Proprioception Test (FPT)  |
| Cross-modal (C-M)              | Reaching Test (RT)<br>Matching to a Visual image (MV)<br>Shape/Length Discrimination (SLD)  |

contrast, the task cannot be performed in the retinal space, since the target and the effector do not share the same spatial location.

**Cross-Modal Tasks** differ from the other three categories in that the target information is given visually (or remembered visually) whereas only proprioceptive information is provided for the effector (the moving hand, Figure 1, C-M). Thus, these tasks always require cross-reference sensory processing. For this reason, their categorization based on the direct encoding in the joint and/or retinal space is not fully applicable. Both Reaching Test and Matching to a Visual image share this characteristic. Similar sensory processing could also be involved in the tasks used in Perfetti’s neurocognitive approach, such as the Shape or Length Discrimination test.

Overall, this new categorization (summarized in Table 1) allows to discriminate the above-mentioned tests in terms of sensory requirements. In the following section, we will present the multisensory integration theory based on MLP and its application to the most representative clinical tests among those reported here.

## OPTIMAL MULTISENSORY INTEGRATION THEORY AND STROKE

In this section we will present the MLP and its application to generic target-oriented movements (first subsection). Then we will use this theoretical framework to describe the information processing underlying the proprioceptive assessments according to their categorization (second subsection).

### Statistical Optimality in Multisensory Integration for Goal-Oriented Hand Movements

When reaching to grasp an object, visual and proprioceptive sensory information about the target and the hand (effector) is used to control movement execution. In a first step, each sensory modality is encoded in the reference frame of the respective receptors: retinal and joint reference for vision and proprioception, respectively. Several studies have shown that redundant sensory

signals are then optimally combined and weighted according to MLP in order to statistically minimize the variability of the estimated movement parameters (Ernst and Banks, 2002).

**Figure 2A** shows how sensory signals are conceptually processed for goal-oriented upper limb movements. To match the target position with the effector, that is to reach the target with the hand, the latter must be displaced by a distance and in a direction that are represented by the movement vector  $\Delta$ . To compute  $\Delta$ , the target and effector positions are compared concurrently in the visual,  $v$ , and proprioceptive,  $p$ , space (Tagliabue and McIntyre, 2011). This is represented by the following equations of the visual and proprioceptive target-effector comparisons  $v$  and  $p$ :

$$\begin{aligned} \Delta V &= x_{T,v} - x_{E,v} \\ \Delta P &= x_{T,p} - x_{E,p} \end{aligned} \tag{1}$$

where  $T$  and  $E$  subscripts indicate an information about the target and the effector, respectively. For each sensory modality, the comparison is characterized by a variance corresponding to

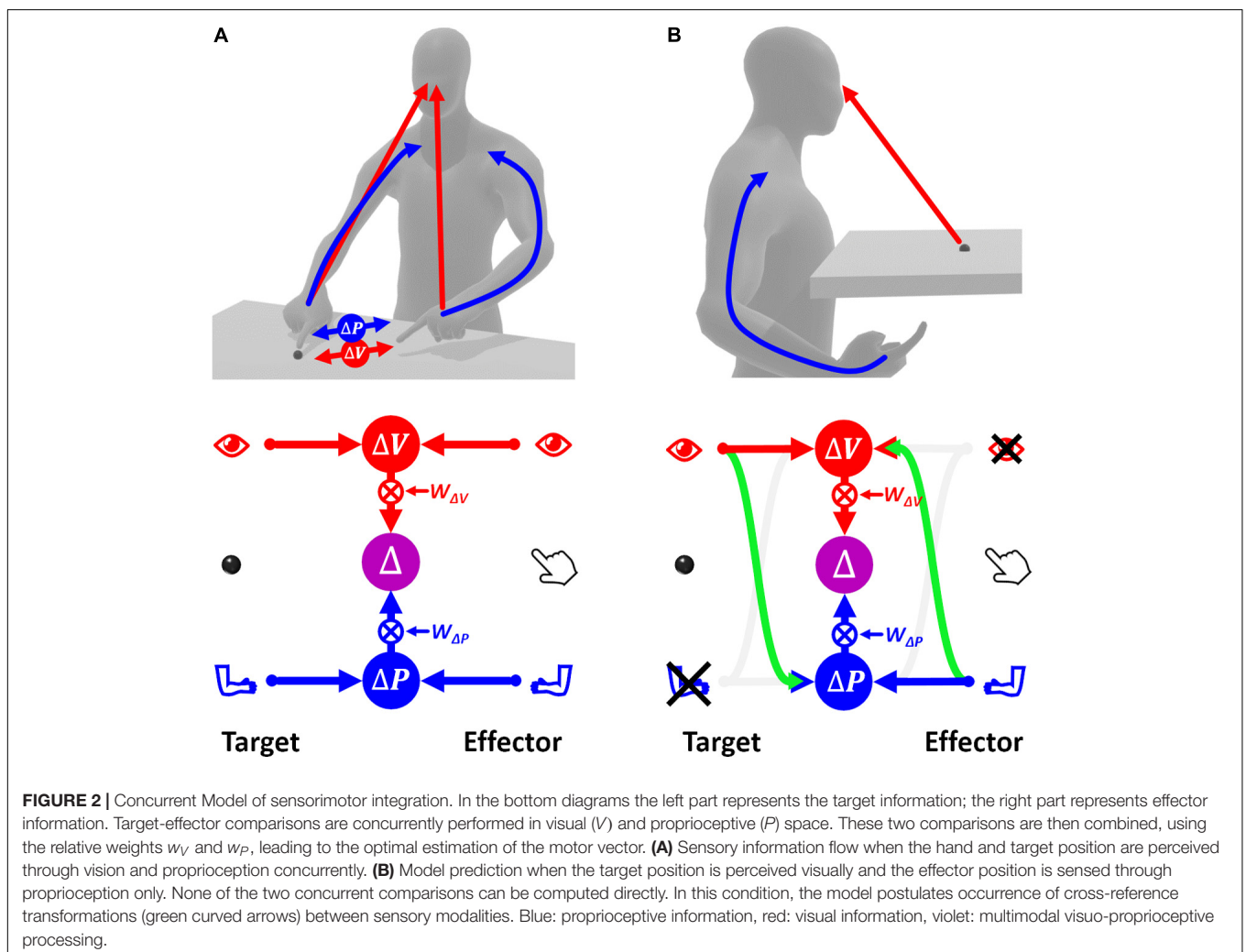
the sum of the variances of the target and effector information (Eq. 2).

$$\begin{aligned} \sigma_{\Delta V}^2 &= \sigma_{T,v}^2 + \sigma_{E,v}^2 \\ \sigma_{\Delta P}^2 &= \sigma_{T,p}^2 + \sigma_{E,p}^2 \end{aligned} \tag{2}$$

The MLP predicts that in order to maximize the precision of the estimated movement vector  $\Delta$ , the concurrent visual and proprioceptive comparisons must be combined (summed), as in Eq. 3.

$$\begin{aligned} \Delta &= w_{\Delta V} \cdot \Delta V + w_{\Delta P} \cdot \Delta P \\ w_{\Delta V} &= \frac{\sigma_{\Delta P}^2}{\sigma_{\Delta V}^2 + \sigma_{\Delta P}^2} \\ w_{\Delta P} &= \frac{\sigma_{\Delta V}^2}{\sigma_{\Delta V}^2 + \sigma_{\Delta P}^2} \end{aligned} \tag{3}$$

Thus, the movement vector is the weighted sum of the concurrent target-effector comparisons, and each comparison is associated to a weight,  $w_{\Delta V}$  and  $w_{\Delta P}$ , whose value depends on the relative variability of the two comparisons.



If this MLP formulation, called “Concurrent Model,” is straightforward when both target and effector positions can be perceived through vision and proprioception (Figure 2A), the information processing seems more complex when some information is not available, e.g., when the target position can be perceived only visually while the effector position only through proprioception (Figure 2B). In this case, none of the two concurrent comparisons can be computed directly, because the target and the effector cannot be perceived through the same sensory modality. However, these comparisons can be performed through two mutually not exclusive possibilities: first, the visually perceived position of the target may be encoded in a proprioceptive space; second, the effector position, provided through proprioception, may be encoded in visual space.

In this condition the variability associated with the two concurrent comparisons is given in Eq. 4 where  $\sigma_{p \rightarrow v}^2$  and  $\sigma_{v \rightarrow p}^2$  represent the variance associated with the cross-reference transformations from proprioception to vision, and vice-versa. The indentation is used to facilitate the distinction between the variance associated with the target and effector encoding (the same type of indentation will be used throughout).

|  |   |   |     |  |
|--|---|---|-----|--|
|  | Target  | Effector  |     |  |
|  | $\sigma_{\Delta V}^2 = \sigma_{T,v}^2$                              | $+ \sigma_{E,p}^2 + \sigma_{p \rightarrow v}^2$ | (4) |  |
|  | $\sigma_{\Delta P}^2 = \sigma_{T,v}^2 + \sigma_{v \rightarrow p}^2$ | $+ \sigma_{E,p}^2$                              |     |  |

In contrast to the task represented in Figure 2A and Eq. 3, in this condition the two concurrent comparisons are not fully independent, because they are partially computed from the same information. In this case, Eq. 3 must be modified to take into account the covariance between proprioceptive and visual target-effector comparisons,  $cov(\Delta P, \Delta V)$  (see Supplementary Section 1 for details):

$$w_{\Delta V} = \frac{\sigma_{\Delta P}^2 - cov(\Delta P, \Delta V)}{\sigma_{\Delta V}^2 + \sigma_{\Delta P}^2 - 2 \cdot cov(\Delta P, \Delta V)} \tag{5}$$

$$w_{\Delta P} = \frac{\sigma_{\Delta V}^2 - cov(\Delta P, \Delta V)}{\sigma_{\Delta V}^2 + \sigma_{\Delta P}^2 - 2 \cdot cov(\Delta P, \Delta V)}$$

For the example of Figure 2B  $cov(\Delta P, \Delta V) = \sigma_{T,v}^2 + \sigma_{E,p}^2$ , that is the common variance component between  $\sigma_{\Delta P}^2$  and  $\sigma_{\Delta V}^2$ . Therefore, Eq. 5 become:

$$w_{\Delta V} = \frac{\sigma_{v \rightarrow p}^2}{\sigma_{v \rightarrow p}^2 + \sigma_{p \rightarrow v}^2} \tag{6}$$

$$w_{\Delta P} = \frac{\sigma_{p \rightarrow v}^2}{\sigma_{v \rightarrow p}^2 + \sigma_{p \rightarrow v}^2}$$

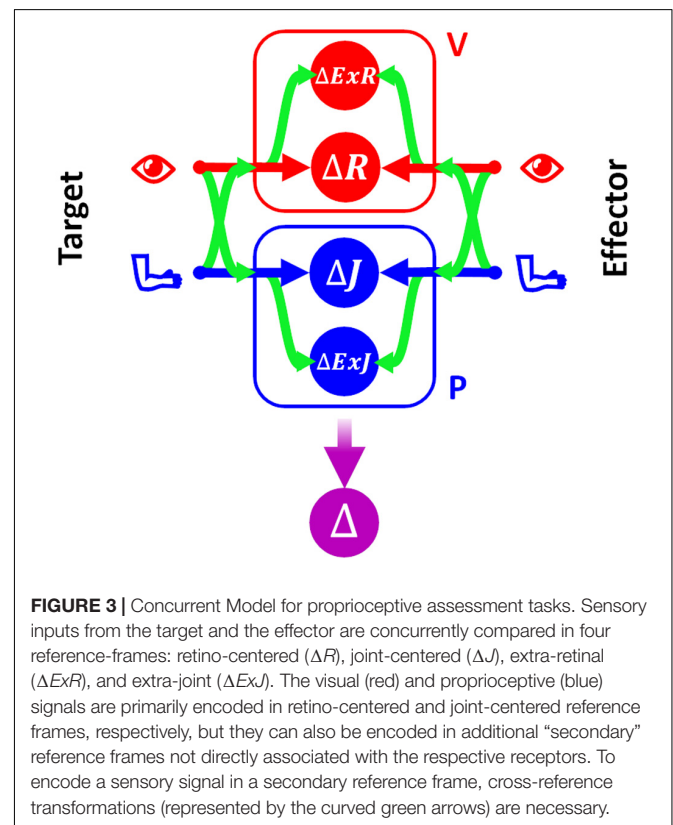
It follows that the relative weights between the two concurrent object-effector comparisons depend on the noisiness of the two cross-modal transformations, which is consistent with experimental observations (Burns and Blohm, 2010; Tagliabue et al., 2013).

## Application of the Optimal Sensory Integration Theory to Proprioception Assessment Tests

In the following we will show whether the MLP predicts clear differences between the sensory processing necessary to accomplish the tasks depending on their categorization described in the previous section.

In order to be able to represent consistently the type of sensory processing underlying the execution of tasks within these four categories, we will use a slightly modified formulation of the Concurrent Model with respect to the one presented in section above. This formulation, represented in Figure 3, explicitly distinguishes between the reference frames in which the sensory signals are natively encoded (the joint,  $J$ , and the retinal,  $R$ , reference frames for proprioception and vision, respectively) and the reference frames which correspond to a combination of the original sensory signal about target and response position, with additional sensory information. For instance, the hand position perceived through joint receptors can be encoded with respect to different body parts or even with respect to external references, such as gravity or visual landmarks (Tagliabue and McIntyre, 2014). To refer to this type of indirect sensory encodings we use the generic term “extra-joint,”  $ExJ$ , for proprioception and “extra-retinal,”  $ExR$ , for vision.

Although both visual and proprioceptive information can potentially be encoded in multiple “extra-” reference frames, we have reduced the model formulation to its simplest version



allowing an accurate description of the sensory processing underlying the analyzed tasks. As a consequence, the present formulation of MLP includes four concurrent target-effector comparisons:  $\Delta J$ ,  $\Delta R$ ,  $\Delta ExJ$ ,  $\Delta ExR$ . In this formulation of the concurrent model the estimation of the motor vector  $\Delta$  corresponds to the following weighted sum:

$$\Delta = w_{\Delta J} \Delta J + w_{\Delta ExJ} \Delta ExJ + w_{\Delta R} \Delta R + w_{\Delta ExR} \Delta ExR \quad (7)$$

To represent all possible cross-reference transformations between these four reference frames, this model includes not only the possibility to perform cross-reference transformations between proprioceptive, joint-centered, and visual, retino-centered reference frames ( $J \leftrightarrow R$ ), but also the possibility to encode joint and retinal signals in the extra-joint and extra-retinal reference frames, respectively ( $J \rightarrow ExJ$  and  $R \rightarrow ExR$ ).

In the following this statistical model will be used to evaluate, for each of the categories of proprioceptive assessments, the relative weights that must be associated with the four concurrent target-effector comparisons to optimize the precision of the movement vector estimation,  $\Delta$ . The precise values of the sensory weight and details of the methods used are reported in **Supplementary Sections 2, 3**. In the following paragraphs these results will be only graphically described in the figures representing the information flow theoretically associated with each category of tasks. The analytical equation of the variability of the optimal motor vector estimation predicted by MLP will be reported for each test and will then be quantitatively compared to the results of experimental studies.

### Within-Arm Proprioceptive Tasks (W-AP)

In this test the memorized target and the effector positions are perceived through the same set of joint sensors. Thus, their position can be compared “directly” in the joint space  $J$ . All three other concurrent comparisons would require some cross-reference transformation. The variance associated with each of the four concurrent target-response comparisons for the W-AP tasks is reported in Eq. 8, where  $\sigma_{J \rightarrow R}^2$  is the variance associated with the cross-reference transformation from the joint-centered to the retino-centered reference frame.  $\sigma_{J \rightarrow ExJ}^2$ ,  $\sigma_{R \rightarrow ExR}^2$  are the variances corresponding to the intra-modal transformations from joint to extra-joint and from retinal to extra-retinal references, respectively.

$$\begin{aligned} \sigma_{\Delta J}^2 &= \sigma_J^2 && + \sigma_J^2 \\ \sigma_{\Delta ExJ}^2 &= \sigma_J^2 + \sigma_{J \rightarrow ExJ}^2 && + \sigma_J^2 + \sigma_{J \rightarrow ExJ}^2 \\ \sigma_{\Delta R}^2 &= \sigma_J^2 + \sigma_{J \rightarrow R}^2 && + \sigma_J^2 + \sigma_{J \rightarrow R}^2 \\ \sigma_{\Delta ExR}^2 &= \sigma_J^2 + \sigma_{J \rightarrow R}^2 + \sigma_{R \rightarrow ExR}^2 && + \sigma_J^2 + \sigma_{J \rightarrow R}^2 + \sigma_{R \rightarrow ExR}^2 \end{aligned} \quad (8)$$

The optimal information flow predicted by MLP is represented in **Figure 4A**: the model predicts no use of the reconstructed representations of the task, and the “exclusive” use of the comparison in the joint space does not require any cross-reference transformation. This phenomenon was clearly shown

in unimodal, proprioceptive tasks involving only one arm (Tagliabue and McIntyre, 2011, 2013; Arnoux et al., 2017). The variance of the movement vector estimation corresponding to this optimal sensory processing is

$$\sigma_{\Delta}^2 = 2\sigma_J^2 \quad (9)$$

### Asymmetric Between-Arms Proprioceptive Tasks (aB-AP)

The asymmetric configuration of the limb during this test results in the impossibility to achieve the task by simply matching the joint signals from the two arms. Mathematically, this impossibility is represented by a large variance associated with the transformation of the proprioceptive joint signals between the left and right arm:  $\sigma_{J_l \rightarrow r}^2 = \sigma_{J_r \rightarrow l}^2 \rightarrow \infty$ . The variances associated with the four concurrent target-effector comparisons are thus:

$$\begin{aligned} \sigma_{\Delta J}^2 &= \sigma_{J_l}^2 + \sigma_{J_l \rightarrow r}^2 && + \sigma_{J_r}^2 + \sigma_{J_r \rightarrow l}^2 \\ \sigma_{\Delta ExJ}^2 &= \sigma_{J_l}^2 + \sigma_{J_l \rightarrow ExJ}^2 && + \sigma_{J_r}^2 + \sigma_{J_r \rightarrow ExJ}^2 \\ \sigma_{\Delta R}^2 &= \sigma_{J_l}^2 + \sigma_{J_l \rightarrow R}^2 && + \sigma_{J_r}^2 + \sigma_{J_r \rightarrow R}^2 \\ \sigma_{\Delta ExR}^2 &= \sigma_{J_l}^2 + \sigma_{J_l \rightarrow R}^2 + \sigma_{R \rightarrow ExR}^2 && + \sigma_{J_r}^2 + \sigma_{J_r \rightarrow R}^2 + \sigma_{R \rightarrow ExR}^2 \end{aligned} \quad (10)$$

If we assume that the cross-reference transformations from the left and right arm joints are characterized by the same variance ( $\sigma_{J_l \rightarrow ExJ}^2 = \sigma_{J_r \rightarrow ExJ}^2$  and  $\sigma_{J_l \rightarrow R}^2 = \sigma_{J_r \rightarrow R}^2$ ), the optimal sensory weighting predicted by MLP (**Figure 4B**), consists in encoding the position of the two hands perceived through proprioception in alternative reference frames, including the retinal one, rather than in joint space. This prediction is consistent with experimental observations on healthy subjects suggesting that retinal and external references contribute to the encoding of asymmetric between-arm tasks (Pouget et al., 2002; McGuire and Sabes, 2009; Jones and Henriques, 2010; Tagliabue and McIntyre, 2013; Arnoux et al., 2017). Tagliabue and McIntyre (2013) showed that it is the use of tasks that require asymmetric joint configurations in the above-mentioned studies that led to the visual reconstruction of proprioceptive signals.

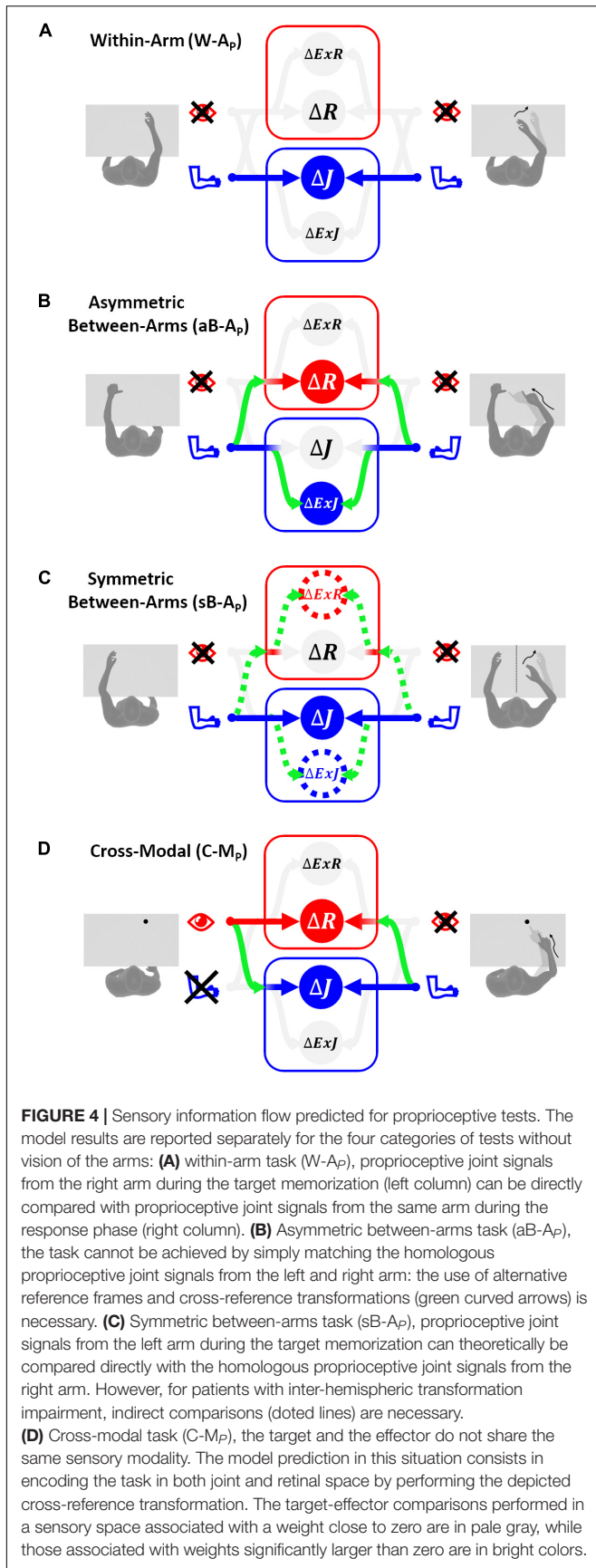
The minimal achievable variability of the  $\Delta$  estimation for these tasks is:

$$\sigma_{\Delta}^2 = \sigma_{J_r}^2 + \sigma_{J_l}^2 + \frac{2\sigma_{J \rightarrow R}^2 \sigma_{J \rightarrow ExJ}^2}{\sigma_{J \rightarrow R}^2 + \sigma_{J \rightarrow ExJ}^2} \quad (11)$$

Thus in the aB-AP tasks, the predicted variability of  $\Delta$  is higher than for the W-A tasks, as experimentally observed (Tagliabue and McIntyre, 2013; Arnoux et al., 2017).

### Symmetric Between-Arms Proprioceptive Tasks (sB-AP)

Experiments on healthy subjects have shown that, in contrast to what has been observed for the aB-AP tests, the precision of this type of symmetric tasks is very similar to the one observed in within-arm tasks, W-AP, and no evidence of visual encoding was



found (Arnoux et al., 2017). These similarities appear to be due to the same joint configuration of the arm holding the target and the arm performing the movement when achieving sB-A<sub>p</sub> tasks. Hence, the movement can be controlled by a “direct” comparison between proprioceptive signals from homologous joints of the two limbs (**Figure 4C**).

The variances associated with the four concurrent target-effector comparisons for the mirroring tasks can be expressed as reported in Eq. 12.

$$\begin{aligned}
 \sigma_{\Delta J}^2 &= \sigma_{J_l}^2 + \sigma_{J_l \rightarrow r}^2 && + \sigma_{J_r}^2 + \sigma_{J_r \rightarrow l}^2 \\
 \sigma_{\Delta ExJ}^2 &= \sigma_{J_l}^2 + \sigma_{J_l \rightarrow ExJ}^2 && + \sigma_{J_r}^2 + \sigma_{J_r \rightarrow ExJ}^2 \\
 \sigma_{\Delta R}^2 &= \sigma_{J_l}^2 + \sigma_{J_l \rightarrow R}^2 && + \sigma_{J_r}^2 + \sigma_{J_r \rightarrow R}^2 + \sigma_{R, Mir}^2 \\
 \sigma_{\Delta ExR}^2 &= \sigma_{J_l}^2 + \sigma_{J_l \rightarrow R}^2 + \sigma_{R \rightarrow ExR}^2 && + \sigma_{J_r}^2 + \sigma_{J_r \rightarrow R}^2 + \sigma_{R \rightarrow ExR}^2
 \end{aligned}
 \tag{12}$$

These equations appear very similar to those describing the asymmetric between-arms tasks (Eq. 10), but there are two important differences, which reflect the different nature of the mirror task and the above-mentioned experimental observations. First, the parameter  $\sigma_{R, Mir}^2$  is added to  $\sigma_{\Delta R}^2$ . This parameter, which is very large ( $\sigma_{R, Mir}^2 \rightarrow \infty$ ), reflects the impossibility to perform the task directly in retinal space: since the two hands must be in two distinct spatial locations, the task cannot be accomplished by matching the reconstructed image of the two hands on the retina. Second, the possibility of directly comparing proprioceptive signals from the two arms is represented by very low values of the variance associated to the transformation of the joint signals between the left and right arm:  $\sigma_{J_l \rightarrow r}^2 = \sigma_{J_r \rightarrow l}^2 \rightarrow 0$ . However, these parameters have not been removed from the equations to be able to describe the behavior of some of the stroke patients. An increase of the value of  $\sigma_{J_l \rightarrow r}^2$  and  $\sigma_{J_r \rightarrow l}^2$  can indeed be used to represent the observed difficulties of some patients in performing sB-A<sub>p</sub> test with respect to the W-A<sub>p</sub> tasks (Gurari et al., 2017).

**Figure 4C** reports the information flow predicted by MLP for two categories of patients: those that have difficulties in performing inter-hemispheric transformations ( $\sigma_{J_r \leftrightarrow l}^2 > 0$ ; dashed lines) and those that do not have this problem ( $\sigma_{J_r \leftrightarrow l}^2 \rightarrow 0$ ). For the latter category of patients, the proprioceptive information is encoded in joint space only, as for the within-arm tasks. For the patients with inter-hemispheric transformation issues MLP predicts an encoding of the information also in Extra-Joint and Extra-Retinal space.

Equation 13 reports the minimally achievable variability of the motor vector estimation.

$$\begin{aligned}
 \sigma_{\Delta}^2 &= \sigma_{J_r}^2 + \sigma_{J_l}^2 + \frac{2\sigma_{J_r \leftrightarrow l}^2 \sigma_{J_r \rightarrow ExJ}^2 (\sigma_{J \rightarrow R}^2 + \sigma_{R \rightarrow ExR}^2)}{(\sigma_{J \rightarrow R}^2 + \sigma_{R \rightarrow ExR}^2)(\sigma_{J \rightarrow ExJ}^2 + \sigma_{J_r \leftrightarrow l}^2) + \sigma_{J \rightarrow ExJ}^2 \sigma_{J_r \leftrightarrow l}^2} \\
 &\rightarrow \sigma_{J_r}^2 + \sigma_{J_l}^2
 \end{aligned}
 \tag{13}$$

In healthy subjects or in patients without inter-hemispheric transformation problems ( $\sigma_{J_r \leftrightarrow l}^2 \rightarrow 0$ ), **Figure 4C** and Eq. 13 suggest that the sensory weighting and the motor vector

variance tend to those predicted for the W-AP tasks (Figure 4A and Eq. 9): encoding of the information in joint space only and minimal variability of the responses. This prediction is consistent with the experimentally observed similarities between the performances in sB-AP and W-AP tasks for healthy subjects (Tagliabue and McIntyre, 2013; Arnoux et al., 2017) and with the performances of some stroke patients (Herter et al., 2019).

The MLP prediction for stroke patients with a difficulty to compare joint signals from the affected to the less-affected side ( $\sigma_{J \leftrightarrow I}^2 > 0$ ) appears to provide some interesting insight into the patient's deterioration of performances in the Mirror Position Test, with respect to the Within-arm Position Test (Gurari et al., 2017) discussed in section "Upper Limb Proprioceptive Deficits Post-stroke." Equation 13 shows that the increased variability in the mirror task can be correctly predicted if the noise associated with the inter-hemispheric comparison of the joint signals ( $\sigma_{J \leftrightarrow I}^2$ ) is significantly larger than that for healthy patients. In other words, lower performances in patients assessed by the Mirror Position Test could be due to a problem in the neural inter-hemispheric processing and not due to a proprioceptive problem *per se*.

### Cross-Modal Tasks (C-M<sub>P</sub>)

Contrary to the other categories of tasks, C-M<sub>P</sub> tasks involve a visually memorized target which the patient has to match with the eyes closed (Figure 4D). In these tasks no direct comparison is possible between the target and effector. Thus, cross-reference transformations are strictly necessary. The variability associated with the four concurrent comparisons is:

$$\begin{aligned} \sigma_{\Delta J}^2 &= \sigma_R^2 + \sigma_{R \rightarrow J}^2 + \sigma_J^2 \\ \sigma_{\Delta ExJ}^2 &= \sigma_R^2 + \sigma_{R \rightarrow J}^2 + \sigma_{J \rightarrow ExJ}^2 + \sigma_J^2 + \sigma_{J \rightarrow ExJ}^2 \\ \sigma_{\Delta R}^2 &= \sigma_R^2 + \sigma_J^2 + \sigma_{J \rightarrow R}^2 \\ \sigma_{\Delta ExR}^2 &= \sigma_R^2 + \sigma_{R \rightarrow ExR}^2 + \sigma_J^2 + \sigma_{J \rightarrow R}^2 + \sigma_{R \rightarrow ExR}^2 \end{aligned} \tag{14}$$

$\sigma_R^2$  refers to the variability associated with the retinal inputs of the target location. If we assume that the noise associated with the transformation of the sensory signals from retinal to joint space and from joint to retinal space are similar ( $\sigma_{R \rightarrow J}^2 = \sigma_{J \rightarrow R}^2 = \sigma_{J \leftrightarrow R}^2$ ), then the sensory weights predicted by the MLP are those represented in Figure 4D and the corresponding minimal variance of the estimated movement vector  $\Delta$  is:

$$\sigma_{\Delta}^2 = \sigma_J^2 + \sigma_R^2 + \frac{\sigma_{J \leftrightarrow R}^2}{2} \tag{15}$$

It follows that degraded performances of stroke patients when performing this category of tasks could be due, not only to a noisy proprioceptive system, but also to difficulties in the encoding of retinal information in joint space or, vice-versa, proprioceptive information in a retinal reference.

## Application of the Optimal Sensory Integration Theory to Visual Compensation Tests

The MLP also renders predictions for the visual compensation tests in which stroke patients can use visual feedback to perform the tasks. In the following we will apply the Concurrent Model to the execution of the same four categories of tasks analyzed in the previous section (W-A, aB-A, sB-A, and C-M) but including the availability of visual information about both target and effector position.  $\sigma_R^2$  will be used to refer to the variability associated with the retinal inputs of both target and effector locations.

### Within-Arm Visuo-Proprioceptive Tasks (W-A<sub>VP</sub>)

Equations 16 represent the variance associated with the four concurrent comparisons for the within-arm tasks using both proprioceptive and visual information.

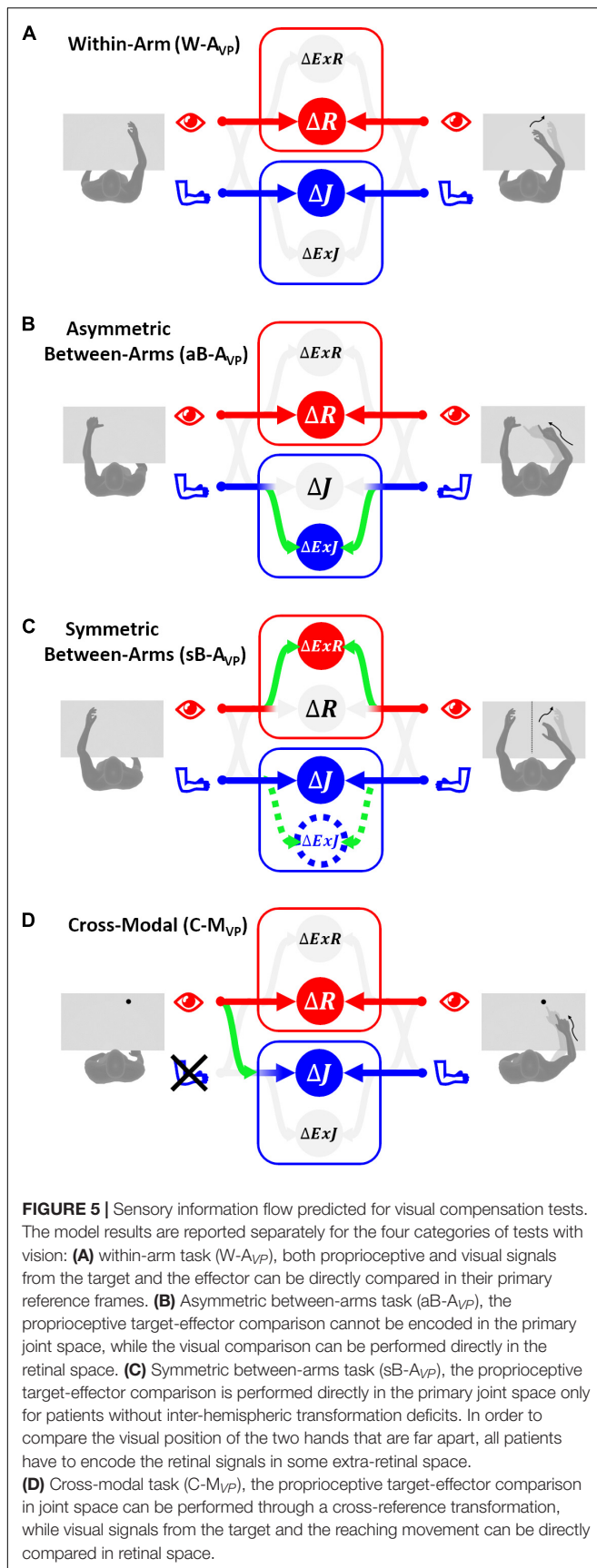
$$\begin{aligned} \sigma_{\Delta J}^2 &= \sigma_J^2 + \sigma_J^2 \\ \sigma_{\Delta ExJ}^2 &= \sigma_J^2 + \sigma_{J \rightarrow ExJ}^2 + \sigma_J^2 + \sigma_{J \rightarrow ExJ}^2 \\ \sigma_{\Delta R}^2 &= \sigma_R^2 + \sigma_R^2 \\ \sigma_{\Delta ExR}^2 &= \sigma_R^2 + \sigma_{R \rightarrow ExR}^2 + \sigma_R^2 + \sigma_{R \rightarrow ExR}^2 \end{aligned} \tag{16}$$

The first two equations, representing the proprioceptive comparison in Joint and Extra-Joint space, are identical to those reported for the W-AP tasks in Eq. 8. The last two equations represent the visual comparison in Retinal and Extra-Retinal space. The target and effector images on the retina can be compared directly. Therefore, the variability of the retinal comparison,  $\sigma_{\Delta R}^2$ , simply corresponds to the sum of the variability of the retinal information about the target and the effector position. The visual extra-retinal comparison,  $\Delta ExR$ , on the other hand, must include the terms  $\sigma_{R \rightarrow ExR}^2$ , associated with the transformation from the retina to the extra-retinal reference frame.

As shown in Figure 5A, MLP predicts that for the W-A<sub>VP</sub> task there would be no sensory encoding in extra-joint or extra-retinal reference. This is due to the fact that, for both visual and proprioceptive modality, the information can be directly compared in the reference frame corresponding to the originating sensory system. The retinal and joint comparisons are weighted as predicted by the standard MLP formulation (Eq. 3), taking into account only the relative variance of the available sources of information (Ernst and Banks, 2002). The variability of the estimation of the movement vector  $\Delta$  corresponding to this optimal sensory weighting is:

$$\sigma_{\Delta}^2 = \frac{2\sigma_J^2\sigma_R^2}{\sigma_J^2 + \sigma_R^2} \tag{17}$$

The comparison of these results with the corresponding prediction for the proprioceptive task (Eq. 9) suggests that patients should be able to visually compensate in this category of tasks, independently from their ability to perform cross-reference transformations:  $\frac{2\sigma_J^2\sigma_R^2}{\sigma_J^2 + \sigma_R^2}$  is always smaller than  $2\sigma_J^2$



and this difference is not affected by the variance of the sensory transformations reported in Eq. 16. This comparison also shows that, the stronger the proprioceptive deficit, the larger will be the advantage provided by using visual information. This prediction is consistent with the observation that stroke patients can compensate through vision for their proprioceptive deficits in this type of tasks (Torre et al., 2013).

### Asymmetric Between-Arms Visuo-Proprioceptive Tasks (aB-A<sub>VP</sub>)

In these tasks, as previously explained for the aB-A<sub>P</sub> tests, a direct comparison between the proprioceptive information in joint space is not possible ( $\sigma_{J_l \leftrightarrow r}^2 \rightarrow \infty$ ). On the other hand, target and effector can be compared directly in retinal coordinates because the task achievement corresponds to the matching of their respective positions on the retina. As a consequence, the concurrent comparison for these tasks are associated with the following variances:

$$\begin{aligned}\sigma_{\Delta J}^2 &= \sigma_{J_l}^2 + \sigma_{J_l \rightarrow r}^2 + \sigma_{J_r}^2 + \sigma_{J_r \rightarrow l}^2 \\ \sigma_{\Delta ExJ}^2 &= \sigma_{J_l}^2 + \sigma_{J_l \rightarrow ExJ}^2 + \sigma_{J_r}^2 + \sigma_{J_r \rightarrow ExJ}^2 \\ \sigma_{\Delta R}^2 &= \sigma_R^2 + \sigma_R^2 \\ \sigma_{\Delta ExR}^2 &= \sigma_R^2 + \sigma_{R \rightarrow ExR}^2 + \sigma_R^2 + \sigma_{R \rightarrow ExR}^2\end{aligned}\quad (18)$$

Figure 5B shows that the sensory information flow corresponding to the minimal variability of the aB-A<sub>VP</sub> task consists, theoretically, in the encoding of proprioceptive information in extra-joint spaces, while visual information is directly encoded in retinal space. Proprioceptive information is not encoded in the joint reference frame, because, as discussed for the corresponding proprioceptive task aB-A<sub>P</sub>, the comparison in the joint space is not possible. The visual information is not encoded in extra-retinal references, because, although  $\Delta ExR$  would be theoretically possible, it would fully covary with  $\Delta R$ . In other words, the extra-retinal encoding would not provide any additional information over the retinal encoding, and would not contribute to reduce the variance of the motor vector estimate, which is given in Eq. 19.

$$\sigma_{\Delta}^2 \rightarrow \frac{2\sigma_R^2(\sigma_{J_r}^2 + \sigma_{J_l}^2 + 2\sigma_{J_r \rightarrow ExJ}^2)}{\sigma_{J_r}^2 + \sigma_{J_l}^2 + 2\sigma_{J_r \rightarrow ExJ}^2 + 2\sigma_R^2}\quad (19)$$

The comparison of this result with the one obtained in Eq. 11 for the corresponding proprioceptive task aB-A<sub>P</sub> (see the **Supplementary Section 4**), shows that in normal conditions the noisiness of the motor vector estimation in the visuo-proprioceptive task is always smaller than for the proprioceptive task. Thus, MLP predicts for this kind of asymmetric tasks that the patients should be able to compensate their proprioceptive deficits by using vision, consistent with experimental observations (Scalha et al., 2011).

## Symmetric Between-Arms Visuo-Proprioceptive Tasks (sB-A<sub>VP</sub>)

For these tasks, the considerations about inter-hemispheric transfer of joint signals presented for the corresponding proprioceptive tasks (sB-A<sub>P</sub>) remain valid: the value of the  $\sigma_{J_{r \leftrightarrow l}}^2$  parameter allows distinguishing patients with problems in comparing joint information from the two arms ( $\sigma_{J_{r \leftrightarrow l}}^2 > 0$ ) from healthy subjects and patients not showing this deficit ( $\sigma_{J_{r \leftrightarrow l}}^2 \rightarrow 0$ ). The considerations about the impossibility of performing the task by directly comparing the visual feedback about the target and the effector ( $\sigma_{R, Mir}^2 \rightarrow \infty$ ) also remain valid.

Equations 20, which describe the variability associated with the four concurrent comparisons for this type of tasks, differ from the analogous equations of the proprioceptive sB-A<sub>P</sub> task (Eq. 12), simply by the fact that  $\Delta R$  and  $\Delta ExR$  are computed from the available retinal information ( $R$ ) and not through cross-reference transformations of proprioceptive signals ( $J \rightarrow R$ ).

$$\begin{aligned}\sigma_{\Delta J}^2 &= \sigma_{J_l}^2 + \sigma_{J_l \rightarrow r}^2 + \sigma_{J_r}^2 + \sigma_{J_r \rightarrow l}^2 \\ \sigma_{\Delta ExJ}^2 &= \sigma_{J_l}^2 + \sigma_{J_l \rightarrow ExJ}^2 + \sigma_{J_r}^2 + \sigma_{J_r \rightarrow ExJ}^2 \\ \sigma_{\Delta R}^2 &= \sigma_R^2 + \sigma_{R \rightarrow J}^2 + \sigma_{R \rightarrow ExR}^2 + \sigma_{R, Mir}^2 \\ \sigma_{\Delta ExR}^2 &= \sigma_R^2 + \sigma_{R \rightarrow ExR}^2 + \sigma_{R \rightarrow J}^2 + \sigma_{R \rightarrow ExJ}^2\end{aligned}\quad (20)$$

The optimal weights associated with the four concurrent target-response comparisons are represented in **Figure 5C**. The predicted sensory information flow is reported for patients both with and without inter-hemispheric transformation deficits. The MLP prediction suggests that to achieve optimal performance stroke patients with problems in comparing joint signals from the two arms should encode proprioceptive information in both joint and extra-joint space, and visual information in extra-retinal space only. Patients without inter-hemispheric communication issues, on the other hand, should encode proprioceptive information in joint space only and visual information in extra-retinal references only.

The variability of the optimal motor vector estimation is shown in Eq. 21. The equation reports, first, the prediction for patients with inter-hemispheric transformation deficits ( $\sigma_{J_{r \leftrightarrow l}}^2 > 0$ ) and then for patients without problems in comparing the sensory information coming from the two arms ( $\sigma_{J_{r \leftrightarrow l}}^2 \rightarrow 0$ ).

$$\begin{aligned}\sigma_{\Delta}^2 &\rightarrow \frac{2(\sigma_R^2 + \sigma_{R \rightarrow ExR}^2)((\sigma_{J_r}^2 + \sigma_{J_l}^2)(\sigma_{J_r \rightarrow ExJ}^2 + \sigma_{J_r \leftrightarrow l}^2) + 2\sigma_{J_r \rightarrow ExJ}^2 \sigma_{J_r \leftrightarrow l}^2)}{(\sigma_{J_r \rightarrow ExJ}^2 + \sigma_{J_r \leftrightarrow l}^2)(\sigma_{J_r}^2 + \sigma_{J_l}^2 + 2\sigma_R^2 + 2\sigma_{R \rightarrow ExR}^2) + 2\sigma_{J_r \rightarrow ExJ}^2 \sigma_{J_r \leftrightarrow l}^2} \\ &\rightarrow \frac{2(\sigma_R^2 + \sigma_{R \rightarrow ExR}^2)(\sigma_{J_r}^2 + \sigma_{J_l}^2)}{(2\sigma_R^2 + 2\sigma_{R \rightarrow ExR}^2) + (\sigma_{J_r}^2 + \sigma_{J_l}^2)}\end{aligned}\quad (21)$$

The comparison of these results with those reported in Eq. 13 for the corresponding proprioceptive task, sB-A<sub>P</sub> (see **Supplementary Section 4** for details) suggests different visual compensation mechanism for the patient with and without inter-hemispheric transformation issues. For patients without problems in comparing joint signals from the two arms, the availability of visual information should result in a direct

reduction of the noisiness of the estimation of the motor vector. For the patients with problems in comparing joint information from the two arms, the possibility to reduce the noise of the motor vector estimate appears to be more limited and to depend on the relative noisiness associated to cross-reference transformations. The inability observed in some stroke patients to use visual information to improve their performances with respect to analogous proprioceptive tasks (Semrau et al., 2018; Herter et al., 2019) could, therefore, be due to difficulties in performing inter-hemispheric and cross-reference transformations.

## Cross-Modal Tasks (C-M<sub>VP</sub>)

As shown in **Figure 5D**, since the target is not perceived proprioceptively, no direct comparison is possible between the target and effector in joint space in this task. Hence a cross-reference transformation ( $\sigma_{R \rightarrow J}^2$ ) would be necessary to make use of the proprioceptive signal on effector position. The variability associated with the four concurrent comparisons is given in Eq. 22.

$$\begin{aligned}\sigma_{\Delta J}^2 &= \sigma_R^2 + \sigma_{R \rightarrow J}^2 + \sigma_J^2 \\ \sigma_{\Delta ExJ}^2 &= \sigma_R^2 + \sigma_{R \rightarrow J}^2 + \sigma_{J \rightarrow ExJ}^2 + \sigma_J^2 + \sigma_{J \rightarrow ExJ}^2 \\ \sigma_{\Delta R}^2 &= \sigma_R^2 + \sigma_{R \rightarrow ExR}^2 + \sigma_{R \rightarrow J}^2 + \sigma_{R \rightarrow ExJ}^2 \\ \sigma_{\Delta ExR}^2 &= \sigma_R^2 + \sigma_{R \rightarrow ExR}^2 + \sigma_{R \rightarrow J}^2 + \sigma_{R \rightarrow ExJ}^2\end{aligned}\quad (22)$$

MLP predicts that the optimal solution for this type of tasks is to encode the proprioceptive and visual information directly in joint and retinal space, respectively. The variance of the estimated movement vector corresponding to this optimal solution is given in Eq. 23.

$$\sigma_{\Delta}^2 = \frac{\sigma_R^2(2\sigma_J^2 + \sigma_R^2 + 2\sigma_{R \rightarrow J}^2)}{\sigma_J^2 + \sigma_{R \rightarrow J}^2 + \sigma_R^2}\quad (23)$$

The comparison between this result and the variability of the movement vector estimation in the corresponding proprioceptive task C-M<sub>P</sub> of Eq. 15 (see **Supplementary Section 4**) shows that, unless visual information is extremely noisy, its availability should lead to a reduction of the variance of  $\Delta$ . It follows that, for this category of task, MLP predicts that the patients should show a clear visual compensation of their proprioceptive deficit. This prediction is in agreement with the visual compensation experimentally observed in stroke patients for this category of tasks (Darling et al., 2008; Scalha et al., 2011).

## REINTERPRETATION OF EXPERIMENTAL OBSERVATIONS ABOUT PROPRIOCEPTIVE DEFICITS AND VISUAL COMPENSATION

After having described the theoretical sensory information flow underlying the four categories of tasks used to test proprioception and visual compensation, we assess the ability of the model to capture the relevant experimental findings described in the first

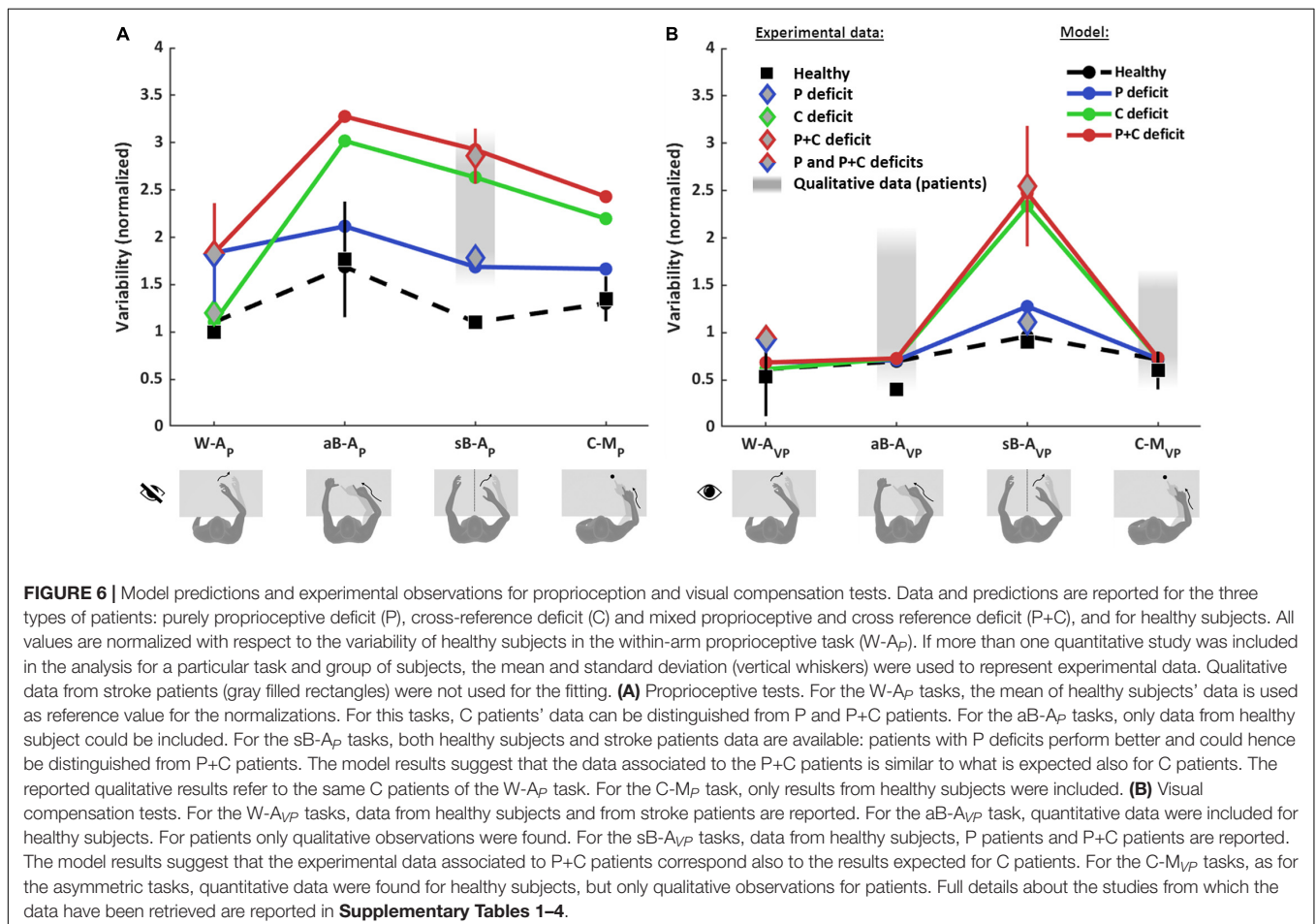
sections. In order to avoid data overfitting, the number of model parameters is reduced to six: the noise of the joint ( $\sigma_J^2$ ) and retinal ( $\sigma_R^2$ ) signals and the noise associated to sensory transformations ( $\sigma_T^2$ ) in healthy subjects; for patients, three terms representing the noise added to the joint signal of the more affected ( $N_{J_m}$ ) and less affected arm ( $N_{J_l}$ ) and to the sensory transformations ( $N_T$ ) due to the deficit of stroke patients.

For this analysis, we will consider three distinct type of patients: P, with proprioceptive deficits only ( $N_{J_m}$  and  $N_{J_l} > 0$  and  $N_T = 0$ ); C, with cross-reference processing deficits only ( $N_{J_m}$   $N_{J_l} = 0$  and  $N_T > 0$ ); and P+C, with combined proprioceptive and cross-reference processing deficits ( $N_{J_m}$ ,  $N_{J_l}$  and  $N_T > 0$ ). In patients of type P, only the noisiness of the proprioceptive joint signals  $\sigma_J^2$  is increased with respect to healthy subjects. For patients of type C, only the noise associated to the sensory transformation ( $\sigma_{R \leftrightarrow J}^2$ ,  $\sigma_{R \rightarrow ExR}^2$ ,  $\sigma_{J \rightarrow ExJ}^2$ ,  $\sigma_{J \leftrightarrow l}^2$ ) is increased with respect to healthy subjects. For patients of type P+C the noise is increased for both proprioception and transformations.

**Figure 6** shows the comparison between the quantitative experimental data found in the literature and the prediction of the MLP model for the four categories of proprioceptive tasks (**Figure 6A**) and for the same four tasks performed using

vision to compensate for proprioceptive deficits (**Figure 6B**). In order to be able to apply the model to the whole dataset, the results from different studies have to be comparable. This was achieved through their normalization with respect to a reference task. To be able to perform the normalization, among the numerous studies that can be found in the literature, only those reporting a quantitative comparison between at least two of the four categories of tasks (W-A, sB-A, aB-A, and C-M) could be included in the dataset. Performance data of healthy subjects were retrieved from Van Beers et al. (1996), Ernst and Banks (2002), Butler et al. (2004), Monaco et al. (2010), Tagliabue and McIntyre (2011), Torre et al. (2013), Khanafer and Cressman (2014), Cameron and López-Moliner (2015), Arnoux et al. (2017), Herter et al. (2019), and Marini et al. (2019) and those of stroke patients from Scalha et al. (2011), Torre et al. (2013), Dos Santos et al. (2015), Contu et al. (2017), Gurari et al. (2017), Rinderknecht et al. (2018), Herter et al. (2019), and Ingemanson et al. (2019). Details about the dataset, the fitting algorithm and the quantification of the obtained results are given in **Supplementary Section 5**.

**Figure 6** shows that the model predicts very different results for healthy subjects and for the three type of patients (P, C, and P+C), depending on the considered task.



For healthy subjects, MLP reproduces well the experimentally observed modulations of the precision among the eight tasks. In particular, the model correctly predicts that the asymmetric test (aB- $A_P$ ) is the least precise (largest variability) among the proprioceptive tasks (**Figure 6A**) and that the symmetric test (sB- $A_{VP}$ ) is the less precise among the tasks using vision (**Figure 6B**).

For stroke patients, the results of **Figure 6A** show that the model seems to capture the different experimental data for the within-arm tasks ( $W-A_P$ ), suggesting that the heterogeneity of the results would be partially explained by differentiating C patients (Gurari et al., 2017) from P and P+C patients (Dos Santos et al., 2015; Contu et al., 2017; Rinderknecht et al., 2018). For the asymmetric tasks (aB- $A_P$ ), the model predicts a very high variability for the C and P+C patients while the increase with respect to the  $W-A_P$  task is moderate for P patients. We do not have, however, experimental data to validate the predictions for the patients in this task. For the sB- $A_P$  task, the model well captures the heterogeneity of the patients' dataset by distinguishing P patients (Herter et al., 2019) from C and P+C patients (Herter et al., 2019; Ingemanson et al., 2019). Interestingly, this classification is consistent with the fact that P patients were able to visually compensate in the sB- $A_{VP}$  task, whereas C and P+C patients were not able to compensate (Herter et al., 2019). The experimental data represented by a red diamond for sB- $A_P$  task were associated with to P+C patients in the fitting procedure, because observations in the literature suggest that P+C patients are more common than C patients. The model prediction suggests, however, that these data could also include C patients. The prediction for the sB- $A_P$  task is also consistent with qualitative observations of Gurari et al. (2017) that the same patients that performed without difficulties the  $W-A_P$  task (classified as C patients) showed significant deficits in a symmetric task. For the cross-modal tasks ( $C-M_P$ ), the model predicts that performances of C and P+C patients would be characterized by a variability significantly larger than that of P patients, similarly to the sB- $A_P$  task.

Concerning the patients' ability to visually compensate for their proprioceptive deficits (**Figure 6B**), the model predicts that in the  $W-A_{VP}$  task all three types of patients (P, C and P+C) should be able to use visual information to improve performance to that of healthy subjects. This prediction is consistent with the experimental observation of Torre et al. (2013) that stroke patients can fully compensate with vision when performing this kind of task, where the information about the target and the effector could be compared directly in both joint and retinal space. For the aB- $A_{VP}$  tasks, the model predicts the same full visual compensation as for the within-arm task. Although we could not find any quantitative experimental results for patients in this type of tasks, the model prediction is coherent with the qualitative observation of Scilha et al. (2011) that patients can significantly improve their performances with vision. For the sB- $A_{VP}$  tasks, the model prediction is very different from the other tasks and it matches the different results obtained by Herter et al. (2019) for patients with low and high levels of visual compensation. The model predictions for this task suggests that the group of patients showing low

visual compensation (higher variability) could confound C and P+C patients, although the patients with the ability to visually compensate (lower variability) are probably of type P. For this task, as for the corresponding proprioceptive test sB- $A_P$ , the model prediction suggests that the experimental data point represented by a red diamond could confound C and P+C patients. For the  $C-M_{VP}$  tasks, the same considerations apply as for the aB- $A_{VP}$  task, in terms of model predictions and of matching with qualitative observations.

Altogether, these results suggest that only the  $W-A_P$  tasks can be considered as "pure proprioception tests." This expression here refers to those tests whose outcome is affected only by deficits of the proprioceptive system, and not by other factors, such as the inability to perform sensory transformations. In contrast, sB- $A_P$ , aB- $A_P$ , and  $C-M_P$  tasks appear to confound proprioceptive deficits and cross-reference transformation deficits, since they are affected by P, C, or P+C deficits. These results also suggest that the visual compensation tests for sB- $A_{VP}$  tasks can assess the patients' ability to perform cross-reference transformations. The reinterpretation of the data of the literature through the MLP framework represented in **Figure 6** additionally suggests that most of the tested stroke patients have mixed P+C deficits (Dos Santos et al., 2015; Contu et al., 2017; Rinderknecht et al., 2018; Herter et al., 2019), but that there are also clear examples of C (Gurari et al., 2017) and P (Herter et al., 2019) categories of patients.

In conclusion, the proposed stratification of patients presented here based on their deficits (P, C, and P+C) appears to be able to explain, and at least partially reconcile, the different outcomes experimentally obtained with various assessments currently in use in clinical research.

## INSIGHTS FROM BRAIN LESIONS AND FUNCTIONAL ANATOMY STUDIES

The neural network responsible for proprioceptive processing seems widely distributed over cortical and subcortical structures (Ben-Shabat et al., 2015; Kessner et al., 2016; Semrau et al., 2018). Beyond the integrity of S1, with a clear impact on proprioception, neural correlates of proprioceptive deficits after stroke remain incompletely understood (Ingemanson et al., 2019). Moreover, no study has yet been undertaken to stratify stroke patients according to the categorization of deficits described in the previous section. However, to probe the clinical potential of this approach we present here a short non-systematic review on brain structures involved in either "pure" proprioceptive perception or cross-reference processing. To that end, we reviewed studies that used functional imaging (fMRI, PET, and EEG after a non-systematic PubMed screening) during proprioceptive and visuo-proprioceptive tasks, as well as imaging-based lesion-symptom mapping (LSM) studies. This should provide a first approximative view on whether brain areas may potentially be dissociated as a function of their involvement in proprioceptive processing according to the described task affordances.

However, there is a caveat: as discussed in the previous section, most stroke patients likely have mixed deficits affecting both

proprioception and cross-reference processing. Since a mixed deficit would alter the patients' performances in all task categories (Figure 6), only a dedicated protocol would allow dissociating the structures specifically involved in tasks requiring cross-reference processing or not. Unsurprisingly, cortical networks seemed to overlap to a large extent among the reviewed articles, and proprioceptive test categorization did not provide a clear dissociation between the cortical areas activated during tests belonging to one or the other category.

In addition to S1, a number of regions within the posterior parietal cortex (PPC) were identified as critical for proprioceptive perception, assessed with either a W- $A_P$  (Rinderknecht et al., 2018; Kessner et al., 2019) task or a sB- $A_P$  task (Dukelow et al., 2010; Findlater et al., 2016, 2018; Meyer et al., 2016). But the lack of between-task comparisons does not allow for a distinction between the lesions sites affecting primarily the proprioceptive sense *per se* or cross-reference processing. Furthermore, based on these results we cannot conclude whether hemispheric dominance may be related to either proprioception or cross-reference processing.

A comparative approach with different types of tasks is needed to elucidate the sensory deficit and to eventually associate a given sensory deficit to particular brain regions. Unless the study assesses and compares different tasks (Semrau et al., 2018; Herter et al., 2019), or uses functional imaging (Van de Winckel et al., 2012; Ben-Shabat et al., 2015), we cannot draw clear conclusions on which brain areas are important for either sensory function.

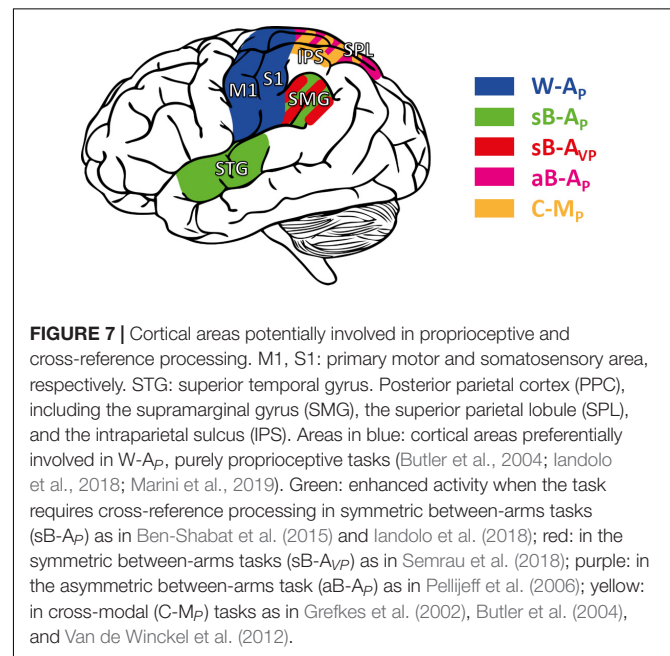
According to the presented MLP predictions, we consider W- $A_P$  assessments to be “purely” proprioceptive (Figure 4A) in contrast to assessments which involve cross-reference processing (aB- $A_P$ , sB- $A_P$ , C- $M_P$ : see Figures 4B–D). We therefore attempted to classify the reviewed functional brain imaging studies accordingly and to probe whether this categorization might result in a processing-specific topological cerebral organization.

“Pure” proprioceptive processing, assessed with a W- $A_P$  tasks seemed to entail primarily the activation of M1 and S1 (Butler et al., 2004; Marini et al., 2019). W- $A_P$  (Figure 4A) tasks, the simplest tasks in terms of computational load (see section “Application of the Optimal Sensory Integration Theory to Proprioception Assessment Tests”), are presumably based on simpler networks. In contrast, the mirror task (a sB- $A_P$  task) seem to involve cross-reference processing. And fMRI revealed that a larger brain network was involved compared to W- $A_P$  tasks, with higher activation of the supramarginal gyrus (SMG) and superior temporal gyrus (STG) (Iandolo et al., 2018), in line with Ben-Shabat et al. (2015). In theory, the same mirror task with visual feedback also involves cross-reference processing (sB- $A_{VP}$ : Figure 5C). An LSM study showed that patients with lesions to the SMG did not improve their performance when adding visual feedback in the mirror test (sB- $A_P$  vs. sB- $A_{VP}$ ), a result presumably related to cross-reference processing deficit (Semrau et al., 2018). Patients that improved to normal performance with vision, i.e., presumably patients with “pure” proprioceptive deficit (Figure 6), had smaller lesions that primarily affected white-matter tracts carrying proprioceptive information rather than lesions in parietal association areas

(Semrau et al., 2018). This result is therefore consistent with a specific role of the parietal association areas in cross-reference processing.

Other proprioceptive tasks such as aB- $A_P$  and C- $M_P$ , known for the visual encoding of proprioceptive information requiring cross-reference transformations, have also been associated to parietal activation. Pellijeff et al. (2006) showed that the fMRI response was specifically enhanced in the superior parietal lobule (SPL) and Precuneus (medial part of the PPC) in a thumb and chin pointing task requiring an update of the limb posture to achieve the task. Similarly, using PET, Butler et al. (2004) showed a greater activity in the SPL in the C- $M_P$  reaching task. Within the PPC, Grefkes et al. (2002) showed that the activity in the anterior intraparietal sulcus (IPS) was specifically enhanced during tactile object recognition. This task, requiring cross-modal visuo-tactile information transfer, involved the anterior IPS in stroke patients (Van de Winckel et al., 2012).

Overall, these studies tended to show that “pure” proprioceptive processing involves mainly S1, whereas cross-reference processing recruits specifically the parietal associative cortex. Figure 7 shows the main trends for task-specific involvement that might be read out as: (i) Tasks excluding visual inputs and that do not require cross-reference processing (W- $A_P$ ) showed a trend for activating preferentially anterior parietal areas (M1, S1). (ii) Tasks excluding visual inputs but requiring cross-reference processing (sB- $A_P$ ), or for which visual processing requires cross-reference transformations (sB- $A_{VP}$ ), seemed to entail additional activation of superior temporal and inferior-lateral PPC areas. (iii) Tasks that impose cross-modal processing, for which a visual encoding of the proprioceptive information has been reported in healthy subjects (aB- $A_P$ , C- $M_P$ : Tagliabue and McIntyre, 2011, 2013), tended to activate the superior-medial PPC areas. There might thus be a gradient



within PPC from inferior-lateral to more superior-medial activation with increasing cross-reference processing demands.

## DISCUSSION

Here, we present a reinterpretation of proprioceptive post-stroke deficits affecting manual control, and of the ability of patients to compensate for these deficits using vision. This theoretical analysis uses the MLP (Ernst and Banks, 2002) and a new formulation of the “Concurrent Model” for multi-sensory integration (Tagliabue and McIntyre, 2011, 2014). The rationale for this work hinges on the conceptual approach that the sensory space in which the information is encoded is not limited to the sensory system from which the signal originates. This concept is supported by evidence that retinal encoding of purely proprioceptive task-contingent stimuli (i.e., in absence of vision) occurs in some pointing tasks (Pouget et al., 2002; Sarlegna and Sainburg, 2007; McGuire and Sabes, 2009; Jones and Henriques, 2010; Tagliabue and McIntyre, 2013; Arnoux et al., 2017). Hence, it is questionable whether some tasks, traditionally classified as being proprioceptive, can be considered as relying on proprioceptive processing only. Moreover, there is evidence that the efficacy of visual compensation is task-dependent (Scalha et al., 2011; Torre et al., 2013; Semrau et al., 2018; Herter et al., 2019). Therefore, it is also questionable whether different visual compensation tasks imply similar sensory processing.

### A Useful Categorization of Proprioceptive Assessments

Applying this concept to clinical proprioceptive deficits and visual compensation tests, we attempt to dissociate purely proprioceptive deficits from those affecting cross-reference processing. We were able to show that tasks described as proprioceptive in clinical practice are likely to involve cross-reference processing. As a consequence, task performances in patients may not specifically depend on a strictly proprioceptive deficit, but may also depend on deficits in performing cross-reference transformations. Clinical and nonclinical methods as well as tasks that assess proprioceptive function and visual compensation have been reviewed and compared through this new conceptual framework. This process led to a new classification of methods for proprioceptive assessments into four categories, which differ by the requirement of performing a task by encoding the information directly in the reference frame associated with sensory receptors: proprioceptive (joint) space and visual (retinal) spaces, respectively. In the first category both visual and proprioceptive information can be encoded in the primary sensory space. The second category includes those tasks in which visual, but not proprioceptive, information can be encoded in the primary sensory space. In the tasks of the third category, proprioceptive, but not visual, information can be encoded in the primary sensory space. The tasks of the fourth category require encoding in non-primary sensory space for both proprioception and vision.

The present analysis suggests that only assessments using a within-arm task represent a “pure” proprioceptive test,

because their execution does not require any cross-reference transformation of proprioceptive information. On the contrary, tasks including a between-arms condition, and in particular those that are asymmetric with respect to the body-midline, likely require cross-reference transformations, among which a reconstruction of the task in visual space. As a consequence, these tests do not specifically assess proprioceptive integrity *per se*, but also the ability to perform sensory transformations. Lesion-symptom and functional imaging studies support this hypothesis (Grefkes et al., 2002; Butler et al., 2004; Pellijeff et al., 2006; Van de Winckel et al., 2012; Ben-Shabat et al., 2015; Iandolo et al., 2018; Semrau et al., 2018). The neural network involved in between-arms tasks is wider compared to the network involved in simpler, within-arm, proprioceptive tasks (Ben-Shabat et al., 2015; Iandolo et al., 2018) and includes the PPC which is known to be involved in cross-modal processing (Grefkes et al., 2002; Yau et al., 2015). Moreover, the use of visual information in between-arms mirror (symmetric) tasks might be dependent on the ability to perform cross-reference transformations (Semrau et al., 2018; Herter et al., 2019). Hence, the common practice in neurorehabilitation, to encourage the use of vision for guiding limb movements post-stroke (Pumpa et al., 2015), might be effective when using only one arm or a between-arms asymmetric configuration, but not in the mirror configuration, unless the target is on the body midline (Torre et al., 2013). Since activities of daily living usually involve objects (e.g., grasping), visual feedback on hand position and orientation can often be used to compensate for proprioceptive deficits, as previously suggested (Scalha et al., 2011).

### An Enhanced Patient Stratification

According to the present reasoning, the commonly interpreted proprioceptive deficits might often encompass a larger and in part multi-modal spectrum of dysfunctions. Taking cross-reference processing into account in the assessment may potentially provide a more detailed patient stratification. The deficits may be reclassified into three distinct categories: (P) pure proprioceptive deficits, (C) pure cross-reference processing deficits, and (P+C) mixed proprioceptive and cross-reference processing deficit. **Table 2** lists the expected test performance as a function of assessment type and deficit category: although no single test can potentially differentiate these three clinical groups, the different combination of these tests could.

This model has limits, since it focuses on stroke deficits in terms of sensory processing. Other factors can interfere with post-stroke performance in the different type of assessments, which are not taken into account by our model, such as age, hand dominance, target memorization, task workspace (Goble, 2010), active or passive reaching (Gurari et al., 2017), position or movement sense (Semrau et al., 2019). However, it provides a framework which reconciles apparently contradictory results from proprioceptive assessments (Torre et al., 2013; Dos Santos et al., 2015; Contu et al., 2017; Gurari et al., 2017; Rinderknecht et al., 2018; Herter et al., 2019; Ingemanson et al., 2019) and from visual compensation tests (Darling et al., 2008; Scalha et al., 2011; Torre et al., 2013; Semrau et al., 2018; Herter et al., 2019),

and it adequately predicts tendencies which fit experimental data (Figure 6).

According to the predicted effect of the three type of deficits (P, C, and P+C) on the tests results (Table 2 and Figure 6), the best candidates for stratifying patients, among the assessments that are currently used, would be the combined use of the W- $A_P$  task (eyes closed) and a sB- $A_{VP}$  task (mirror, with visual feedback). Together, these two complementary assessments may help to better stratify patients. In addition to these two methods, adding visual feedback in common proprioceptive tasks (Scalha et al., 2011; Torre et al., 2013; Semrau et al., 2018; Herter et al., 2019; Marini et al., 2019), or using graphesthesia, shape or length discrimination (Van de Winckel et al., 2012; De Diego et al., 2013; Turville et al., 2017) or reaching to visual targets with the unseen hand (Tagliabue and McIntyre, 2011; Elangovan et al., 2019) could help to further explore the complexity of sensorimotor deficits. In the future, to help explore this complexity, robot-assisted tests may enter clinical routine: the tasks are relatively easy and rapid, and 2D robotic manipulators are affordable (Contu et al., 2017; Rinderknecht et al., 2018). Moreover, robotic devices can overcome major limits of current clinical assessment: a quantitative measurement, without ceiling or floor effect, allowing for a more reliable, precise and reproducible evaluation of proprioceptive deficits (Dukelow et al., 2010; Lambercy et al., 2011; Simo et al., 2014; Dos Santos et al., 2015; Contu et al., 2017; Semrau et al., 2017; Deblock-Bellamy et al., 2018; Rinderknecht et al., 2018; Ingemanson et al., 2019).

The proposed stratification of patients may also provide insights about the neural correlates. We would expect that lesions of different brain areas would correspond to the three

different categories of deficits. Hypothetically, and informed by the reviewed brain-mapping literature, injury affecting S1 may primarily relate to purely proprioceptive deficits, whereas lesions in the PPC and STG may cause deficits in the ability of performing cross-reference transformations. Patients with mixed deficits would likely tend to have larger lesions affecting both proprioceptive and associative areas. Further lesion-symptom studies examining the correlation of brain lesions in different categories of tasks may offer better identification of brain structures in relation to proprioception or cross-reference processing.

## Application for a More Personalized Rehabilitation Approach

A more accurate stratification of post-stroke patients suffering from proprioceptive deficits should be relevant also for rehabilitation protocols. Given that sensory recovery is a predictor for motor and functional recovery (Bolognini et al., 2016), training of proprioception and cross-reference processing may be key to improve recovery. Currently the effectiveness of sensory rehabilitation is rather weak (Doyle et al., 2010; Findlater and Dukelow, 2017), in part due to heterogeneity in interventions, in outcomes measures (Doyle et al., 2010), and in the precision and reliability of the assessment (Findlater and Dukelow, 2017). A more accurate diagnostic stratification would potentially allow for sensory rehabilitation interventions targeting either proprioception alone, cross-reference processing alone, or both of them; although this would need validation. Adequate training needs to match the symptoms: training restricted to the proprioceptive modality may not address dysfunction in cross-modal processing, and vice versa. Table 3 summarizes hypothetical treatment options based on the present novel stratification of patients with specific deficits. A more accurate assessment of the different sensory functions could also provide a better assessment of the progress made during rehabilitation.

## CONCLUSION

Proprioception is a prerequisite for normal hand function, in particular for reaching, grasping and object manipulation. Using a theoretical approach, based on statistical models of optimal multi-sensory integration, we have reinterpreted post-stroke proprioceptive deficits, as well as the ability of patients to visually compensate for their deficit. The present analyses highlight that proprioceptive control of the hand may be largely affected by the inability to perform cross-reference transformations, that is to process proprioceptive information in order to encode it, not only in joint space, but also in alternative (often visual) reference frames. This finding allowed us to propose an improved classification of post-stroke deficits, which distinguishes between deficits of the proprioceptive system *per se*, deficits of cross-reference processing, and the combined deficits of the former two. This distinction could lead to a new stratification of stroke patients and may result in more personalized rehabilitation plans.

**TABLE 2** | Tasks for which the model predicts an impairment (X) depending on the type of deficit present in patients: (P) deficit of purely proprioceptive origin, (C) cross-reference transformation deficit only, and (C+P) combined deficits.

|              | P | C | P+C |
|--------------|---|---|-----|
| W- $A_P$     | X |   | X   |
| W- $A_{VP}$  |   |   |     |
| aB- $A_P$    | X | X | X   |
| aB- $A_{VP}$ |   |   |     |
| sB- $A_P$    | X | X | X   |
| sB- $A_{VP}$ |   | X | X   |
| C- $M_P$     | X | X | X   |
| C- $M_{VP}$  |   |   |     |

**TABLE 3** | Possible strategies for differential rehabilitation methods depending on the observed sensory deficit: proprioceptive (P), cross-reference (C), and combined (P+C) deficits.

|   | P | C | P+C |
|---|---|---|-----|
| Proprioceptive, within-arm training             | X |   | X   |
| Proprioceptive, between-arm training            |   | X | X   |
| Cross-modal training                            |   | X | X   |
| Visual compensation (matching spatial location) | X | X | X   |
| Visual compensation (mirror configuration)      | X |   |     |

Xs identify appropriate rehabilitation methods.

## DATA AVAILABILITY STATEMENT

The manuscript presents only experimental data from the literature. All datasets generated for this study are included in the article/**Supplementary Material**, further inquiries can be directed to the corresponding author/s.

## AUTHOR CONTRIBUTIONS

MT conceptualized the topic of the manuscript. JB-E wrote the initial draft of the manuscript and prepared the figures. All authors contributed to writing the manuscript, and read and approved the submitted version.

## FUNDING

JB-E was supported by a Ph.D. fellowship of the École Doctorale Cerveau-Cognition-Comportement (ED3C,

## REFERENCES

- Arnoux, L., Fromentin, S., Farotto, D., Beranek, M., McIntyre, J., and Tagliabue, M. (2017). The visual encoding of purely proprioceptive intermanual tasks is due to the need of transforming joint signals, not to their interhemispheric transfer. *J. Neurophysiol.* 118, 1598–1608. doi: 10.1152/jn.00140.2017
- Ben-Shabat, E., Matyas, T. A., Pell, G. S., Brodtmann, A., and Carey, L. M. (2015). The right supramarginal gyrus is important for proprioception in healthy and stroke-affected participants: a functional mri study. *Front. Neurol.* 6:248. doi: 10.3389/fneur.2015.00248
- Birchenaill, J., Térémetz, M., Roca, P., Lamy, J. C., Oppenheim, C., Maier, M. A., et al. (2019). Individual recovery profiles of manual dexterity, and relation to corticospinal lesion load and excitability after stroke – a longitudinal pilot study. *Neurophysiol. Clin.* 49, 149–164. doi: 10.1016/j.neucli.2018.10.065
- Bolognini, N., Russo, C., and Edwards, D. J. (2016). The sensory side of post-stroke motor rehabilitation. *Restor. Neurol. Neurosci.* 34, 571–586. doi: 10.3233/RNN-150606
- Burns, J. K., and Blohm, G. (2010). Multi-sensory weights depend on contextual noise in reference frame transformations. *Front. Hum. Neurosci.* 4:221. doi: 10.3389/fnhum.2010.00221
- Butler, A. J., Fink, G. R., Dohle, C., Wunderlich, G., Tellmann, L., Seitz, R. J., et al. (2004). Neural mechanisms underlying reaching for remembered targets cued kinesthetically or visually in left or right hemispace. *Hum. Brain Mapp.* 21, 165–177. doi: 10.1002/hbm.20001
- Cameron, B. D., and López-Moliner, J. (2015). Target modality affects visually guided online control of reaching. *Vision Res.* 110, 233–243. doi: 10.1016/j.visres.2014.06.010
- Carlsson, H., Ekstrand, E., and Brogårdh, C. (2019). Sensory function, measured as active discriminative touch, is associated with dexterity after stroke. *PM R* 11, 821–827. doi: 10.1002/pmrj.12044
- Connell, L. A., Lincoln, N. B., and Radford, K. A. (2008). Somatosensory impairment after stroke: frequency of different deficits and their recovery. *Clin. Rehabil.* 22, 758–767. doi: 10.1177/0269215508090674
- Contu, S., Hussain, A., Kager, S., Budhota, A., Deshmukh, V. A., Kuah, C. W. K., et al. (2017). Proprioceptive assessment in clinical settings: evaluation of joint position sense in upper limb post-stroke using a robotic manipulator, edited by François Tremblay. *PLoS One* 12:e0183257. doi: 10.1371/journal.pone.0183257
- Darling, W. G., Bartelt, R., Pizzimenti, M. A., and Rizzo, M. (2008). Spatial perception errors do not predict pointing errors by individuals with brain lesions. *J. Clin. Exp. Neuropsychol.* 30, 102–119. doi: 10.1080/13803390701249036

n°158, Sorbonne Université and Université de Paris). This work was supported by the *Centre National d'Études Spatiales*, the *Centre National de la Recherche Scientifique* (CNRS), and the *Université de Paris*. This study contributes to the IdEx Université de Paris ANR-18-IDEX-0001.

## ACKNOWLEDGMENTS

We wish to thank Martino Trassinelli, from the Institut des Nanosciences de Paris (CNRS – Sorbonne Université), for the useful discussion about constrained optimization methods.

## SUPPLEMENTARY MATERIAL

The Supplementary Material for this article can be found online at: <https://www.frontiersin.org/articles/10.3389/fnhum.2021.646698/full#supplementary-material>

- De Diego, C., Puig, S., and Navarro, X. (2013). A sensorimotor stimulation program for rehabilitation of chronic stroke patients. *Restor. Neurol. Neurosci.* 31, 361–371. doi: 10.3233/RNN-120250
- De Santis, D., Zenzeri, J., Casadio, M., Masia, L., Riva, A., Morasso, P., et al. (2015). Robot-assisted training of the kinesthetic sense: enhancing proprioception after stroke. *Front. Hum. Neurosci.* 8:1037. doi: 10.3389/fnhum.2014.01037
- Deblock-Bellamy, A., Batcho, C. S., Mercier, C., and Blanchette, A. K. (2018). Quantification of upper limb position sense using an exoskeleton and a virtual reality display. *J. Neuroeng. Rehabil.* 15:24. doi: 10.1186/s12984-018-0367-x
- Dos Santos, G. L., García Salazar, L. F., Lazarin, A. C., and Russo, T. L. (2015). Joint position sense is bilaterally reduced for shoulder abduction and flexion in chronic hemiparetic individuals. *Topics Stroke Rehabil.* 22, 271–280. doi: 10.1179/1074935714Z.00000000014
- Doyle, S., Bennett, S., Fasoli, S. E., and McKenna, K. T. (2010). Interventions for sensory impairment in the upper limb after stroke. *Cochrane Database Syst. Rev.* 2010:CD006331. doi: 10.1002/14651858.CD006331.pub2
- Dukelow, S. P., Herter, T. M., Bagg, S. D., and Scott, S. H. (2012). The independence of deficits in position sense and visually guided reaching following stroke. *J. Neuroeng. Rehabil.* 9:72. doi: 10.1186/1743-0003-9-72
- Dukelow, S. P., Herter, T. M., Moore, K. D., Demers, M. J., Glasgow, J. I., Bagg, S. D., et al. (2010). Quantitative assessment of limb position sense following stroke. *Neurorehabil. Neural Repair* 24, 178–187. doi: 10.1177/1545968309345267
- Elangovan, N., Yeh, I. L., Holst-Wolf, J., and Konczak, J. (2019). “A robot-assisted sensorimotor training program can improve proprioception and motor function in stroke survivors,” in *Proceedings of the 2019 IEEE 16th International Conference on Rehabilitation Robotics (ICORR)* (Toronto, ON: IEEE), 660–664. doi: 10.1109/ICORR.2019.8779409
- Ernst, M. O., and Banks, M. S. (2002). Humans integrate visual and haptic information in a statistically optimal fashion. *Nature* 415, 429–433. doi: 10.1038/415429a
- Findlater, S. E., Desai, J. A., Semrau, J. A., Kenzie, J. M., Rorden, C., Herter, T. M., et al. (2016). Central Perception of Position Sense Involves a Distributed Neural Network – Evidence from Lesion-Behavior Analyses. *Cortex* 79, 42–56. doi: 10.1016/j.cortex.2016.03.008
- Findlater, S. E., and Dukelow, S. P. (2017). Upper extremity proprioception after stroke: bridging the gap between neuroscience and rehabilitation. *J. Mot. Behav.* 49, 27–34. doi: 10.1080/00222895.2016.1219303
- Findlater, S. E., Hawe, R. L., Semrau, J. A., Kenzie, J. M., Yu, A. Y., Scott, S. H., et al. (2018). Lesion locations associated with persistent proprioceptive impairment in the upper limbs after stroke. *Neuroimage Clin.* 20, 955–971. doi: 10.1016/j.nicl.2018.10.003

- Frenkel-Toledo, S., Fridberg, G., Ofir, S., Bartur, G., Lowenthal-Raz, J., Granot, O., et al. (2019). Lesion location impact on functional recovery of the hemiparetic upper limb." edited by mariella pazzaglia. *PLoS One* 14:e0219738. doi: 10.1371/journal.pone.0219738
- Goble, D. J. (2010). Proprioceptive acuity assessment via joint position matching: from basic science to general practice. *Phys. Ther.* 90, 1176–1184. doi: 10.2522/ptj.20090399
- Grefkes, C., Weiss, P. H., Zilles, K., and Fink, G. R. (2002). Crossmodal processing of object features in human anterior intraparietal cortex: an fmri study implies equivalencies between humans and monkeys. *Neuron* 35, 173–184. doi: 10.1016/s0896-6273(02)00741-9
- Gurari, N., Drogos, J. M., and Dewald, J. P. A. (2017). Individuals with chronic hemiparetic stroke can correctly match forearm positions within a single arm. *Clin. Neurophysiol.* 128, 18–30. doi: 10.1016/j.clinph.2016.10.009
- Herter, T. M., Scott, S. H., and Dukelow, S. P. (2019). Vision does not always help stroke survivors compensate for impaired limb position sense. *J. Neuroeng. Rehabil.* 16:129. doi: 10.1186/s12984-019-0596-7
- Hirayama, K., Fukutake, T., and Kawamura, M. (1999). Thumb localizing test' for detecting a lesion in the posterior column-medial lemniscal system. *J. Neurol. Sci.* 167, 45–49. doi: 10.1016/s0022-510x(99)00136-7
- Iandolo, R., Bellini, A., Saiote, C., Marre, I., Bommarito, G., Oesingmann, N., et al. (2018). Neural correlates of lower limbs proprioception: an fmri study of foot position matching. *Hum. Brain Mapp.* 39, 1929–1944. doi: 10.1002/hbm.23972
- Iandolo, R., Squeri, V., De Santis, D., Giannoni, P., Morasso, P., and Casadio, M. (2014). "Testing proprioception in intrinsic and extrinsic coordinate systems: is there a difference?" in *Proceedings of the 2014 36th Annual International Conference of the IEEE Engineering in Medicine and Biology Society* (Chicago, IL: IEEE), 6961–6964. doi: 10.1109/EMBC.2014.6945229
- Ingemanson, M. L., Rowe, J. R., Chan, V., Riley, J., Wolbrecht, E. T., Reinkensmeyer, D. J., et al. (2019). Neural correlates of passive position finger sense after stroke. *Neurorehabil. Neural Repair* 33, 740–750. doi: 10.1177/1545968319862556
- Jones, S. A. H., and Henriques, D. Y. P. (2010). Memory for proprioceptive and multisensory targets is partially coded relative to gaze. *Neuropsychologia* 48, 3782–3792. doi: 10.1016/j.neuropsychologia.2010.10.001
- Kenzie, J. M., Semrau, J. A., Hill, M. D., Scott, S. H., and Dukelow, S. P. (2017). A composite robotic-based measure of upper limb proprioception. *J. Neuroeng. Rehabil.* 14:114. doi: 10.1186/s12984-017-0329-8
- Kessner, S. S., Bingel, U., and Thomalla, G. (2016). Somatosensory deficits after stroke: a scoping review. *Topics Stroke Rehabil.* 23, 136–146. doi: 10.1080/10749357.2015.1116822
- Kessner, S. S., Schlemm, E., Cheng, B., Bingel, U., Fiehler, J., Gerloff, C., et al. (2019). Somatosensory deficits after ischemic stroke: time course and association with infarct location. *Stroke* 50, 1116–1123. doi: 10.1161/STROKEAHA.118.023750
- Khanafar, S., and Cressman, E. K. (2014). Sensory integration during reaching: the effects of manipulating visual target availability. *Exp. Brain Res.* 232, 3833–3846. doi: 10.1007/s00221-014-4064-0
- Körding, K. P., Beierholm, U., Ma, W. J., Quartz, S., Tenenbaum, J. B., and Shams, L. (2007). Causal inference in multisensory perception." edited by olaf sporns. *PLoS ONE* 2:e943. doi: 10.1371/journal.pone.0000943
- Lambercy, O., Robles, A. J., Kim, Y., and Gassert, R. (2011). "Design of a robotic device for assessment and rehabilitation of hand sensory function," in *Proceedings of the 2011 IEEE International Conference on Rehabilitation Robotics* (Zurich: IEEE), 1–6. doi: 10.1109/ICORR.2011.5975436
- Lanska, D. J., and Kryscio, R. (2000). Thumb localizing test' for detecting a lesion in the posterior column-medial lemniscal system. *J. Neurol. Sci.* 174, 152–154. doi: 10.1016/s0022-510x(99)00321-4
- Lemon, R. N. (2008). Descending pathways in motor control. *Annu. Rev. Neurosci.* 31, 195–218. doi: 10.1146/annurev.neuro.31.060407.125547
- Marini, F., Zenzeri, J., Pippo, V., Morasso, P., and Campus, C. (2019). Neural correlates of proprioceptive upper limb position matching. *Hum. Brain Mapp.* 40, 4813–4826. doi: 10.1002/hbm.24739
- Matsuda, K., Satoh, M., Tabei, K. I., Ueda, Y., Itoh, A., Ishikawa, H., et al. (2019). Subregional heterogeneity of somatosensory dysfunction in the insula. *J. Neurol. Neurosurg. Psychiatry* 90, 957–958. doi: 10.1136/jnnp-2018-319174
- McGuire, L. M. M., and Sabes, P. N. (2009). Sensory transformations and the use of multiple reference frames for reach planning. *Nat. Neurosci.* 12, 1056–1061. doi: 10.1038/nn.2357
- Metzger, J. C., Lambercy, O., Califfi, A., Conti, F. M., and Gassert, R. (2014). Neurocognitive robot-assisted therapy of hand function. *IEEE Trans. Haptics* 7, 140–149. doi: 10.1109/TOH.2013.72
- Meyer, S., De Bruyn, N., Lafosse, C., Van Dijk, M., Michielsens, M., Thijs, L., et al. (2016). Somatosensory impairments in the upper limb poststroke: distribution and association with motor function and visuospatial neglect. *Neurorehabil. Neural Repair* 30, 731–742. doi: 10.1177/1545968315624779
- Meyer, S., Karttunen, A. H., Thijs, V., Feys, H., and Verheyden, G. (2014). How do somatosensory deficits in the arm and hand relate to upper limb impairment, activity, and participation problems after stroke? a systematic review. *Phys. Ther.* 94, 1220–1231. doi: 10.2522/ptj.20130271
- Monaco, S., Króliczak, G., Quinlan, D. J., Fattori, P., Galletti, C., Goodale, M. A., et al. (2010). Contribution of visual and proprioceptive information to the precision of reaching movements. *Exp. Brain Res.* 202, 15–32. doi: 10.1007/s00221-009-2106-9
- Pellijeff, A., Bonilha, L., Morgan, P. S., McKenzie, K., and Jackson, S. R. (2006). Parietal updating of limb posture: an event-related fmri study. *Neuropsychologia* 44, 2685–2690. doi: 10.1016/j.neuropsychologia.2006.01.009
- Pennati, G. V., Plantin, J., Carment, L., Roca, P., Baron, J. C., Pavlova, E., et al. (2020). Recovery and prediction of dynamic precision grip force control after stroke. *Stroke* 51, 944–951. doi: 10.1161/STROKEAHA.119.026205
- Pouget, A., Ducom, J. C., Torri, J., and Bavelier, D. (2002). Multisensory spatial representations in eye-centered coordinates for reaching. *Cognition* 83, B1–B11. doi: 10.1016/S0010-0277(01)00163-9
- Pumpa, L. U., Cahill, L. S., and Carey, L. M. (2015). Somatosensory assessment and treatment after stroke: an evidence-practice gap. *Aust. Occup. Ther. J.* 62, 93–104. doi: 10.1111/1440-1630.12170
- Rand, D. (2018). Proprioception deficits in chronic stroke—upper extremity function and daily living. Edited by Sliman J. Bensmaia. *PLoS One* 13:e0195043. doi: 10.1371/journal.pone.0195043
- Rinderknecht, M. D., Lambercy, O., Raible, V., Büsching, I., Sehle, A., Liepert, J., et al. (2018). Reliability, validity, and clinical feasibility of a rapid and objective assessment of post-stroke deficits in hand proprioception. *J. Neuroeng. Rehabil.* 15:47. doi: 10.1186/s12984-018-0387-6
- Saeyns, W., Vereeck, L., Truijien, S., Lafosse, C., Wuyts, F. P., and Van de Heyning, P. (2012). Influence of sensory loss on the perception of verticality in stroke patients. *Disabil. Rehabil.* 34, 1965–1970. doi: 10.3109/09638288.2012.671883
- Sallés, L., Martín-Casas, P., Gironès, X., Durà, M. J., Lafuente, J. V., and Perfetti, C. (2017). A Neurocognitive approach for recovering upper extremity movement following subacute stroke: a randomized controlled pilot study. *J. Phys. Ther. Sci.* 29, 665–672. doi: 10.1589/jpts.29.665
- Santisteban, L., Térémets, M., Bleton, J. P., Baron, J. C., Maier, M. A., and Lindberg, P. G. (2016). Upper limb outcome measures used in stroke rehabilitation studies: a systematic literature review." edited by françois tremblay. *PLoS One* 11:e0154792. doi: 10.1371/journal.pone.0154792
- Sarlegna, F. R., and Sainburg, R. L. (2007). The effect of target modality on visual and proprioceptive contributions to the control of movement distance. *Exp. Brain Res.* 176, 267–280. doi: 10.1007/s00221-006-0613-5
- Scalha, T. B., Miyasaki, E., Lima, N. M., and Borges, G. (2011). Correlations between motor and sensory functions in upper limb chronic hemiparetics after stroke. *Arq. Neuropsiquiatr.* 69, 624–629. doi: 10.1590/S0004-282X2011000500010
- Semrau, J. A., Herter, T. M., Scott, S. H., and Dukelow, S. P. (2017). Inter-rater reliability of kinesthetic measurements with the kinarm robotic exoskeleton. *J. Neuroeng. Rehabil.* 14:42. doi: 10.1186/s12984-017-0260-z
- Semrau, J. A., Herter, T. M., Scott, S. H., and Dukelow, S. P. (2018). Vision of the upper limb fails to compensate for kinesthetic impairments in subacute stroke. *Cortex* 109, 245–259. doi: 10.1016/j.cortex.2018.09.022
- Semrau, J. A., Herter, T. M., Scott, S. H., and Dukelow, S. P. (2019). Differential loss of position sense and kinesthesia in sub-acute stroke. *Cortex* 121, 414–426. doi: 10.1016/j.cortex.2019.09.013
- Simo, L., Botzer, L., Ghez, C., and Scheidt, R. A. (2014). A robotic test of proprioception within the hemiparetic arm post-stroke. *J. Neuroeng. Rehabil.* 11:77. doi: 10.1186/1743-0003-11-77
- Tagliabue, M., Arnoux, L., and McIntyre, J. (2013). Keep your head on straight: facilitating sensori-motor transformations for eye–hand coordination. *Neuroscience* 248, 88–94. doi: 10.1016/j.neuroscience.2013.05.051

- Tagliabue, M., and McIntyre, J. (2008). *Multiple and Multimodal Reference Frames for Eye-Hand Coordination Program Neuroscience Meeting*. Washington, DC: Society for Neuroscience.
- Tagliabue, M., and McIntyre, J. (2011). Necessity is the mother of invention: reconstructing missing sensory information in multiple, concurrent reference frames for eye-hand coordination. *J. Neurosci.* 31, 1397–1409. doi: 10.1523/JNEUROSCI.0623-10.2011
- Tagliabue, M., and McIntyre, J. (2013). When kinesthesia becomes visual: a theoretical justification for executing motor tasks in visual space. *Edited by Robert J. van Beers. PLoS One* 8:e68438. doi: 10.1371/journal.pone.0068438
- Tagliabue, M., and McIntyre, J. (2014). A modular theory of multisensory integration for motor control. *Front. Comput. Neurosci.* 8:1. doi: 10.3389/fncom.2014.00001
- Torre, K., Hammami, N., Trotter, J., Van Dokkum, L., Coroian, F., Mottet, D., et al. (2013). Somatosensory-related limitations for bimanual coordination after stroke. *Neurorehabil. Neural Repair* 27, 507–515. doi: 10.1177/1545968313478483
- Turville, M., Carey, L. M., Matyas, T. A., and Blennerhassett, J. (2017). Change in functional arm use is associated with somatosensory skills after sensory retraining poststroke. *Am. J. Occup. Ther.* 71, 7103190070p1-7103190070p9. doi: 10.5014/ajot.2017.024950
- Valdes, B. A., Khoshnam, M., Neva, J. L., and Menon, C. (2019). “Robot-aided upper-limb proprioceptive training in three-dimensional space,” in *Proceedings of the 2019 IEEE 16th International Conference on Rehabilitation Robotics (ICORR)* (Toronto, ON: IEEE), 121–126. doi: 10.1109/ICORR.2019.8779529
- Van Beers, R. J., Sittig, A. C., and Gon, J. J. (1996). How humans combine simultaneous proprioceptive and visual position information. *Exp. Brain Res.* 111, 253–261. doi: 10.1007/BF00227302
- Van de Winckel, A., Wenderoth, N., De Weerd, W., Sunaert, S., Peeters, R., Van Hecke, W., et al. (2012). Frontoparietal involvement in passively guided shape and length discrimination: a comparison between subcortical stroke patients and healthy controls. *Exp. Brain Res.* 220, 179–189. doi: 10.1007/s00221-012-3128-2
- Yau, J. M., DeAngelis, J. C., and Angelaki, D. E. (2015). Dissecting neural circuits for multisensory integration and crossmodal processing. *Philos. Trans. R. Soc. B Biol. Sci.* 370:20140203. doi: 10.1098/rstb.2014.0203
- Zackowski, K. M., Dromerick, A. W., Sahrman, S. A., Thach, W. T., and Bastian, A. J. (2004). How do strength, sensation, spasticity and joint individuation relate to the reaching deficits of people with chronic hemiparesis? *Brain* 127, 1035–1046. doi: 10.1093/brain/awh116
- Zandvliet, S. B., Kwakkel, G., Nijland, R. H. M., Van Wegen, E. E. H., and Meskers, C. G. M. (2020). Is recovery of somatosensory impairment conditional for upper-limb motor recovery early after stroke? *Neurorehabil. Neural Repair* 34, 403–416. doi: 10.1177/1545968320907075

**Conflict of Interest:** The authors declare that the research was conducted in the absence of any commercial or financial relationships that could be construed as a potential conflict of interest.

Copyright © 2021 Bernard-Espina, Beraneck, Maier and Tagliabue. This is an open-access article distributed under the terms of the Creative Commons Attribution License (CC BY). The use, distribution or reproduction in other forums is permitted, provided the original author(s) and the copyright owner(s) are credited and that the original publication in this journal is cited, in accordance with accepted academic practice. No use, distribution or reproduction is permitted which does not comply with these terms.

## Supplementary Material

### 1 Equations for optimal sensory weighting, case with 2 reference frames

The motor vector  $\Delta_i$  is defined by the weighted sum of the sensory estimates in the visual ( $\Delta V_i$ ) and proprioceptive ( $\Delta P_i$ ) modality:

$$\Delta_i = w_{\Delta P} \cdot \Delta P_i + w_{\Delta V} \cdot \Delta V_i \quad (\text{S1})$$

with  $w_{\Delta P}$  and  $w_{\Delta V}$  the sensory weights for the concurrent target-effector comparisons in the proprioceptive and visual modality respectively, assuming the constraint  $C(w_{\Delta P}, w_{\Delta V})$ :

$$C(w_{\Delta P}, w_{\Delta V}) = w_{\Delta P} + w_{\Delta V} - 1 = 0 \quad (\text{S2})$$

Without loss of generality, let  $\Delta$  have a mean of zero. The variance of  $\Delta$  is:

$$\sigma_{\Delta}^2 = \frac{1}{n} \sum_{i=1}^n (\Delta_i)^2 \quad (\text{S3})$$

$$\sigma_{\Delta}^2 = \frac{1}{n} \sum_{i=1}^n (w_{\Delta P} \cdot \Delta P_i + w_{\Delta V} \cdot \Delta V_i)^2 \quad (\text{S4})$$

$$\sigma_{\Delta}^2 = (w_{\Delta P})^2 \cdot \frac{1}{n} \sum_{i=1}^n (\Delta P_i)^2 + (w_{\Delta V})^2 \cdot \frac{1}{n} \sum_{i=1}^n (\Delta V_i)^2 + 2 \cdot w_{\Delta P} \cdot w_{\Delta V} \cdot \frac{1}{n} \sum_{i=1}^n \Delta P_i \cdot \Delta V_i \quad (\text{S5})$$

$$\sigma_{\Delta}^2(w_{\Delta P}, w_{\Delta V}) = w_{\Delta P}^2 \cdot \sigma_{\Delta P}^2 + w_{\Delta V}^2 \cdot \sigma_{\Delta V}^2 + 2 \cdot w_{\Delta P} \cdot w_{\Delta V} \cdot \text{cov}(\Delta P, \Delta V) \quad (\text{S6})$$

In order to optimize the sensory weighting, the sensory weights  $w_{\Delta P}$  and  $w_{\Delta V}$  should be defined to minimize the motor vector's variance  $\sigma_{\Delta}^2$ , under the constraint (S2). We use Lagrange Multiplier technique to minimize the function  $\sigma_{\Delta}^2(w_{\Delta P}, w_{\Delta V})$  with the constraint  $C(w_{\Delta P}, w_{\Delta V}) = 0$ . We need to solve the following equation system, with  $\lambda$  as the Lagrange multiplier:

$$\begin{cases} \nabla \sigma_{\Delta}^2(w_{\Delta P}, w_{\Delta V}) = \lambda \cdot \nabla C(w_{\Delta P}, w_{\Delta V}) \\ C(w_{\Delta P}, w_{\Delta V}) = 0 \end{cases} \quad (\text{S7})$$

$$\begin{cases} \frac{\partial \sigma_{\Delta}^2(w_{\Delta P}, w_{\Delta V})}{\partial w_{\Delta P}} = \lambda \cdot \frac{\partial C(w_{\Delta P}, w_{\Delta V})}{\partial w_{\Delta P}} \\ \frac{\partial \sigma_{\Delta}^2(w_{\Delta P}, w_{\Delta V})}{\partial w_{\Delta V}} = \lambda \cdot \frac{\partial C(w_{\Delta P}, w_{\Delta V})}{\partial w_{\Delta V}} \\ w_{\Delta P} + w_{\Delta V} - 1 = 0 \end{cases} \quad (\text{S8})$$

$$\begin{cases} 2 \cdot w_{\Delta P} \cdot \sigma_{\Delta P}^2 + 2 \cdot w_{\Delta V} \cdot \text{cov}(\Delta P, \Delta V) = \lambda \\ 2 \cdot w_{\Delta V} \cdot \sigma_{\Delta V}^2 + 2 \cdot w_{\Delta P} \cdot \text{cov}(\Delta P, \Delta V) = \lambda \\ w_{\Delta P} + w_{\Delta V} - 1 = 0 \end{cases} \quad (\text{S9})$$

which gives the solutions:

$$\begin{aligned}
 w_{\Delta P} &= \frac{\sigma_{\Delta V}^2 - \text{cov}(\Delta P, \Delta V)}{\sigma_{\Delta P}^2 + \sigma_{\Delta V}^2 - 2 \cdot \text{cov}(\Delta P, \Delta V)} \\
 w_{\Delta V} &= \frac{\sigma_{\Delta P}^2 - \text{cov}(\Delta P, \Delta V)}{\sigma_{\Delta P}^2 + \sigma_{\Delta V}^2 - 2 \cdot \text{cov}(\Delta P, \Delta V)}
 \end{aligned} \tag{S10}$$

Replacing  $w_{\Delta P}$  and  $w_{\Delta V}$  in equation S6 gives the variance of the optimal motor vector  $\sigma_{\Delta}^2$ :

$$\sigma_{\Delta}^2 = \frac{\sigma_{\Delta P}^2 \cdot \sigma_{\Delta V}^2 - \text{cov}(\Delta P, \Delta V)^2}{\sigma_{\Delta P}^2 + \sigma_{\Delta V}^2 - 2 \cdot \text{cov}(\Delta P, \Delta V)} \tag{S11}$$

## 2 Equations for optimal sensory weighting, case with 4 reference frames

Following the same reasoning, to find the sensory weights  $w_{\Delta J}$ ,  $w_{\Delta ExJ}$ ,  $w_{\Delta R}$ , and  $w_{\Delta ExR}$  for the joint-centered ( $J$ ), extra-joint ( $ExJ$ ), retino-centered ( $R$ ) and extra-retinal ( $ExR$ ) reference-frames respectively, we need to solve the following system of equations:

$$\begin{cases}
 \nabla \sigma_{\Delta}^2(w_{\Delta J}, w_{\Delta ExJ}, w_{\Delta R}, w_{\Delta ExR}) = \lambda \cdot \nabla C(w_{\Delta J}, w_{\Delta ExJ}, w_{\Delta R}, w_{\Delta ExR}) \\
 C(w_{\Delta J}, w_{\Delta ExJ}, w_{\Delta R}, w_{\Delta ExR}) = 0
 \end{cases} \tag{S12}$$

The general formulation for the variance of the optimal motor vector estimate weights is:

$$\begin{aligned}
 \sigma_{\Delta}^2 = & w_{\Delta J}^2 \cdot \sigma_{\Delta J}^2 + w_{\Delta ExJ}^2 \cdot \sigma_{\Delta ExJ}^2 + w_{\Delta R}^2 \cdot \sigma_{\Delta R}^2 + w_{\Delta ExR}^2 \cdot \sigma_{\Delta ExR}^2 \\
 & + 2 \cdot w_{\Delta J} \cdot w_{\Delta ExJ} \cdot \text{cov}(\Delta J, \Delta ExJ) \\
 & + 2 \cdot w_{\Delta J} \cdot w_{\Delta R} \cdot \text{cov}(\Delta J, \Delta R) \\
 & + 2 \cdot w_{\Delta J} \cdot w_{\Delta ExR} \cdot \text{cov}(\Delta J, \Delta ExR) \\
 & + 2 \cdot w_{\Delta ExJ} \cdot w_{\Delta R} \cdot \text{cov}(\Delta ExJ, \Delta R) \\
 & + 2 \cdot w_{\Delta ExJ} \cdot w_{\Delta ExR} \cdot \text{cov}(\Delta ExJ, \Delta ExR) \\
 & + 2 \cdot w_{\Delta R} \cdot w_{\Delta ExR} \cdot \text{cov}(\Delta R, \Delta ExR)
 \end{aligned} \tag{S13}$$

The equation S12 thus becomes:

$$\begin{cases}
 2 \cdot w_{\Delta J} \cdot \sigma_{\Delta J}^2 + 2 \cdot w_{\Delta ExJ} \cdot \text{cov}(\Delta J, \Delta ExJ) + 2 \cdot w_{\Delta R} \cdot \text{cov}(\Delta J, \Delta R) + 2 \cdot w_{\Delta ExR} \cdot \text{cov}(\Delta J, \Delta ExR) = \lambda \\
 2 \cdot w_{\Delta ExJ} \cdot \sigma_{\Delta ExJ}^2 + 2 \cdot w_{\Delta J} \cdot \text{cov}(\Delta J, \Delta ExJ) + 2 \cdot w_{\Delta R} \cdot \text{cov}(\Delta ExJ, \Delta R) + 2 \cdot w_{\Delta ExR} \cdot \text{cov}(\Delta ExJ, \Delta ExR) = \lambda \\
 2 \cdot w_{\Delta R} \cdot \sigma_{\Delta R}^2 + 2 \cdot w_{\Delta J} \cdot \text{cov}(\Delta J, \Delta R) + 2 \cdot w_{\Delta ExJ} \cdot \text{cov}(\Delta ExJ, \Delta R) + 2 \cdot w_{\Delta ExR} \cdot \text{cov}(\Delta R, \Delta ExR) = \lambda \\
 2 \cdot w_{\Delta ExR} \cdot \sigma_{\Delta ExR}^2 + 2 \cdot w_{\Delta J} \cdot \text{cov}(\Delta J, \Delta ExR) + 2 \cdot w_{\Delta ExJ} \cdot \text{cov}(\Delta ExJ, \Delta ExR) + 2 \cdot w_{\Delta R} \cdot \text{cov}(\Delta R, \Delta ExR) = \lambda \\
 w_{\Delta J} + w_{\Delta ExJ} + w_{\Delta R} + w_{\Delta ExR} - 1 = 0
 \end{cases} \tag{S14}$$

The general solution for the sensory weights  $w_{\Delta J}$ ,  $w_{\Delta ExJ}$ ,  $w_{\Delta R}$ , and  $w_{\Delta ExR}$  is too large to be printed, but is easily calculable using Matlab® (R2019b, with the Symbolic Toolbox).

## 3 Task specific solutions

Using the general equations for the 4 sensory weights associated to the 4 reference-frames, we can compute the sensory weights for each reference-frame for a given proprioceptive or visuo-proprioceptive task.

### 3.1 Within-arm proprioceptive tasks (W-AP)

The variance for the 4 concurrent target-effector comparisons are described in the main text (equations 8). The covariances between the concurrent comparisons in the 4 reference frames are:

$$\begin{aligned} cov(\Delta J, \Delta ExJ) &= cov(\Delta J, \Delta R) = cov(\Delta J, \Delta ExR) = cov(\Delta ExJ, \Delta R) = cov(\Delta ExJ, \Delta ExR) = \sigma_j^2 + \sigma_j^2 \\ cov(\Delta R, \Delta ExR) &= \sigma_j^2 + \sigma_{j \rightarrow R}^2 + \sigma_j^2 + \sigma_{j \rightarrow R}^2 \end{aligned} \quad (\text{S15})$$

Replacing these terms (equations 8, and equations S15) in the system S14 gives the optimal weights:

$$\begin{aligned} w_{\Delta J} &= 1 \\ w_{\Delta ExJ} &= 0 \\ w_{\Delta R} &= 0 \\ w_{\Delta ExR} &= 0 \end{aligned} \quad (\text{S16})$$

Using this optimal set of weights (equations S16), the variances (equations 8) and covariances (equations S15), we obtain the variance for the optimal motor vector by replacing these terms in equation S13 as described in the manuscript (equation 9).

### 3.2 Asymmetric between-arms proprioceptive tasks (aB-AP)

The variance for the 4 concurrent target-effector comparisons are described in the main text (equations 10). The covariances between the concurrent comparisons in the 4 reference frames are:

$$\begin{aligned} cov(\Delta J, \Delta ExJ) &= cov(\Delta J, \Delta R) = cov(\Delta J, \Delta ExR) = cov(\Delta ExJ, \Delta R) = cov(\Delta ExJ, \Delta ExR) = \sigma_{j_r}^2 + \sigma_{j_l}^2 \\ cov(\Delta R, \Delta ExR) &= \sigma_{j_r}^2 + \sigma_{j_r \rightarrow R}^2 + \sigma_{j_l}^2 + \sigma_{j_l \rightarrow R}^2 \end{aligned} \quad (\text{S17})$$

For the asymmetric configuration, since the joint signals are not directly comparable, we consider  $\sigma_{j_r \leftrightarrow l}^2 \rightarrow \infty$ . Moreover, because the hand and the target have the same position in space, the visual reconstruction of hand and target are directly comparable. Therefore we consider  $\sigma_{M_r \leftrightarrow l}^2 \rightarrow 0$ . Replacing these terms (equations 10, and equations S17) in the system S14 gives the optimal weights:

$$\begin{aligned} w_{\Delta J} &\rightarrow 0 \\ w_{\Delta ExJ} &\rightarrow \frac{\sigma_{j \rightarrow R}^2}{\sigma_{j \rightarrow R}^2 + \sigma_{j \rightarrow ExJ}^2} \\ w_{\Delta R} &\rightarrow \frac{\sigma_{j \rightarrow ExJ}^2}{\sigma_{j \rightarrow R}^2 + \sigma_{j \rightarrow ExJ}^2} \\ w_{\Delta ExR} &\rightarrow 0 \end{aligned} \quad (\text{S18})$$

Using this optimal set of weights (equations S18), the variances (equations 10) and covariances (equations S17), we obtain the variance for the optimal motor vector by replacing these terms in equation S13 as described in the manuscript (equation 11).

### 3.3 Symmetric between-arms proprioceptive tasks (sB-AP)

The variance for the 4 concurrent target-effector comparisons are described in the main text (equations 12). The covariances between the concurrent comparisons in the 4 reference frames are:

$$\begin{aligned} cov(\Delta J, \Delta ExJ) &= cov(\Delta J, \Delta R) = cov(\Delta J, \Delta ExR) = cov(\Delta ExJ, \Delta R) = cov(\Delta ExJ, \Delta ExR) = \sigma_{J_r}^2 + \sigma_{J_l}^2 \\ cov(\Delta R, \Delta ExR) &= \sigma_{J_r}^2 + \sigma_{J_r \rightarrow R}^2 + \sigma_{J_l}^2 + \sigma_{J_l \rightarrow R}^2 \end{aligned} \quad (\text{S19})$$

For the symmetric configuration, since the analogous joint signals from both arms are theoretically comparable, we consider  $\sigma_{J_{r \leftrightarrow l}}^2 \rightarrow 0$ . Moreover, because the hand and the target do not have the same position in space, the visual reconstruction of hand and target on the retina are not directly comparable. Therefore we consider  $\sigma_{R, Mir}^2 \rightarrow \infty$ . Replacing these terms (equations 12, and equations S19) in the system S14 gives the optimal weights:

$$\begin{aligned} W_{\Delta J} &\rightarrow 1 \\ W_{\Delta ExJ} &\rightarrow 0 \\ W_{\Delta R} &\rightarrow 0 \\ W_{\Delta ExR} &\rightarrow 0 \end{aligned} \quad (\text{S20})$$

However, considering a patient with brain lesions affecting the ability to perform easily inter-hemispheric transformations, we cannot postulate that  $\sigma_{J_{r \leftrightarrow l}}^2 \rightarrow 0$ . The set of weights becomes:

$$\begin{aligned} W_{\Delta J} &\rightarrow \frac{\sigma_{J \rightarrow ExJ}^2 (\sigma_{J \rightarrow R}^2 + \sigma_{R \rightarrow ExR}^2)}{(\sigma_{J \rightarrow ExJ}^2 + \sigma_{J_{r \leftrightarrow l}}^2) (\sigma_{J \rightarrow R}^2 + \sigma_{R \rightarrow ExR}^2) + \sigma_{J_{r \leftrightarrow l}}^2 \sigma_{J \rightarrow ExJ}^2} \\ W_{\Delta ExJ} &\rightarrow \frac{\sigma_{J_{r \leftrightarrow l}}^2 (\sigma_{J \rightarrow R}^2 + \sigma_{R \rightarrow ExR}^2)}{(\sigma_{J \rightarrow ExJ}^2 + \sigma_{J_{r \leftrightarrow l}}^2) (\sigma_{J \rightarrow R}^2 + \sigma_{R \rightarrow ExR}^2) + \sigma_{J_{r \leftrightarrow l}}^2 \sigma_{J \rightarrow ExJ}^2} \\ W_{\Delta R} &\rightarrow 0 \\ W_{\Delta ExR} &\rightarrow \frac{\sigma_{J \rightarrow ExJ}^2 \sigma_{J_{r \leftrightarrow l}}^2}{(\sigma_{J \rightarrow ExJ}^2 + \sigma_{J_{r \leftrightarrow l}}^2) (\sigma_{J \rightarrow R}^2 + \sigma_{R \rightarrow ExR}^2) + \sigma_{J_{r \leftrightarrow l}}^2 \sigma_{J \rightarrow ExJ}^2} \end{aligned} \quad (\text{S21})$$

Using this optimal sets of weights (equations S20 and S21), the variances (equations 12) and covariances (equations S19), we obtain the variance for the optimal motor vector by replacing these terms in equation S13 as described in the manuscript (equation 13).

### 3.4 Cross-modal task (C-Mp)

The variance for the 4 concurrent target-effector comparisons are described in the main text (equations 14). The covariances between the concurrent comparisons in the 4 reference frames are:

$$\begin{aligned} cov(\Delta J, \Delta ExJ) &= \sigma_R^2 + \sigma_{R \rightarrow J}^2 + \sigma_J^2 \\ cov(\Delta R, \Delta ExR) &= \sigma_R^2 + \sigma_J^2 + \sigma_{J \rightarrow R}^2 \\ cov(\Delta J, \Delta R) &= cov(\Delta J, \Delta ExR) = cov(\Delta ExJ, \Delta R) = cov(\Delta ExJ, \Delta ExR) = \sigma_R^2 + \sigma_J^2 \end{aligned} \quad (\text{S22})$$

Replacing these terms (equations 14, and equations S22) in the system S14 gives the optimal weights:

$$\begin{aligned} W_{\Delta J} &= \frac{\sigma_{J \rightarrow R}^2}{\sigma_{J \rightarrow R}^2 + \sigma_{R \rightarrow J}^2} \\ W_{\Delta ExJ} &= 0 \\ W_{\Delta R} &= \frac{\sigma_{R \rightarrow J}^2}{\sigma_{J \rightarrow R}^2 + \sigma_{R \rightarrow J}^2} \\ W_{\Delta ExR} &= 0 \end{aligned} \quad (\text{S23})$$

Using this optimal set of weights (equations S23), the variances (equations 14) and covariances (equations S22), and considering  $\sigma_{R \rightarrow J}^2 = \sigma_{J \rightarrow R}^2 = \sigma_{J \leftrightarrow R}^2$ , we obtain the variance for the optimal motor vector by replacing these terms in equation S13 as described in the main text (equation 15).

### 3.5 Within-arm visuo-proprioceptive tasks (W-A<sub>VP</sub>)

The variance for the 4 concurrent target-effector comparisons are described in the main text (equations 16). The covariances between the concurrent comparisons in the 4 reference frames are:

$$\begin{aligned} cov(\Delta J, \Delta ExJ) &= \sigma_J^2 + \sigma_J^2 \\ cov(\Delta R, \Delta ExR) &= \sigma_R^2 + \sigma_R^2 \\ cov(\Delta J, \Delta R) &= cov(\Delta J, \Delta ExR) = cov(\Delta ExJ, \Delta R) = cov(\Delta ExJ, \Delta ExR) = 0 \end{aligned} \quad (\text{S24})$$

Replacing these terms (equations 16, and equations S24) in the system S14 gives the optimal weights:

$$\begin{aligned} w_{\Delta J} &= \frac{\sigma_R^2}{\sigma_J^2 + \sigma_R^2} \\ w_{\Delta ExJ} &= 0 \\ w_{\Delta R} &= \frac{\sigma_J^2}{\sigma_J^2 + \sigma_R^2} \\ w_{\Delta ExR} &= 0 \end{aligned} \quad (\text{S25})$$

Using this optimal set of weights (equations S25), the variances (equations 16) and covariances (equations S24), we obtain the variance for the optimal motor vector by replacing these terms in equation S13 as described in the manuscript (equation 17).

### 3.6 Asymmetric between-arms visuo-proprioceptive task (aB-A<sub>VP</sub>)

The variance for the 4 concurrent target-effector comparisons are described in the main text (equations 18). The covariances between the concurrent comparisons in the 4 reference frames are:

$$\begin{aligned} cov(\Delta J, \Delta ExJ) &= \sigma_{J_r}^2 + \sigma_{J_l}^2 \\ cov(\Delta R, \Delta ExR) &= \sigma_R^2 + \sigma_R^2 \\ cov(\Delta J, \Delta R) &= cov(\Delta J, \Delta ExR) = cov(\Delta ExJ, \Delta R) = cov(\Delta ExJ, \Delta ExR) = 0 \end{aligned} \quad (\text{S26})$$

For the asymmetric configuration, since the joint signals are not directly comparable, we consider  $\sigma_{J_r \leftrightarrow l}^2 \rightarrow \infty$ . However, because the hand and the target have the same position in space, a direct visual comparison is possible. We consider  $\sigma_{M_r \leftrightarrow l}^2 = 0$ . Replacing these terms (equations 18, and equations S26) in the system S14 gives the optimal weights:

$$\begin{aligned} w_{\Delta J} &\rightarrow 0 \\ w_{\Delta ExJ} &\rightarrow \frac{2\sigma_R^2}{2\sigma_R^2 + \sigma_{J_r}^2 + \sigma_{J_l}^2 + 2\sigma_{J \rightarrow ExJ}^2} \\ w_{\Delta R} &\rightarrow \frac{\sigma_{J_r}^2 + \sigma_{J_l}^2 + 2\sigma_{J \rightarrow ExJ}^2}{2\sigma_R^2 + \sigma_{J_r}^2 + \sigma_{J_l}^2 + 2\sigma_{J \rightarrow ExJ}^2} \\ w_{\Delta ExR} &\rightarrow 0 \end{aligned} \quad (\text{S27})$$

Using this optimal set of weights (equations S27), the variances (equations 18) and covariances (equations S26), we obtain the variance for the optimal motor vector by replacing these terms in equation S13 as described in the main text (equation 19).

### 3.7 Symmetric between-arms visuo-proprioceptive task (sB-A<sub>VP</sub>)

The variance for the 4 concurrent target-effector comparisons are described in the main text (equations 20). The covariances between the concurrent comparisons in the 4 reference frames are:

$$\begin{aligned} cov(\Delta J, \Delta ExJ) &= \sigma_{J_r}^2 + \sigma_{J_l}^2 \\ cov(\Delta R, \Delta ExR) &= \sigma_R^2 + \sigma_{R'}^2 \\ cov(\Delta J, \Delta R) &= cov(\Delta J, \Delta ExR) = cov(\Delta ExJ, \Delta R) = cov(\Delta ExJ, \Delta ExR) = 0 \end{aligned} \quad (\text{S28})$$

For the symmetric configuration, since the analogous joint signals from both arms are theoretically comparable, we consider  $\sigma_{J_r \leftrightarrow l}^2 \rightarrow 0$ . Moreover, because the hand and the target do not have the same position in space, the visual reconstruction of hand and target on the retina are not directly comparable. Therefore we consider  $\sigma_{R, Mir}^2 \rightarrow \infty$ . Replacing these terms (equations 20, and equations S28) in the system S14 gives the optimal weights:

$$\begin{aligned} W_{\Delta J} &\rightarrow \frac{2 \cdot (\sigma_R^2 + \sigma_{R \rightarrow ExR}^2)}{\sigma_{J_r}^2 + \sigma_{J_l}^2 + 2 \cdot \sigma_R^2 + 2 \cdot \sigma_{R \rightarrow ExR}^2} \\ W_{\Delta ExJ} &\rightarrow 0 \\ W_{\Delta R} &\rightarrow 0 \\ W_{\Delta ExR} &\rightarrow \frac{\sigma_{J_r}^2 + \sigma_{J_l}^2}{\sigma_{J_r}^2 + \sigma_{J_l}^2 + 2 \cdot \sigma_R^2 + 2 \cdot \sigma_{R \rightarrow ExR}^2} \end{aligned} \quad (\text{S29})$$

However, considering a patient with brain lesions affecting the ability to perform easily cross-reference transformations, we cannot postulate that  $\sigma_{J_r \leftrightarrow l}^2 \rightarrow 0$ . The set of weights becomes:

$$\begin{aligned} W_{\Delta J} &\rightarrow \frac{2 \cdot \sigma_{J \rightarrow ExJ}^2 (\sigma_R^2 + \sigma_{R \rightarrow ExR}^2)}{(\sigma_{J \rightarrow ExJ}^2 + \sigma_{J_r \leftrightarrow l}^2) (\sigma_{J_r}^2 + \sigma_{J_l}^2 + 2 \cdot \sigma_R^2 + 2 \cdot \sigma_{R \rightarrow ExR}^2) + 2 \cdot \sigma_{J \rightarrow ExJ}^2 \cdot \sigma_{J_r \leftrightarrow l}^2} \\ W_{\Delta ExJ} &\rightarrow \frac{2 \cdot \sigma_{J_r \leftrightarrow l}^2 (\sigma_R^2 + \sigma_{R \rightarrow ExR}^2)}{(\sigma_{J \rightarrow ExJ}^2 + \sigma_{J_r \leftrightarrow l}^2) (\sigma_{J_r}^2 + \sigma_{J_l}^2 + 2 \cdot \sigma_R^2 + 2 \cdot \sigma_{R \rightarrow ExR}^2) + 2 \cdot \sigma_{J \rightarrow ExJ}^2 \cdot \sigma_{J_r \leftrightarrow l}^2} \\ W_{\Delta R} &\rightarrow 0 \\ W_{\Delta ExR} &\rightarrow \frac{(\sigma_{J_r}^2 + \sigma_{J_l}^2) (\sigma_{J \rightarrow ExJ}^2 + \sigma_{J_r \leftrightarrow l}^2) + 2 \cdot \sigma_{J \rightarrow ExJ}^2 \cdot \sigma_{J_r \leftrightarrow l}^2}{(\sigma_{J \rightarrow ExJ}^2 + \sigma_{J_r \leftrightarrow l}^2) (\sigma_{J_r}^2 + \sigma_{J_l}^2 + 2 \cdot \sigma_R^2 + 2 \cdot \sigma_{R \rightarrow ExR}^2) + 2 \cdot \sigma_{J \rightarrow ExJ}^2 \cdot \sigma_{J_r \leftrightarrow l}^2} \end{aligned} \quad (\text{S30})$$

Using this optimal set of weights (equations S29 and S30), the variances (equations 20) and covariances (equations S28), we obtain the variance for the optimal motor vector by replacing these terms in equation S13 as described in the main text (equation 21).

### 3.8 Cross-modal task, with full visual feedback (C-M<sub>VP</sub>)

The variance for the 4 concurrent target-effector comparisons are described in the main text (equations 22). The covariances between the concurrent comparisons in the 4 reference frames are:

$$\begin{aligned}
cov(\Delta J, \Delta ExJ) &= \sigma_R^2 + \sigma_{R \rightarrow J}^2 + \sigma_J^2 \\
cov(\Delta R, \Delta ExR) &= \sigma_R^2 + \sigma_R^2 \\
cov(\Delta J, \Delta R) &= cov(\Delta J, \Delta ExR) = cov(\Delta ExJ, \Delta R) = cov(\Delta ExJ, \Delta ExR) = \sigma_R^2
\end{aligned} \tag{S31}$$

Replacing these terms (equations 22, and equations S31) in the system S14 gives the optimal weights:

$$\begin{aligned}
w_{\Delta J} &= \frac{\sigma_R^2}{\sigma_J^2 + \sigma_{R \rightarrow J}^2 + \sigma_R^2} \\
w_{\Delta ExJ} &= 0 \\
w_{\Delta R} &= \frac{\sigma_J^2 + \sigma_{R \rightarrow J}^2}{\sigma_J^2 + \sigma_{R \rightarrow J}^2 + \sigma_R^2} \\
w_{\Delta ExR} &= 0
\end{aligned} \tag{S32}$$

Using this optimal set of weights (equations S32), the variances (equations 22) and covariances (equations S31), we obtain the variance for the optimal motor vector by replacing these terms in equation S13 as described in the main text (equation 23).

## 4 Visual compensation

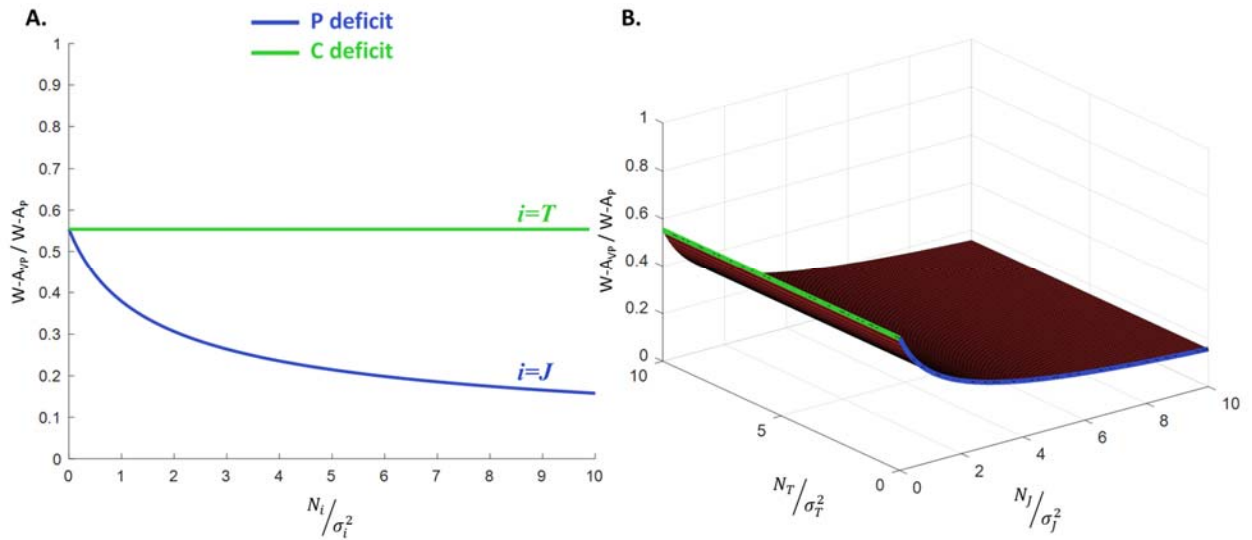
To illustrate the ability of patients to compensate for their proprioceptive deficits with vision, we can express, for each task category, the ratio between the variance of the motor vector in the visuo-proprioceptive task and the proprioceptive task. We analyzed the contribution of the sensory deficit nature (either pure proprioceptive deficit (P), pure cross-reference processing deficit (C) or mixed deficit (P+C)) to the relative performance of task with and without vision.

### 4.1 Within-arm tasks

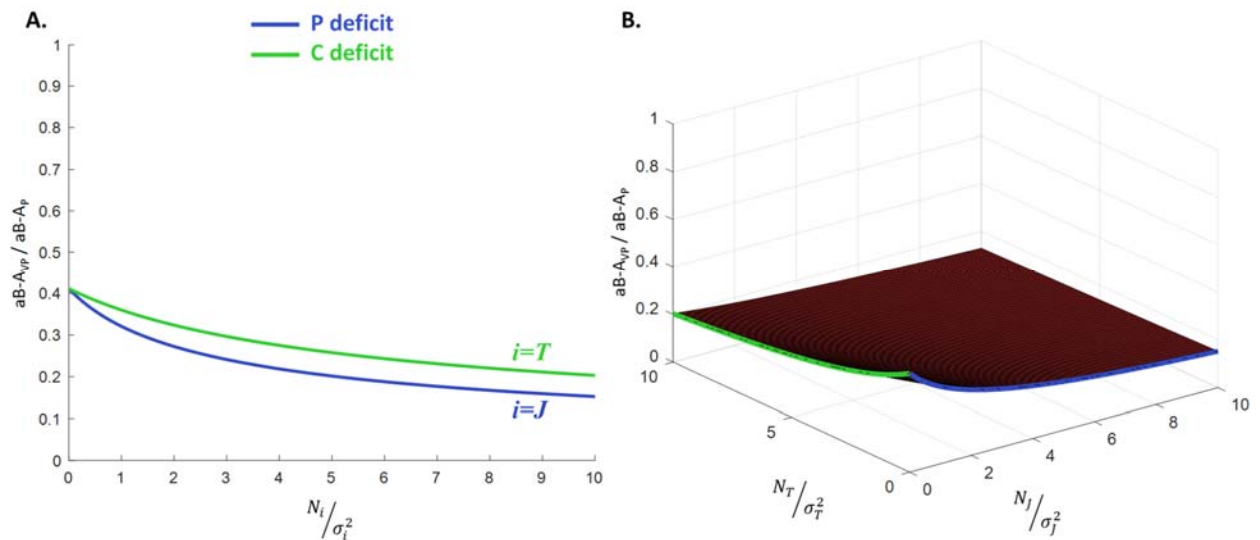
For the W-A task (see manuscript, equations 9 and 17), the performance of the proprioceptive task, relative to the visuo-proprioceptive task, is only affected by the proprioceptive noisiness (represented by the additional joint signal noise  $N_J$ ): the more proprioception is affected, the less the proprioceptive task (W-A<sub>P</sub>) is precise relative to the visuo-proprioceptive task (W-A<sub>VP</sub>). This means patients can always improve performance with visual feedback to compensate for the proprioceptive deficit in the W-A<sub>P</sub> task. Moreover, the stronger the proprioceptive deficit, the larger will be the advantage provided by using visual information (Supplementary Figure 1).

### 4.2 Asymmetric between-arms tasks

Similarly, for the aB-A task (see manuscript, equations 11 and 19), the performance of the proprioceptive task, relative to the visuo-proprioceptive task, is affected by both the proprioceptive cross-reference transformations noisiness (represented by the deficit factors  $N_J$  and  $N_T$  respectively): the more proprioception or cross-reference transformations are affected, the less the proprioceptive task (aB-A<sub>P</sub>) is precise relative to the visuo-proprioceptive task (aB-A<sub>VP</sub>). This means patients can always improve performance with visual feedback to compensate for the proprioceptive and cross-reference deficits in the aB-A<sub>P</sub> task. As well, the stronger the sensory deficit (proprioceptive, cross-reference or mixed), the larger will be the advantage provided by using visual information (Supplementary Figure 2).



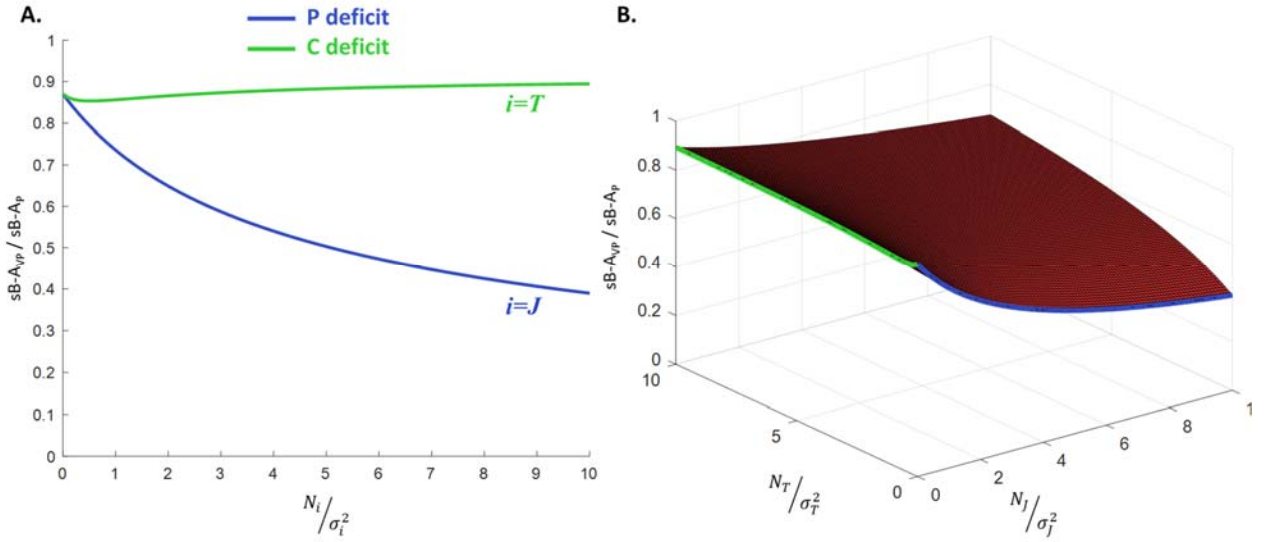
**Supplementary Figure 1.** Ratio between the variance of the within-arm proprioceptive and visuo-proprioceptive tasks ( $W-A_{vp}/W-A_p$ ) as function of the additional noise associated to stroke deficits. **(A)** represents patients with either pure proprioceptive deficit (P:  $N_J > 0$  and  $N_T = 0$ ) or pure cross-reference deficits (C:  $N_J = 0$  and  $N_T > 0$ ). **(B)** represents patients with mixed (P+C:  $N_J > 0$  and  $N_T > 0$ ) deficit. For these plots, we used the values associated to healthy subjects ( $\sigma_J^2$ ,  $\sigma_R^2$  and  $\sigma_T^2$ ) obtained with our fitting algorithm (figures 6A and 6B).



**Supplementary Figure 2.** Ratio between the variance of the asymmetric between-arms proprioceptive and visuo-proprioceptive tasks ( $aB-A_{vp}/aB-A_p$ ) as function of the additional noise associated to stroke deficits. **(A)** represents patients with either pure proprioceptive deficit (P:  $N_J > 0$  and  $N_T = 0$ ) or pure cross-reference deficits (C:  $N_J = 0$  and  $N_T > 0$ ). **(B)** represents patients with mixed (P+C:  $N_J > 0$  and  $N_T > 0$ ) deficit. For these plots, we used the values associated to healthy subjects ( $\sigma_J^2$ ,  $\sigma_R^2$  and  $\sigma_T^2$ ) obtained with our fitting algorithm (figures 6A and 6B).

### 4.3 Symmetric between-arms tasks

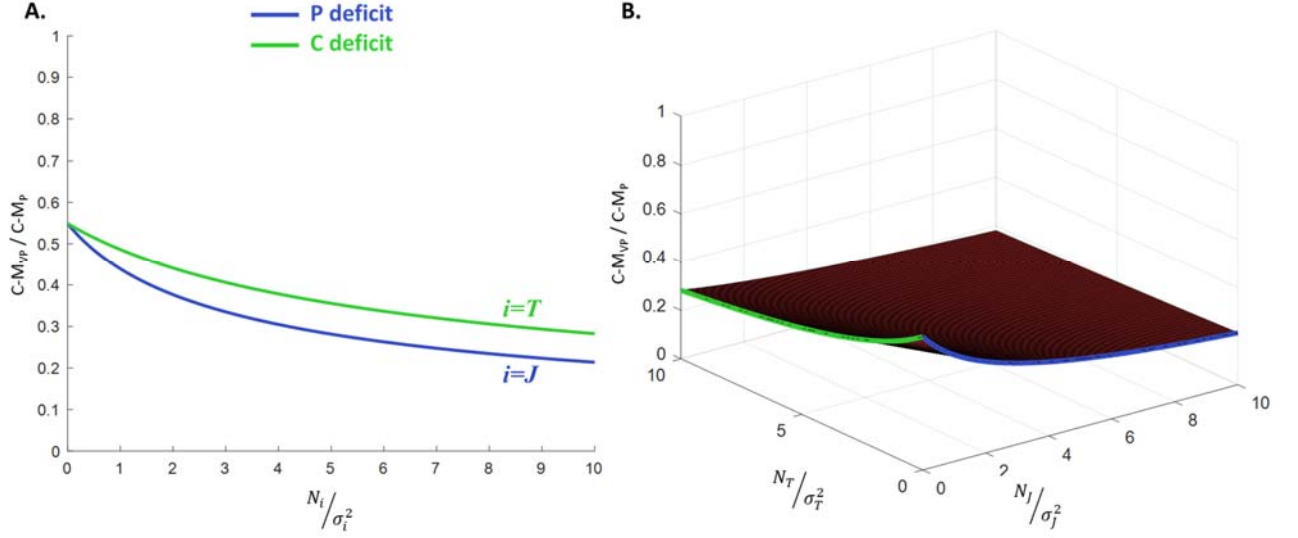
For the sB-A task (see manuscript, equations 13 and 21), the performance of the proprioceptive task (sB-A<sub>P</sub>), relative to the visuo-proprioceptive task (sB-A<sub>VP</sub>), is also affected by both the proprioceptive and cross-reference transformations noisiness (represented by the deficit factors  $N_J$  and  $N_T$  respectively). If we consider a patient with pure proprioceptive deficit ( $N_J > 0$  and  $N_T = 0$ ), the stronger the proprioceptive deficit, the larger will be the advantage provided by using visual information (Supplementary Figure 3). But, in contrast with the aB-A<sub>P</sub> tasks, vision hardly compensate for the cross-reference deficit in patients with sensory transformation deficits: the more cross-reference transformations are affected, the less patients can improve with visual feedback. Indeed, the performance in the sB-A<sub>VP</sub> task tends to the performance in the sB-A<sub>P</sub> task.



**Supplementary Figure 3.** Ratio between the variance of the symmetric between-arms proprioceptive and visuo-proprioceptive tasks ( $sB-A_{VP}/sB-A_P$ ) as function of the additional noise associated to stroke deficits. (A) represents patients with either pure proprioceptive deficit (P:  $N_J > 0$  and  $N_T = 0$ ) or pure cross-reference deficits (C:  $N_J = 0$  and  $N_T > 0$ ). (B) represents patients with mixed (P+C:  $N_J > 0$  and  $N_T > 0$ ) deficit. For these plots, we used the values associated to healthy subjects ( $\sigma_J^2$ ,  $\sigma_R^2$  and  $\sigma_T^2$ ) obtained with our fitting algorithm (figures 6A and 6B).

### 4.4 Cross-modal tasks

For the C-M task (see manuscript, equations 15 and 23), as for the W-A and aB-A tasks, patients can always improve performance with visual feedback to compensate for the proprioceptive or cross-reference deficits. The stronger the sensory deficit (proprioceptive, cross-reference or mixed), the larger will be the advantage provided by using visual information (Supplementary Figure 4).



**Supplementary Figure 4.** Ratio between the variance of the cross-modal proprioceptive and visuo-proprioceptive tasks ( $C-M_{vp}/C-M_p$ ) as function of the additional noise associated to stroke deficits. **(A)** represents patients with either pure proprioceptive deficit (P:  $N_j > 0$  and  $N_t = 0$ ) or pure cross-reference deficits (C:  $N_j = 0$  and  $N_t > 0$ ). **(B)** represents patients with mixed (P+C:  $N_j > 0$  and  $N_t > 0$ ) deficit. For these plots, we used the values associated to healthy subjects ( $\sigma_j^2$ ,  $\sigma_R^2$  and  $\sigma_T^2$ ) obtained with our fitting algorithm (figures 6A and 6B).

## 5 Model fitting

### 5.1 Experimental data used for the fitting

We used 17 data points, extracted from the literature, for fitting our model parameters. The data are shown in Supplementary Table 1 for healthy subjects, and in Supplementary Tables 2, 3 and 4 for patients with P, C and P+C deficits respectively.

The data were most often extracted from graphs. Therefore, its lecture was not always precise. For this reason, we rounded the data at the first digit. The following tables combine absolute and variable errors, as not all selected studies use the same parameter to describe the performance variability.

### 5.2 Algorithm

For fitting our model to the experimental data, we used Matlab® built-in “fmincon” function (R2019b, with the Optimization Toolbox) to minimize the  $l_2$ -norm of the fitting errors, represented by the following cost function  $cf$ :

$$cf = \sum_{i=1}^n (\sigma_{exp_i} - \sigma_{th_i})^2$$

Where  $n$  is the number of data points ( $n = 17$ ),  $\sigma_{exp_i}$  is the normalized variability of the responses for a given task, and  $\sigma_{th_i}$  is the normalized variability for the same task predicted by the model.

In order to avoid data overfitting, the number of independent variables in the model was reduced to six ( $v = 6$ ): the noise of the joint ( $\sigma_J^2$ ) and retinal ( $\sigma_R^2$ ) signals and the noise associated to sensory transformations ( $\sigma_T^2$ ) in healthy subjects; for patients, three terms representing the noise added to the joint signal of the more affected ( $N_{J_m}$ ) and less affected arm ( $N_{J_l}$ ) and to the sensory transformations ( $N_T$ ) due to the stroke lesions.

The number of degrees of freedom,  $d$ , of the fitting procedure, which is defined as the difference between the number of data points to be fitted,  $n$ , and the number of parameters of the model,  $v$ , is therefore:

$$d = n - v = 17 - 6 = 11$$

**Supplementary Table 1.** Performance variability reported in studies involving healthy subjects. These data points are represented by black squares on the Figure 6 in the main text. The data are normalized with respect to the W-A<sub>P</sub> task precision. When the W-A<sub>P</sub> was not part of the study (Herter et al. 2019; Cameron and López-Moliner 2015; Khanafer and Cressman 2014; Monaco et al. 2010), a different experimental task, represented by “X”, was used as a reference. Then, this ratio was normalized to the W-A<sub>P</sub> task. For example, in Herter et al. 2019, the performance in the sB-A<sub>VP</sub> was first normalized by the performance in the sB-A<sub>P</sub> task. Finally, the ratio sB-A<sub>VP</sub>/sB-A<sub>P</sub> was multiplied by the normalized value for the sB-A<sub>P</sub> task (sB-A<sub>P</sub>/W-A<sub>P</sub>). So that sB-A<sub>VP</sub>/sB-A<sub>P</sub> \* sB-A<sub>P</sub>/W-A<sub>P</sub> = sB-A<sub>VP</sub>/W-A<sub>P</sub> corresponds to the variability of the sB-A<sub>VP</sub> task, normalized by the W-A<sub>P</sub> task.

| Study                          | Task | W-A <sub>P</sub> | aB-A <sub>P</sub> | sB-A <sub>P</sub> | C-M <sub>P</sub> | W-A <sub>VP</sub> | aB-A <sub>VP</sub> | sB-A <sub>VP</sub> | C-M <sub>VP</sub> |
|--------------------------------|------|------------------|-------------------|-------------------|------------------|-------------------|--------------------|--------------------|-------------------|
|                                |      |                  |                   |                   |                  |                   |                    |                    |                   |
| Van Beers et al. 1996          |      |                  | X                 |                   | 1.6              |                   |                    |                    |                   |
| Ernst and Banks 2002           |      | 1                |                   |                   |                  | 0.2               |                    |                    |                   |
| Butler et al. 2004             |      | 1                | 1.1               |                   | 1.2              |                   |                    |                    |                   |
| Monaco et al. 2010             |      |                  | 1.9               |                   | X                |                   | 0.4                |                    | 0.4               |
| Tagliabue and McIntyre 2011    |      | 1                |                   |                   | 1.1              |                   |                    |                    | 0.6               |
| Torre et al. 2013              |      | 1                |                   |                   |                  | 1                 |                    |                    |                   |
| Khanafer and Cressman 2014     |      |                  | X                 |                   | 1.5              |                   |                    |                    |                   |
| Cameron and López-Moliner 2015 |      |                  |                   |                   | X                |                   |                    |                    | 0.8               |
| Arnoux et al. 2017             |      | 1                | 2.3               | 1.1               |                  |                   |                    |                    |                   |
| Herter et al. 2019             |      |                  |                   | X                 |                  |                   |                    | 0.9                |                   |
| Marini et al. 2019             |      | 1                |                   |                   |                  | 0.4               |                    |                    |                   |
| mean (±SD)                     |      | 1                | 1.8±0.6           | 1.1               | 1.3±0.2          | 0.5±0.4           | 0.4                | 0.9                | 0.6±0.2           |

**Supplementary Table 2.** Performance variability reported in studies involving patients with proprioceptive only (P) deficits. These data points are represented by blue diamonds on the Figure 6 of the main text. The data are first expressed as a ratio of the performance of healthy subjects in the same study, and then normalized to the W-A<sub>P</sub> task precision of healthy participants. The letter “Q” represents qualitative results that were not used for the fitting, but that appear on the Figure 6, as gray rectangles.

| Study                    | Task | W-A <sub>P</sub> | aB-A <sub>P</sub> | sB-A <sub>P</sub> | C-M <sub>P</sub> | W-A <sub>VP</sub> | aB-A <sub>VP</sub> | sB-A <sub>VP</sub> | C-M <sub>VP</sub> |
|--------------------------|------|------------------|-------------------|-------------------|------------------|-------------------|--------------------|--------------------|-------------------|
|                          |      |                  |                   |                   |                  |                   |                    |                    |                   |
| Scalha et al. 2011       |      |                  |                   |                   |                  |                   | Q                  |                    | Q                 |
| Torre et al. 2013        |      | 1.4              |                   |                   |                  | 0.9               |                    |                    |                   |
| Dos Santos et al. 2015   |      | 2.5              |                   |                   |                  |                   |                    |                    |                   |
| Contu et al. 2017        |      | 1.4              |                   |                   |                  |                   |                    |                    |                   |
| Rinderknecht et al. 2018 |      | 1.9              |                   |                   |                  |                   |                    |                    |                   |
| Herter et al. 2019       |      |                  |                   | 1.8               |                  |                   |                    | 1.1                |                   |
| mean (±SD)               |      | 1.8±0.5          |                   | 1.8               |                  | 0.9               |                    | 1.1                |                   |

**Supplementary Table 3.** Performance variability reported in the selected studies involving patients with cross-reference only (C) deficits. These data points are represented by green diamonds on the Figure 6. The data are first expressed as a ratio of the performance of healthy subjects in the same study, and then normalized to the W-A<sub>P</sub> task precision of healthy participants. The letter “Q” represents qualitative results that were not used for the fitting, but that appear on the Figure 6, as the gray rectangles.

| Study \ Task       | W-A <sub>P</sub> | aB-A <sub>P</sub> | sB-A <sub>P</sub> | C-M <sub>P</sub> | W-A <sub>VP</sub> | aB-A <sub>VP</sub> | sB-A <sub>VP</sub> | C-M <sub>VP</sub> |
|--------------------|------------------|-------------------|-------------------|------------------|-------------------|--------------------|--------------------|-------------------|
| Scalha et al. 2011 |                  |                   |                   |                  |                   | Q                  |                    | Q                 |
| Gurari et al. 2017 | 1.2              |                   | Q                 |                  |                   |                    |                    |                   |
| mean (±SD)         | 1.2              |                   |                   |                  |                   |                    |                    |                   |

**Supplementary Table 4.** Performance variability reported in the selected studies involving patients with proprioceptive and cross-reference (P+C) deficits. These data points are represented by red diamonds on the Figure 6. Data points for the sB-A<sub>P</sub> and sB-A<sub>VP</sub> tasks were associated P+C patients, because in the absence of cues allowing a more specific discrimination between C and P+C types of deficits, it is statically more likely that the majority of patients tested in Herter et al. (2019) and Ingemanson et al. (2019) were P+C patients. It cannot be totally excluded, however, that these data could confound C and P+C patients. The data are first expressed as a ratio of the performance of healthy subjects in the same study, and then normalized to the W-A<sub>P</sub> task precision of healthy participants. The letter “Q” represents qualitative results that were not used for the fitting, but that appear on the Figure 6, as the gray rectangles.

| Study \ Task             | W-A <sub>P</sub> | aB-A <sub>P</sub> | sB-A <sub>P</sub> | C-M <sub>P</sub> | W-A <sub>VP</sub> | aB-A <sub>VP</sub> | sB-A <sub>VP</sub> | C-M <sub>VP</sub> |
|--------------------------|------------------|-------------------|-------------------|------------------|-------------------|--------------------|--------------------|-------------------|
| Scalha et al. 2011       |                  |                   |                   |                  |                   | Q                  |                    | Q                 |
| Torre et al. 2013        | 1.4              |                   |                   |                  | 0.9               |                    |                    |                   |
| Dos Santos et al. 2015   | 2.5              |                   |                   |                  |                   |                    |                    |                   |
| Contu et al. 2017        | 1.4              |                   |                   |                  |                   |                    |                    |                   |
| Rinderknecht et al. 2018 | 1.9              |                   |                   |                  |                   |                    |                    |                   |
| Herter et al. 2019 (a)   |                  |                   | 3.0               |                  |                   |                    | 3.0                |                   |
| Herter et al. 2019 (b)   |                  |                   | 3.0               |                  |                   |                    | 2.1                |                   |
| Ingemanson et al. 2019   |                  |                   | 2.5               |                  |                   |                    |                    |                   |
| mean (±SD)               | 1.8±0.5          |                   | 2.8±0.3           |                  | 0.9               |                    | 2.5±0.6            |                   |

(a) patients who showed no improvement in the sB-A<sub>VP</sub> task, with respect to the sB-A<sub>P</sub> task.

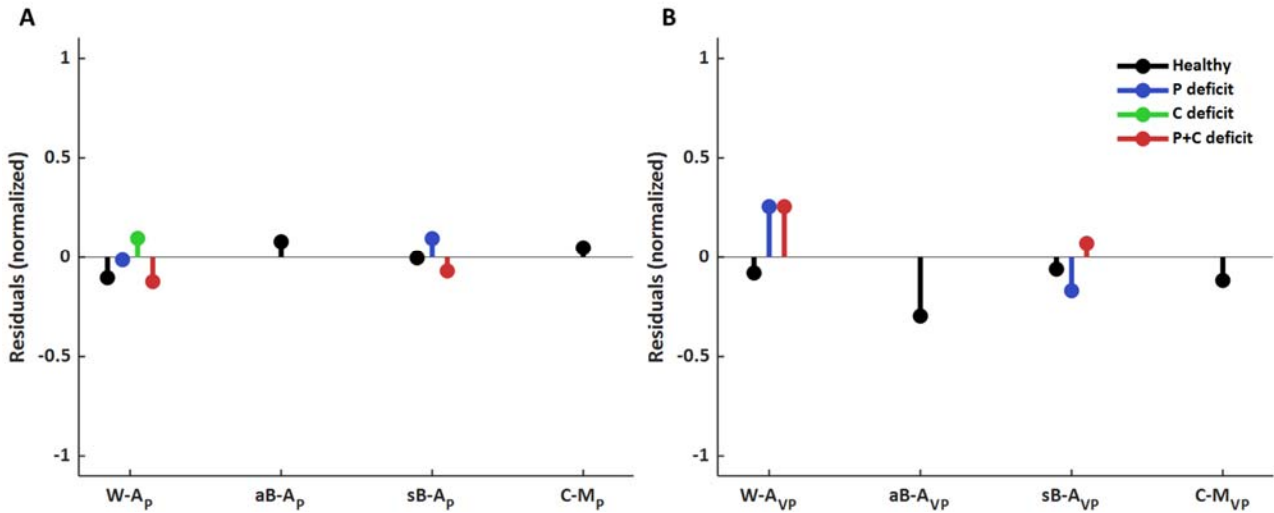
(b) patients who showed only partial improvement in the sB-A<sub>VP</sub> task, with respect to the sB-A<sub>P</sub> task.

### 5.3 Fitting results

The best fitting between the model predictions and the experimental data is obtained when the six parameters of the model have the following values:

$$\begin{cases} \sigma_f^2 = 0.61 \\ \sigma_R^2 = 0.27 \\ \sigma_T^2 = 1.63 \\ N_{J_m} = 1.08 \\ N_{J_l} = 0.55 \\ N_T = 6.25 \end{cases}$$

The residuals from the fitting procedure are displayed in Supplementary Figure 5. For testing if the residuals are normally distributed, we used the Shapiro-Wilk parametric hypothesis test of composite normality. The statistical test did not reject the normality assumption ( $W=0.96$ ,  $p=0.71$ ).



**Supplementary Figure 5.** Residuals from the fitting procedure, for each sensory condition.

The Root Mean Square (RMS) of the residuals is 0.14.

The adjusted R-Squared (with 11 degrees of freedom) is 0.93, meaning our model accounts for 93% of the total variability in the experimental data.



# How Tilting the Head Interferes With Eye-Hand Coordination: The Role of Gravity in Visuo-Proprioceptive, Cross-Modal Sensory Transformations

Jules Bernard-Espina<sup>1</sup>, Daniele Dal Canto<sup>1</sup>, Mathieu Beraneck<sup>1</sup>, Joseph McIntyre<sup>1,2,3</sup> and Michele Tagliabue<sup>1\*</sup>

<sup>1</sup> Université de Paris, CNRS, Integrative Neuroscience and Cognition Center, Paris, France, <sup>2</sup> Ikerbasque Science Foundation, Bilbao, Spain, <sup>3</sup> TECNALIA, Basque Research and Technology Alliance (BRTA), San Sebastian, Spain

## OPEN ACCESS

### Edited by:

Pierre Denise,

INSERM U1075 Université de Caen Normandie - Pôle des Formations et de Recherche en Santé, France

### Reviewed by:

Maria Gallagher,

Cardiff University, United Kingdom

Michael Jenkin,

York University, Canada

### \*Correspondence:

Michele Tagliabue

michele.tagliabue@u-paris.fr

**Received:** 03 October 2021

**Accepted:** 03 February 2022

**Published:** 10 March 2022

### Citation:

Bernard-Espina J, Dal Canto D, Beraneck M, McIntyre J and Tagliabue M (2022) How Tilting the Head Interferes With Eye-Hand Coordination: The Role of Gravity in Visuo-Proprioceptive, Cross-Modal Sensory Transformations. *Front. Integr. Neurosci.* 16:788905. doi: 10.3389/fnint.2022.788905

To correctly position the hand with respect to the spatial location and orientation of an object to be reached/grasped, visual information about the target and proprioceptive information from the hand must be compared. Since visual and proprioceptive sensory modalities are inherently encoded in a retinal and musculo-skeletal reference frame, respectively, this comparison requires cross-modal sensory transformations. Previous studies have shown that lateral tilts of the head interfere with the visuo-proprioceptive transformations. It is unclear, however, whether this phenomenon is related to the neck flexion or to the head-gravity misalignment. To answer to this question, we performed three virtual reality experiments in which we compared a grasping-like movement with lateral neck flexions executed in an upright seated position and while lying supine. In the main experiment, the task requires cross-modal transformations, because the target information is visually acquired, and the hand is sensed through proprioception only. In the other two control experiments, the task is unimodal, because both target and hand are sensed through one, and the same, sensory channel (vision and proprioception, respectively), and, hence, cross-modal processing is unnecessary. The results show that lateral neck flexions have considerably different effects in the seated and supine posture, but only for the cross-modal task. More precisely, the subjects' response variability and the importance associated to the visual encoding of the information significantly increased when supine. We show that these findings are consistent with the idea that head-gravity misalignment interferes with the visuo-proprioceptive cross-modal processing. Indeed, the principle of statistical optimality in multisensory integration predicts the observed results if the noise associated to the visuo-proprioceptive transformations is assumed to be affected by gravitational signals, and not by neck proprioceptive signals *per se*. This finding is also consistent with the observation of otolithic projections in the posterior parietal cortex, which is involved in the

visuo-proprioceptive processing. Altogether these findings represent a clear evidence of the theorized central role of gravity in spatial perception. More precisely, otolithic signals would contribute to reciprocally align the reference frames in which the available sensory information can be encoded.

**Keywords:** multisensory integration, cross-modal transformation, gravity, reaching/grasping movement, eye-hand coordination, vision, proprioception, otolith

## INTRODUCTION

When reaching to grasp an object, arm proprioceptive signals and the visually acquired object position/orientation must be compared. A typical situation in which visuo-proprioceptive communication is strictly necessary is at the beginning of the reaching movement if the hand is out of sight. There are, however other common situations where cross-modal transformations, i.e., the encoding of visual information in a proprioceptive space and vice-versa, is necessary during the whole reaching movement: for instance, when trying to insert a bolt from beneath a plate on which the threaded hole location is visually identified from above. There is also evidence that the visuo-proprioceptive interaction is performed even when it is not strictly necessary, that is even when object and hand can be both seen, or both sensed through proprioception, before the movement onset (Sober and Sabes, 2005; Sarlegna and Sainburg, 2007, 2009; Sarlegna et al., 2009) and during movement execution (Tagliabue and McIntyre, 2011, 2013, 2014; Cluff et al., 2015; Crevecoeur et al., 2016; Arnoux et al., 2017).

It has been shown that tilting laterally the head when seating interferes with the communication between visual and proprioceptive systems (Burns and Blohm, 2010; Tagliabue and McIntyre, 2011) and we demonstrated that this phenomenon is independent from the phase of the movement during which the head is tilted (Tagliabue et al., 2013; Tagliabue and McIntyre, 2014). These studies, however, did not allow understanding whether the neck on trunk lateral flexion *per se* (the signals originating from the neck muscles), or the head misalignment with respect to the vertical (gravitational signals), interferes with cross-modal transformations. The first option, that we call here the *Neck Hypothesis*, would be consistent with the contribution of the neck flexion angle information to the kinematic chain linking the hand to the eyes and that may be thus used to compute visuo-proprioceptive transformations (Sabes, 2011). This hypothesis has two possible variants: “*Neck1 Hp*,” wherein the lateral neck flexions *per se* interferes with eye-hand transformation, because of the rarity of adopting such neck postures when performing reaching/grasping tasks; “*Neck2 Hp*,” wherein lateral neck flexions require an increase of the muscle activations to support the weight of the head, resulting in increased signal-dependent noise that would interfere with eye-hand transformations (Abedi Khoozani and Blohm, 2018). An alternative option, called here the *Gravity Hypothesis* (*Gravity Hp*), is related to the idea that gravity might play a fundamental role in the reciprocal calibration between visual and proprioceptive senses (Paillard, 1991), since it can be both seen (the visual environment provides information about the vertical)

and felt (mechano-receptors detect gravity action). The head-vertical misalignment might hence perturb the ability of using gravity as reference for visuo-proprioceptive transformations. This could be due to an increase of the otolithic noise with the lateral head tilt (Vrijer et al., 2008) or to the fact that eye-hand coordination tasks are more commonly performed with the head straight and sensorimotor precision has been shown to be proportional to the task usualness (Howard et al., 2009).

To discriminate between these hypotheses, we performed a first virtual reality experiment in which the subject had to perform in a *Seated* and in a *Supine* position the same cross-modal task: align the hand to “grasp” a visual target with the unseen hand (Tagliabue and McIntyre, 2011; Tagliabue et al., 2013). To test the effect of the neck flexion, the subjects are asked to laterally tilt the head between the target acquisition and the hand movement onset. If “*Neck1 Hp*” is correct, the subjects’ performance should not change notably between postures, because the tasks performed in the seated and supine condition do not significantly differ in terms of lateral neck flexion. On the other hand, “*Neck2 Hp*” predicts an improvement of the precision when supine, because, thanks to a special head support, in this position the neck muscles never have to sustain the head weight, resulting in spindle-noise reduction (Abedi Khoozani and Blohm, 2018). Neck proprioceptive degradation is not to be expected with the head-support, because there is evidence that a decrease of the muscle tone, as experienced by astronauts in weightlessness, does not reduce the sensitivity of the muscle receptors (Roll et al., 1993). Finally, “*Gravity Hp*” will be supported by a decrease of precision when supine, because when lying on their back the subject’s head is misaligned with respect to gravity during the whole task and not only during the response phase, as in the seated configuration.

Two control experiments were performed to test whether potential effect of posture observed in the cross-modal task could be due to an effect of posture on visual and/or proprioceptive perception, and not on the sensory transformations. In the first control experiment the subjects performed a unimodal visual task: only vision could be used for both target acquisition and response control. In the second control experiment a unimodal proprioceptive task was tested: both target and response could be sensed through proprioception only.

In order to compare the *Neck* and *Gravity Hypotheses* predictions with the measured subjects’ precision and sensory weighting, we applied our “*Concurrent Model*” (see below) of multisensory integration (Tagliabue and McIntyre, 2008, 2011, 2012, 2013, 2014; Tagliabue et al., 2013; Arnoux et al., 2017; Bernard-Espina et al., 2021) to the cross- and uni-modal tasks tested here.

To confirm our interpretation of the first set of results, we performed an additional experiment in which the subjects were tested seated and supine, but without lateral neck flexions. The goal was to specifically test the effect of the modulation of the gravitational information without interference from neck muscle-spindles' signals.

## MATERIALS AND METHODS

### Ethics Statement

The experimental protocol was approved by the Ethical Committee of the University of Paris (N° CER 2014-34/2018-115) and all participant gave written informed consent in line with the Declaration of Helsinki.

### Experimental Setup and Procedure

The setup is very similar to what used in our previous studies (Tagliabue and McIntyre, 2011, 2012), consisting of the following components: an active-marker motion-analysis system (CODAmotion; Charnwood Dynamics) used for real-time recording of the three-dimensional position of 19 infrared LEDs (sub-millimeter accuracy, 200-Hz sampling frequency). Eight markers were distributed ~10 cm apart on the surface of stereo virtual reality goggles (nVisor sx60, NVIS) worn by the subjects (field of view: 60°, frame rate: 60 Hz, resolution: 1,280 × 1,024 pixels, adjustable inter-pupillary distance); eight on the surface of a tool (350 g, isotropic inertial moment around the roll axis) that was attached to the subjects' dominant hand; and three attached to a fixed reference frame placed in the laboratory. Custom C++ code was developed by the research team to optimally combine the information about the three-dimensional position of the infrared markers and the angular information from an inertial sensor (IS-300 Plus system from InterSense) placed on the VR headset to estimate in real-time the position and the orientation of the subject's viewpoint and thus to update accordingly the stereoscopic images shown in the virtual reality goggles. For tracking the hand movement only infrared markers were used.

The three-dimensional virtual environment shown to the subjects through the head mounted display consisted of a cylindrical tunnel (Figure 1). Longitudinal marks parallel to the tunnel axis were added on the walls to help the subjects to perceive their own spatial orientation in the virtual world. The fact that the marks went from white in the "ceiling" to black on the "floor" facilitated the identification of the visual vertical.

### Experimental Paradigm

The task consisted of three phases: (1) memorization of the target orientation, (2) lateral neck flexion, and (3) alignment of the tool to the remembered target orientation. As in our previous studies (Tagliabue and McIntyre, 2011, 2012, 2013, 2014; Tagliabue et al., 2013; Arnoux et al., 2017), we took advantage of the head rotation to introduce a sensory conflict with the subjects not noticing it (see below). The target could be laterally tilted with respect to the virtual vertical of  $-45^\circ$ ,  $-30^\circ$ ,  $-15^\circ$ ,  $0^\circ$ ,  $+15^\circ$ ,  $+30^\circ$  or  $+45^\circ$ . The subjects had 2.5 s to memorize its orientation. After

the target disappeared, the subject was guided to laterally tilt the head  $15^\circ$  to the right or to the left by a sound with a left-right balance and a volume corresponding to the direction and the distance from the desired inclination. If the subject was unable to extinguish the sound within 5 sec, the trial was interrupted and repeated later on, otherwise a go signal was given to indicate that he/she had to reproduce the target orientation with the tool. The subject clicked on the trigger of a trackball held in the hand to validate the response.

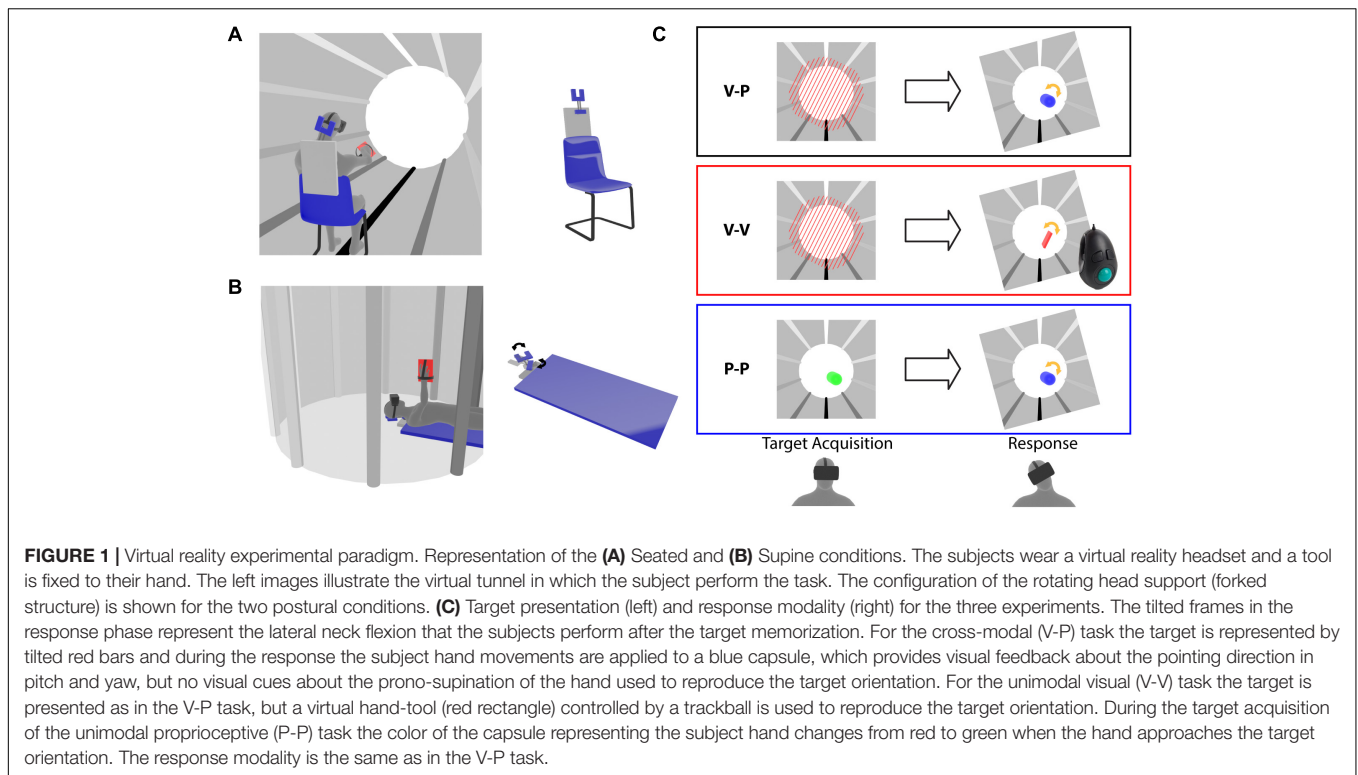
In order to quantify the sensory weighting in each experimental condition a sensory conflict was artificially introduced (Tagliabue and McIntyre, 2011): tracking the virtual reality goggles was normally used to hold the visual scene stable with respect to the real world during the lateral head tilt, but in half of the trials, a gradual, imperceptible conflict was generated such that, when the subjects laterally flex the neck, they received visual information corresponding to a larger head tilt. The amplitude of the angle between the visual vertical and subject body axis varied proportionally (by a factor of 0.6) with the actual head tilt, so that for a  $15^\circ$  lateral head roll a  $9^\circ$  conflict was generated. When, at the end of the experiment, the subjects were interviewed about the conflict perception, none of them reported to have noticed the tilt of the visual scene.

Each subject was tested in two postural conditions: Seated and Supine (Figures 1A,B). In order to compensate for possible learning effects, half of the subjects were tested first seated and then supine, and the other half in the opposite order. When the subjects performed the task in the supine position, they lay in a medical bed with their head supported by an articulated mechanical structure allowing for lateral neck flexions (Figure 1B). When the subject performed the task in a seated position the same head support was fixed to the back of the chair to restrain the head movements in a way similar to the supine condition (Figure 1A). Since the main axis of the virtual tunnel always corresponded to the anterior-posterior subject direction, it was horizontal and vertical in the Seated and Supine Condition, respectively.

As detailed below, the first three experiments presented in this study differed only by the sensory information available to acquire the target and to control the tool during the response (Figure 1C). The task used in the fourth, additional experiment was the same as for the main cross-modal experiment with the exception that the subject always kept the head aligned to the body.

### Cross-Modal Experiment

The target was presented visually and during the response the tool orientation could be controlled through arm proprioception only (V-P task). As shown in the top part of Figure 1C, the target consisted of parallel beams blocking the tunnel in front of the subject. In the response phase, subjects raised their hand and reproduced the memorized beams orientation by pronosupinating the palm. The subjects' hands were represented in the virtual environment as a capsule with the same main axis so that all its degrees of freedom except the roll (hand pronosupination) could be visually controlled. It follows that only arm proprioception could be used to control the alignment task.



### Uni-Modal Visual Experiment

Both target acquisition and tool control orientation could be performed by using vision only (V-V task). The target was represented by the beams as in Experiment 1. For the response, subjects did not move the hand, which was kept next to the body. A virtual representation of the tool fixed to the subject hand appeared in front of their eyes with a random roll orientation (see middle part of **Figure 1C**). They used a trackball to change its roll angle and to align it to the memorized beams. In this way only visual information could be used to evaluate the task achievement.

### Uni-Modal Proprioceptive Experiment

Both target and tool orientation could be sensed through proprioception only (P-P task). The beams were not shown to the subjects. To sense the target orientation, they raised the hand, which was represented by a capsule, as in the response phase of Experiment 1. In this phase the color of the capsule changed as a function of the hand roll turning from red to green as the hand approached the target roll angle. Thus, subjects had to pronate or supinate the hand to find the target orientation. After 2.5 s with the correct hand orientation an audio signal instructed the subject to lower the arm. The only information available to memorize the roll orientation of the target was the proprioceptive feedback related to forearm pronation-supination. The target orientation was in this way presented proprioceptively, without any visual feedback about the desired orientation. The response was controlled using proprioception only, as in Experiment 1.

In total 54 subjects were tested, 18 for each experiment (average age: V-P  $26.5 \pm 9$ ; V-V  $30 \pm 6$ ; P-P  $24.5 \pm 6$ ). The

number of male and female participants was balanced and about 17% of the subjects were left-handed. The subjects performed two trials for each combination of target orientation, head inclination and sensory conflict, for a total of 56 ( $= 2 \times 7 \times 2 \times 2$ ) trials per posture. The order of the trials was randomized.

### Neck Straight Experiment

The task is very similar to the one tested in the “Cross-modal Experiment” except that the subjects were not asked to laterally flex the neck after the target memorization. Twelve subjects participated to the experiment (age:  $38.5 \pm 8$ ). Half of them performed the Seated condition before the Supine condition, the other half did the opposite to compensate for possible learning effects. As for the previous experiment, each target orientation was tested twice per postural condition, for a total of 28 ( $= 2 \times 2 \times 7$ ) responses. The head mounted display used for these tests was an Oculus Rift (field of view:  $90^\circ$ , frame rate: 90 Hz, resolution:  $1,080 \times 1,200$  pixels, adjustable inter-pupillary distance). As for the main experiments, a custom C++ code was developed by the research team to integrate optical (Codamotion system) and inertial (embedded in the Oculus-Rift) sensors and to update the stereo images provided in virtual reality headset.

### Data Analysis

The subjects’ performance was analyzed using Matlab (MathWorks, RRID: SCR\_001622) in terms of the lateral inclination (roll) of the tool when they validated the response. In order to describe the variability of the subject responses, we computed the root mean square of the difference, *RMSd*, between

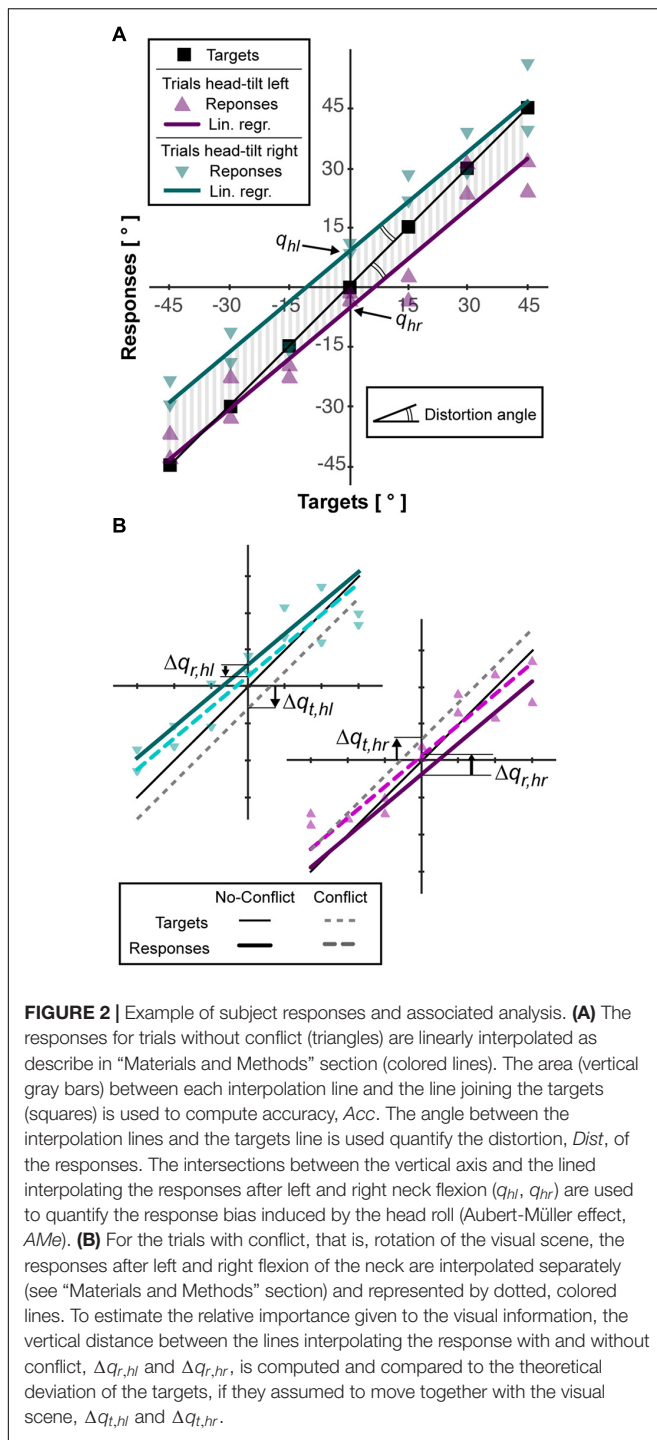


**FIGURE 2** | Example of subject responses and associated analysis. **(A)** The responses for trials without conflict (triangles) are linearly interpolated as describe in “Materials and Methods” section (colored lines). The area (vertical gray bars) between each interpolation line and the line joining the targets (squares) is used to compute accuracy, *Acc*. The angle between the interpolation lines and the targets line is used quantify the distortion, *Dist*, of the responses. The intersections between the vertical axis and the lined interpolating the responses after left and right neck flexion ( $q_{hl}$ ,  $q_{hr}$ ) are used to quantify the response bias induced by the head roll (Aubert-Müller effect, *AME*). **(B)** For the trials with conflict, that is, rotation of the visual scene, the responses after left and right flexion of the neck are interpolated separately (see “Materials and Methods” section) and represented by dotted, colored lines. To estimate the relative importance given to the visual information, the vertical distance between the lines interpolating the response with and without conflict,  $\Delta q_{r,hl}$  and  $\Delta q_{r,hr}$ , is computed and compared to the theoretical deviation of the targets, if they assumed to move together with the visual scene,  $\Delta q_{t,hl}$  and  $\Delta q_{t,hr}$ .

the two responses,  $r$ , to each combination of target,  $t$ , and head,  $h$ , inclination in the trials without conflict.

$$RMSd = \sqrt{\frac{\sum_{h=1}^2 \sum_{t=1}^7 (r_{t,h,1} - r_{t,h,2})^2}{14}} \quad (1)$$

To describe the characteristics of the average behavior of the subjects, the linear regression lines of their responses after tilting

the head to the right and to the left were computed imposing their parallelism (see **Figure 2A**). Each of the two regression lines have the form  $r = mt + q_i$ , where  $r$  and  $t$  are the response and target orientation, respectively. The parameter “ $m$ ,” common for the two lines, represents their slope. The intersection with the response axis “ $q_i$ ” is different for the trials with rotation of the head to the right ( $i = hr$ ) and to the left ( $i = hl$ ). The parameters of the lines were used to quantify the following variables:

- The *accuracy* (*Acc*), that is average response-target distance, was represented by the average absolute distance between the regression lines and the line passing through the targets position (vertical gray lines in **Figure 2A**).
- The *Aubert-Müller effect* (*AME*), corresponding to the global response bias due to the lateral neck flexion (Guerraz et al., 1998), was quantified as half of the algebraic distance between the intersection point of the two regression lines with the vertical axis:  $AME = (q_{hl} - q_{hr})/2$ .
- The *distortion* (*Dist*), representing possible over/under-estimation of the distance between two targets’ orientation (McIntyre and Lipshits, 2008), is represented by the angle between the regression lines and the line passing through the targets’ orientations:  $Dist = \text{atan}(m) - 45^\circ$  (double arcs in **Figure 2A**). Positive and negative values of *Dist* correspond to a global over- and under- estimation of the angular distances, respectively.

## Sensory Weighting Quantification

To quantify the specific effect of the sensory conflict in each condition we linearly interpolated the responses of the conflict-trials with right and left neck flexion constraining the lines to be parallel to regression lines of the no-conflict-trials (see **Figure 2B**). This procedure provides the responses-axis intercepts for the conflict trials. Subtracting to these parameters the corresponding values in the no-conflict-trials we obtain the average deviations in the response due to the tilt of the visual scene:  $\Delta q_{r,hi}$ . In order to convert the response deviation into the percentage weight given to visual information, we computed, for each conflict trial, the virtual displacement of the target expected if only visual information was used to code its orientation, which corresponds to  $t - \text{head\_angle} \times 0.6$ . We linearly interpolated these theoretical responses for right and left neck flexion separately, constraining the lines to be parallel to the one joining the targets ( $m = 1$ ) and we obtained the response-axis intercepts (see **Figure 2B**). Subtracting from these parameters the intercept of the line joining the target in the no-conflict trials ( $q = 0$ ), we obtain the average target deviation expected in case of fully visual encoding of their orientation:  $\Delta q_{t,hi}$ . The percentage weight given to the visual information,  $\omega_V$ , can be then computed as it follows:

$$\omega_V = \frac{1}{2} \sum_{i=l,r} \frac{\Delta q_{r,hi}}{\Delta q_{t,hi}} \cdot 100\% \quad (2)$$

## Statistical Analysis

For each experiment, we assessed the effect of the subject posture on the subject performances by performing mixed

model ANOVAs on the *AME*, *Dist*, *Acc*, *RMSd*, and  $\omega_V$  dependent variables, with the *Posture* (Seated, Supine) and *Order* (Seated-First and Supine-First) as within- and between- subjects independent variable, respectively. No between-experiment comparisons were performed, because they do not correspond to the goal of this study. Since we performed three distinct experiments, we applied a Bonferroni correction ( $n = 3$ ) to the resulting p-values to reduce the probability of type I errors (false positive). Therefore, in the following,  $p < 0.05/3$  ( $\approx 0.0167$ ),  $p < 0.01/3$  ( $\approx 0.0033$ ), and  $p < 0.001/3$  ( $\approx 0.00033$ ) will be indicated with “\*,” “\*\*,” “\*\*\*,” respectively. For the straight-neck experiment, we specifically wanted to test the “Gravity Hp,” that is whether the Supine position increased the subjects’ variable and constant errors. We therefore performed one-tail Student’s *t*-tests on *RMSd* and *Acc*. Since the subjects did not rotate their head, no conflict could be generated and no quantification of the sensory weighting was possible. All statistical analyses were performed using the Statistica 8 software (Statsoft, SCR\_014213).

## Optimal Integration of Non-independent Sensory Signals Based on the Maximum Likelihood Principle

In order to quantify the predictions associated with the *Gravity* and *Neck* Hypotheses and compare them with the experimental results, we apply our *Concurrent Model* of optimal sensory integration (Tagliabue and McIntyre, 2011, 2014) to describe the information flow associated with the Seated and Supine postures for each of the three experiments. An illustration of the general model structure is reported in **Figure 3A**.

This model is based on the assumption that the target and hand position are compared in the visual and proprioceptive space concurrently ( $\Delta V$  and  $\Delta P$ ) and then these two parallel comparisons are combined based on the Maximum Likelihood Principle (Ernst and Banks, 2002). From this optimality principle it follows that the relative weight,  $W_{\Delta V}$  and  $W_{\Delta P}$ , given to each comparison depends on their variance  $\sigma_{\Delta V}^2$  and  $\sigma_{\Delta P}^2$  as it follows:

$$W_{\Delta V} = \frac{\sigma_{\Delta P}^2 - \text{cov}(\Delta V, \Delta P)}{\sigma_{\Delta V}^2 + \sigma_{\Delta P}^2 - 2\text{cov}(\Delta V, \Delta P)}$$

$$W_{\Delta P} = \frac{\sigma_{\Delta V}^2 - \text{cov}(\Delta V, \Delta P)}{\sigma_{\Delta V}^2 + \sigma_{\Delta P}^2 - 2\text{cov}(\Delta V, \Delta P)} \quad (3)$$

which corresponds to the minimal achievable variance of motor vector estimation  $\Delta$

$$\sigma_{\Delta}^2 = \frac{\sigma_{\Delta V}^2 \sigma_{\Delta P}^2 - \text{cov}(\Delta V, \Delta P)^2}{\sigma_{\Delta V}^2 + \sigma_{\Delta P}^2 - 2\text{cov}(\Delta V, \Delta P)} \quad (4)$$

In Equations 3 and 4 the covariance between  $\Delta V$  and  $\Delta P$ ,  $\text{cov}(\Delta V, \Delta P)$ , is used to take into account the situations in which the two concurrent comparisons are not fully independent (Tagliabue and McIntyre, 2013). The application of MLP to multi-sensory integration therefore assumes that the brain can estimate the variability of the signals to be combined ( $\sigma_{\Delta V}^2$  and  $\sigma_{\Delta P}^2$ ) and to which extent they are independent ( $\text{cov}(\Delta V, \Delta P)$ ). Although

it is not clear whether, and how, the brain would actually estimate these specific parameters, perceptive and behavioral studies have shown that human sensory weighting is clearly modulated by signals’ variability as predicted by the MLP (Ernst and Banks, 2002) and that performances cannot be improved by combining two fully dependent signals (Tagliabue and McIntyre, 2013–2014), as expected if their covariance is taken into account.

For the cross-modal task without head rotation (**Figure 3B**), the model predicts a reconstruction of the proprioceptive target representation from the visual information and of a visual hand representation from the proprioceptive feedback (green arrows). These cross-modal transformations, which introduce additional errors, are associated to specific variance terms  $\sigma_{V \rightarrow P}^2$  and  $\sigma_{P \rightarrow V}^2$ , and, as show in section 1 of **Supplementary Material**, Equations 3 and 4 become:

$$W_{\Delta V} = \frac{\sigma_{V \rightarrow P}^2}{\sigma_{V \rightarrow P}^2 + \sigma_{P \rightarrow V}^2} \quad W_{\Delta P} = \frac{\sigma_{P \rightarrow V}^2}{\sigma_{V \rightarrow P}^2 + \sigma_{P \rightarrow V}^2}$$

$$\sigma_{\Delta}^2 = \sigma_{T_V}^2 + \sigma_{H_P}^2 + \frac{\sigma_{V \rightarrow P}^2 \sigma_{P \rightarrow V}^2}{\sigma_{V \rightarrow P}^2 + \sigma_{P \rightarrow V}^2} \quad (5)$$

As illustrated in **Figures 3C,D**, the model predicts no cross-modal reconstructions for the unimodal tasks (Tagliabue and McIntyre, 2013): in these tasks, the direct comparison between the available information about the target and the hand fully covaries with any comparison reconstructed from the available cues. From equation 4 it follows that the reconstruction of concurrent comparisons cannot improve the precision of  $\Delta$  and using equations 3 it results that the predicted sensory weights and the motor vector variance are:

$$W_{\Delta V} = 1 \quad W_{\Delta P} = 0 \quad \sigma_{\Delta}^2 = \sigma_{T_V}^2 + \sigma_{H_V}^2 \quad (6)$$

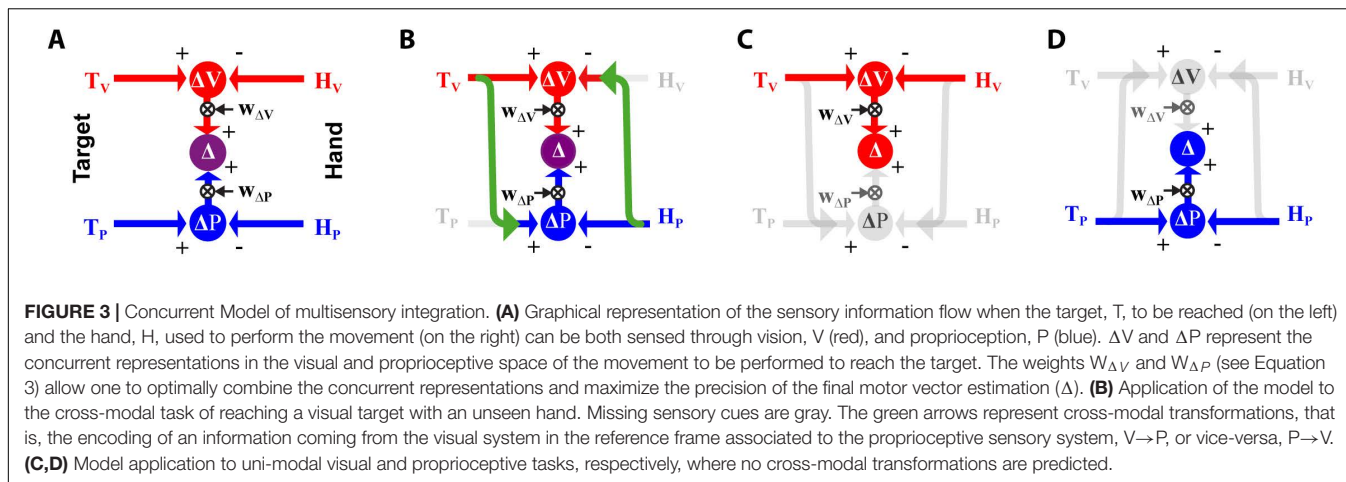
$$W_{\Delta V} = 0 \quad W_{\Delta P} = 1 \quad \sigma_{\Delta}^2 = \sigma_{T_P}^2 + \sigma_{H_P}^2 \quad (7)$$

for the visual and proprioceptive task, respectively.

For all tasks, once the motor vector is estimated, the motor system generates the muscle activations necessary to displace the hand in the defined direction and distance. This step introduces some additional noise, that we will call motor noise,  $\sigma_m^2$ , so that the variance of the movement execution is  $\sigma_{ME}^2 = \sigma_{\Delta}^2 + \sigma_m^2$ . There might be additional factors, as the concentration and fatigue levels of the subject, that can contribute to the movement execution variability. For sake of simplicity, the present version of the model does not include them separately and they are all combined together in the  $\sigma_m^2$  term.

To simulate the effect on the information processing of head inclination with respect to gravity, or of the neck flexion, in these three tasks, the variance,  $\sigma_N^2$ , is added to the  $\sigma_{V \rightarrow P}^2$ ,  $\sigma_{P \rightarrow V}^2$  terms. This extra noise is added to the cross-modal sensory transformations performed with the neck flexed, with neck muscle acting against gravity or with the head misaligned with respect to gravity, depending on the hypothesis to be tested.

In order to test which hypothesis, between the “Neck1,” “Neck2,” and “Gravity,” better predicts the experimental results, we compare the observed effect of posture on the subjects’



responses' variability,  $DMSd = RMSd_{Supine}^2 - RMSd_{Seated}^2$ , and on the response deviation due to visual scene rotation,  $D\omega_V = \omega_{V,Supine} - \omega_{V,Seated}$ , with corresponding parameters of the model: the difference between the Supine and Seated posture predicted by the model for the movement execution variability,  $D\sigma_{ME}^2 = \sigma_{ME,Supine}^2 - \sigma_{ME,Seated}^2$ , and for the weight associated with visual representation of the task,  $DW_{\Delta V} = W_{\Delta V,Supine} - W_{\Delta V,Seated}$ .

As shown in **Supplementary Material (sections 3 and 4)**, the theoretical predictions depend only on two main parameters: the variance associated to the cross-modal sensory transformation,  $\sigma_{P \leftrightarrow V}^2$ , and to the noise added to these transformations when performed with the head misaligned with respect to gravity and/or the body,  $\sigma_N^2$ . In order to reduce even further the degrees of freedom of the model, and thus the possibility of overfitting the experimental data, the value of  $\sigma_{P \leftrightarrow V}^2$  is set to  $23.19^\circ^2$ ; a value that is computed from the results of Tagliabue and McIntyre (2011) in section 4.2 of **Supplementary Material**. To statistically test whether the predictions of the various hypotheses differed from the experimental data, a multivariate Hotelling's  $T^2$  test is performed with six dependent variables ( $D\omega_V$  and  $DMSd$  for each of the three experiments) and the six corresponding model predictions ( $DW_{\Delta V}$  and  $D\sigma_{ME}^2$ ) as reference values.

## RESULTS

The subjects' average responses in the three main experiments (Cross-modal, Unimodal Visual and Unimodal Proprioceptive tasks) for the two tested postures (Seated and Supine) are depicted in **Figure 4A**, where specific deviations of the responses away from the target can be seen for each task and each posture. The statistical analyses show that none of the analyzed parameters were significantly affected by the posture *Order* and that the *Order* did not significantly interact with the *Posture* effect. Neither did *Posture* appear to have had a significant effect on the average error (accuracy) in any of three experiments (**Figure 4B**). More detailed analyses of the pattern of errors, however, reveal some specific effects of *Posture* (see statistics reported on **Table 1**): the global response deviation in relation with the lateral neck flexion, close to zero in the Seated

condition, significantly increased in all three experiments when the subjects were Supine (Aubert-Müller effect in **Figure 4C**). The effect of posture on the perceptive distortion appears to have differed among the three experiments (**Figure 4D**): a significant modulation, but in opposite directions, for cross-modal and unimodal proprioceptive tasks and no difference for the unimodal visual experiment. In conclusion, subjects' posture appears to affect some specific aspect of the average response patterns, but the average error (accuracy) does not significantly change when supine.

On the other hand, the variability of the responses RMSd, reported in **Figure 5A**, appears to have been affected by the subject's posture: in the cross-modal experiment the subjects were significantly less precise when supine, but this was not the case in the unimodal visual and proprioceptive experiments. The change, or lack thereof, in response variability was accompanied by a similar modulation of the sensory weighting shown in **Figure 5B**: only in the cross-modal task did the visual weight significantly increase in the supine posture.

Overall, these results suggest that the use of sensory information during the cross-modal paradigm differs from that of unimodal tasks, and that this weighted processing is significantly affected by posture.

## Analysis of Between-Subjects Differences

To go beyond average responses, we then assessed whether inter-individual variability can provide more insight on the sensory processing underlying the responses observed in the three experiments.

For the Seated condition of the unimodal visual and proprioceptive experiments, the concurrent model predicts, respectively, a negative and positive correlation between the visual weighting and the variability of the motor vector estimation. In fact, a visual weight smaller than 100% in the V-V task, or the larger than 0% in the P-P task, would both correspond to suboptimal solutions and thus to an increase of the variability of the motor vector estimation (see **Supplementary Material, section 2**). The correlation between visual weighting and the variability of the motor vector estimation measured in inter-individuals is reported in **Table 2**.

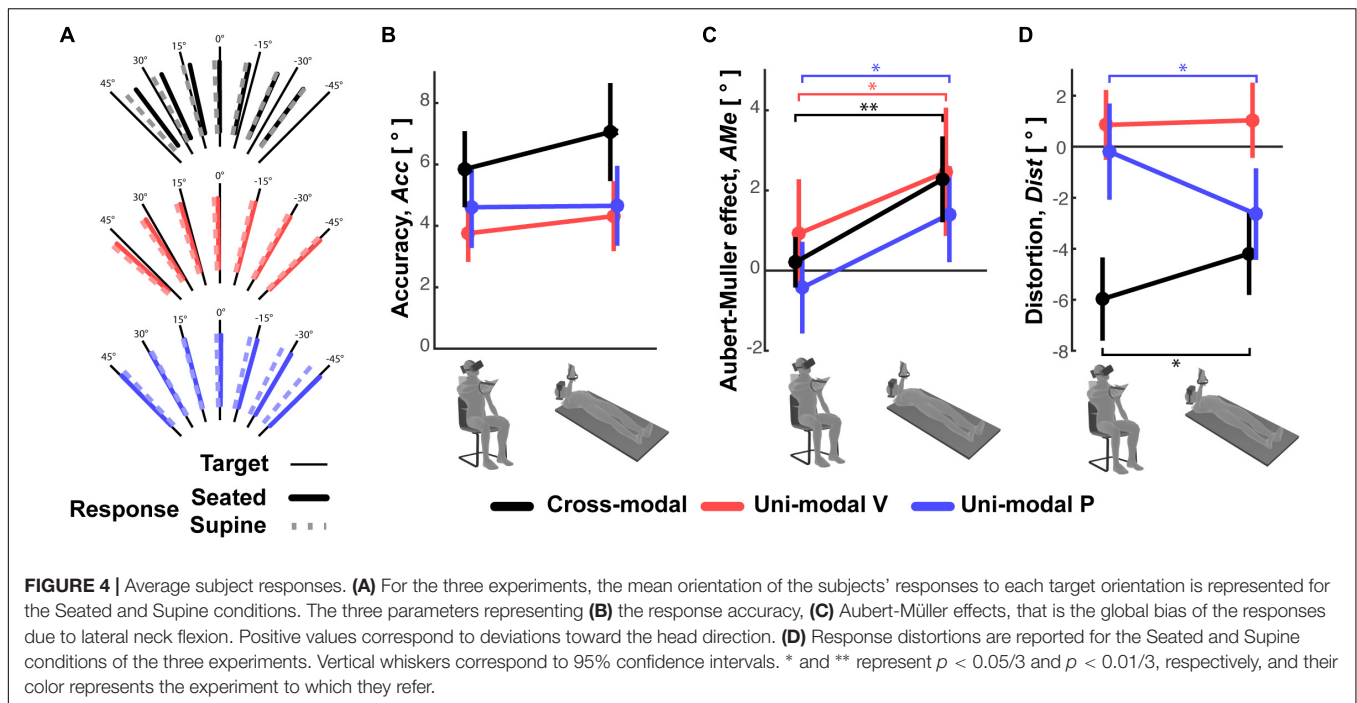


**TABLE 1 |** For each of the experiments (cross-modal, V-P; unimodal visual V-V; unimodal proprioceptive, P-P) the ANOVA main effect of Posture, posture Order and the interaction between these two factors are reported for the Aubert-Müller effect, AMe, the response distortion, Dist, accuracy, Acc, and variability, RMSd, as well as for the relative weight associated to visual information,  $\omega_V$ .

| Exp | Param.     | Effects  |                               |                                |
|-----|------------|--|-------------------------------|--------------------------------|
|     |            | Posture  | Order                         | Posture x Order                |
| V-P | AMe        | $F_{(1,16)} = 12.7, p = \mathbf{0.0026}$           | $F_{(1,16)} = 0.18, p = 0.67$ | $F_{(1,16)} = 0.01, p = 0.89$  |
|     | Dist       | $F_{(1,16)} = 10.6, p = \mathbf{0.0049}$           | $F_{(1,16)} = 0.23, p = 0.63$ | $F_{(1,16)} = 0.61, p = 0.44$  |
|     | Acc        | $F_{(1,16)} = 0.97, p = 0.34$                      | $F_{(1,16)} = 0.97, p = 0.33$ | $F_{(1,16)} = 0.34, p = 0.57$  |
|     | RMSd       | $F_{(1,16)} = 15.3, p = \mathbf{0.0012}$           | $F_{(1,16)} = 0.01, p = 0.91$ | $F_{(1,16)} = 1.41, p = 0.25$  |
|     | $\omega_V$ | $F_{(1,16)} = 23.9, p = \mathbf{16 \cdot 10^{-5}}$ | $F_{(1,16)} = 0.00, p = 0.97$ | $F_{(1,16)} = 0.57, p = 0.46$  |
| V-V | AMe        | $F_{(1,16)} = 9.16, p = \mathbf{0.0080}$           | $F_{(1,16)} = 0.19, p = 0.67$ | $F_{(1,16)} = 2.91, p = 0.11$  |
|     | Dist       | $F_{(1,16)} = 0.01, p = 0.93$                      | $F_{(1,16)} = 0.20, p = 0.65$ | $F_{(1,16)} = 2.49, p = 0.13$  |
|     | Acc        | $F_{(1,16)} = 1.63, p = 0.22$                      | $F_{(1,16)} = 0.42, p = 0.52$ | $F_{(1,16)} = 0.86, p = 0.37$  |
|     | RMSd       | $F_{(1,16)} = 0.10, p = 0.76$                      | $F_{(1,16)} = 0.07, p = 0.79$ | $F_{(1,16)} = 0.85, p = 0.37$  |
|     | $\omega_V$ | $F_{(1,16)} = 2.36, p = 0.14$                      | $F_{(1,16)} = 0.25, p = 0.62$ | $F_{(1,16)} = 3.54, p = 0.08$  |
| P-P | AMe        | $F_{(1,16)} = 10.9, p = \mathbf{0.0044}$           | $F_{(1,16)} = 0.98, p = 0.34$ | $F_{(1,16)} = 2.11, p = 0.16$  |
|     | Dist       | $F_{(1,16)} = 10.7, p = \mathbf{0.0048}$           | $F_{(1,16)} = 0.01, p = 0.92$ | $F_{(1,16)} = 6.93, p = 0.018$ |
|     | Acc        | $F_{(1,16)} = 0.01, p = 0.93$                      | $F_{(1,16)} = 4.94, p = 0.04$ | $F_{(1,16)} = 0.04, p = 0.83$  |
|     | RMSd       | $F_{(1,16)} = 0.85, p = 0.37$                      | $F_{(1,16)} = 2.89, p = 0.11$ | $F_{(1,16)} = 0.98, p = 0.33$  |
|     | $\omega_V$ | $F_{(1,16)} = 0.02, p = 0.89$                      | $F_{(1,16)} = 0.71, p = 0.41$ | $F_{(1,16)} = 4.31, p = 0.054$ |

The significant results after the Bonferroni correction ( $p < 0.05/3$ ) are reported in bold fonts.

Although not statistically significant, the tendency to a negative correlation in the unimodal visual task reported in **Table 2**, is consistent with the model prediction, while the absence of correlation in the P-P experiment is not. This could be due to a significant contribution of the motor noise to *RMSd* in this task, because both memorization and response require active hand movements. Motor noise affects the response variability but not the sensory weight,

thus it might hide an existing correlation between the variability of motor vector estimation and the sensory weighting. The potential influence of motor noise is supported by the fact that the expected correlation seems to exist for the V-V task, where the motor component should be irrelevant.

For the V-P task no clear correlation between  $\omega_V$  and *RMSd* is to be expected, because, as shown in Equation 5, the sensory

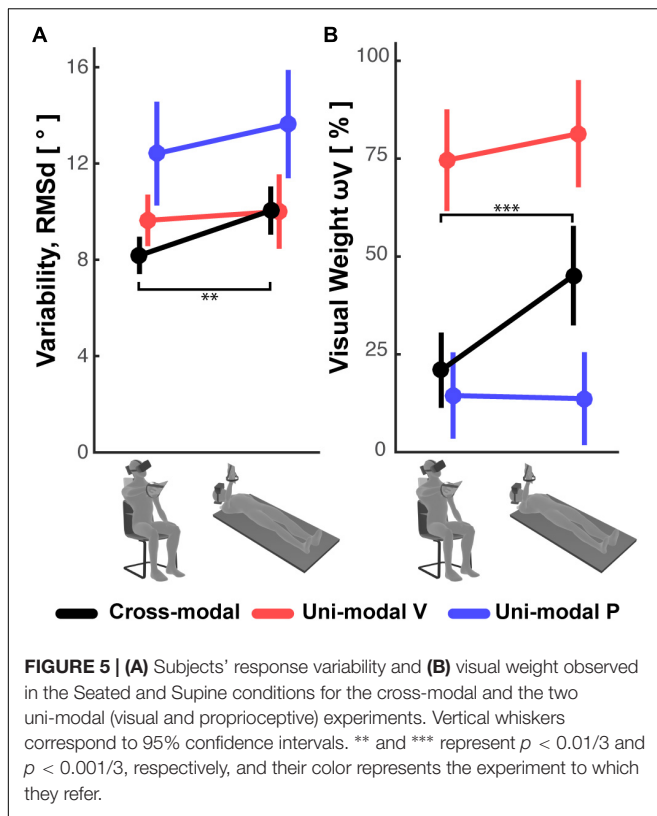


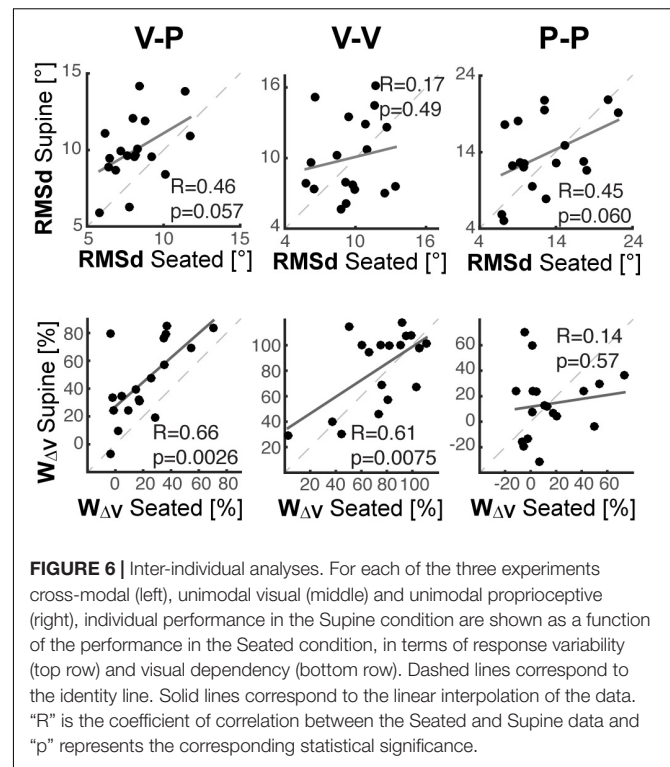
**TABLE 2 |** Coefficient of correlation  $R$  (and associated  $p$ -value) between the variability, RMSd, and visual dependency,  $\omega_V$ , in the Seated condition of the three experiments (Exp).

| Exp | $R$   | $p$  |
|-----|-------|------|
| V-P | 0.11  | 0.65 |
| V-V | -0.41 | 0.09 |
| P-P | 0.17  | 0.51 |

weight theoretically depends only on the noise attributed to the cross-modal sensory transformations, whilst the response variability depends also on the subject's visual and proprioceptive acuity. Moreover, motor noise could play a role, as in the P-P task.

In order to understand whether between-subject differences while seated would affect an individual's performance when supine, we evaluated the correlation between the individual performance in the Seated and Supine conditions. As shown in **Figure 6**, we evaluated the performance in terms of response variability, RMSd, and visual weight,  $\omega_V$ .

The top part of **Figure 6** shows that the ranking of the subject in terms of response precision in the Seated condition tends to be preserved when Supine, but only in the tasks with relevant proprioceptive and motor components (V-P and P-P). Consistent with the results of **Table 2**, this finding suggests that the individual motor noise contributes to the observed response variability and tends to be preserved between postures. The bottom part of **Figure 6** show that in the tasks with a relevant visual component (V-P, V-V), the subjects that are



most visuo-(in)dependent when seated, remain the most visuo-(in)dependent when supine. These correlations suggest that, although different levels of visual-dependency can be observed among the subjects, their visual-dependency ranking was not altered by posture. It follows that the effect of the postural change in the cross-modal task was quite consistent among all of participants.

## Model Predictions

**Figure 7A** graphically represents the model predictions associated with the hypotheses that the lateral neck flexion per se (Neck1 Hp), the increase of the noise in the neck muscles-spindles (Neck2 Hp) or the head misalignment with respect to gravity (Gravity Hp), interferes with the ability to perform cross-modal transformation (detailed model equations are presented in **Supplementary Material, section 3**). Their quantitative comparison with the experimental results is shown in **Figure 7B** in terms of differences between the Seated and Supine condition. Focusing these predictions on the effect of the postural change has two main advantages: first, it compensates for a possible role of individual motor precision or sensory acuity that, as we have shown above, might increase between-subject variability. Second, it simplifies the model by allowing a significant reduction of the number of parameters estimated.

**Figure 7B** show that the "Neck1 Hp," which predicts no changes between Seated and Supine postures for all three, Cross-Modal, Unimodal Visual and Unimodal Proprioceptive tasks, is significantly different from the experimental observations [Hotelling's test:  $T^2 = 93.0$ ,  $F_{(6,12)} = 10.9$ ,  $p = 0.0003$ ]. The "Neck2 Hp" prediction also significantly differs from the experimental

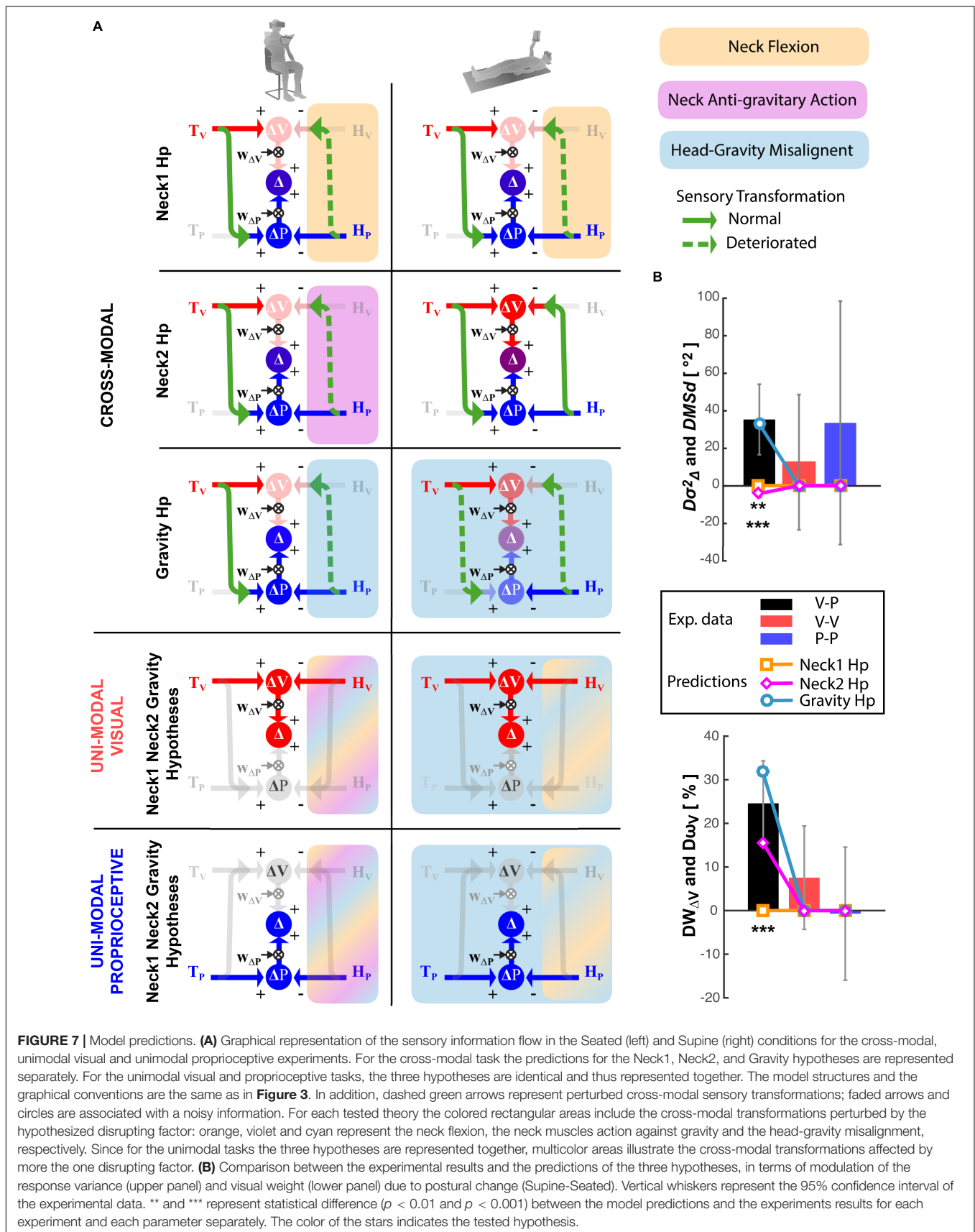


**FIGURE 7 |** Model predictions. **(A)** Graphical representation of the sensory information flow in the Seated (left) and Supine (right) conditions for the cross-modal, unimodal visual and unimodal proprioceptive experiments. For the cross-modal task the predictions for the Neck1, Neck2, and Gravity hypotheses are represented separately. For the unimodal visual and proprioceptive tasks, the three hypotheses are identical and thus represented together. The model structures and the graphical conventions are the same as in Figure 3. In addition, dashed green arrows represent perturbed cross-modal sensory transformations; faded arrows and circles are associated with a noisy information. For each tested theory the colored rectangular areas include the cross-modal transformations perturbed by the hypothesized disrupting factor: orange, violet and cyan represent the neck flexion, the neck muscles action against gravity and the head-gravity misalignent, respectively. Since for the unimodal tasks the three hypotheses are represented together, multicolor areas illustrate the cross-modal transformations affected by more the one disrupting factor. **(B)** Comparison between the experimental results and the predictions of the three hypotheses, in terms of modulation of the response variance (upper panel) and visual weight (lower panel) due to postural change (Supine-Seated). Vertical whiskers represent the 95% confidence interval of the experimental data. \*\* and \*\*\* represent statistical difference ( $p < 0.01$  and  $p < 0.001$ ) between the model predictions and the experiments results for each experiment and each parameter separately. The color of the stars indicates the tested hypothesis.

observations [Hotelling's test:  $T^2 = 34.93$   $F_{(6,12)} = 4.11$ ,  $p = 0.017$ ]. Indeed, although this hypothesis appears to better match the increase of the visual weight when supine, it cannot account for the increase in response variability; since in the Supine posture the neck muscles never act against gravity the model must predict a decrease of the response variability with respect to task performed with the Seated posture, which require a neck muscles' activation during the response phase to support the tilted head.

"Gravity Hp" appears to well capture the fact that the Supine posture increases both the response variability and the visual weight in the cross-modal task only [Hotelling's test:  $T^2 = 9.65$ ,  $F_{(6,12)} = 1.13$ ,  $p = 0.40$ ]. The matching between the Gravity Hp prediction and the experimental data is obtained with  $\sigma_N^2 = 81^2$ , which means that the variance associated with the cross-modal transformation would increase by about 3.5 times when the head is not aligned with gravity.

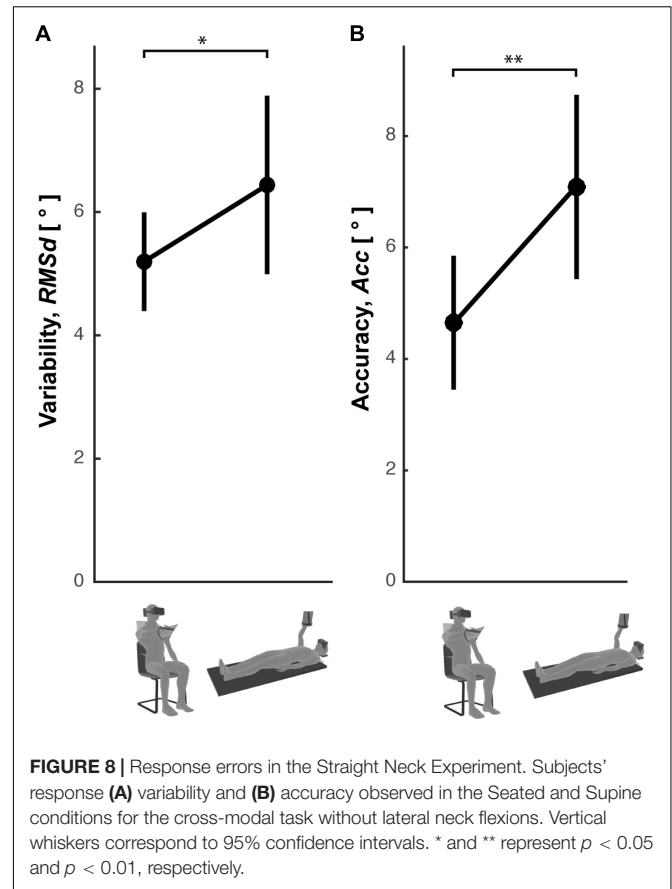
### Straight-Neck Experiment

To confirm the role of the head-gravity alignment on the visuo-proprioceptive transformations (experimental results and the model prediction of **Figure 7**) the precision and the accuracy of the subjects' responses was compared between the Seated and Supine conditions of a cross-modal task performed without lateral neck movements. **Figure 8** shows that, as for the main Cross-Modal Experiment, when supine the subjects are significantly less precise [one-tailed  $t$ -test:  $t_{(11)} = 3.42$ ,  $p = 0.04$ ] and less accurate [one-tailed  $t$ -test:  $t_{(11)} = 2.79$ ,  $p = 0.009$ ] than when seated.

## DISCUSSION

We have performed experiments to try to understand why lateral neck flexions appear to interfere with the visuo-proprioceptive transformations used during reaching/grasping movements (Burns and Blohm, 2010; Tagliabue and McIntyre, 2011, 2014; Tagliabue et al., 2013). This type of cross-modal transformation consists of encoding retinal visual signals into a proprioceptive joint space and, vice-versa, encoding the position/orientation of the hand sensed through joint proprioception in a visual space.

Our first working hypothesis was that neck flexion might perturb the sensory information coming from the eye-hand kinematic chain, which can be used for computing the cross-modal transformation (Sabes, 2011). The lateral neck flexion interference could have two main origins: the rarity of performing eye-hand coordination tasks with such neck configuration (Neck1 Hp) or degradation of the proprioceptive neck information due to the muscle effort necessary to sustain the head's weight (Neck2 Hp). "Neck1 Hp" is related to the difficulty of interpreting correctly the "unusual" sensory signals coming from the flexed neck. As observed for different tasks, motor performance appears indeed to correlate with the relative incidence of the type of movement during everyday life (Howard et al., 2009). "Neck2 Hp" is based on the signal-dependent nature of noisiness of the neck muscles spindles (Abedi Khoozani and Blohm, 2018). An alternative hypothesis,



one that does not involve the eye-hand kinematic chain, was that head misalignment with respect to gravity, and not lateral neck flexion, would mainly interfere with visuo-proprioceptive transformations (Gravity Hp). This hypothesis is based on the fundamental role that gravity would have in reciprocal calibration of the retinal and proprioceptive reference frame (Paillard, 1991).

To test which of these hypotheses better describe the actual functioning of the human central nervous system (CNS) we asked volunteers to perform a virtual-reality task requiring cross-modal transformations, i.e., matching with an unseen hand a memorized visual target orientation, as to grab it, after a lateral neck flexion. The subjects performed this task both in a Seated and Supine position.

The expected effect of changing posture is very different for the three hypotheses. To try to formalize and quantify these predictions we applied an optimal theory of multi-sensory integration to the above-described task. This statistical model, in which the task is concurrently represented in the visual and proprioceptive space (Tagliabue and McIntyre, 2008, 2011, 2012, 2013, 2014; McGuire and Sabes, 2009; Tagliabue et al., 2013; Arnoux et al., 2017; Bernard-Espina et al., 2021) allowed to compute the effects of changing posture in terms of subjects' responses variability and in terms of the relative importance given to the visual and proprioceptive encoding of the information.

The model results show that the "Neck1 Hp" predicts no significant changes in subject precision nor in sensory weighting,

because the lateral neck flexion is the same in the two postural conditions. If the “Neck2 Hp” is correct a decrease of the response variability and an increase of the importance given to visual encoding is to be expected, because when supine a special head support always sustained the head, reducing the neck muscles activation, and hence the neck proprioceptive noise. The “Gravity Hp” predicts an increase of both response variability and weight associated to visual space, because when supine the subject head is always misaligned with respect to gravity, continuously perturbing cross-modal transformations. The results of the “Cross-Modal Experiment” show a significant increase of the response variability and visual weight when supine, so that the “Gravity Hp” prediction is the closest to the experimental observations. With the “Neck-Straight Experiment,” which does not involve lateral head rotations, we were able to disentangle even further the role of gravitational afferences from those generated by neck movements, such as neck muscle spindles and semi-circular canals signals. The persistence, in this experiment as in the task with head rotations, of an increase of subject errors in the supine posture confirms and reinforces the importance of the gravity-head alignment. Overall, these results clearly support the hypothesis of a fundamental role of gravity in the ability of performing cross-modal transformations. More precisely, these findings are consistent with the idea that a misalignment of the head with respect to gravity interferes with the ability of performing cross-modal transformations, that is the encoding of a visual information in the proprioceptive space and vice-versa.

Although the present results support the central role of the external gravitational reference, a role of the neck and of the rest of eye-hand kinematic chain, which is associated with an egocentric processing of the information, should not be fully discarded. We have indeed already reported evidence supporting the coexistence of ego- and exo-centric information processes (Tagliabue and McIntyre, 2012, 2014). Moreover, a role of the visual vertical in the ability to perform cross-modal sensory transformations cannot be excluded, as it has been shown that the vertical direction perception is a highly multisensory process, with gravity, body and scene information interacting (Dyde et al., 2006).

The posture effect on the cross-modal transformations reported here, however, is ascribable to gravitational signals, because in all used experimental paradigms the head/body axis information and the visual information contributing to the vertical perception were identical in the seated and supine condition and the only factor that changed was the misalignment with respect to the gravitational vector.

To be able to exclude the hypothesis that the observed effect of the posture in the cross-modal task could be ascribed to a degradation of the visual or proprioceptive acuity *per se* and not of the sensory transformations, we added two control experiments in which the subjects performed visual and proprioceptive tasks not requiring sensory transformations. The lack of significant differences between the seated and supine condition in terms of response variability and sensory weighting in these uni-modal experiments suggests that the head misalignment with respect to gravity does not significantly alter the unimodal sensory precision *per se*, and thus supports

the idea of a specific effect of posture/gravity on the sensory transformations. The different effect of the posture on the response precision between the cross-modal and unimodal tasks is perfectly in line with the results of the orientation reproduction experiment of McIntyre and Lipshits (2008). They showed indeed that laterally tilting the whole body of subjects by 22.5° clearly increases their response errors in a cross-modal (haptic-visual) task, and not so in two unimodal tasks (visual-visual and haptic-haptic). The consistency with the present results also suggests that the head tilt effects are independent of the tilt axis (pitch or roll).

In our three first experiments we observed that posture also influences some features of the average pattern of subjects' responses. Although our theoretical framework does not provide predictions on this aspect of the subjects' performance, it is interesting to note that the response shifts due to the lateral neck flexion (Aubert-Müller effect) significantly increased when supine, in all three experiments. This result suggests that gravity direction would also contribute to the encoding of the target and response orientation, no matter the modality of the information. This is consistent with Darling and Gilchrist (1991) study on hand orientation reproduction tasks showing that gravitational information influences the encoding of the hand roll. Similarly, the disappearance of the oblique effect when the subject' whole body is laterally tilted in purely visual (McIntyre et al., 2001) and cross-modal (McIntyre and Lipshits, 2008) orientation reproduction tasks was interpreted as an evidence of the use of gravity as a reference to encode orientation cues. In addition to its role in perception, gravity was shown to contribute also to motor encoding, since lateral tilts affected the perception of hand movements direction (Darling et al., 2008) and the control of eye saccades (Pelt et al., 2005).

## Inter-Individual Differences

The analyses of the between-subjects differences suggest that the effect of the head-gravity misalignments on cross-modal transformations is quite robust, since it does not appear to depend on individual characteristics such as visual dependency or precision, which can vary significantly between subjects. The observed inter-subject variability in the Seated condition also suggests that not all subjects perform optimally, in the “Maximum Likelihood” sense (Ernst and Banks, 2002), that is, some subjects sub-optimally combine the visual and proprioceptive representations of the task. As expected, however, those subjects who deviate from the theoretical optimal sensory weighting tends to show larger level of variability.

Lastly, the inter-subject analyses also suggest that the noise of the motor component of the task, which can be different between participants, might represent a relevant part of the performance variability. These observations confirm the rationale of basing our conclusions on within-subject comparisons.

## Vestibular Pathways to Cortical Networks Involved in Visuo-Proprioceptive Transformations

The present section aims at discussing whether the behavioral findings reported here are compatible with the current knowledge

about the anatomy and physiology of the central nervous system. First, the brain areas involved in visuo-proprioceptive transformations will be presented. Second, it will be discussed how the signals related to head orientation with respect to gravity might interact with these brain areas and hence with the cross-modal processing.

The idea that the brain performs cross-modal transformations is supported by several electrophysiological and brain imaging studies. For instance, the encoding of visual stimuli in somatosensory space is consistent with the observation that brain regions such as the somatosensory areas (S) and Brodmann's Area 5 (BA5), which are known to encode the hand grasping configuration and the position of tactile stimulation in the peripersonal space (Koch and Fuster, 1989; Deshpande et al., 2008; Lacey et al., 2009), are activated also by visual stimuli such as images of glossy and rough surfaces, which have a strong "tactile content" (Sun et al., 2016), and by images of familiar manipulable objects (Vingerhoets, 2008). Similarly, the encoding of haptic/proprioceptive information in visual space is fully compatible with the finding that the visual area in the Lateral Occipital Complex, called LOTv, is activated not only by 3D objects images (Moore and Engel, 2001), but also when sensing familiar objects with the hand (Deshpande et al., 2008; Lacey et al., 2009).

A brain area which appears to be a good candidate for performing cross-modal transformations is the Intra-Parietal Sulcus (IPS) which has been shown to have neural activation compatible with the computation of visuo-tactile transformations in monkey (Avillac et al., 2005) and which is known to be involved in the visuo-motor transformations performed during grasp movements (McGuire and Sabes, 2011; Janssen and Scherberger, 2015). Monkey experiments have shown that, in this brain area, the information can be reencoded from the retinal space to the somatosensory space, and vice-versa, thanks to recurrent basis function neural networks (Pouget et al., 2002) which would use the sensory signals relative to the eye-body kinematic chain to "connect" the two sensory spaces. In humans, the Anterior part of IPS is strongly activated when comparing visual to haptic objects, and vice-versa (Grefkes et al., 2002) or when reaching a visual target without visual feedback of the hand (Beurze et al., 2010). Virtual lesions of this area through TMS interfere with visuo-tactile transformations, but not with uni-modal, visual and tactile, tasks (Buelte et al., 2008). The planning of cross-modal tasks, such as reach-and-grasp visual objects with an unseen hand, also appears affected by TMS of the anterior IPS (Verhagen et al., 2012).

Focusing on the main finding of the present study, one can ask through which neural pathway the head-gravity misalignment can affect the visuo-proprioceptive transformations occurring in the IPS. At the peripheral level, the information about the head orientation with respect to gravity is mainly provided by a complex integration of the signals from different areas of the otolithic organ (Chartrand et al., 2016) arising from both the left and right organs (Uchino and Kushiro, 2011). Semicircular canal and neck proprioception, which are combined to otolithic information already at the level of the vestibular nuclei (Gdowski and McCrea, 2000; Dickman and Angelaki,

2002), can also contribute to the head orientation estimation. However, since in the Straight Neck Experiment the posture effect was also observed when no head rotations, nor neck flexions, occurred, we can conclude that the otolithic signals are sufficient to affect visuo-proprioceptive transformations. At the central level, it is known that the vestibular-otolithic information can reach the parietal cortex through the posterior vestibular thalamocortical pathway (Hitier et al., 2014; Cullen, 2019). Specific otolithic afferences have been indeed observed in the IPS: otolithic stimulations activate neurons of Ventral IPS in monkeys (Schlack et al., 2002; Chen et al., 2011), with half of the neurons in this area which receive vestibular inputs (Bremmer, 2005), and human fMRI studies also show IPS activations resulting from saccular stimulations (Miyamoto et al., 2007; Schlindwein et al., 2008). Electrical stimulations of the anterior-IPS have also been reported to elicit linear vestibular sensations in a patient (Blanke et al., 2000). Since head-gravity misalignment modulates the otolithic inputs and the otolithic system projects to the IPS, it is plausible that gravitational information would be integrated in the recurrent basis-function neural network of this brain areas (Pouget et al., 2002; Avillac et al., 2005) to "connect" the visual and the proprioceptive space. As a consequence, it is reasonable that an alteration of the otolithic gravitational input due to the head tilt can alter cross-modal transformations.

There are other neural structures involved in motor control, such as the cerebellum, that receive otolithic inputs (Büttner-Ennever, 1999), and could therefore contribute to the effect of the head-gravity misalignment observed here. However, the predictive functions of the cerebellum (Blakemore and Sirigu, 2003), which is fundamental for the control of rapid movements, probably plays only a marginal role in the slow, quasi-static, movements tested here.

## Otolithic Signal-Dependent Noise or Unusualness?

Once we have established that the head-gravity misalignment affects visuo-proprioceptive transformations and which neural circuits could be responsible for this phenomenon, the following question remains open: "How does tilting the head interfere with the cross-modal sensory processing?" At least two possible explanations exist: first, the unusualness of performing eye-hand coordination tasks with the head tilted; second, a possible signal-dependent increase of the otolithic noise with the head tilt.

Some studies have been able to correctly predict the effect of tilting the head on subjective vertical experiments by assuming that the noise of the otolithic signals linearly increases with the signal amplitude (Vrijer et al., 2008), hence the second hypothesis appears reasonable. To our knowledge, however, there are no electrophysiological studies clearly supporting the signal-dependent modulation of the otolithic noise (Fagerson and Barmack, 1995; Yu et al., 2012), therefore, the fact that unusual tilt of the head could interfere with cross-modal sensory transformations should not be "*a priori*" discarded. The "usualness effect" appears consistent with IPS recurrent neural networks functioning (Pouget et al., 2002) in which the synaptic weights necessary to perform visuo-proprioceptive

transformations are learnt through experience. Since the upright position is largely the most common head orientation in our everyday life, it is possible that these neural networks become “optimized” for such head position and significantly less effective when otolithic afferences signal a head tilt for which we have a limited experience. A way to test this hypothesis could be to perform experiments on subjects that are in a tilted position, or in weightlessness, for a long period of time and see whether they can learn to perform cross-modal transformations as effectively as in the upright position, despite the altered or lacking otolithic signals.

## CONCLUSION AND PERSPECTIVES

The results of the present study show the relevant role of the head-gravity alignment in the ability of performing visuo-proprioceptive transformations necessary to correctly reach and grasp objects. This finding suggests that the neural networks in the parietal cortex involved in the cross-modal processing of sensory information are more efficient when the otolithic afferences correspond to an upright head position.

This finding has interesting implications: for instance, the application of this idea to the clinical field suggests that vestibular pathologies might perturb not only equilibrium and eye movements, but also the eye-hand coordination, which is rarely assessed in these patients. Our findings might be beneficial also to healthy subjects, in that they can contribute to the ergonomic principles used when conceiving a new working station: avoiding visuo-manual tasks when the operator is tilted would indeed maximize their execution precision. Finally, there are potential space-related applications: the astronauts’ eye-hand coordination might be perturbed in weightlessness, because of the lack of the gravitational reference used for visuo-proprioceptive transformations. To prevent potential deterioration of performances in delicate visuo-manual tasks, as controlling robotic-arms or piloting space vehicles, specific training performed in “altered” posture could therefore be beneficial.

## DATA AVAILABILITY STATEMENT

The raw data supporting the conclusions of this article will be made available by the authors, without undue reservation.

## REFERENCES

- Abedi Khoozani, P., and Blohm, G. (2018). Neck muscle spindle noise biases reaches in a multisensory integration task. *J. Neurophysiol.* 120, 893–909. doi: 10.1152/jn.00643.2017
- Arnoux, L., Fromentin, S., Farotto, D., Beraneck, M., McIntyre, J., and Tagliabue, M. (2017). The visual encoding of purely proprioceptive intermanual tasks is due to the need of transforming joint signals, not to their interhemispheric transfer. *J. Neurophysiol.* 118, 1598–1608. doi: 10.1152/jn.00140.2017
- Avillac, M., Deneve, S., Olivier, E., Pouget, A., and Duhamel, J.-R. (2005). Reference frames for representing visual and tactile locations in parietal cortex. *Nat. Neurosci.* 8, 941–949. doi: 10.1038/nn1480

## ETHICS STATEMENT

The studies involving human participants were reviewed and approved by CER Université de Paris. The patients/participants provided their written informed consent to participate in this study.

## AUTHOR CONTRIBUTIONS

MT conceived and supervised the experiments, performed the final data analysis, and wrote the first draft of the manuscript. JB-E performed the experiments and data analyses. DD developed the experimental setup and performed the experiments. All authors contributed to manuscript revisions, read and approved the submitted version.

## FUNDING

This work was supported by the *Centre National d’Etudes Spatiales* (DAR 2017/4800000906, DAR 2018/4800000948, 2019/4800001041). JB-E was supported by a Ph.D. fellowship of the *École Doctorale Cerveau-Cognition-Comportement* (ED3C, n°158, Sorbonne Université and Université de Paris). The research team is supported by the *Centre National de la Recherche Scientifique* and the *Université de Paris*. This study contributes to the IdEx Université de Paris ANR-18-IDEX-0001.

## ACKNOWLEDGMENTS

We wish to thank Patrice Jegouzo from the mechanical workshop of the Université de Paris for the precious help in conceiving and realizing the head support for the experiments.

## SUPPLEMENTARY MATERIAL

The Supplementary Material for this article can be found online at: <https://www.frontiersin.org/articles/10.3389/fnint.2022.788905/full#supplementary-material>

- Bernard-Espina, J., Beraneck, M., Maier, M. A., and Tagliabue, M. (2021). Multisensory integration in stroke patients: a theoretical approach to reinterpret upper-limb proprioceptive deficits and visual compensation’. *Front. Neurosci.* 15:319. doi: 10.3389/fnins.2021.646698
- Beurze, S. M., Toni, I., Pisella, L., and Medendorp, W. P. (2010). Reference frames for reach planning in human parietofrontal cortex. *J. Neurophysiol.* 104, 1736–1745. doi: 10.1152/jn.01044.2009
- Blakemore, S. J., and Sirigu, A. (2003). Action prediction in the cerebellum and in the parietal lobe. *Exp. Brain Res.* 153, 239–245. doi: 10.1007/s00221-003-1597-z
- Blanke, O., Perrig, S., Thut, G., Landis, T., and Seeck, M. (2000). Simple and complex vestibular responses induced by electrical cortical stimulation of the parietal cortex in humans. *J. Neurol. Neurosurg. Psychiatry* 69, 553–556. doi: 10.1136/jnnp.69.4.553

- Bremmer, F. (2005). Navigation in space—the role of the macaque ventral intraparietal area. *J. Physiol.* 566, 29–35. doi: 10.1111/jphysiol.2005.082552
- Buelte, D., Meister, I. G., Staedtgen, M., Dambeck, N., Sparing, R., Grefkes, C., et al. (2008). The role of the anterior intraparietal sulcus in crossmodal processing of object features in humans: an rTMS study. *Brain Res.* 1217, 110–118. doi: 10.1016/j.brainres.2008.03.075
- Burns, J. K., and Blohm, G. (2010). Multi-sensory weights depend on contextual noise in reference frame transformations. *Front. Hum. Neurosci.* 4:221. doi: 10.3389/fnhum.2010.00221
- Büttner-Ennever, J. A. (1999). A review of otolith pathways to brainstem and cerebellum. *Ann. N. Y. Acad. Sci.* 871, 51–64. doi: 10.1111/j.1749-6632.1999.tb09175.x
- Chartrand, T., McCollum, G., Hanes, D. A., and Boyle, R. D. (2016). Symmetries of a generic utricular projection: neural connectivity and the distribution of utricular information. *J. Math. Biol.* 72, 727–753. doi: 10.1007/s00285-015-0900-5
- Chen, A., DeAngelis, G. C., and Angelaki, D. E. (2011). Representation of vestibular and visual cues to self-motion in ventral intraparietal cortex. *J. Neurosci.* 31, 12036–12052. doi: 10.1523/JNEUROSCI.0395-11.2011
- Cluff, T., Crevecoeur, F., and Scott, S. H. (2015). A perspective on multisensory integration and rapid perturbation responses. *Vis. Res.* 110, 215–222. doi: 10.1016/j.visres.2014.06.011
- Crevecoeur, F., Munoz, D. P., and Scott, S. H. (2016). Dynamic multisensory integration: somatosensory speed trumps visual accuracy during feedback control. *J. Neurosci.* 36, 8598–8611. doi: 10.1523/JNEUROSCI.0184-16.2016
- Cullen, K. E. (2019). Vestibular processing during natural self-motion: implications for perception and action. *Nat. Rev. Neurosci.* 20, 346–363. doi: 10.1038/s41583-019-0153-1
- Darling, W. G., and Gilchrist, L. (1991). Is there a preferred coordinate system for perception of hand orientation in three-dimensional space? *Exp. Brain Res.* 85, 405–416. doi: 10.1007/BF00229417
- Darling, W. G., Viaene, A. N., Peterson, C. R., and Schmiedeler, J. P. (2008). Perception of hand motion direction uses a gravitational reference. *Exp. Brain Res.* 186, 237–248. doi: 10.1007/s00221-007-1227-2
- Deshpande, G., Hu, X., Stilla, R., and Sathian, K. (2008). Effective connectivity during haptic perception: a study using Granger causality analysis of functional magnetic resonance imaging data. *NeuroImage* 40, 1807–1814. doi: 10.1016/j.neuroimage.2008.01.044
- Dickman, J. D., and Angelaki, D. E. (2002). Vestibular convergence patterns in vestibular nuclei neurons of alert primates. *J. Neurophysiol.* 88, 3518–3533. doi: 10.1152/jn.00518.2002
- Dyde, R. T., Jenkin, M. R., and Harris, L. R. (2006). The subjective visual vertical and the perceptual upright. *Exp. Brain Res.* 173, 612–622. doi: 10.1007/s00221-006-0405-y
- Ernst, M. O., and Banks, M. S. (2002). Humans integrate visual and haptic information in a statistically optimal fashion. *Nature* 415, 429–433. doi: 10.1038/415429a
- Fagerson, M. H., and Barmack, N. H. (1995). Responses to vertical vestibular stimulation of neurons in the nucleus reticularis gigantocellularis in rabbits. *J. Neurophysiol.* 73, 2378–2391. doi: 10.1152/jn.1995.73.6.2378
- Gdowski, G. T., and McCreary, R. A. (2000). Neck proprioceptive inputs to primate vestibular nucleus neurons. *Exp. Brain Res.* 135, 511–526. doi: 10.1007/s002210000542
- Grefkes, C., Weiss, P. H., Zilles, K., and Fink, G. R. (2002). Crossmodal processing of object features in human anterior intraparietal cortex: an fMRI study implies equivalencies between humans and monkeys. *Neuron* 35, 173–184. doi: 10.1016/s0896-6273(02)00741-9
- Guerraz, M., Poquin, D., and Ohlmann, T. (1998). The role of head-centric spatial reference with a static and kinetic visual disturbance. *Percept. Psychophys.* 60, 287–295. doi: 10.3758/bf03206037
- Hitier, M., Besnard, S., and Smith, P. F. (2014). Vestibular pathways involved in cognition. *Front. Integr. Neurosci.* 8:59. doi: 10.3389/fnint.2014.00059
- Howard, I. S., Ingram, J. N., Körding, K. P., and Wolpert, D. M. (2009). Statistics of natural movements are reflected in motor errors. *J. Neurophysiol.* 102, 1902–1910. doi: 10.1152/jn.00013.2009
- Janssen, P., and Scherberger, H. (2015). Visual guidance in control of grasping. *Annu. Rev. Neurosci.* 38, 69–86. doi: 10.1146/annurev-neuro-071714-034028
- Koch, K. W., and Fuster, J. M. (1989). Unit activity in monkey parietal cortex related to haptic perception and temporary memory. *Exp. Brain Res.* 76, 292–306. doi: 10.1007/BF00247889
- Lacey, S., Tal, N., Amedi, A., and Sathian, K. (2009). A putative model of multisensory object representation. *Brain Topogr.* 21, 269–274. doi: 10.1007/s10548-009-0087-4
- McGuire, L. M. M., and Sabes, P. N. (2009). Sensory transformations and the use of multiple reference frames for reach planning. *Nat. Neurosci.* 12, 1056–1061. doi: 10.1038/nn.2357
- McGuire, L. M. M., and Sabes, P. N. (2011). Heterogeneous representations in the superior parietal lobule are common across reaches to visual and proprioceptive targets. *J. Neurosci.* 31, 6661–6673. doi: 10.1523/JNEUROSCI.2921-10.2011
- McIntyre, J., and Lipshits, M. (2008). Central processes amplify and transform anisotropies of the visual system in a test of visual-haptic coordination. *J. Neurosci.* 28, 1246–1261. doi: 10.1523/JNEUROSCI.2066-07.2008
- McIntyre, J., Lipshits, M., Zaoui, M., Berthoz, A., and Gurfinkel, V. (2001). Internal reference frames for representation and storage of visual information: the role of gravity. *Acta Astronaut.* 49, 111–121. doi: 10.1016/s0094-5765(01)00087-x
- Miyamoto, T., Fukushima, K., Takada, T., de Waele, C., and Vidal, P.-P. (2007). Saccular stimulation of the human cortex: a functional magnetic resonance imaging study. *Neurosci. Lett.* 423, 68–72. doi: 10.1016/j.neulet.2007.06.036
- Moore, C., and Engel, S. A. (2001). Neural response to perception of volume in the lateral occipital complex. *Neuron* 29, 277–286. doi: 10.1016/s0896-6273(01)00197-0
- Paillard, J. (1991). “Knowing where and knowing how to get there,” in *Brain And Space*, ed. J. Paillard (Oxford: Oxford University Press), 461–481.
- Pelt, S. V., Gisbergen, J. A. M. V., and Mendendorp, W. P. (2005). Visuospatial memory computations during whole-body rotations in roll. *J. Neurophysiol.* 94, 1432–1442. doi: 10.1152/jn.00018.2005
- Pouget, A., Deneve, S., and Duhamel, J.-R. (2002). A computational perspective on the neural basis of multisensory spatial representations. *Nat. Rev. Neurosci.* 3, 741–747. doi: 10.1038/nrn914
- Roll, J. P., Popov, K., Gurfinkel, V., Lipshits, M., André-Deshays, C., Gilhodes, J. C., et al. (1993). Sensorimotor and perceptual function of muscle proprioception in microgravity. *J. Vestib. Res.* 3, 259–273.
- Sabes, P. N. (2011). Sensory integration for reaching: models of optimality in the context of behavior and the underlying neural circuits. *Prog. Brain Res.* 191, 195–209. doi: 10.1016/B978-0-444-53752-2.00004-7
- Sarlegna, F. R., and Sainburg, R. L. (2007). The effect of target modality on visual and proprioceptive contributions to the control of movement distance. *Exp. Brain Res.* 176, 267–280. doi: 10.1007/s00221-006-0613-5
- Sarlegna, F. R., and Sainburg, R. L. (2009). The roles of vision and proprioception in the planning of reaching movements. *Adv. Exp. Med. Biol.* 629, 317–335. doi: 10.1007/978-0-387-77064-2\_16
- Sarlegna, F. R., Przybyla, A., and Sainburg, R. L. (2009). The influence of target sensory modality on motor planning may reflect errors in sensori-motor transformations. *Neuroscience* 164, 597–610. doi: 10.1016/j.neuroscience.2009.07.057
- Schlack, A., Hoffmann, K.-P., and Bremmer, F. (2002). Interaction of linear vestibular and visual stimulation in the macaque ventral intraparietal area (VIP). *Eur. J. Neurosci.* 16, 1877–1886. doi: 10.1046/j.1460-9568.2002.02251.x
- Schwindwein, P., Mueller, M., Bauermann, T., Brandt, T., Stoeter, P., and Dieterich, M. (2008). Cortical representation of saccular vestibular stimulation: VEMPs in fMRI. *NeuroImage* 39, 19–31. doi: 10.1016/j.neuroimage.2007.08.016
- Sober, S. J., and Sabes, P. N. (2005). Flexible strategies for sensory integration during motor planning. *Nat. Neurosci.* 8, 490–497. doi: 10.1038/nn1427
- Sun, H.-C., Welchman, A. E., Chang, D. H. F., and Di Luca, M. (2016). Look but don't touch: visual cues to surface structure drive somatosensory cortex. *NeuroImage* 128, 353–361. doi: 10.1016/j.neuroimage.2015.12.054
- Tagliabue, M., and McIntyre, J. (2008). “Multiple and multimodal reference frames for eye-hand coordination,” in *Proceedings of the Program Neuroscience meeting*, (Washington, DC: Society for Neuroscience), 466.15.

- Tagliabue, M., and McIntyre, J. (2011). Necessity is the mother of invention: reconstructing missing sensory information in multiple, concurrent reference frames for eye-hand coordination. *J. Neurosci.* 31, 1397–1409. doi: 10.1523/JNEUROSCI.0623-10.2011
- Tagliabue, M., and McIntyre, J. (2012). Eye-hand coordination when the body moves: Dynamic egocentric and exocentric sensory encoding. *Neurosci. Lett.* 513, 78–83. doi: 10.1016/j.neulet.2012.02.011
- Tagliabue, M., and McIntyre, J. (2013). When kinesthesia becomes visual: a theoretical justification for executing motor tasks in visual space. *PLoS One* 8:e68438. doi: 10.1371/journal.pone.0068438
- Tagliabue, M., and McIntyre, J. (2014). A modular theory of multisensory integration for motor control. *Front. Comput. Neurosci.* 8:1. doi: 10.3389/fncom.2014.00001
- Tagliabue, M., Arnoux, L., and McIntyre, J. (2013). Keep your head on straight: facilitating sensori-motor transformations for eye-hand coordination. *Neuroscience* 248, 88–94. doi: 10.1016/j.neuroscience.2013.05.051
- Uchino, Y., and Koshiro, K. (2011). Differences between otolith- and semicircular canal-activated neural circuitry in the vestibular system. *Neurosci. Res.* 71, 315–327. doi: 10.1016/j.neures.2011.09.001
- Verhagen, L., Dijkerman, H. C., Medendorp, W. P., and Toni, I. (2012). Cortical dynamics of sensorimotor integration during grasp planning. *J. Neurosci.* 32, 4508–4519. doi: 10.1523/jneurosci.5451-11.2012
- Vingerhoets, G. (2008). Knowing about tools: neural correlates of tool familiarity and experience. *NeuroImage* 40, 1380–1391. doi: 10.1016/j.neuroimage.2007.12.058
- Vrijer, M. D., Medendorp, W. P., and Gisbergen, J. A. M. V. (2008). Shared computational mechanism for tilt compensation accounts for biased verticality percepts in motion and pattern vision. *J. Neurophysiol.* 99, 915–930. doi: 10.1152/jn.00921.2007
- Yu, X.-J., Dickman, J. D., and Angelaki, D. E. (2012). Detection thresholds of macaque otolith afferents. *J. Neurosci.* 32, 8306–8316. doi: 10.1523/JNEUROSCI.1067-12.2012

**Conflict of Interest:** The authors declare that the research was conducted in the absence of any commercial or financial relationships that could be construed as a potential conflict of interest.

**Publisher's Note:** All claims expressed in this article are solely those of the authors and do not necessarily represent those of their affiliated organizations, or those of the publisher, the editors and the reviewers. Any product that may be evaluated in this article, or claim that may be made by its manufacturer, is not guaranteed or endorsed by the publisher.

Copyright © 2022 Bernard-Espina, Dal Canto, Beranek, McIntyre and Tagliabue. This is an open-access article distributed under the terms of the Creative Commons Attribution License (CC BY). The use, distribution or reproduction in other forums is permitted, provided the original author(s) and the copyright owner(s) are credited and that the original publication in this journal is cited, in accordance with accepted academic practice. No use, distribution or reproduction is permitted which does not comply with these terms.

## *Supplementary Material*

### 1 Optimality in multisensory integration

The motor vector  $\Delta$  is the weighted sum of the sensory estimates in the visual ( $\Delta V$ ) and proprioceptive ( $\Delta P$ ) modality, and its variance is:

$$\sigma_{\Delta}^2 = W_{\Delta P}^2 \sigma_{\Delta P}^2 + W_{\Delta V}^2 \sigma_{\Delta V}^2 + 2W_{\Delta P}W_{\Delta V}cov(\Delta P, \Delta V) \quad (\text{S1})$$

where  $W_{\Delta P} + W_{\Delta V} = 1$ .

According to the Maximum Likelihood Principle (MLP), to minimize the motor vector's variance  $\sigma_{\Delta}^2$ , the sensory weights  $W_{\Delta V}$  and  $W_{\Delta P}$  are the following:

$$W_{\Delta V} = \frac{\sigma_{\Delta P}^2 - cov(\Delta V, \Delta P)}{\sigma_{\Delta V}^2 + \sigma_{\Delta P}^2 - 2cov(\Delta V, \Delta P)}, \quad W_{\Delta P} = \frac{\sigma_{\Delta V}^2 - cov(\Delta V, \Delta P)}{\sigma_{\Delta V}^2 + \sigma_{\Delta P}^2 - 2cov(\Delta V, \Delta P)} \quad (\text{S2})$$

The optimal solutions for the cross-modal task (V-P), unimodal visual task (V-V) and unimodal proprioceptive task (P-P) are described in the Manuscript (equations 5-7). For further details on the mathematical procedure, please refer to Supplementary Material of Bernard-Espina et al. (2021).

### 2 Predictions for sub-optimal strategies

For the unimodal tasks, the MLP predicts that a visual weight smaller than 100% in the V-V task, or larger than 0% in the P-P task, would correspond to a suboptimal strategy, increasing the variance of the motor vector.

The experimental results suggest that not all subjects used the sensory information in an optimal fashion (see Manuscript, section "Analysis of between-subjects differences" in Results).

#### 2.1 Unimodal visual task (V-V)

For the V-V task, the variance associated with the visual and proprioceptive representations are the following:

$$\begin{array}{l|l} \text{Target} & \text{Hand} \\ \hline \sigma_{\Delta V}^2 = \sigma_{T_V}^2 & + \sigma_{H_V}^2 \\ \sigma_{\Delta P}^2 = \sigma_{T_V}^2 + \sigma_{V \rightarrow P}^2 & + \sigma_{H_V}^2 + \sigma_{V \rightarrow P}^2 \end{array} \quad (\text{S3})$$

Since there is no proprioceptive information, the proprioceptive representation of both the target and the hand need to be reconstructed from the visual information. Therefore, the covariance between visual and proprioceptive representations is:

$$\text{cov}(\Delta P, \Delta V) = \sigma_{T_V}^2 + \sigma_{H_V}^2 = \sigma_{\Delta V}^2 \quad (\text{S4})$$

If we assume a generic, therefore possibly suboptimal, visual weight  $W$  (with  $W \in [0, 1]$ ), and replacing S3 and S4 in S1, we obtain:

$$\sigma_{\Delta}^2 = \sigma_{\Delta V}^2 + (1 - W)^2 (2\sigma_{V \rightarrow P}^2) \quad (\text{S5})$$

To complete this formulation, we must take into consideration the head tilt occurring during the response phase which induces a noise in the cross-modal sensory transformation  $\sigma_N^2$ . Therefore, equation S5 becomes:

$$\sigma_{\Delta}^2 = \sigma_{\Delta V}^2 + (1 - W)^2 (2\sigma_{V \rightarrow P}^2 + \sigma_N^2) \quad (\text{S6})$$

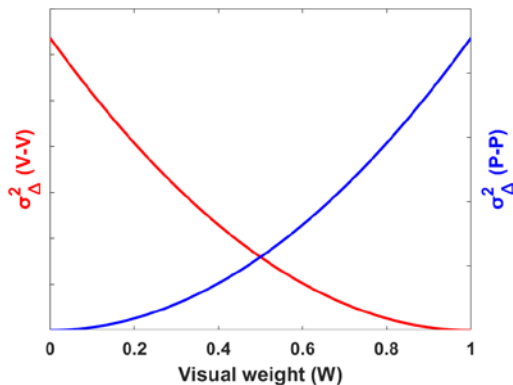
It follows that, if  $W$  is smaller than the optimal visual weight  $W_{\Delta V} = 1$  (equation 6 in the main text), the variability of the associated movement vector estimation is larger than the variability of the optimal MLP solution  $\sigma_{\Delta}^2 = \sigma_{\Delta V}^2$  (Supplementary Figure 1). A negative correlation between  $W$  and  $\sigma_{\Delta}^2$  is hence to be expected.

## 2.2 Unimodal proprioceptive task (P-P)

Similarly, for the P-P task, we obtain the following:

$$\sigma_{\Delta}^2 = \sigma_{\Delta P}^2 + W^2 (2\sigma_{P \rightarrow V}^2 + \sigma_N^2) \quad (\text{S7})$$

Therefore, if  $W$  is larger than the optimal solution  $W_{\Delta V} = 0$  (equation 7 in the main text), the variability of the associated movement vector estimation is larger than the variability of the optimal MLP solution  $\sigma_{\Delta}^2 = \sigma_{\Delta P}^2$  (Supplementary Figure 1). A positive correlation between  $W$  and  $\sigma_{\Delta}^2$  is hence to be expected.



**Supplementary Figure 1.** Graphical representation of the variance value for the unimodal V-V task (see equation S6) and P-P task (see equation S7), depending on the visual weight  $W$ . The minimal variance is observed for the optimal weights, as described in the main text (equations 6 and 7).

### 3 Model predictions for the difference between seated and supine postures

Based on the optimal equations for multi-sensory integration (see equations 5-7 in the Manuscript), we present here the equations for the difference between the Supine and Seated posture predicted by the model for the movement execution variance,  $D\sigma_{ME}^2$ , and for the weight associated with visual representation of the task,  $DW_{\Delta V}$ , for the ‘Neck1’, ‘Neck2’ and ‘Gravity’ hypotheses.

#### 3.1 Unimodal tasks

For unimodal tasks (V-V and P-P), since no cross-modal sensory transformations are involved, the equations of both movement execution variance and visual weight do not contain  $\sigma_N^2$  terms representing the effect of head tilt and/or neck flexions on sensory transformation.

$$\text{V-V: } \begin{cases} \sigma_{\Delta, Seated}^2 = \sigma_{T_V}^2 + \sigma_{H_V}^2 \\ \sigma_{\Delta, Supine}^2 = \sigma_{T_V}^2 + \sigma_{H_V}^2 \end{cases} \quad (\text{S8})$$

$$\text{P-P: } \begin{cases} \sigma_{\Delta, Seated}^2 = \sigma_{T_P}^2 + \sigma_{H_P}^2 \\ \sigma_{\Delta, Supine}^2 = \sigma_{T_P}^2 + \sigma_{H_P}^2 \end{cases} \quad (\text{S9})$$

It follows that all the three hypotheses predict no effect of posture on the subject performances for both unimodal tasks:

$$\boxed{\begin{aligned} D\sigma_{ME}^2 &= 0 \\ DW_{\Delta V} &= 0 \end{aligned}} \quad (\text{S10})$$

#### 3.2 Cross-modal visuo-proprioceptive task

For the cross-modal task (V-P), the three hypotheses differ by where the noise ( $\sigma_N^2$ ) added to the cross-modal sensory transformations is involved. For simplicity we assume that noise associated with the transformations from vision to proprioception of the target information ( $\sigma_{V \rightarrow P}^2$ ) and from proprioception to vision of the reaching hand information ( $\sigma_{P \rightarrow V}^2$ ) are characterized by a similar variance.

$$\sigma_{V \rightarrow P}^2 = \sigma_{P \rightarrow V}^2 = \sigma_T^2 \quad (\text{S11})$$

##### 3.2.1 Neck1 hypothesis

According to Neck1 hypothesis, noise ( $\sigma_N^2$ ) should be added to the cross-modal sensory transformations when the neck is laterally flexed, that is during the response phase ( $\sigma_{P \rightarrow V}^2 + \sigma_N^2$ ), and not during the target memorization ( $\sigma_{V \rightarrow P}^2$ ), and this regardless of the body posture.

For the variances, we have:

$$\begin{cases} \sigma_{ME,Seated}^2 = \sigma_{\Delta,Seated}^2 + \sigma_m^2 \\ \sigma_{ME,Supine}^2 = \sigma_{\Delta,Supine}^2 + \sigma_m^2 \end{cases} \quad (\text{S12})$$

with:

$$\begin{cases} \sigma_{\Delta,Seated}^2 = \sigma_{TV}^2 + \sigma_{HP}^2 + \frac{\sigma_{V \rightarrow P}^2 (\sigma_{P \rightarrow V}^2 + \sigma_N^2)}{\sigma_{V \rightarrow P}^2 + \sigma_{P \rightarrow V}^2 + \sigma_N^2} \\ \sigma_{\Delta,Supine}^2 = \sigma_{TV}^2 + \sigma_{HP}^2 + \frac{\sigma_{V \rightarrow P}^2 (\sigma_{P \rightarrow V}^2 + \sigma_N^2)}{\sigma_{V \rightarrow P}^2 + \sigma_{P \rightarrow V}^2 + \sigma_N^2} \end{cases} \quad (\text{S13})$$

Then,  $D\sigma_{ME}^2 = \sigma_{ME,Supine}^2 - \sigma_{ME,Seated}^2$  is:

$$D\sigma_{ME}^2 = 0 \quad (\text{S14})$$

For the visual weights, we have:

$$\begin{cases} W_{\Delta V,Seated} = \frac{\sigma_{V \rightarrow P}^2}{\sigma_{V \rightarrow P}^2 + \sigma_{P \rightarrow V}^2 + \sigma_N^2} \\ W_{\Delta V,Supine} = \frac{\sigma_{V \rightarrow P}^2}{\sigma_{V \rightarrow P}^2 + \sigma_{P \rightarrow V}^2 + \sigma_N^2} \end{cases} \quad (\text{S15})$$

Then,  $DW_{\Delta V} = W_{\Delta V,Supine} - W_{\Delta V,Seated}$  is:

$$DW_{\Delta V} = 0 \quad (\text{S16})$$

The Neck1 hypothesis predicts no difference between postures in terms of variance and visual weight.

### 3.2.2 Neck2 hypothesis

According to Neck2 hypothesis, noise ( $\sigma_N^2$ ) should be added to the cross-modal sensory transformations when the neck muscles are active against gravity, that is when the neck is laterally flexed during the response phase of the seated condition ( $\sigma_{P \rightarrow V}^2 + \sigma_N^2$ ). No additional noise is added during the memorization phase of the Seated condition ( $\sigma_{V \rightarrow P}^2$ ) and during both task phases in the Supine condition ( $\sigma_{V \rightarrow P}^2$  and  $\sigma_{P \rightarrow V}^2$ ).

For the variances, we have:

$$\begin{cases} \sigma_{\Delta, Seated}^2 = \sigma_{T_V}^2 + \sigma_{H_P}^2 + \frac{\sigma_{V \rightarrow P}^2 (\sigma_{P \rightarrow V}^2 + \sigma_N^2)}{\sigma_{V \rightarrow P}^2 + \sigma_{P \rightarrow V}^2 + \sigma_N^2} \\ \sigma_{\Delta, Supine}^2 = \sigma_{T_V}^2 + \sigma_{H_P}^2 + \frac{\sigma_{V \rightarrow P}^2 \sigma_{P \rightarrow V}^2}{\sigma_{V \rightarrow P}^2 + \sigma_{P \rightarrow V}^2} \end{cases} \quad (\text{S18})$$

Therefore,  $D\sigma_{ME}^2 = \frac{\sigma_{V \rightarrow P}^2 \sigma_{P \rightarrow V}^2}{\sigma_{V \rightarrow P}^2 + \sigma_{P \rightarrow V}^2} - \frac{\sigma_{V \rightarrow P}^2 (\sigma_{P \rightarrow V}^2 + \sigma_N^2)}{\sigma_{V \rightarrow P}^2 + \sigma_{P \rightarrow V}^2 + \sigma_N^2}$

If we apply S11, we can simplify  $D\sigma_{ME}^2$  as follows:

$$D\sigma_{ME}^2 = -\frac{\sigma_T^2 \sigma_N^2}{2(2\sigma_T^2 + \sigma_N^2)} \quad (\text{S18})$$

For the visual weights, we have:

$$\begin{cases} W_{\Delta V, Seated} = \frac{\sigma_{V \rightarrow P}^2}{\sigma_{V \rightarrow P}^2 + \sigma_{P \rightarrow V}^2 + \sigma_N^2} \\ W_{\Delta V, Supine} = \frac{\sigma_{V \rightarrow P}^2}{\sigma_{V \rightarrow P}^2 + \sigma_{P \rightarrow V}^2} \end{cases} \quad (\text{S19})$$

Therefore,  $DW_{\Delta V} = \frac{\sigma_{V \rightarrow P}^2}{\sigma_{V \rightarrow P}^2 + \sigma_{P \rightarrow V}^2} - \frac{\sigma_{V \rightarrow P}^2}{\sigma_{V \rightarrow P}^2 + \sigma_{P \rightarrow V}^2 + \sigma_N^2}$

If we apply S11, we can simplify  $DW_{\Delta V}$  as follows:

$$DW_{\Delta V} = \frac{\sigma_N^2}{2(2\sigma_T^2 + \sigma_N^2)} \quad (\text{S20})$$

The Neck2 hypothesis predicts for the supine posture a smaller variance, and a larger visual weight, than in the seated position.

### 3.2.3 Gravity hypothesis

According to the Gravity hypothesis, noise ( $\sigma_N^2$ ) should be added to the cross-modal sensory transformations when the head is not aligned with the gravity vector, that is when the neck is laterally flexed during the response phase in the Seated condition ( $\sigma_{P \rightarrow V}^2 + \sigma_N^2$ ), and during both task's phases in the Supine condition ( $\sigma_{V \rightarrow P}^2 + \sigma_N^2$  and  $\sigma_{P \rightarrow V}^2 + \sigma_N^2$ ). No noise is added during the target memorization phase in the Seated condition ( $\sigma_{V \rightarrow P}^2$ ).

For the variances, we have:

$$\begin{cases} \sigma_{\Delta, Seated}^2 = \sigma_{T_V}^2 + \sigma_{H_P}^2 + \frac{\sigma_{V \rightarrow P}^2 (\sigma_{P \rightarrow V}^2 + \sigma_N^2)}{\sigma_{V \rightarrow P}^2 + \sigma_{P \rightarrow V}^2 + \sigma_N^2} \\ \sigma_{\Delta, Supine}^2 = \sigma_{T_V}^2 + \sigma_{H_P}^2 + \frac{(\sigma_{V \rightarrow P}^2 + \sigma_N^2)(\sigma_{P \rightarrow V}^2 + \sigma_N^2)}{\sigma_{V \rightarrow P}^2 + \sigma_{P \rightarrow V}^2 + 2\sigma_N^2} \end{cases} \quad (\text{S21})$$

$$\text{Therefore, } D\sigma_{ME}^2 = \frac{(\sigma_{V \rightarrow P}^2 + \sigma_N^2)(\sigma_{P \rightarrow V}^2 + \sigma_N^2)}{\sigma_{V \rightarrow P}^2 + \sigma_{P \rightarrow V}^2 + 2\sigma_N^2} - \frac{\sigma_{V \rightarrow P}^2 (\sigma_{P \rightarrow V}^2 + \sigma_N^2)}{\sigma_{V \rightarrow P}^2 + \sigma_{P \rightarrow V}^2 + \sigma_N^2}$$

If we apply S11, we can simplify  $D\sigma_{ME}^2$  as follows:

$$\sigma_{ME}^2 = \frac{\sigma_N^2 (\sigma_T^2 + \sigma_N^2)}{2(2\sigma_T^2 + \sigma_N^2)} \quad (\text{S22})$$

For the visual weights, we have:

$$\begin{cases} W_{\Delta V, Seated} = \frac{\sigma_{V \rightarrow P}^2}{\sigma_{V \rightarrow P}^2 + \sigma_{P \rightarrow V}^2 + \sigma_N^2} \\ W_{\Delta V, Supine} = \frac{\sigma_{V \rightarrow P}^2 + \sigma_N^2}{\sigma_{V \rightarrow P}^2 + \sigma_{P \rightarrow V}^2 + 2\sigma_N^2} \end{cases} \quad (\text{S23})$$

$$\text{Therefore, } DW_{\Delta V} = \frac{\sigma_{V \rightarrow P}^2 + \sigma_N^2}{\sigma_{V \rightarrow P}^2 + \sigma_{P \rightarrow V}^2 + 2\sigma_N^2} - \frac{\sigma_{V \rightarrow P}^2}{\sigma_{V \rightarrow P}^2 + \sigma_{P \rightarrow V}^2 + \sigma_N^2}$$

If we apply S11, we can simplify  $DW_{\Delta V}$  as follows:

$$DW_{\Delta V} = \frac{\sigma_N^2}{2(2\sigma_T^2 + \sigma_N^2)} \quad (\text{S24})$$

The Gravity hypothesis predicts a larger variance, and a larger visual weight, in the supine posture, in comparison to the seated posture.

## 4 Fitting experimental data

### 4.1 Algorithm

For fitting our model to the experimental data, we used Matlab® built-in “fmincon” function (R2019b, with the Optimization Toolbox) to minimize the l2-norm of the fitting errors, represented by the following cost functions,  $cf1$  for the variance, and  $cf2$  for the visual weigh:

$$cf1 = \sum_{i=1}^n (DMSd - D\sigma_{ME}^2)^2 \text{ and } cf2 = \sum_{i=1}^n (D\omega_V - DW_{\Delta V})^2 \quad (\text{S25})$$

### 4.2 Independent variables

In order to avoid data overfitting, the number of independent variables in the model was reduced to one ( $\sigma_N^2$ ): the variance associated to the cross-modal sensory transformations ( $\sigma_T^2$ ) was computed from Tagliabue & McIntyre (2011).

In Tagliabue & McIntyre (2011), the cross-modal task V-P, as well as the unimodal tasks P-P and V-V, were tested with a similar protocol in the seated posture, with the head straight. Using their results, and the equations for optimal sensory integration (see main text, equations 5-7), we have:

$$\begin{cases} \sigma_{\Delta V-P}^2 = \sigma_{T_V}^2 + \sigma_{H_P}^2 + \frac{\sigma_{V \rightarrow P}^2 \sigma_{P \rightarrow V}^2}{\sigma_{V \rightarrow P}^2 + \sigma_{P \rightarrow V}^2} = 33.65 \\ \sigma_{\Delta V-V}^2 = \sigma_{T_V}^2 + \sigma_{H_V}^2 = 16.0 \\ \sigma_{\Delta P-P}^2 = \sigma_{T_P}^2 + \sigma_{H_P}^2 = 28.1 \end{cases} \quad (\text{S26})$$

For simplicity, we assume:

$$\sigma_{T_V}^2 = \sigma_{H_V}^2 = \sigma_V^2 \text{ and } \sigma_{T_P}^2 = \sigma_{H_P}^2 = \sigma_P^2 \quad (\text{S27})$$

If we apply S11 and S27, the system of equations S26 becomes:

$$\begin{cases} \sigma_V^2 + \sigma_P^2 + \frac{\sigma_T^2}{2} = 33.65 \\ 2\sigma_V^2 = 16.0 \\ 2\sigma_P^2 = 28.1 \end{cases} \quad (\text{S28})$$

Therefore, we have:

$$\sigma_T^2 = 23.2^{\circ 2} \quad (\text{S29})$$